Length 14281

Copy No.

NASA CR-144920

FINAL REPORT

STUDY OF A FAIL-SAFE ABORT SYSTEM FOR AN ACTIVELY COOLED HYPERSONIC AIRCRAFT

VOLUME II

Technical Report
by
M.E. Peeples and R.L. Herring
January 1976

Prepared under Contract No. NAS1-13631
for
NATIONAL AERONAUTICS AND SPACE ADMINISTRATION
Langley Research Center, Hampton, Va. 23665

by

McDonnell Aircraft Company (MCAIR)
McDonnell Douglas Corporation, St. Louis, Mo. 63166

1. Report No.	2. Government Accession No.	3. Recipient's Catalog No.
NASA CR-144920		

4. Title and Subtitle	5. Report Date
Study of a Fail-Safe Abort System for an Actively Cooled Hypersonic Aircraft, Volume II, Technical Report	January 1976
	6. Performing Organization Code
7. Author(s)	8. Performing Organization Report No.
C. J. Pirrello and R. L. Herring	MDC A3313, Vol. II
	10. Work Unit No.
9. Performing Organization Name and Address	11. Contract or Grant No.
McDonnell Aircraft Company McDonnell Douglas Corporation Post Office Box 516 St. Louis, Mo. 63166	NAS1-13631
	13. Type of Report and Period Covered
12. Sponsoring Agency Name and Address	Contractor Report
National Aeronautics and Space Administration Washington, D.C. 20546	14. Sponsoring Agency Code

15. Supplementary Notes

16. Abstract

Conceptual designs of a fail-safe abort system for hydrogen fueled actively cooled high speed aircraft are examined. The fail-safe concept depends on basically three factors: (1) a reliable method of detecting a failure or malfunction in the active cooling system, (2) the optimization of abort trajectories which minimize the descent heat load to the aircraft, and (3) fail-safe thermostructural concepts to minimize both the weight and the maximum temperature the structure will reach during descent. These factors are examined and promising approaches are evaluated based on weight, reliability, ease of manufacture and cost.

17. Key Words (Suggested by Author(s))	18. Distribution Statement
Actively cooled structure Hypersonic heat loads Thermal protection systems	Unclassified - Unlimited

19. Security Classif. (of this report)	20. Security Classif. (of this page)	21. No. of Pages	22. Price*
Unclassified	Unclassified	232	

*For sale by the National Technical Information Service, Springfield, Virginia 22151

FOREWORD

This report presents the results of a "Study of a Fail-Safe Abort System for an Actively Cooled Hypersonic Aircraft" performed from 6 January 1975 through 15 January 1976 under National Aeronautics and Space Administration Contract NAS-1-13631 by McDonnell Aircraft Company (MCAIR), St. Louis, Missouri, a division of McDonnell Douglas Corporation.

The study was sponsored by the High-Speed Aerodynamics Division, Hypersonic Aerodynamics Branch, with Mr. Charles B. Johnson as Study Monitor.

Mr. Charles J. Pirrello was the MCAIR Study Manager, with Mr. Ralph L. Herring as Principal Investigator. The study was conducted within MCAIR Advanced Engineering which is managed by Mr. Harold D. Altis, Director, Advanced Engineering Division. The study team was an element of Advanced Systems Concepts, supervised by Mr. Dwight H. Bennett.

The overall objective of this study was to conceptually design and evaluate a fail-safe active cooling system which will be used in an abort mode from cruise Mach numbers of 3 to 6. The study was conducted in accordance with the requirements and instructions of NASA RFP 1-15-4807 and McDonnell Technical Proposal, Report MDC A2961, with minor revisions as mutually agreed upon by NASA and MCAIR. The study was conducted using customary units for the principal measurements and calculations. Results were converted to the International System of Units (S.I.) for the final report.

This is one of two reports detailing the technical results of the study. The other report is "Volume I, Technical Summary", Reference (1).

The primary contributors to the contents of this report were M. E. Peeples and R. L. Herring. Other contributors were C. D. Snyder (Aerodynamics), J. P. O'Connor (Materials), J. E. Stone (Thermodynamics). K. L. Wilkinson (Production Design) and L. C. Koch and D. J. Thies (Structural Analyses).

TABLE OF CONTENTS

LIST OF ILLUSTRATIONS

LIST OF ILLUSTRATIONS (CONT'D)

LIST OF ILLUSTRATIONS (CONT'D)

LIST OF ILLUSTRATIONS (CONT'D)

LIST OF ILLUSTRATIONS (CONT'D)

LIST OF ILLUSTRATIONS (CONT'D)

LIST OF ILLUSTRATIONS (CONT'D)

LIST OF ABBREVIATIONS AND SYMBOLS

Abbreviations	Definitions
ACS	Active Cooling System
Al	Aluminum
APU	Auxiliary Power Unit
BIT	Built-In-Test
c.g.	Center of Gravity
EMF	Electromotive Force
FDS	Failure Detection System
FS	Fuselage Station
H/C	Honeycomb
HP	Horse Power
H-X	Heat Exchanger
IR	Infrared
NM	Nautical Mile
PCM	Phase Change Material
TPS	Thermal Protection System
Wt	Weight
Symbols	
A	Area
Btu	British Thermal Unit
$\mathfrak{C}_L$	Centerline
C_{N_β}	Yawing moment coefficient due to sideslip
D	Diameter
F	Allowable Stress
°F	Degrees Fahrenheit
ft	Feet
g	Acceleration due to gravity
H_2	Hydrogen
h	Heat transfer coefficient, honeycomb depth
h'	Distance between centroids of outer and inner skin
hr	Hour
in	Inch
L	Length

LIST OF ABBREVIATIONS AND SYMBOLS (CONT'D)

Abbreviations	Definitions
lbf	Pounds force
lbm	Pounds mass
L/D	Lift to Drag ratio
LH_2	Liquid Hydrogen
$\dot{m}$	Coolant flowrate
min	Minute
N	Running load
n_z	Limit load factor in vertical plane (positive up)
P	Pitch, pressure
psia	Pounds force per square inch, absolute
psid	Pounds force per square inch, differential
q	Dynamic pressure
$\dot{q}$	Heating rate per unit area
Q	Integrated heat per unit area = $\int \dot{q} d\tau$
$\dot{Q}$	Integrated heating rate = $\int \dot{q} dA$
S	Reference lifting area
sec	Second
t	Thickness
T	Temperature
UA	Thermal conductance
W	Mass
W/S	Wing loading
X	Distance aft of nose tip
Greek Symbols	
α	Angle of Attack
γ	Specific weight (mass and weight of a unit volume) = ρg
Δ	Difference
ε	Emissivity
μ	Viscosity
ρ	Density (γ/g)
τ	Descent time
θ	Operating time

Greek Symbols (Cont'd)	Definitions
Σ	Summation
ϕ	Bank angle
SI Units	
g	Gram (Mass)
J	Joule (Heat)
K	Kelvin (Temperature)
m	Meter (Length)
N	Newton (Force)
Pa	Pascal (Pressure)
W	Watt (Power)
s	Second (Time)
SI Prefixes	
m	Milli (10^{-3})
c	Centi (10^{-2})
k	Kilo (10^{3})
M	Mega (10^{6})
Subscripts	
avg	Average
aw	Adiabatic wall
b	Bond, adhesive
B	Baseline
c	Coolant
ci	Coolant inlet
co	Coolant outlet
f	Fuel
i	Inner skin
ins	Insulation
L	Lower, line
min	Minimum
max	Maximum
o	Outer skin
p	Panel

LIST OF ABBREVIATIONS AND SYMBOLS (CONT'D)

Subscripts (Cont'd)	Definition
r	Fin root
s	Skin, system
sil	Silicone
t	Tube
U	Upper
W	Wall, wetted
X	Aircraft axis - longitudinal
Z	Aircraft axis - vertical

1. INTRODUCTION

Previous studies of hydrogen fueled, high speed transport aircraft which utilized actively cooled structure showed the concept has potential advantages over hot structures. The use of hydrogen for fuel provides a heat sink source for the active cooling system to use in reducing aircraft skin and structural temperatures. The reduced temperature allows the use of conventional low temperature material which may provide a longer useful life and a reduced cost compared to some of the more exotic high temperature materials.

However, there are still numerous problems which require investigation before an optimum, workable, safe aircraft system is designed. Redundant systems are heavy and may not provide the best overall approach to safe aircraft. In addition, there may be failures which cannot be negated by redundant systems. Reference (2) indicated that with highly efficient aerodynamic and propulsion system approaches, the normal cruise fuel flow would not be sufficient to cool the entire aircraft. Thus, either an additional expendable heat sink source would be required or the heat load to the cooling system would have to be reduced. These are important issues, however, the more compelling issue is insuring the safety of the aircraft in all possible situations.

Reference (3) presented a fail-safe system concept as an alternative to a redundant active cooling system. This concept consisted of an abort maneuver by the aircraft and a passive thermal protection system (TPS) in the form of overcoat material for the aircraft skin. The abort maneuver provides a low-heat-load descent from normal cruise speed to a lower speed at which cooling is unnecessary, and the passive TPS allows the aircraft structure to absorb the abort heat load without exceeding critical structural temperatures. In addition, the passive TPS may solve the fuel flow problem, a consequence which would be most welcome.

The overall objective of this study was to conceptually design and evaluate a fail-safe actively cooled structural system which will be used in an abort mode from cruise Mach numbers of 3 to 6.

The specific objectives of this study were:

o To determine and evaluate means of failure detection of those active cooling system failures requiring abort.

o To optimize abort mode descent trajectories for cruise Mach numbers of 3 to 6 for minimum heat load.

o To define and evaluate thermostructural concepts for actively cooled structure which will absorb the abort heat load.

The overall study plan is shown in Figure 1. Each of the first three tasks, while distinctively different elements, involved an appreciable amount of interaction. The overall integration of the three elements evaluated all the pertinent interactions in the final evaluation and selection process.

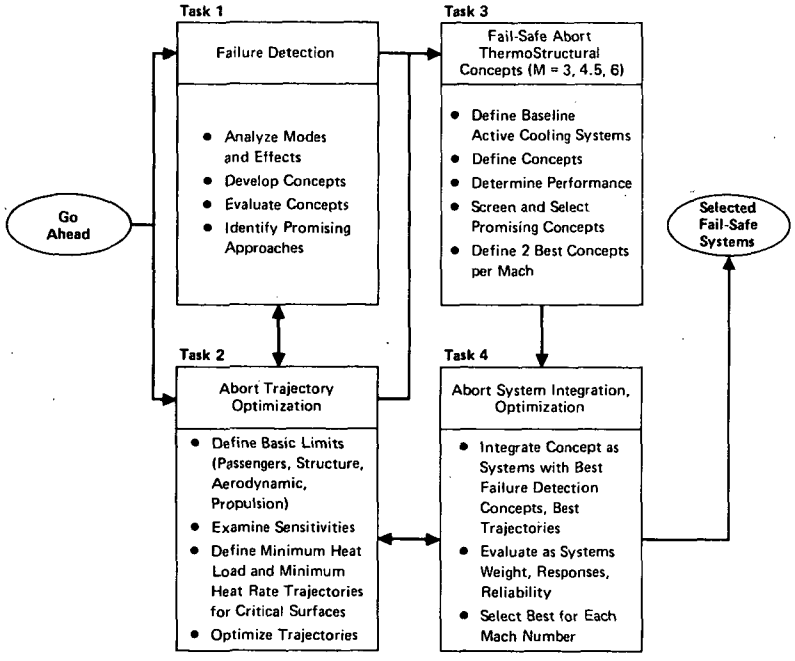

FIGURE 1
FAIL-SAFE ABORT SYSTEM STUDY PLAN

A common set of ground rules and assumptions were established at the beginning of this study that were applicable to the range of investigated cruise Mach numbers. These were:

o The baseline structural design concepts and aerodynamic characteristics were those of the References (2), (4), and (5) blended body Mach 6 transport configuration.

o Structural temperatures were limited to a maximum of 394 K (250°F) during normal cruise and a maximum of 478 K (400°F) during abort.

o Start-of-abort descent was from a nominal cruise dynamic pressure of 24.1 kP_a (504 lb_f/ft^2).

o The coolant was methanol-water at 255 K (0°F) inlet temperature to the cooled structural panels.

o Failure Detection - The primary concern in detection of failures was associated with individual actively cooled structural panel failures such as cracks propagating into, or through, coolant tubes, impact damage or indentation resulting in coolant flow restriction, or separation of a coolant tube from the actively cooled skin.

o Thermostructural Concepts - Aluminum "dee" tube/honeycomb and beaded panel skin/stringer were both to be considered as candidate structural concepts, if applicable. "Precooled" concepts were considered to be material operated well below its maximum useful temperature level to provide heat sink capability in case of abort, e.g., beryllium used in normal operation at a temperature of 394 K (250°F).

o Material/structural life and maintenance requirements are important. Ideally, the airframe structure should be reusable after abort.

o System Integration - Failure modes and detection were reinvestigated after definition of candidate thermostructural concepts.

A brief summary of the overall results of this study are presented as Section 2. The characteristics of the aircraft design used as a baseline vehicle and basic design requirements are described in Section 3.

The technical analyses conducted to meet the study objectives are discussed in Section 4. Failure detection is discussed in Section 4.1. Section 4.2 describes the abort trajectory studies. The abort maneuver, initiated upon detection of a failure, is designed to result in a low heat load descent.

In addition to the low heat load descent trajectory, the fail-safe abort system must have a thermostructural design that can absorb the heat load without exceeding the maximum workable temperature of the aircraft structure. Section 4.3 discusses these fail-safe thermostructural concepts.

Section 4.4 presents the results of integration of failure detection, abort trajectories, and thermostructural concepts as optimized fail-safe systems.

The conclusions resulting from the analyses are discussed in Section 5. The results of this entire study are summarized in Reference (1).

Page intentionally left blank

2. SUMMARY OF FAIL-SAFE ABORT SYSTEMS

It was determined that overall operation of the basic active cooling system can be monitored for failure by conventional instrumentation. The complicating factor in detection of a failure is the large surface area of the aircraft, 2980 m^2 (32,134 ft^2).

Four promising concepts for sensing a high out-of-tolerance skin temperature were identified. The four were: Infrared scanning; Eutectic salt (resistance change) elements; Fluid filled tube elements (thermal expansion of liquid); and Fluid filled tube elements (phase change of contained fluid). The infrared scanning approach was the lowest weight, but is limited in application. Only half of the aircraft surface can be scanned. This concept also is limited by temperature response characteristics of overcoated or shielded surfaces. The system is judged the highest risk due to the potential problems associated with development of sensor windows for operation within the hypersonic environment.

The remaining approaches to detection of skin panel overtemperature are based on the use of temperature sensitive elements attached to the internal surface of the panel skin. The eutectic salt elements work on the principal of electrical resistance change with change in temperature. A solid conductor wire is contained within a porous ceramic which is contained within tubing. The voids between tubing, ceramic and wire, and the porosity of the ceramic are saturated with a eutectic salt mixture. During normal temperature operation the eutectic salt acts as an insulator. At higher temperatures, the salt melts and acts as an electrical conductor. This results in an electrical short detectable by the element circuit signal processor.

The fluid filled tube elements were of two types. The liquid thermal expansion elements contain a fire-resistant hydraulic fluid and utilize a small reservoir and transducer to provide a continuous record of average temperature of each tube element.

The other fluid filled tube elements contain a high vapor pressure liquid. A small reservoir, with pressure transducers and a pressure relief valve, maintains constant system pressure and provides volume for thermal expansion of the contained fluid. During normal operation the liquid level in the reservoir provides a continuous record of average panel temperature. At higher than normal temperatures, the contained liquid boils and provides a pressure signal. The sensor element circuit reservoir pressure relief valve

prevents pressure from exceeding safe levels. The eutectic salt elements represent the minimum development risk approach but the highest unit weight. The high vapor pressure, tube element contained, fluid approach was selected over the others because of its potential overall capability and low unit weight.

The low heat load descent trajectories selected for abort from cruise Mach number are all maximum g-load pull-up maneuvers with transition to a high lift coefficient descent. Aircraft angle of attack was limited to 20 degrees. These descent trajectories were found to be very effective in the reduction of aircraft total heat load. In general, the descent heat load ranged from 32 to 25 percent of normal maximum lift-to-drag ratio descent heat load for start of abort Mach numbers of 3 and 6, respectively.

A large number of potential candidate thermostructural concepts were screened and evaluated for possible application to aircraft designed for operation within the Mach 3 to 6 flight regime. The thermostructural concepts selected for Mach 3 and Mach 4.5 cruise were designed based on cruise considerations and provide more than adequate abort capability. The concepts selected for the Mach 6 cruise aircraft were principally designed by abort capability requirements.

The "Fail-Safe Abort System" elements for Mach 3, 4.5, and 6 cruise are briefly described in the remainder of this section.

2.1 MACH 3 FAIL-SAFE SYSTEM

The design characteristics of the fail-safe abort system selected for Mach 3 cruise are summarized in Figure 2. Failure detection for individual actively cooled panels is provided by Freon filled tube elements. The silicone elastomer overcoats for the upper and lower surfaces were sized to provide matching of available hydrogen fuel flow heat sink capacity with the active cooling system heat load. Maximum lower surface structural temperature during abort is 403 K (266°F). The upper surface structure experiences a maximum of (386K (235°F) during abort.

2.2 MACH 4.5 FAIL-SAFE SYSTEM

The characteristics of the fail-safe abort system selected for Mach 4.5 cruise are illustrated in summary form by Figure 3. Freon filled tube elements are utilized to provide failure detection capability for individual

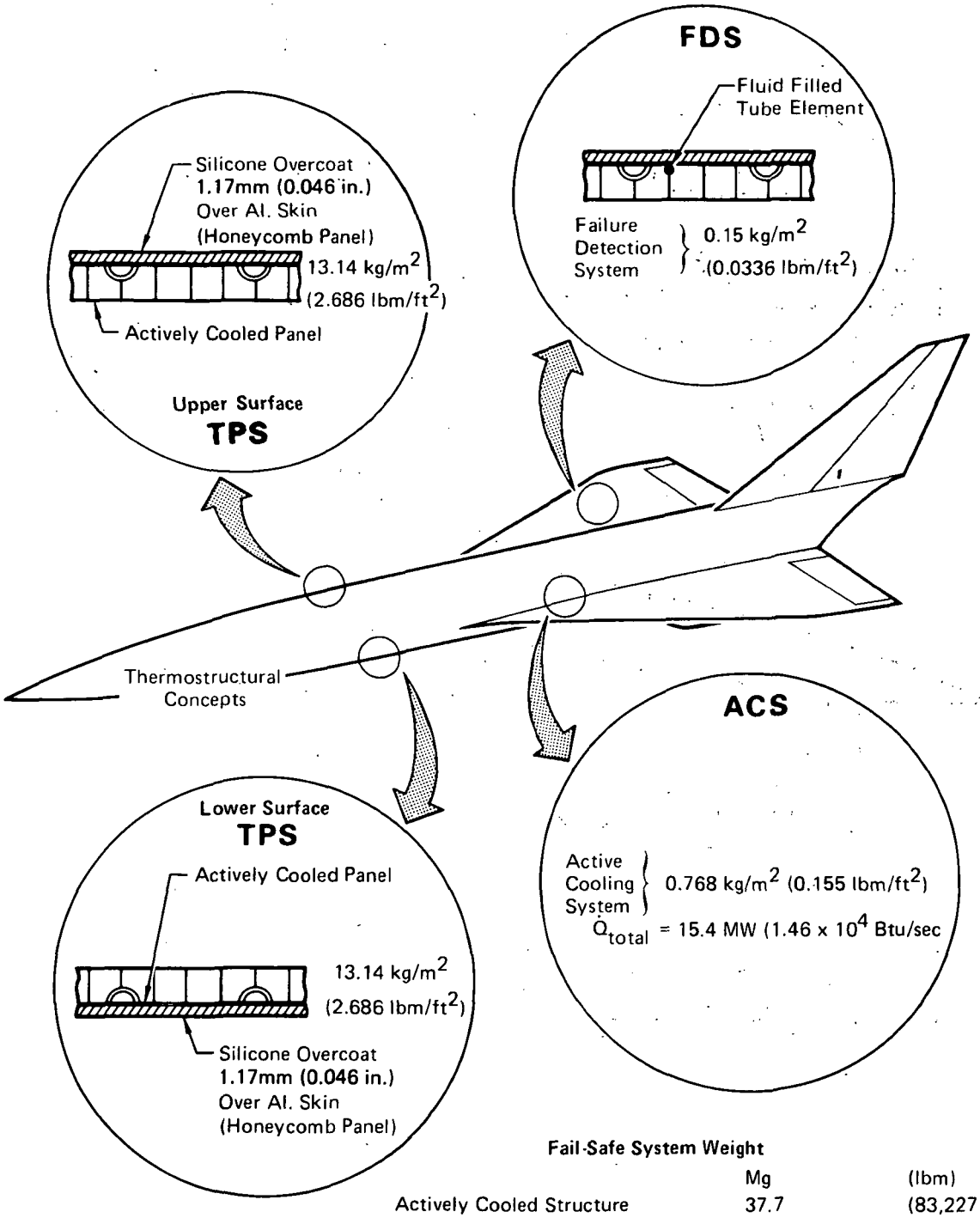

Fail-Safe System Weight

	Mg	(lbm)
Actively Cooled Structure	37.7	(83,227)
(TPS) Thermal Protection Systems	1.5	(3,093)
(ACS) Active Cooling System	2.3	(4,974)
(FDS) Failure Detection System	0.5	(1,081)
Total	42.0	(92,375)

FIGURE 2
MACH 3 FAIL-SAFE SYSTEM SUMMARY

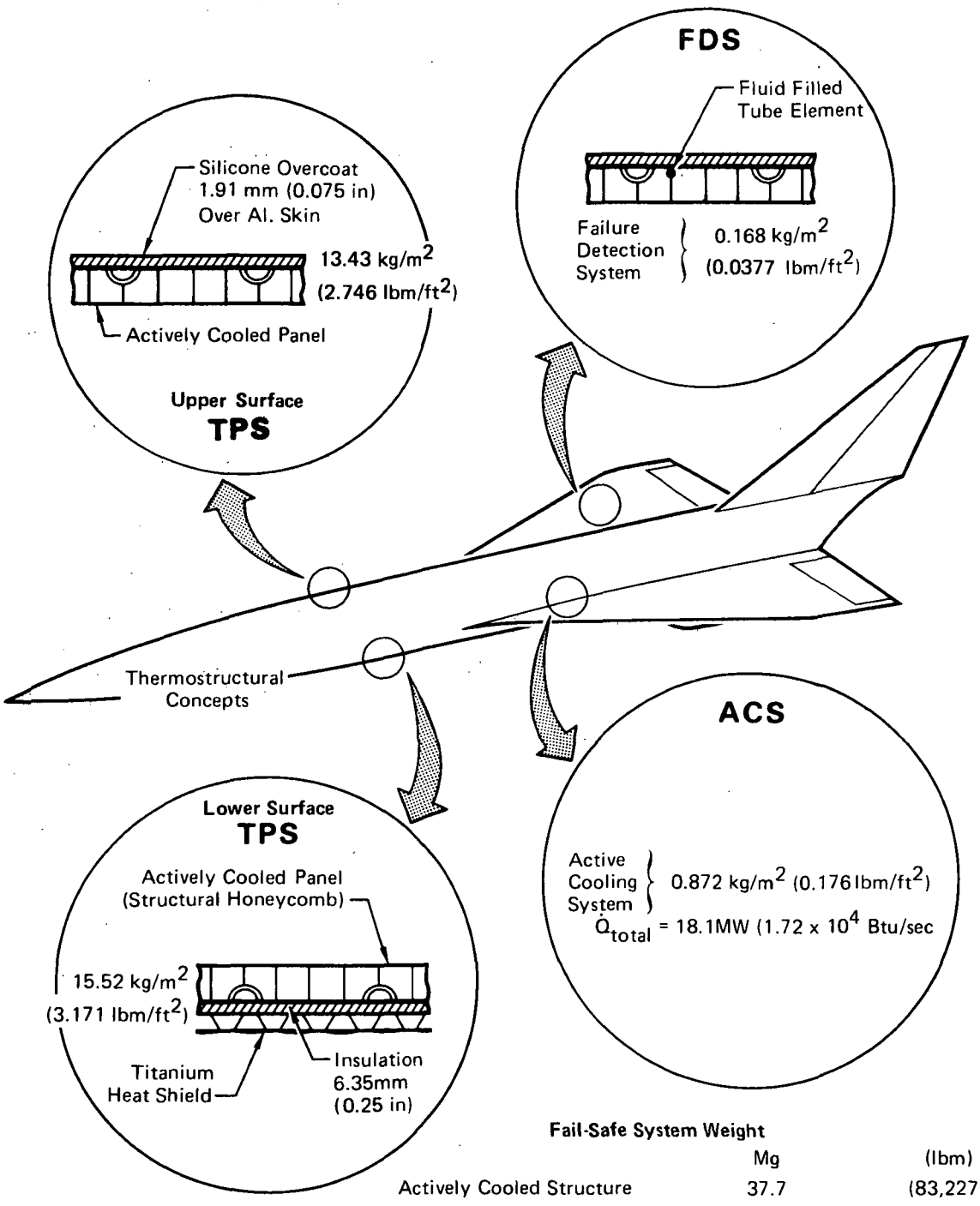

Fail-Safe System Weight

	Mg	(lbm)
Actively Cooled Structure	37.7	(83,227)
(TPS) Thermal Protection Systems	5.2	(11,254)
(ACS) Active Cooling System	2.6	(5,645)
(FDS) Failure Detection System	0.5	(1,212)
Total	46.0	(101,338)

FIGURE 3
MACH 4.5 FAIL-SAFE SYSTEM SUMMARY

actively cooled panels. Silicone elastomer overcoats are used on the aircraft upper surfaces. Insulation and corrugation stiffened beaded titanium skin heat shields cover the lower surface aluminum actively cooled structure. During cruise the absorbed heat is only 41 percent of the available fuel heat sink capacity. Maximum structural temperatures during abort are only 409 K (276°F) and 420 K (296°F) for the upper and lower surface, respectively.

2.3 MACH 6 FAIL-SAFE SYSTEM

The Mach 6 fail-safe system is summarized by Figure 4. Rene' 41 corrugation stiffened beaded skin heat shields over insulated aluminum actively cooled panels are used on the lower aircraft surfaces. The upper surfaces are protected during abort by a silicone elastomer overcoat. Maximum temperatures of the aluminum structure during abort reach a level of 443 K (337°F) for upper surfaces and 465 K (377°F) for lower surfaces. Only 46 percent of the hydrogen fuel heat sink capacity is required to absorb the active cooling system heat load.

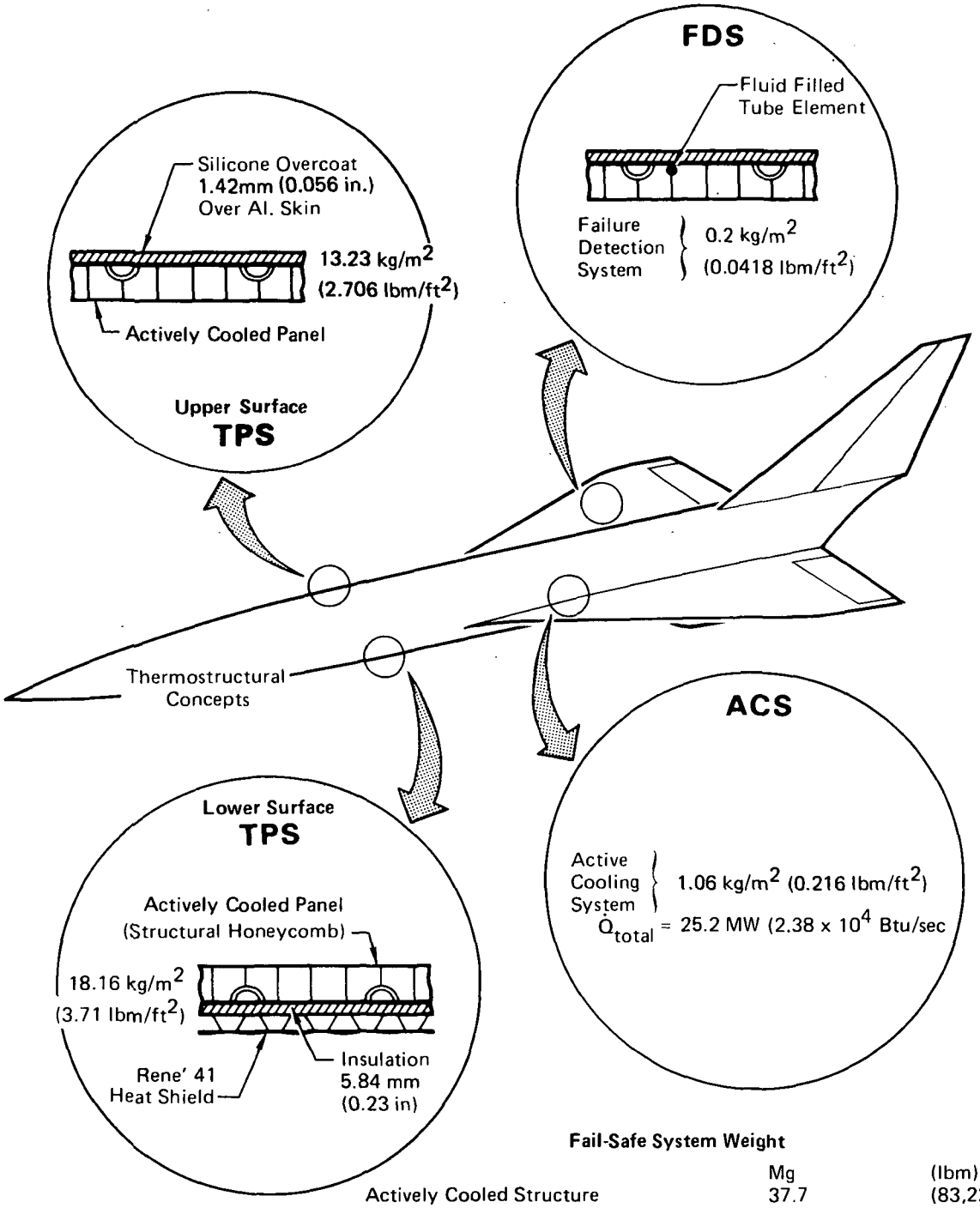

Fail-Safe System Weight

	Mg	(lbm)
Actively Cooled Structure	37.7	(83,227)
(TPS) Thermal Protection Systems	8.4	(18,476)
(ACS) Active Cooling System	3.2	(6,955)
(FDS) Failure Detection System	0.6	(1,343)
Total	49.9	(110,001)

FIGURE 4
MACH 6 FAIL-SAFE SYSTEM SUMMARY

3. BASELINE AIRCRAFT CHARACTERISTICS

The baseline aircraft configuration used throughout the study was an actively cooled Mach 6 cruise design, identified in Reference (4) as Concept 3. The aircraft is a blended wing-body configuration, having an elliptical fuselage cross section, incorporating an integral "bubble" fuel tank structure. The aircraft was designed to carry 200 passengers over a range of 9.26 Mm (5000 NM). Takeoff fuel load was 108.9 Mg (240,000 lb_m) of hydrogen. Figure 5 shows the general arrangement of the aircraft and indicates the pertinent wetted areas. The engine nacelle area was uncooled.

Complete details of the active cooling system design of the baseline aircraft are available in Reference (2). Some of these details are shown by Figure 6. This system used methanol/water solution (60 percent methanol by weight) as the coolant. Pumping power requirements associated with methanol/water solutions were shown in the Reference (6) study to be considerably lower than those for a glycol/water solutions. Also, based on the Reference (6) study results, a coolant inlet temperature to the panels of 256 K (0°F) was assumed. The coolant after absorbing the total heat load, was returned to the heat exchanger at approximately 294 K (70°F). This system was used as a reference active cooling system design and consisted of a nonredundant, uninsulated (bare aluminum skin) system designed for a maximum aluminum structural temperature of 394 K (250°F).

The structural design details of the baseline aircraft are available in Reference (5). Actively cooled panels of both honeycomb and beaded construction were compared to determine the most favorable surface covering. Aluminum honeycomb panels were selected. Figure 7 shows, in some detail, the construction of the actively cooled panels used as moldline covering on the baseline aircraft.

The honeycomb construction panel was selected because it results in a lighter aircraft. The honeycomb panels provide fail-safe coolant containment in the event of tube failure, minimize the number of mechanical fasteners, and provide better flexibility in tailoring local load capability.

Aerodynamic characteristics of the baseline aircraft were used for all three Mach number cruise conditions. Performance analyses of the baseline

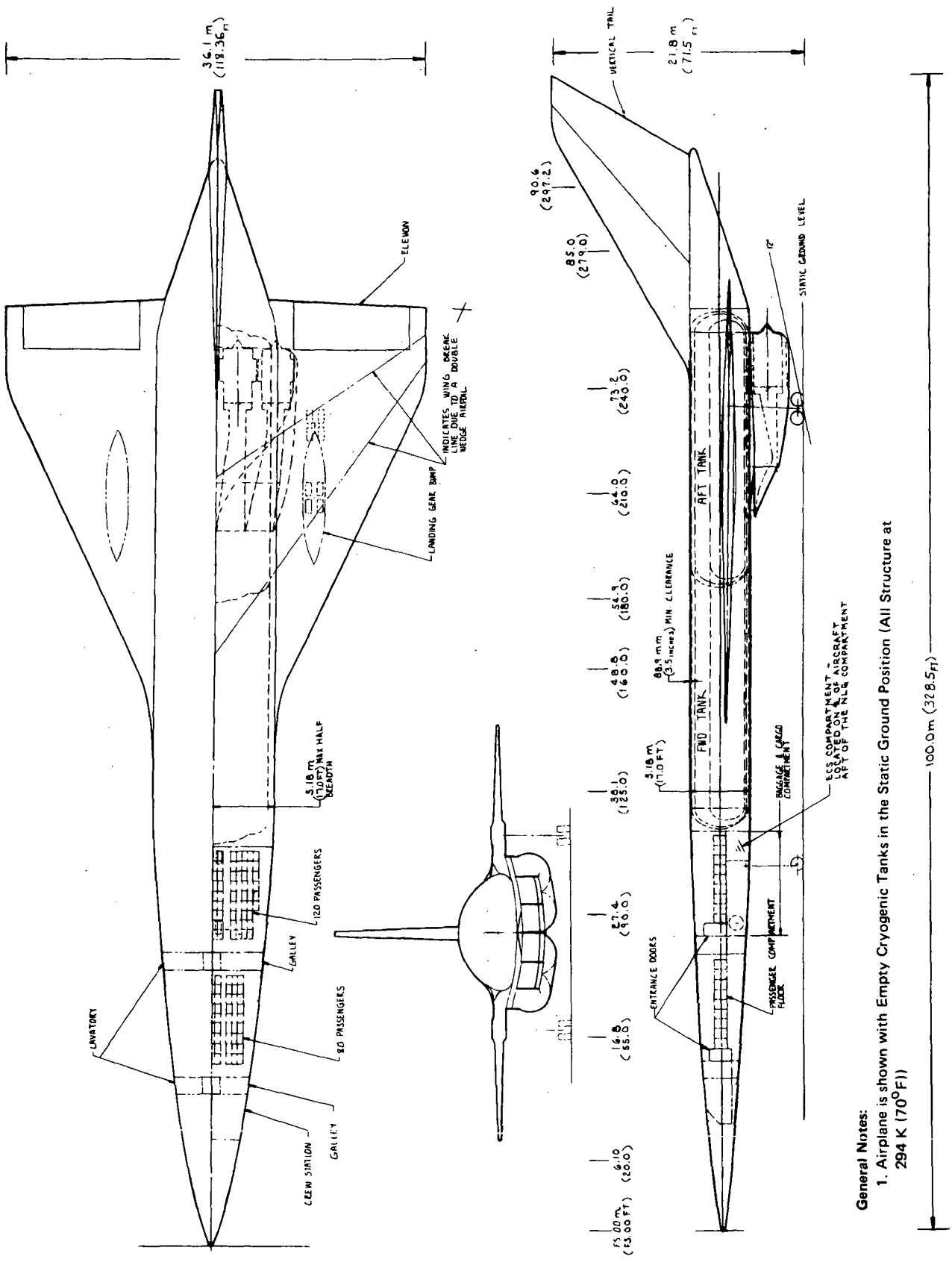

FIGURE 5
BASELINE AIRCRAFT GENERAL ARRANGEMENT

Forward Fuselage	FS 0.00–34m	(FS 0.00–113.5 ft)	0.62 km^3 (22,000 ft^3)
Center Fuselage	FS 34.6–80.0m	(FS 113.5–262.52 ft)	1.84 km^3 (65,100 ft^3)
Aft Fuselage	FS 80.0–93.9m	(FS 262.52–308 ft)	0.11 km^3 (3,800 ft^3)
Total Fuselage			2.57 km^3 90,900 ft^3)
Tank Volume			1.62 km^3 57,200 ft^3)
Tank Volume/Center Fuselage Volume			87.9%
Tank Volume/Total Fuselage Volume			63%

Physical Characteristics

Item	Wing		Vertical Tail	
S_{theo}	0.96 km^2	(10,377 ft^2)	0.14 km^2	(1,535 ft^2)
AR	1.35	–	2.00	–
λ	0.15	–	0.27	–
b	36.1 m	(118.36 ft)	11.9 m	(39.18 ft)
b/2	18.0 m	(59.18 ft)	–	–
C_R	46.5 m	(152.47 ft)	18.6 m	(61.01 ft)
C_T	7.0 m	(22.87 ft)	5.1 m	(16.66 ft)
MAC	31.6 m	(103.64 ft)	13.3 m	(43.49 ft)
Λ LE (deg)	65	–	60	–
Λ TE (deg)	–3	–	30	–
Incidence (deg)	+1/2	–	–	–
Dihedral	0	–	–	–
Thickness Ratio	0.03	–	0.03	–

Performance Summary

Range	9.20 Mg (4,968 NM)
Payload (200 Passengers)	21.8 Mg (48,000 lb)
Operating Weight Empty	187.3 Mg (412,816 lb)
Takeoff Gross Weight	296.1 Mg (652,816 lb)

Propulsion

(4) GE5/JZ6-C 400 kN (90,000 lb) T_{SLS} per Engine Uninstalled

Total Inlet Capture Area (AC_{total}) = 15.8 m^2 (170 ft^2)

	Tire Size
Main Gear	1.27 m x 0.51 m (50 in. x 20 in.)
Nose Gear	1.27 m x 0.51 m (50 in. x 20 in.)

Wetted Area

Fuselage	1.63 km^2 (17,600 ft^2)
Nacelle	0.38 km^2 (4,080 ft^2)
Wing	1.07 km^2 (11,464 ft^2)
Vertical Tail	0.28 km^2 (3,070 ft^2)
Total	3.36 km^2 (36,214 ft^2)

Fuel Distribution

Tank Section	Type	Usable Volume*	Fuel Weight
Forward Fuselage	Integral	0.76 km^3 (26,778 ft^3)	53.7 Mg (118,400 lb)
Aft Fuselage	Integral	0.78 km^3 (27,522 ft^3)	55.2 Mg (121,600 lb)
Total		1.54 km^3 (54,300 ft^3)	108.9 Mg (240,000 lb)

*5% of tank volume allowed for ullage, rings, etc. ∴ Usable volume = 0.95 tank volume

Fuel: Liquid hydrogen @ 20.3 K (−423°F) ρ (density) = 70.8 Kg/m^3 (4.42 lb/ft^3)

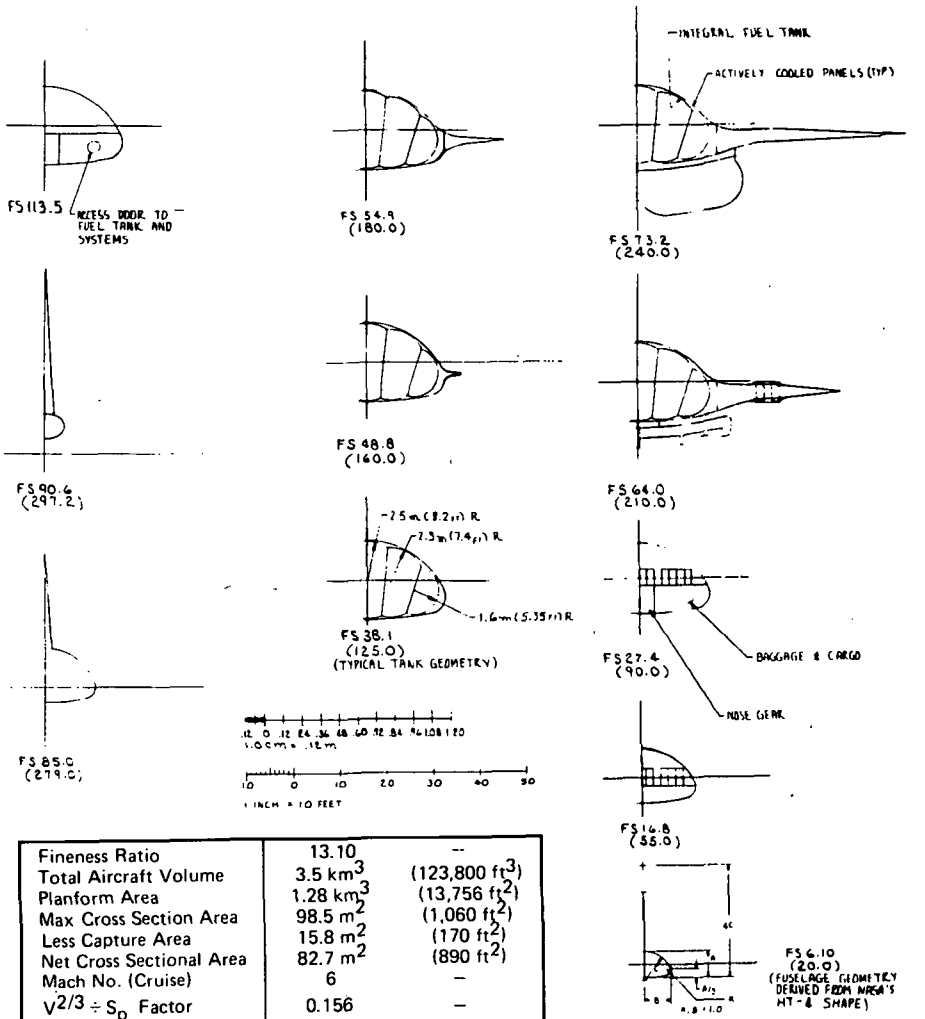

Fineness Ratio	13.10	–
Total Aircraft Volume	3.5 km^3	(123,800 ft^3)
Planform Area	1.28 km^3	(13,756 ft^2)
Max Cross Section Area	98.5 m^2	(1,060 ft^2)
Less Capture Area	15.8 m^2	(170 ft^2)
Net Cross Sectional Area	82.7 m^2	(890 ft^2)
Mach No. (Cruise)	6	–
$V^{2/3} \div S_p$ Factor	0.156	–

FIGURE 5 (Continued)
BASELINE AIRCRAFT GENERAL ARRANGEMENT

Page Intentionally Left Blank

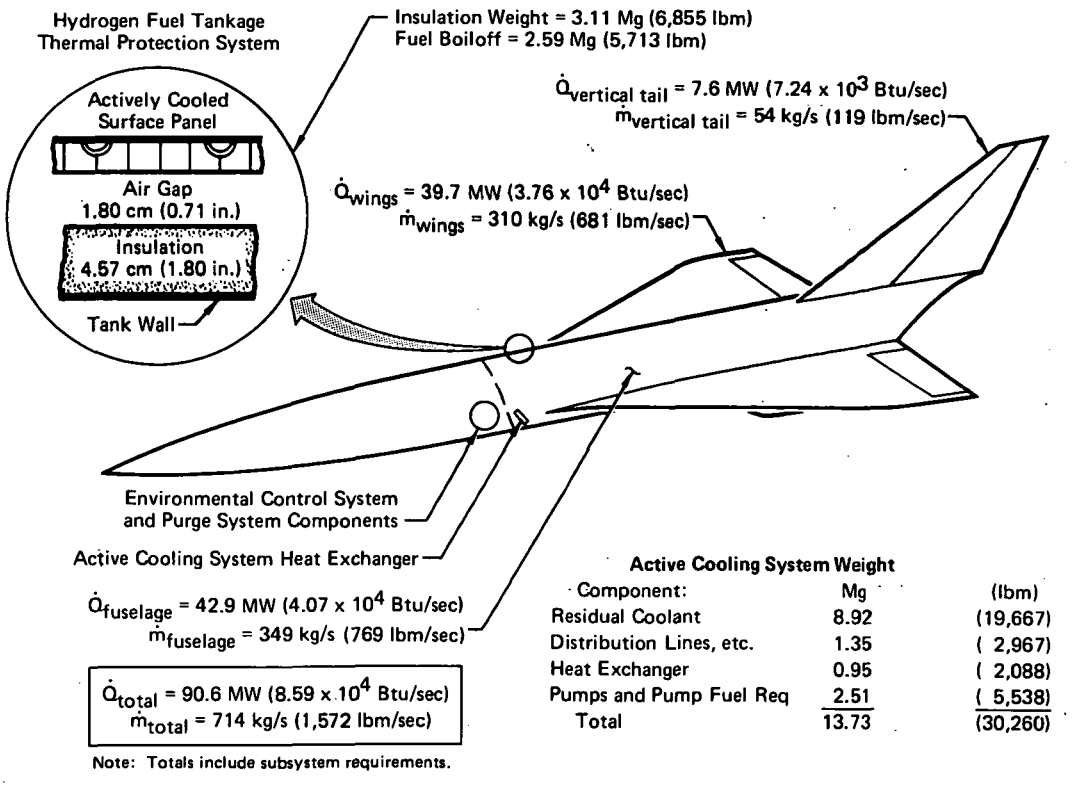

Note: Totals include subsystem requirements.

Active Cooling System Weight

Component:	Mg	(lbm)
Residual Coolant	8.92	(19,667)
Distribution Lines, etc.	1.35	(2,967)
Heat Exchanger	0.95	(2,088)
Pumps and Pump Fuel Req	2.51	(5,538)
Total	13.73	(30,260)

FIGURE 6
THERMODYNAMIC SUMMARY MACH 6 BASELINE

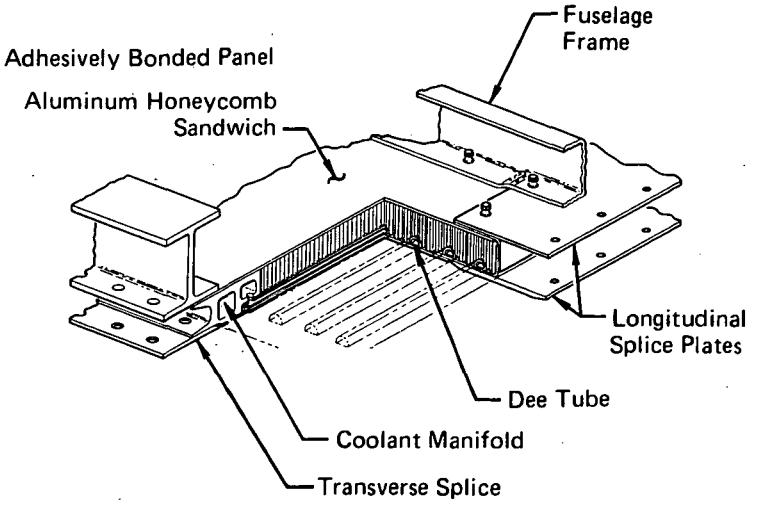

FIGURE 7
ACTIVELY COOLED PANEL CONSTRUCTION

aircraft are available in Reference (4). Aerodynamic coefficients used to compute performance and aerodynamic characteristics, as well as the methods used to obtain them, are described therein. The propulsion system consists of four General Electric advanced hydrogen fueled turboramjet engines. The engine performance data is classified, Reference (7), and therefore is not included in this report. The baseline aircraft Mach number - altitude profile is presented in Figure 8.

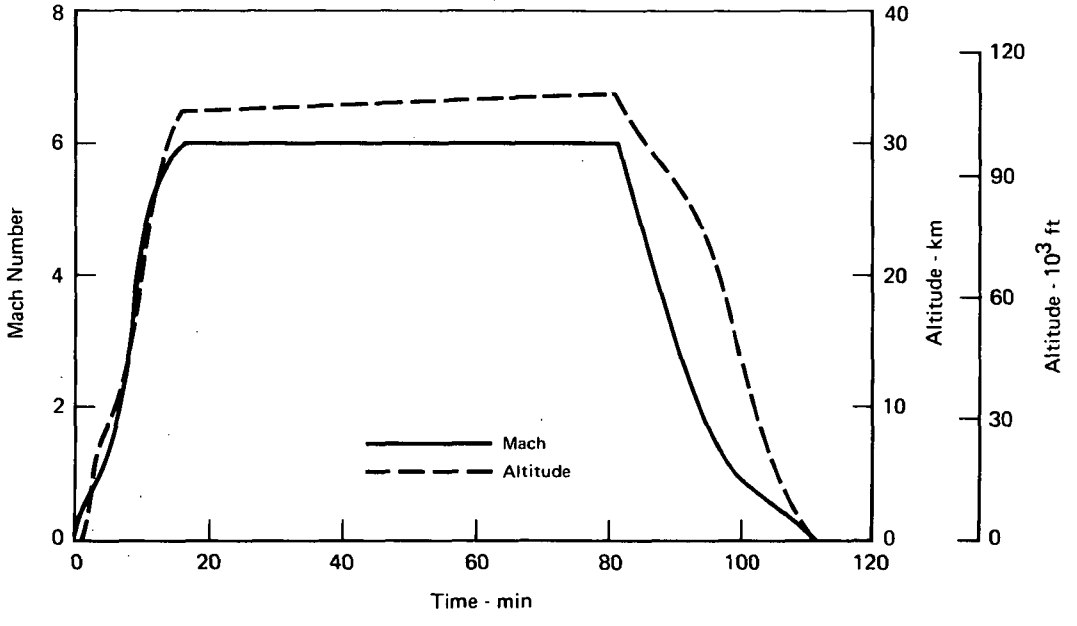

FIGURE 8
MACH NUMBER AND ALTITUDE vs TIME, BASELINE AIRCRAFT

The cooling system design condition was established at that point in the nominal flight trajectory where the total heat absorbed by the cooling system was a maximum. The transient effects of maneuvers on cooling system design were not considered. Parametric data were used to generate generalized heating rates at the design condition of Mach 6, 32 km (105,000 ft) altitude, 7° angle of attack.

Heating zones were defined over the surface area of the aircraft. The number of zones was established in such a manner as to reflect significant variations in local heating rates without creating an unnecessary number of zones to manage. The fuselage was divided into zones that reflected differences in distance from the nose and variations in upper, side, and lower

surface deflection angles. Figure 9 illustrates the zonal definition established. The zones on wings and vertical tail surface areas were distinctly defined to reflect the effect of distance from leading edges and, in the case of wings, differences between upper and lower surface heating. Forward of FS 48.8 m (160 ft), waterline extremes for these zones were determined by finding 45° tangency points on the moldline. Between FS 48.8 m (160 ft) and FS 54.9 m (180 ft) an arbitrary line connecting the waterlines to the wing surfaces was drawn so that aft of FS 54.9 m (180 ft) no side surface heating effects are defined.

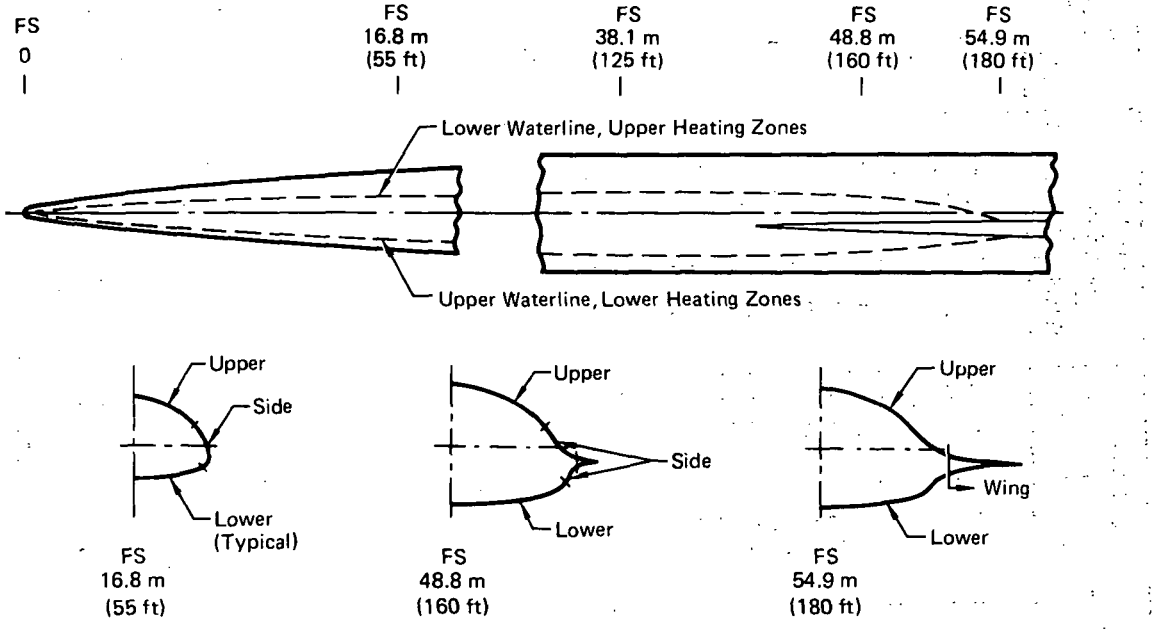

FIGURE 9
TYPICAL FUSELAGE HEATING ZONES, CONCEPT 3

Figure 10 contains the following information for each heating zone: location, surface area (aircraft total), maximum heating rate, average heating rate over the zone, and zonal heating rate (product of the average heating rate and the area). The distribution of the design coolant flow rates established is summarized in Figure 11.

The active cooling system coolant distribution line routing was defined in Reference (2). Distribution line sizes were established per the routing

Zone	Fuselage Station		Fuselage Location	Total Area		Maximum Heating Rate, $\dot{q}$ max		Average Heating Rate, $\dot{q}$ avg		Zonal Heating Rate $\dot{Q}$	
	m	(ft)		m^2	(ft^2)	kW/m^2	(Btu/sec ft^2)	kW/m^2	(Btu/sec ft^2)	MW	(Btu/sec)
Fuselage:											
1	0-6.1	(0-20)	Upper	10.7	(115)	36	(3.2)	28	(2.5)	0.30	(288)
2	↓	(0-20)	Side	4.2	(45)	176	(15.5)	108	(9.5)	0.45	(428)
3	↓	(0-20)	Lower	14.9	(160)	133	(11.7)	98	(8.6)	1.45	(1,376)
4	6.1-12.2	(20-40)	Upper	21.4	(230)	25	(2.2)	23	(2.0)	0.49	(460)
5	↓	(20-40)	Side	20.0	(215)	71	(6.3)	59	(5.2)	1.18	(1,118)
6	↓	(20-40)	Lower	27.4	(295)	83	(7.3)	73	(6.4)	1.99	(1,888)
7	12.2-18.3	(40-60)	Upper	27.9	(300)	20	(1.8)	18	(1.6)	0.51	(480)
8	↓	(40-60)	Side	31.1	(335)	49	(4.3)	43	(3.8)	1.34	(1,273)
9	↓	(40-60)	Lower	34.8	(375)	66	(5.8)	60	(5.3)	2.10	(1,988)
10	18.3-24.4	(60-80)	Upper	33.0	(355)	17	(1.5)	16	(1.4)	0.52	(497)
11	↓	(60-80)	Side	34.8	(375)	37	(3.3)	35	(3.1)	1.23	(1,163)
12	↓	(60-80)	Lower	41.8	(450)	54	(4.8)	51	(4.5)	2.14	(2,025)
13	24.4-30.5	(80-100)	Upper	43.2	(465)	16	(1.4)	15	(1.3)	0.64	(605)
14	↓	(80-100)	Side	38.6	(415)	33	(2.9)	31	(2.7)	1.18	(1,121)
15	↓	(80-100)	Lower	51.1	(550)	48	(4.2)	45	(4.0)	2.32	(2,200)
16	30.5-36.6	(100-120)	Upper	44.1	(475)	15	(1.3)	15	(1.3)	0.65	(618)
17	↓	(100-120)	Side	39.5	(425)	28	(2.5)	24	(2.1)	0.94	(893)
18	↓	(100-120)	Lower	53.4	(575)	42	(3.7)	40	(3.5)	2.12	(2,013)
19	36.6-42.7	(120-140)	Upper	48.8	(525)	14	(1.2)	14	(1.2)	0.66	(630)
20	↓	(120-140)	Side	42.3	(455)	20	(1.8)	19	(1.7)	0.82	(774)
21	↓	(120-140)	Lower	58.1	(625)	37	(3.3)	36	(3.2)	2.11	(2,000)
22	42.7-48.8	(140-160)	Upper	55.7	(600)	14	(1.2)	14	(1.2)	0.76	(720)
23	↓	(140-160)	Side	33.9	(365)	18	(1.6)	18	(1.6)	0.62	(584)
24	↓	(140-160)	Lower	60.4	(650)	36	(3.2)	36	(3.2)	2.19	(2,080)
25	48.8-54.9	(160-180)	Upper	65.0	(700)	14	(1.2)	14	(1.2)	0.89	(840)
26	↓	(160-180)	Side	15.3	(165)	18	(1.6)	18	(1.6)	0.28	(264)
27	↓	(160-180)	Lower	62.7	(675)	35	(3.1)	35	(3.1)	2.21	(2,093)
28	54.9-66.3	(180-217.6)	Upper	134.7	(1,450)	12	(1.1)	12	(1.1)	1.68	(1,595)
29	54.9-70.7	(180-232.1)	Lower	116.1	(1,250)	35	(3.1)	35	(3.1)	4.09	(3,875)
30	66.3-78.0	(217.6-255.8)	Upper	153.3	(1,650)	12	(1.1)	12	(1.1)	1.91	(1,815)
31	78.0-93.9	(255.8-308)	Upper	121.7	(1,310)	12	(1.1)	12	(1.1)	1.52	(1,441)
32	↓	(255.8-308)	Lower	95.2	(1,025)	17	(1.5)	17	(1.5)	1.62	(1,538)
Fuselage Totals:				1,635.1	(17,600)					42.89	(40,683)

FIGURE 10
DESIGN HEATING RATES AND HEAT LOADS
Mach 6, 32 km (105,000 Ft) Altitude

Zone	Location	Total Area		Maximum Heating Rate, $\dot{q}$ max		Average Heating Rate, $\dot{q}$ avg		Zonal Heating Rate $\dot{Q}$	
		m^2	(ft^2)	kW/m^2	(Btu/sec ft^2)	kW/m^2	(Btu/sec ft^2)	MW	(Btu/sec)
Wings:									
33	Upper Surface, Forward 3.05 m (10 ft)	79.1	(851)	24	(2.1)	20	(1.8)	1.62	(1,532)
34	Upper Surface, 3.05-9.14m (10-30 ft) from LE	151.8	(1,634)	23	(2.0)	19	(1.7)	2.93	(2,778)
35	Upper Surface, 9.14+m (30+ ft) from LE	232.4	(2,501)	18	(1.6)	17	(1.5)	3.96	(3,752)
36	Upper Surface, Elevon	78.1	(841)	54	(4.8)	54	(4.8)	4.26	(4,037)
37	Lower Surface, Forward 3.05m (10 ft)	79.1	(851)	75	(6.6)	59	(5.2)	4.67	(4,425)
38	Lower Surface, 3.05-9.14m (10-30 ft) from LE	151.8	(1,634)	54	(4.8)	49	(4.3)	7.41	(7,026)
39	Lower Surface, 9.14+m (30+ ft) from LE	214.7	(2,311)	45	(4.0)	43	(3.8)	9.26	(8,782)
40	Lower Surface, Elevon	78.1	(841)	71	(6.3)	71	(6.3)	5.59	(5,298)
	Wing Totals:	1,065.0	(11,464)					39.68	(37,630)
Vertical Tail:									
41	Forward 3.05m (10 ft)	72.8	(784)	42	(3.7)	33	(2.9)	2.40	(2,274)
42	3.05-9.14m (10-30 ft) from LE	131.0	(1,410)	31	(2.7)	27	(2.4)	2.57	(3,384)
43	9.14+m (30+ ft) from LE)	81.4	(876)	22	(1.9)	20	(1.8)	1.66	(1,577)
	Vertical Tail Totals:	285.2	(3,070)					7.63	(7,235)
	Airframe Totals:	2,985.4	(32,134)					90.20	(85,548)

FIGURE 10 (Continued)
DESIGN HEATING RATES AND HEAD LOADS
Mach 6, 32 km (105,000 Ft) Altitude

Zone (Reference Fig. 10)	Skin Thickness		Tube Spacing		Tubes/ Zone	Flowrate/Tube		Flowrate/Zone	
	mm	(in.)	cm	(in.)		g/s	(lbm/hr)	kg/s	(lbm/hr x 10^{-3})
1	1.016	(0.040)	5.03	(1.98)	34.85	73.1	(580)	2.55	(20.21)
2	1.016	(0.040)	2.74	(1.08)	25.00	266.9	(2,118)	6.67	(52.94)
3	1.016	(0.040)	3.02	(1.19)	80.67	207.0	(1,643)	16.69	(132.50)
4	1.016	(0.040)	5.87	(2.31)	59.74	57.3	(455)	3.42	(27.18)
5	1.016	(0.040)	3.81	(1.50)	86.00	122.0	(968)	10.48	(83.21)
6	1.016	(0.040)	3.61	(1.42)	124.65	137.8	(1,093)	17.16	(136.18)
7	1.016	(0.040)	6.40	(2.52)	71.43	51.0	(405)	3.65	(28.93)
8	1.016	(0.040)	4.45	(1.75)	114.86	90.5	(718)	10.38	(82.41)
9	1.016	(0.040)	3.94	(1.55)	145.16	114.0	(905)	16.55	(131.37)
10	1.016	(0.040)	6.93	(2.73)	78.02	46.4	(368)	3.61	(28.67)
11	1.016	(0.040)	4.95	(1.95)	115.38	74.7	(593)	8.61	(68.36)
12	1.016	(0.040)	4.24	(1.67)	161.68	98.1	(780)	15.89	(126.11)
13	1.600	(0.063)	8.74	(3.44)	81.10	55.0	(436)	4.46	(35.36)
14	1.600	(0.063)	6.32	(2.49)	100.00	90.8	(721)	9.08	(72.10)
15	1.600	(0.063)	5.41	(2.13)	154.93	122.0	(968)	18.90	(149.97)
16	1.600	(0.063)	9.04	(3.56)	80.06	53.0	(417)	4.21	(33.39)
17	1.600	(0.063)	6.76	(2.66)	95.86	81.3	(645)	7.79	(61.83)
18	1.600	(0.063)	5.72	(2.25)	153.33	110.0	(873)	16.87	(133.86)
19	0.635	(0.025)	6.22	(2.45)	128.57	41.6	(330)	5.35	(42.43)
20	0.635	(0.025)	5.23	(2.06)	132.52	51.0	(405)	6.76	(53.67)
21	0.635	(0.025)	4.09	(1.61)	232.92	75.0	(593)	17.39	(138.01)
22	0.635	(0.025)	6.22	(2.45)	146.94	41.6	(330)	6.11	(48.49)
23	0.635	(0.025)	5.51	(2.17)	100.92	47.9	(380)	4.83	(38.35)
24	0.635	(0.025)	4.14	(1.63)	239.26	73.1	(580)	17.48	(138.77)
25	0.635	(0.025)	6.22	(2.45)	171.43	41.6	(330)	7.13	(56.57)
26	0.635	(0.025)	5.51	(2.17)	45.62	47.9	(380)	2.18	(17.34)
27	0.635	(0.025)	4.19	(1.65)	245.45	71.6	(568)	17.55	(139.29)
28	0.635	(0.025)	6.45	(2.54)	342.52	40.1	(318)	13.70	(108.75)
29	0.635	(0.025)	4.19	(1.65)	454.55	71.6	(568)	32.50	(257.96)
30	0.635	(0.025)	6.45	(2.54)	389.76	40.1	(318)	15.59	(123.75)
31	0.635	(0.025)	6.45	(2.54)	309.45	40.1	(318)	12.38	(98.25)
32	0.635	(0.025)	5.66	(2.23)	275.78	46.4	(368)	12.77	(101.35)
33	1.016	(0.040)	5.99	(2.36)	216.36	55.8	(443)	12.06	(95.74)
34	1.016	(0.040)	6.12	(2.41)	406.80	54.2	(430)	22.04	(174.92)
35	1.600	(0.063)	8.23	(3.24)	463.15	59.7	(474)	27.66	(219.53)
36	1.016	(0.040)	4.24	(1.67)	302.16	98.3	(780)	29.70	(235.69)
37	1.016	(0.040)	3.76	(1.48)	345.00	126.6	(1,005)	43.69	(346.73)
38	1.016	(0.040)	4.24	(1.67)	587.07	98.3	(780)	57.70	(457.92)
39	1.600	(0.063)	5.51	(2.17)	638.99	117.2	(930)	74.88	(594.26)
40	1.016	(0.040)	3.81	(1.50)	336.40	122.0	(968)	41.01	(325.47)
41	1.016	(0.040)	4.72	(1.86)	252.90	81.0	(643)	20.47	(162.49)
42	1.270	(0.050)	5.92	(2.33)	363.09	65.3	(518)	23.68	(187.90)
43	1.270	(0.050)	6.88	(2.71)	193.95	52.7	(418)	10.20	(80.97)
Total					9,084.00			711.78	(5,649.16)

FIGURE 11
DESIGN COOLANT FLOWRATES FOR AIRFRAME COOLING
Baseline Aircraft, Mach 6, 32 km (105,000 Ft) Altitude

indicated in Figures 12 and 13. All lines (including feeder lines) were sized based on an allowable pressure drop of 2.26 kPa/m (0.1 psi/ft). An allowance for the differences in coolant density between supply and return lines was included.

The active cooling system weight bases are defined in Reference (2). The total weight for the system was 13.73 Mg (30,260 lb_m). This weight did not include the weight of the actively cooled structural panels covering the aircraft.

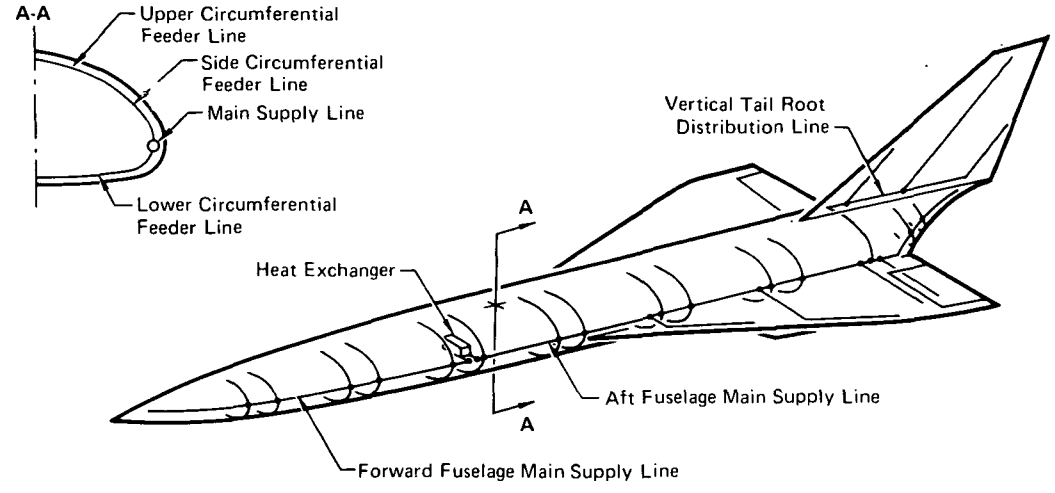

- Supply Lines only are Shown, Return Lines Spaced Similarly
- Lines Represent Those on One Side of Aircraft only, Except for Vertical Tail Lines

FIGURE 12
SIMPLIFIED DISTRIBUTION SYSTEM SCHEMATIC

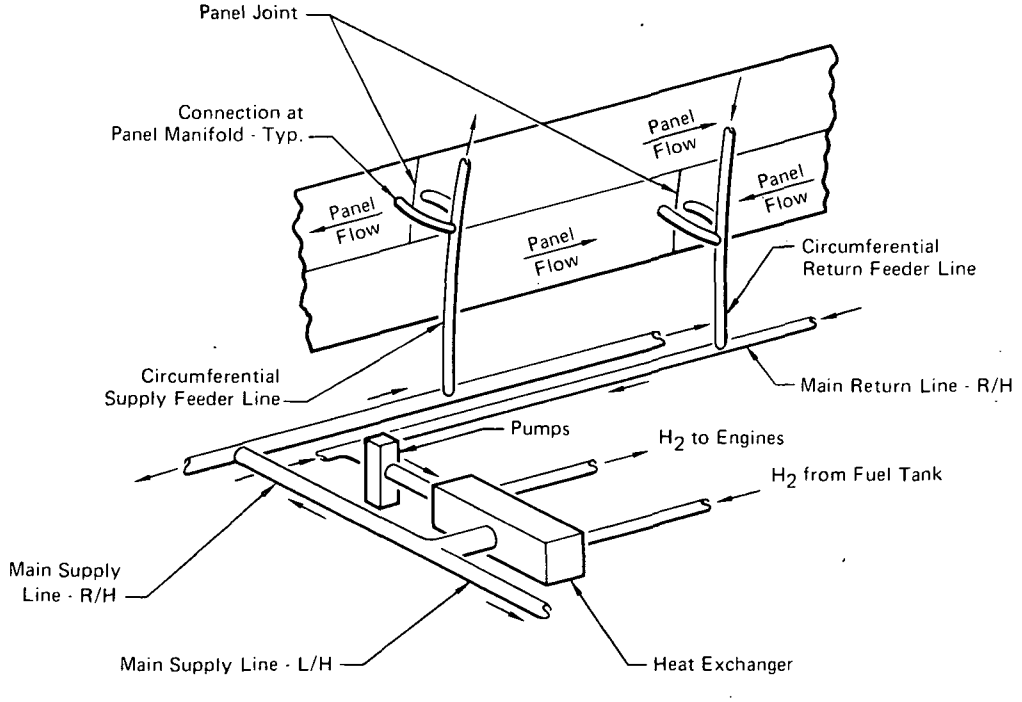

FIGURE 13
TYPICAL COOLANT DISTRIBUTION ROUTING AT MAJOR COMPONENT LOCATION

Page Intentionally Left Blank

4. TECHNICAL DISCUSSION

The integrated "Fail-Safe Abort System" must satisfy three basic requirements:

- o Failure in the cooling system or cooled airframe structural panels must be reliably detected.
- o The aircraft must have the capability of reacting quickly to an abort demand, utilizing abort maneuvers intended to minimize the heat load during descent.
- o The structural design must have the capability to absorb the descent heat load without exceeding the design temperature limits and must do so at minimum weight and cost.

Studies were conducted in the realms of: (1) failure detection, (2) aerodynamic heating during aircraft descent from cruise, (3) thermostructural design, and (4) systems integration. Discussion of these studies follow.

4.1 ACTIVE COOLING SYSTEM FAILURE DETECTION

The study of active cooling system failure detection was subdivided into five areas, starting with the establishment of a baseline model for failure mode and effect analyses and concluding with system integration. Primary emphasis was placed on detecting failures that would result in out-of-tolerance temperatures on individual panels.

4.1.1 Baseline Cooling System - Failure detection analyses were based on the active cooling system shown in Figure 14. This system is a refined version of the Reference (2) system. The system employs APU driven pumps for circulating a 60/40 mixture of methanol and water through coolant tubes attached to external skin panels of the aircraft. Aerodynamic heat absorbed by the coolant flowing through the panels is transferred through a heat exchanger to liquid hydrogen pumped to the aircraft engines. Hydrogen flow through the heat exchanger is modulated to maintain coolant at 255 K (0°F) at the inlet to actively cooled panels. Nominal design coolant temperature is 352 K (120°F) at the heat exchanger inlet (panel outlet). Pressurized coolant reservoirs maintain positive pump inlet pressure, and accommodate volume changes caused by system coolant temperature excursions and leakage. Other system elements shown on Figure 14, such as filters, check valves, relief

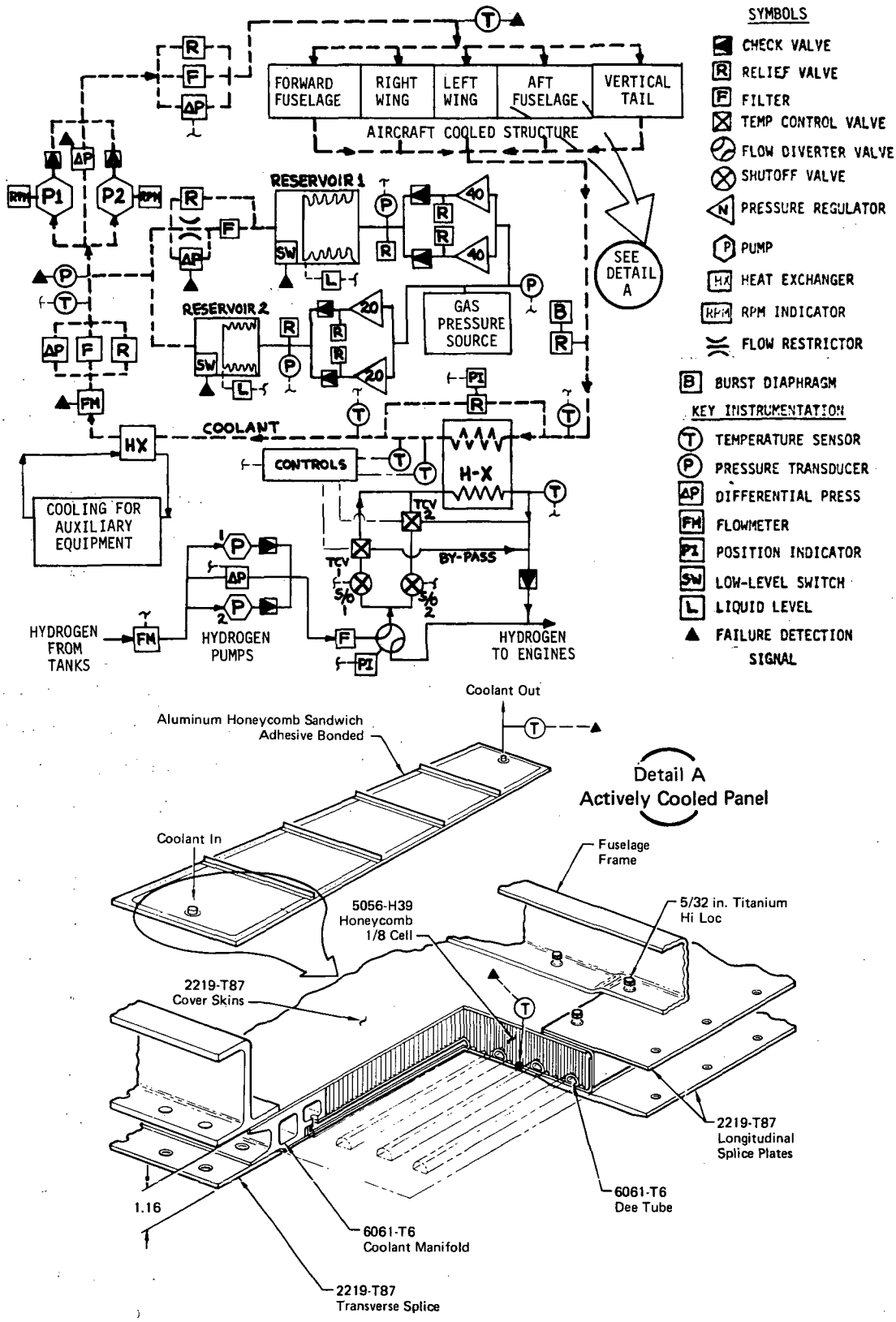

FIGURE 14
BASELINE ACTIVE COOLING SYSTEM SCHEMATIC

valves, etc., are included to provide better visibility in the study of potential failures which might render the system cooling inadequate. In addition, the baseline cooling system employs some redundant components, such as pumps and temperature control valves, to guard against single-point failures. Instrumentation for system monitoring and failure detection is also included.

4.1.2 Failure Modes and Effects - The qualitative evaluation of system failures and effects is presented in Figure 15. It was based on defining those failures which could result in a certain end-failure mode; in this case, structural failure. Various system failures, and how they ultimately might lead to structural failure are illustrated. Failure detection candidates include those which detect the actual failure or any of its subsequent effects. Redundant components/subsystems consistent with Figure 14 are also indicated.

Figure 16 summarizes potential causes and consequences of the most probable failure modes of each of the major system elements. Information is also presented on primary failure detection methods and corrective action to be taken.

It was assumed that abort (to a less severe heating condition) would be in order for any failure that would ultimately lead to excessive skin temperature or system pressure, regardless of component redundancy.

The severity of each failure mode is described in Figure 16. However, in most cases, the severity cannot realistically be stated in qualitative terms alone. In order to assess how rapidly a failure can be detected, and also how much time is available to initiate abort, a more quantitative assessment was made, using typical failure modes in individual actively cooled structural panels. The effects of leaks in coolant tubes and damage causing flow restriction are described.

o External Coolant Leakage - The ultimate effect of coolant leakage is essentially the same anywhere within the system: depletion of the coolant reservoir(s) to the point where pump inlet pressure is reduced and coolant flow rate is degraded. However, the severity of the failure will depend on leakage rate, reservoir volume, flight time, panel design, external heating rate, and the characteristics and response time of the failure detection system.

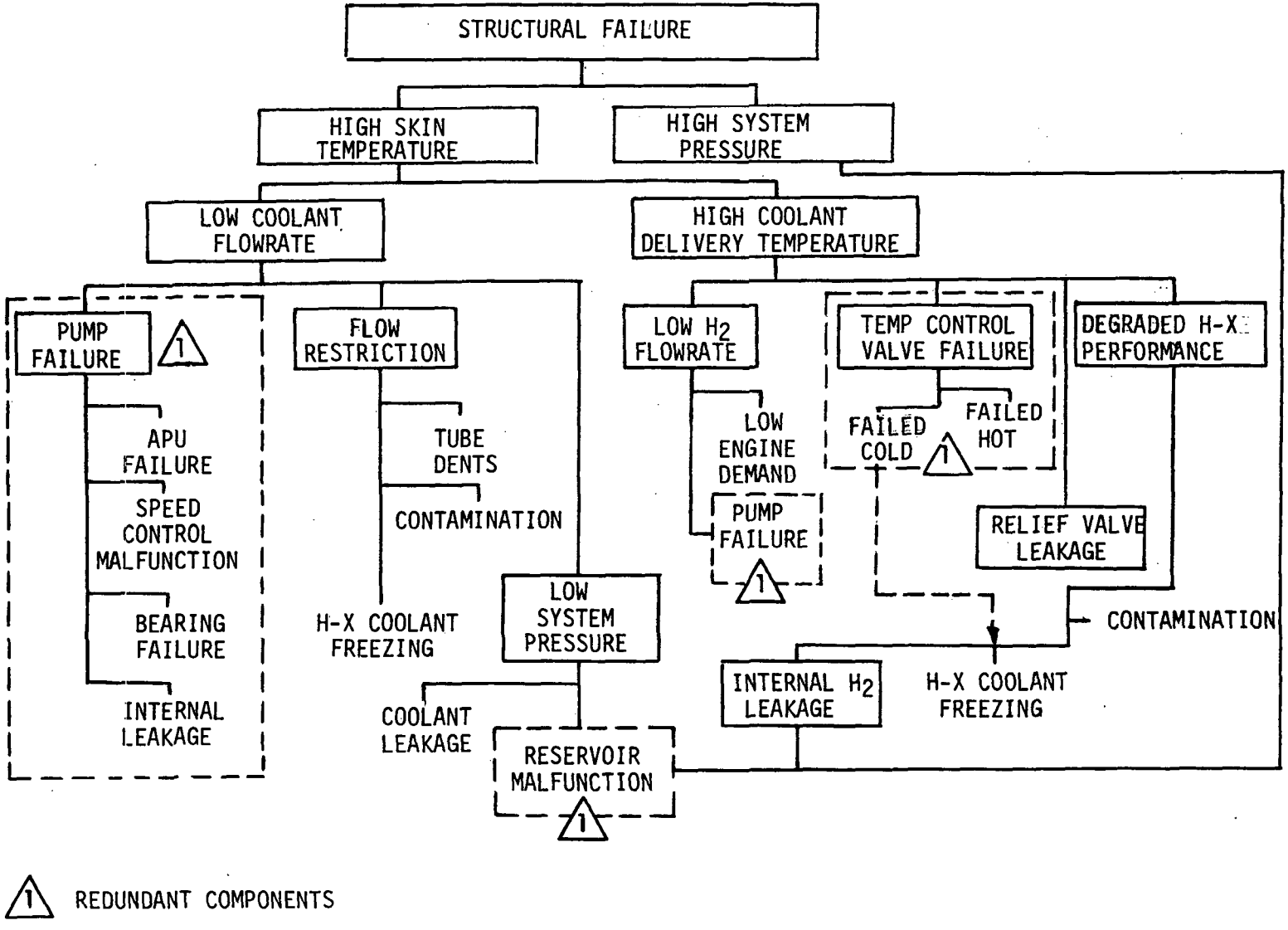

FIGURE 15
SYSTEM FAILURE MODES

Item	Failure Mode	Failure Cause(s)	Failure Effect(s)	Severity of Failure	Primary Failure Detection	Corrective Action
1. Active Cooled Panel	A. Leakage	o Cracks due to over-stress, corrosion, etc. o Accidental damage due to mishandling, collision, etc.	o Coolant reservoir depletion followed sequentially by: o Reduced pump inlet pressure o Degraded pump performance o Fluctuating flow rate (low) o Erratic pump ΔP o High H-X inlet coolant temp o High panel skin temp	o Function of leakage rate, reservoir volume, panel design, heating rate, and failure detection system (FDS) response.	o Reservoir level-low o Reservoir coolant flow-high o Pump inlet pressure-low o Pump ΔP-low o Coolant flow-low	o Abort if two cues are indicated o Reservoir flow-high o Reservoir level-low
	B. Clogged Passage	o Dents due to mis-handling or accidental damage o Contaminant buildup o Crimped tube due to skin buckling	o Reduced coolant flow through affected tube o High skin temp at or adjacent to affected tube	o Function of degree of clogging, panel design, heating rate, and FDS response.	o Local skin temp at panel outlet-high	o Abort if two cues are indicated o Skin temp 1 - high o Skin temp 2 - high
2. Distribu-tion Lines and Fittings	A. Leakage	-Same as 1A-	-Same as 1A-	-Same as 1A-	-Same as 1A-	-Same as 1A-
	B. Flow Restric-tion	o Dents due to mis-handling or accidental damage o Contaminant buildup	o Reduced coolant flow to one or more active cooled panels o High panel skin temp	o Function of degree of restriction, panel design, heating rate, and FDS response.	o Main distribution lines o Coolant flow rate-low o Pump ΔP - high o Panel coolant out temp-high o Panel outlet skin temp-high o Feeder lines o Panel coolant out temp-high o Panel outlet skin temp-high	o Abort if two cues are indicated o Panel outlet coolant temp-high o Panel outlet skin temp-high
3. Coolant Pump	A. External Leakage	-Same as 1A- o Seal deterioration	-Same as 1A-	-Same as 1A-	-Same as 1A-	-Same as 1A-
	B. Internal Leakage	o Pump wear o Seal deterioration o Leaky check valve at adjacent pump exit	o Degraded pump performance o Low coolant flow rate o Low pump ΔP o High H-X inlet coolant temp o High panel skin temp	o Function of leakage rate, flow rate reduction, panel design, heating rate, and FDS response	o Coolant flow rate-low o Pump ΔP - low	o Automatic switchover to redundant pump o Coolant flow rate-low o Pump ΔP - low o Abort after indication of auto pump switchover

FIGURE 16
ACTIVE COOLING SYSTEM FAILURE MODES AND EFFECTS

Item	Failure Mode	Failure Cause(s)	Failure Effect(s)	Severity of Failure	Primary Failure Detection	Corrective Action

3.(Cont'd)	C.Low Flow Rate	o Loss of speed control
		o APU malfunction
		o Bearing failure
		o Cavitation
		  o Low pump inlet pressure
		  o Free gas in loop
		o Contamination
			o High H-X inlet coolant temp
			o High panel skin temp
				o Function of flow rate reduction, panel design, heating rate, and FDS response	o Coolant flow rate-low
					o Pump ΔP - low
					o H-X inlet temp-high
					o Pump speed-low
					o Pump noise/vibration-high
						-Same as 3B-

4.Heat Exchanger	A.External Coolant Leakage	-Same as 1A-	-Same as 1A-	-Same as 1A-	-Same as 1A-	-Same as 1A-

	B.Internal Leakage (H_2 to Coolant)	-Same as 1A-	o Degraded pump performance
			  o Fluctuating flow rate-low
			  o Erratic pump ΔP
			  o High H-X inlet coolant temp
			  o High panel skin temp
			o Increased coolant loop pressure
			  o Coolant vent through overboard relief
				o Function of leakage rate, coolant flow rate reduction, heating rate, and FDS response	o Coolant pressure-high
					o Coolant flow rate-low
					o Pump ΔP - erratic
						o Abort if two cues are indicated
						  o Coolant pressure-high
						  o Coolant flow rate-low

	C.Flow Restriction	o Coolant freezing
		o TCV malfunction
		o Contamination
			o Slight coolant flow rate reduction
			o Increased pump ΔP
			o Increased H-X inlet temp
			o Increased panel inlet temp (If H-X ΔP relief valve setting)
			o High panel skin temp
				o Function of degree of restriction, panel design, heating rate, and failure detection system response	o Relief valve position-open
					o Panel inlet temp-high
					o H-X inlet temp-high
						o Abort if two cues are indicated
						  o Panel inlet temp-high
						  o H-X inlet temp-high

5.Temp Control Valve	A.Failed Cold	o Contamination
		o Mechanical binding
		o Electrical Malfunction
		o Erroneous signal
			o Low coolant temp at H-X outlet followed by:
			  o Increased H-X coolant ΔP
			  o Potential freezing in H-X
			  o Coolant bypass around H-X
			  o Increased panel inlet temp
			o High panel skin temp
				o Function of coolant system heat capacity, panel design, heating rate, and failure detection system response	o H-X out temp-low
					o H-X relief valve position-open
					o Panel inlet temp-high
					H-X inlet temp-low
						o Abort if two cues are indicated
						  o Panel inlet temp-high
						  o H-X inlet temp-high
						o Switch to redundant TCV

FIGURE 16 (Continued)
ACTIVE COOLING SYSTEM FAILURE MODES AND EFFECTS

Item	Failure Mode	Failure Cause(s)	Failure Effect(s)	Severity of Failure	Primary Failure Detection	Corrective Action
5.Temp Control Valve	B.Failed Hot	-Same as 5A-	o High coolant temp at H-X outlet followed by: o Increased panel inlet temp o Increased HX inlet temp o High panel skin temp	o Function of coolant system heat capacity, panel design, heating rate, and failure detection system response	o All coolant temps-high o H-X outlet o Panel inlet o H-X inlet o Etc	o Abort if two cues are indicated o Panel inlet temp high o H-X inlet temp-high o Switch to redundant TCV
6.Coolant Reservoir	A.Coolant Leak	-Same as 1A-	-Same as 1A-	-Same as 1A-	-Same as 1A-	-Same as 1A-
	B.Internal Gas Leak	o Cracks in bladder o Degradation o Overstress	o Gas entrainment in coolant o Pump cavitation o Fluctuating flow rate (low) o Erratic Pump ΔP o High H-X inlet coolant temp o High panel skin temp	o Function of gas permeation through coolant, solubility of gas in coolant, resultant pump cavitation and flow rate reduction, panel design, heating rate, and failure detection system response	o Coolant flow rate-low o Pump ΔP - low o H-X inlet temp-high	o Abort if two cues are indicated o Coolant flow rate-low o H-X inlet temp-high
	C.Loss of Gas Pressure	o Gas leak o Crack in tank or line o Leaky relief valve o Gas supply malfunction	o Reduced reservoir pressure o Reduced pump inlet pressure o Degraded pump performance o Fluctuating flow rate (low) o Erratic Pump ΔP o High H-X inlet coolant temp o High panel skin temp	o Function of leak rate, pump inlet pressure reduction, flow rate reduction, panel design, heating rate, and failure detection system response	o Reservoir gas pressure-low o Pump inlet pressure-low o Affected reservoir level-low o Coolant flow rate-low o Pump ΔP - low o H-X inlet temp-high	o Abort if two cues are indicated o Coolant flow rate-low o H-X inlet temp-high
7.Coolant Filter	A.Leakage	-Same as 1A	-Same as 1A-	-Same as 1A-	-Same as 1A-	-Same as 1A-
	B.Flow Restriction	o Contamination	o Coolant bypass around filter via relief valve o Slight coolant flow reduction o Slight Pump ΔP Increase	o No significant effect on coolant system performance unless the following failure modes are subsequently encountered: 1B, 2B, 3C, 4C, 8B	o Relief valve position - open o Relief valve ΔP - high	o None

FIGURE 16 (Continued)
ACTIVE COOLING SYSTEM FAILURE MODES AND EFFECTS

Item	Failure Mode	Failure Cause(s)	Failure Effect(s)	Severity of Failure	Primary Failure Detection	Corrective Action
8.H-X Relief Valve	A.External Leakage	-Same as 1A-	-Same as 1A-	-Same as 1A-	-Same as 1A-	-Same as 1A-
	B.Internal Leakage	o Contamination o Material degradation o Corrosion o Overstress	o Increased panel inlet temp o Increased H-X inlet temp o High panel skin temp	o Function of leakage rate	o Panel inlet temp-high o H-X inlet temp-high	o Abort if two cues are indicated o Panel inlet temp-high o H-X inlet temp-high
9.Overboard Relief Valve	A.Leakage	o Material degradation o Corrosion o Overstress	-Same as 1A-	-Same as 1A-	-Same as 1A-	-Same as 1A-

FIGURE 16 (Concluded)
ACTIVE COOLING SYSTEM FAILURE MODES AND EFFECTS

For the baseline cooling system described by Figure 17, coolant reservoir volume requirements were determined as a function of the range of bulk coolant temperatures expected on the ground and in flight (Figure 18). As shown, designing to an extremely low minimum coolant temperature requires the maximum reservoir volume, due to coolant expansion at the maximum temperature. However, designing to accommodate these large changes results in a penalty to the aircraft. The only time extremely low coolant temperatures are expected to be encountered are during subsonic operation at high altitude and during cold day ground operation. The active cooling system would not be required to operate under those conditions. Thus, a range of 241 K to 380 K (-25°F to +125°F) was assumed requiring a coolant reservoir volume of 0.85 m^3 (30.0 ft^3), i.e., empty at 241 K (-25°F) and full at 380 K (+125°F).

In order to provide additional failure detection cues, dual reservoirs, with unequal volumes and pressure levels, were assumed. Reservoir #1 was sized for a volume of 0.79 m^3 (28 ft^3) and 276 k Pa (40 lbf/in^2) absolute pressure. Reservoir #2 was sized for 0.057 m^3 (2.0 ft^3) and a pressure of 138 k Pa (20 lbf/in^2) absolute. With this arrangement, Reservoir #1 would accommodate system coolant expansion/contraction and control pump inlet absolute pressure to 276 k Pa (40 lbf/in^2) during normal situations. Reservoir #2 would remain full unless average coolant temperature drops to an abnormal 257 K (3°F) (average normal coolant temperature during flight is approximately 272 K to 278 K (30°F to 40°F)) or a system leak occurs which depletes Reservoir #1.

Reservoir #2 was sized to provide sufficient coolant to sustain a leakage rate of 1.64 kg/s (3.62 lb/sec) for 30 seconds. This leakage rate corresponds to a clean break in one of the 8.64 mm (0.34 in.) dee tubes and a pump ΔP of 689 k Pa (100 lbf/in^2).

The system response was evaluated in terms of elapsed time between a failure and coolant system flow reduction. Figure 19 illustrates, as a function of leak rate, the time to deplete Reservoirs #1 and #2. It would appear that the flight crew would be provided with an indication of coolant leakage in sufficient time to take corrective action unless the leak rate were signficantly higher than those assumed.

- FLIGHT CONDITIONS
  - Cruise Altitude - 32 km (105,000 ft)
  - Cruise Mach No. - 6
  - Flight Duration ~ 106 Minutes
    - Climb - 14 Min
    - Cruise - 68 Min
    - Descent - 24 Min

- ACTIVE COOLING SYSTEM PARAMETERS
  - 60/40 Methanol/H_2O Coolant
  - Total Heat Load = 90.2 MW (308 x 10^6 Btu/hr)
  - Total Coolant Flowrate = 712 kg/s (5.65 x 10^6 Lbm/hr)
  - Coolant Pump $\Delta P \approx$ 689 kPa (100 psid)
  - Coolant Temp - 255K (0°F) Delivery, 291K (65°F) Return
  - Parallel Coolant Flow Delivery/Return Lines:
    - Fuselage - Fore and Aft, Each Side
    - Wings - Each Wing
    - Vertical Tail
  - Cooling System Weight — 13726 kg (30260 lbm)
    - Coolant in Panels — 1751 kg (3860 lbm)
    - Coolant in Lines — 7170 kg (15807 lbm)
    - Heat Exchanger — 947 kg (2088 lbm)
    - Pumps — 263 kg (580 lbm)
    - Lines, Connectors & Misc. — 1346 kg (2967 lbm)
    - H_2 to Drive Pumps — 2249 kg (4958 lbm)

- ACTIVELY COOLED PANEL PARAMETERS:
  - Total Panel Surface Area = 2985 m^2 (32134 ft^2)
  - Range of External Heating Rates = 12 to 108 kW/m^2 (1.1 to 9.5 Btu/sec ft^2)
  - Average External Heating Rate = 30 kW/m^2 (2.66 Btu/sec ft^2)
  - Typical Active Cooled Panel:
    - Size - 1.2 m (4 ft) Wide x 6.1 m (20 ft) Long
    - Coolant Tubes - 8.64 mm (0.34 in.) ID Al. D-Tube, 0.89 mm (0.035 in.) Wall
    - External Skin - 0.635 mm (0.025 in.), 1.02 mm (0.04 in.), 1.27mm (0.050 in.), or 1.6 mm (0.063 in.) Al. Skin
    - Max Design Skin Temp - 394K (250°F)
    - Parallel Coolant Tubes Manifolded at Each End

FIGURE 17
CHARACTERISTICS OF BASELINE AIRCRAFT/COOLING SYSTEM (AIRCRAFT CONCEPT 3 OF REFERENCE 2 STUDY)

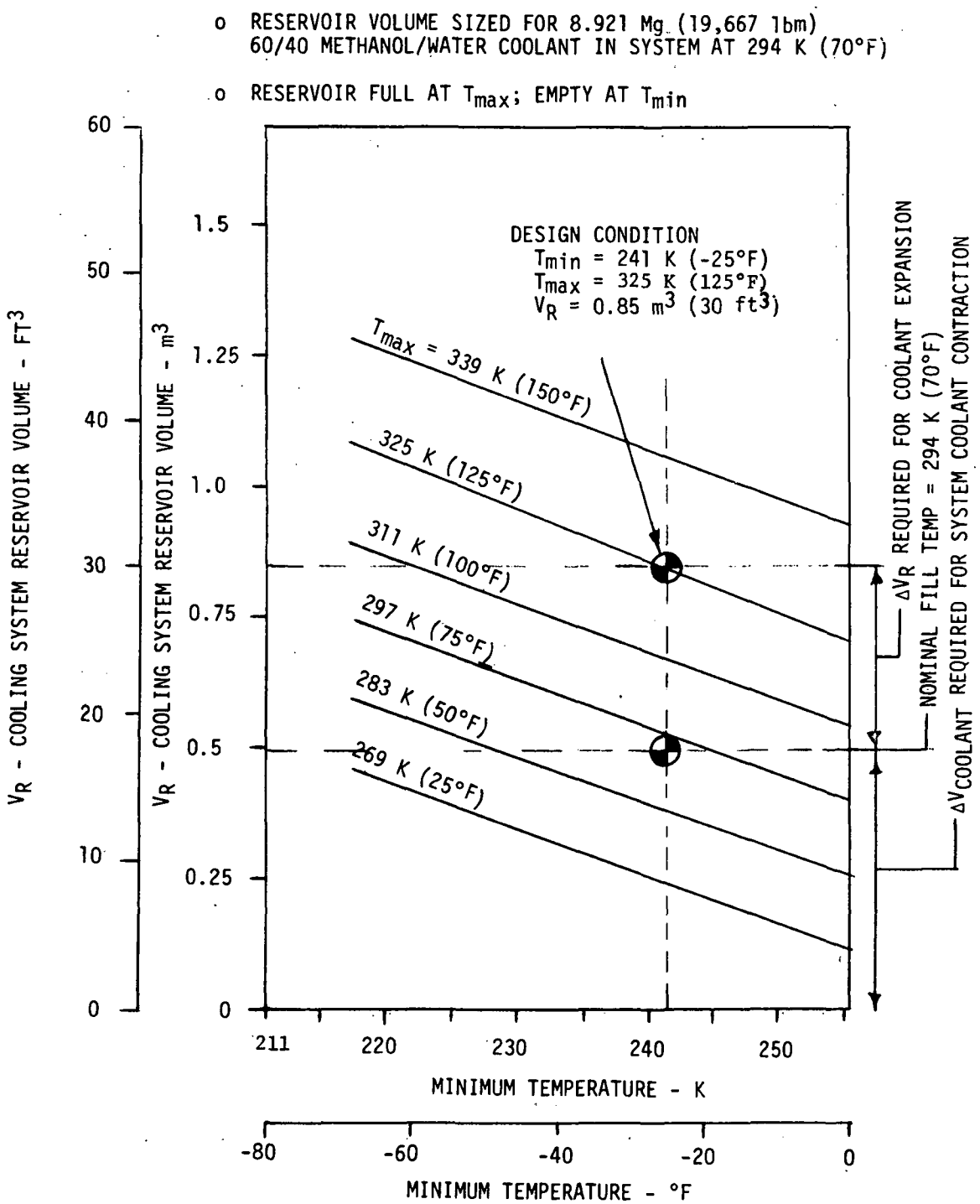

FIGURE 18
COOLANT RESERVOIR VOLUME FOR BASELINE SYSTEM

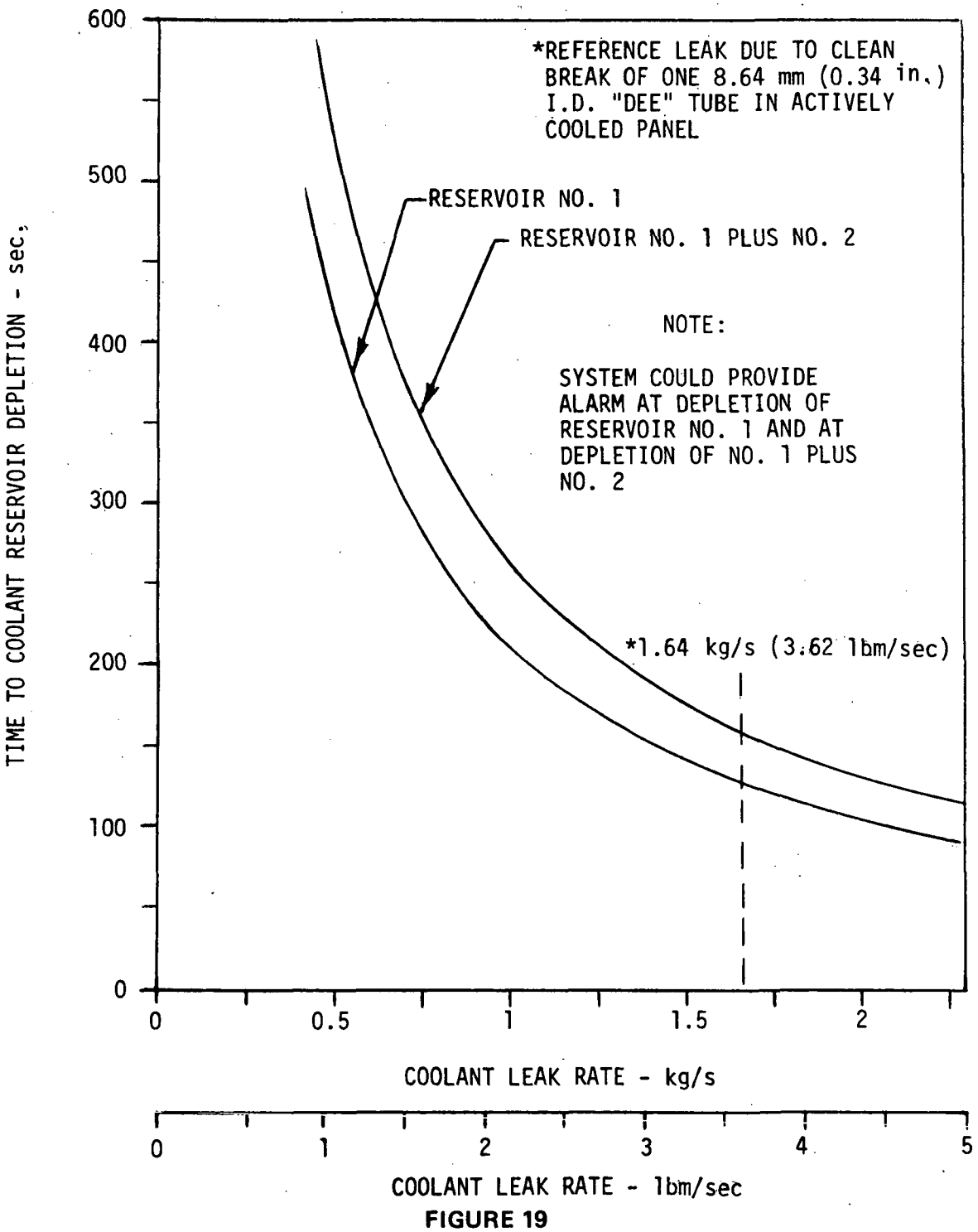

FIGURE 19
COOLANT RESERVOIR RESPONSE TO COOLANT TUBE LEAKAGE

o Clogged Coolant Passage - The temperature rise which occurs with a clogged tube is a function of the degree of flow restriction and the panel design parameters (i.e., external heating rate, tube spacing, and skin thickness). Parametric analyses were made defining combinations of tube spacing (pitch) and aluminum skin thickness required to limit temperatures to 394 K (250°F) at various sustained external heating rates (Figure 20). The maximum expected heating rate is approximately 108 kW/m^2 (9.5 Btu/ft^2 sec). Additional panel heat capacity which would be required for a fail-safe abort design was not included at this time. With a 100 percent clogged tube, the adjacent tubes must handle approximately 50 percent more heat load, which increases coolant temperature at the panel exit. The effective spacing between active tubes is doubled, resulting in a much larger temperature gradient in the skin, and a higher ΔT then occurs between the coolant and the skin. For the baseline panel, peak skin temperatures of 644 K to 700 K (700°F to 800°F) would be experienced. This could result in structural failure if undetected.

Peak skin temperatures resulting from reduced coolant flowrate are presented in Figure 21. The reason for higher peak temperatures for the thicker skin is the larger ΔT between the coolant and skin. Initial flowrate must be higher, and therefore thermal conductance decreases at a greater rate for the same percent reduction in coolant flowrate. Local coolant temperature at the panel exit is independent of skin thickness while panel skin temperature gradients are independent of coolant flow reduction over the range indicated by Figure 21. For the particular panel design assumptions, it is shown that a flowrate reduction to 50 percent of normal will not cause skin temperature to exceed 455 K (360°F). Skin temperatures resulting from constriction of a single tube should not be quite as high as those of Figure 21 because of conduction to adjacent tubes.

A 50 percent reduction in flowrate implies a substantial dent. This is illustrated by Figure 22, which shows that a 50 percent flow reduction requires a blockage of 85 percent of the tube area. This large a dent would be detected by ground inspection, and the D-tube honeycomb type panel would offer substantial protection from a dent of this magnitude in flight.

One might consider reducing the tube spacing or increasing the skin thickness to limit peak skin temperature to a tolerable level (e.g., 478 K (400°F)) in case of a 100 percent clogged tube (Figure 23). However, if the

actively cooled panel were designed to absorb the heating encountered with a clogged tube, the panel, and cooling system, weight would increase. This, in effect, would be comparable to a redundant system.

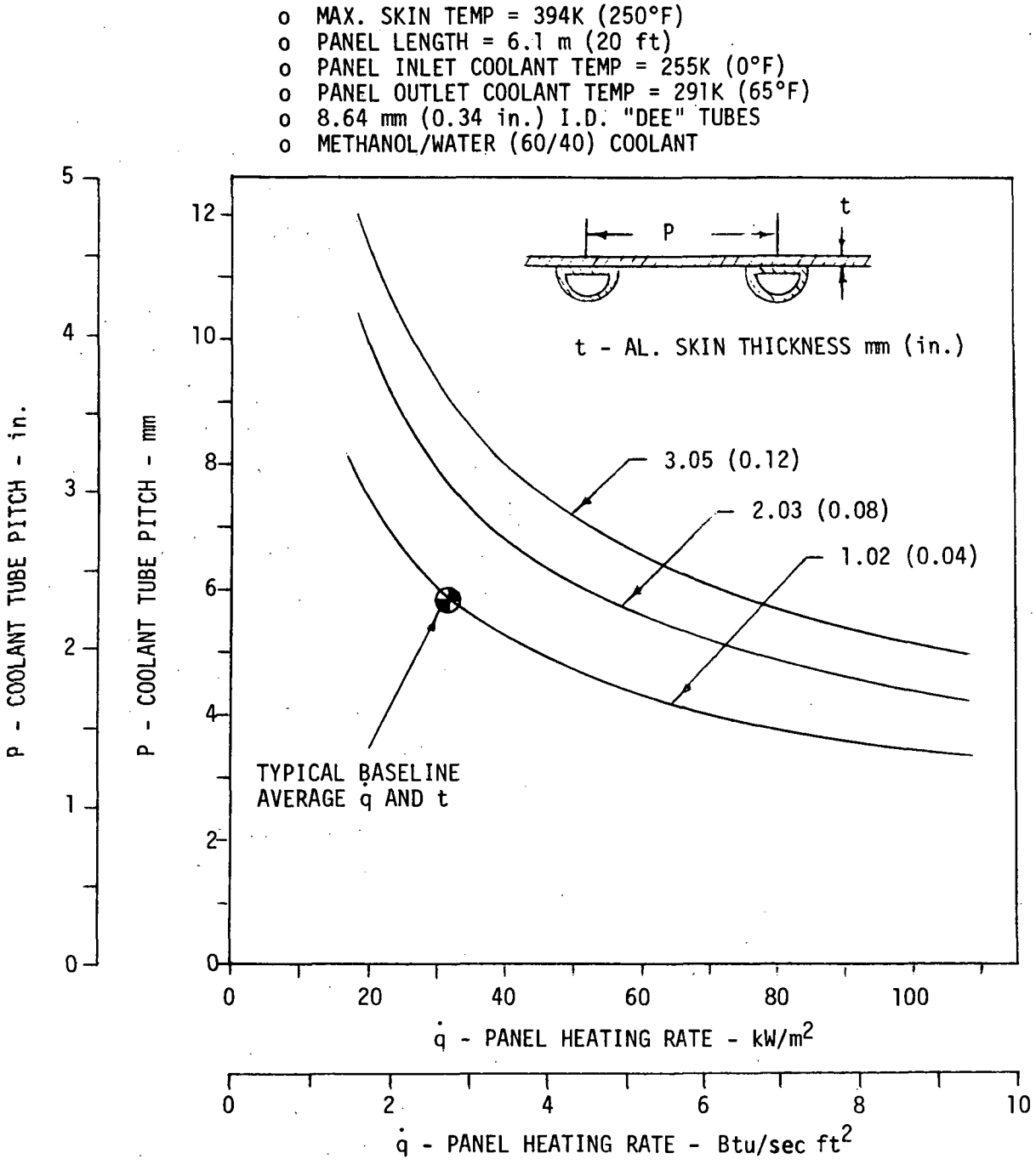

FIGURE 20
ACTIVELY COOLED PANEL DESIGN PARAMETERS

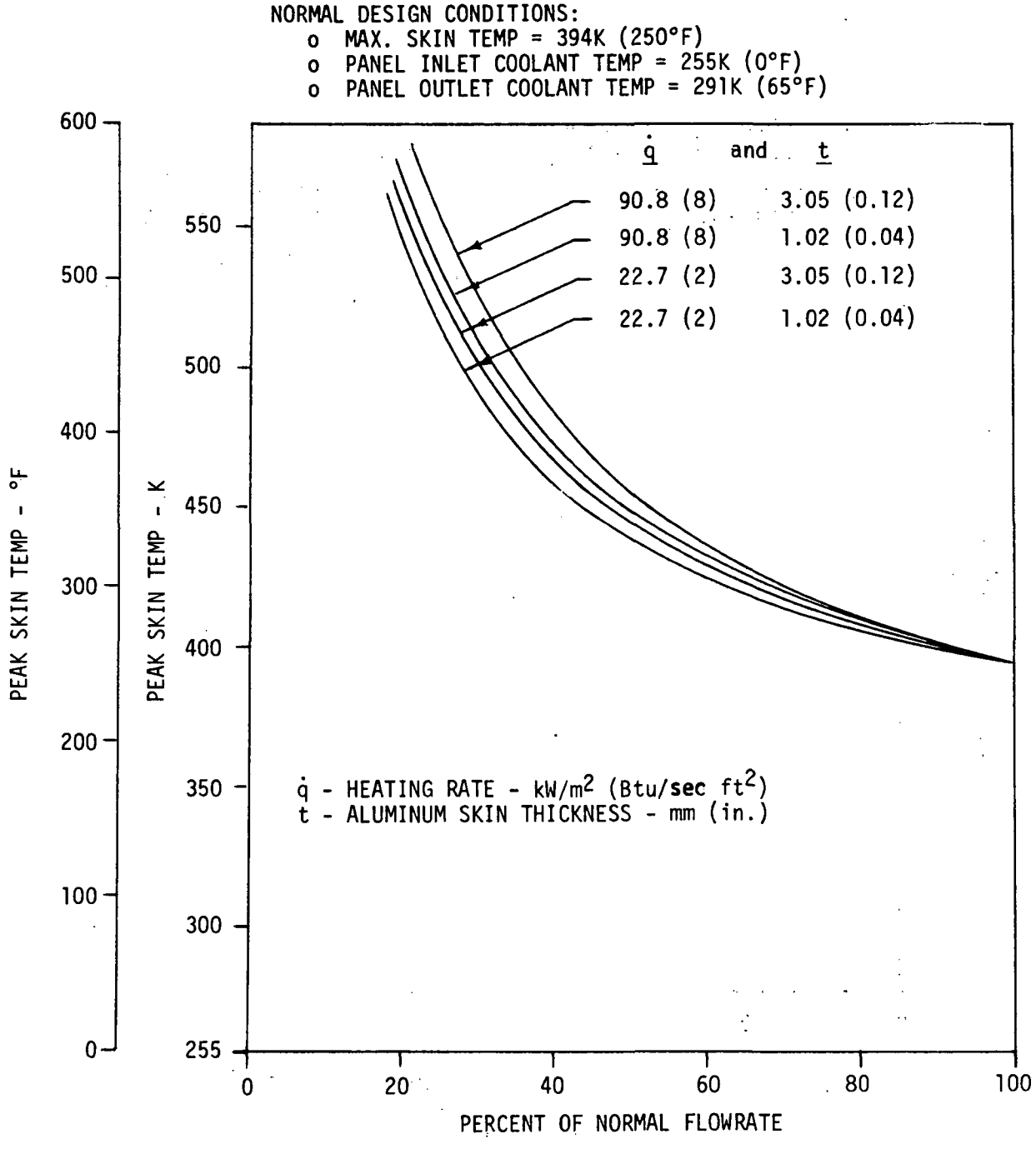

FIGURE 21
ACTIVELY COOLED PANEL PEAK SKIN TEMPERATURE DUE TO REDUCED COOLANT FLOWRATE
Steady State Operation

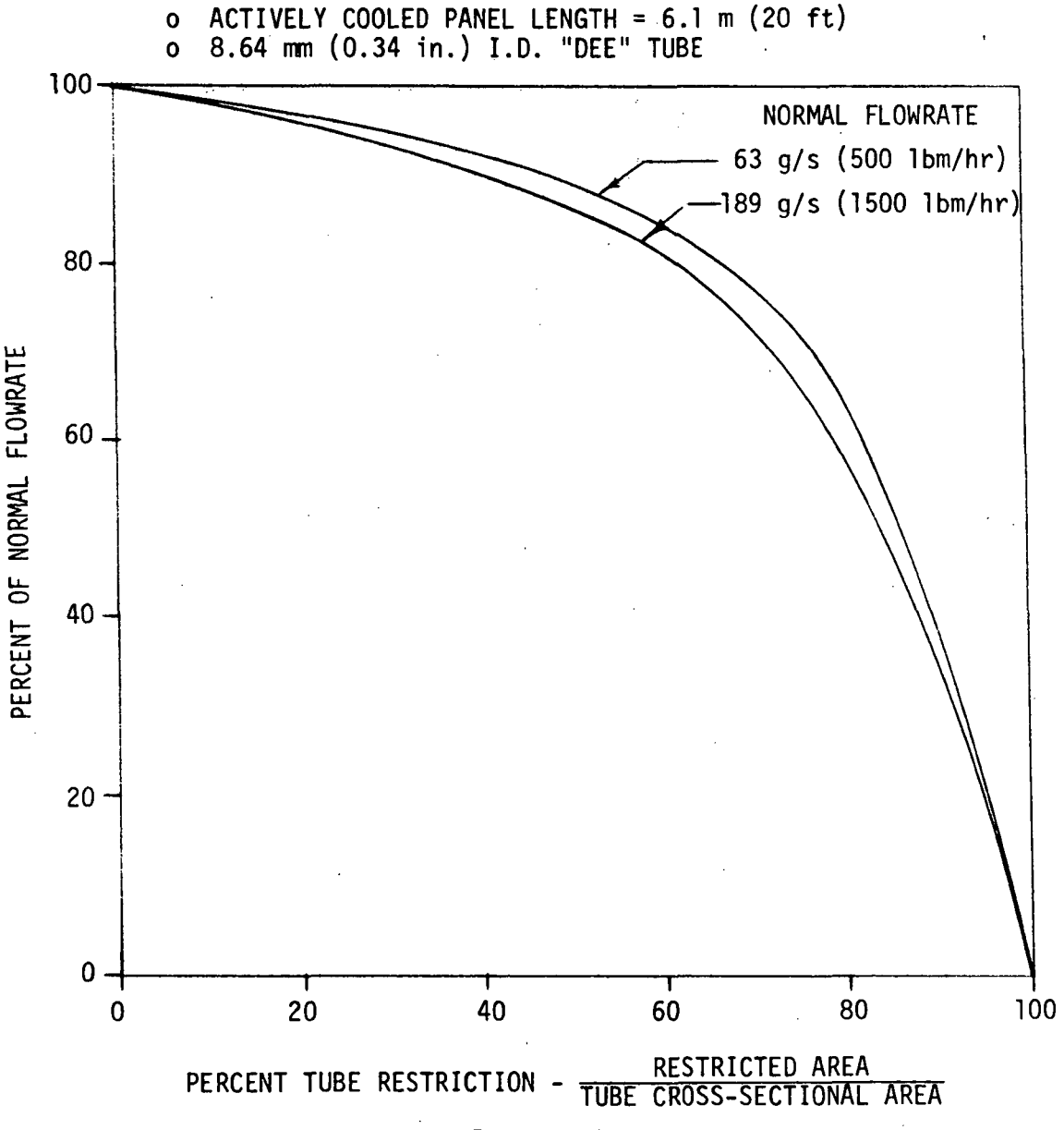

FIGURE 22
COOLANT FLOW RATE REDUCTION DUE TO TUBE RESTRICTION

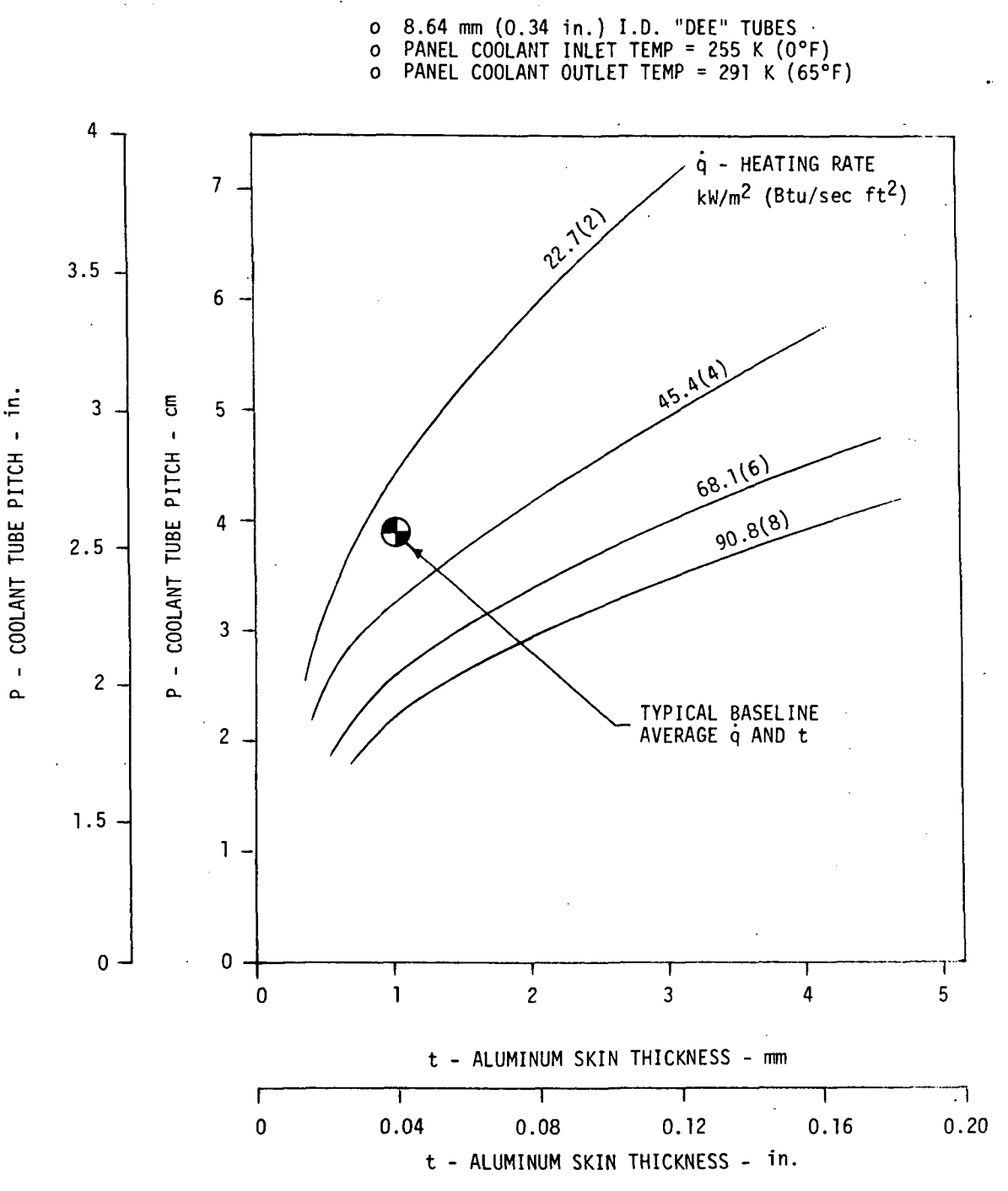

FIGURE 23
SKIN THICKNESS AND COOLANT TUBE PITCH REQUIRED TO LIMIT PEAK TEMPERATURE TO 478 K (400°F) WITH ONE TUBE BLOCKED 100%

4.1.3 Methods of Failure Detection - Figure 24 presents candidate failure detection methods for the failure modes identified for the active cooling system. Failure cues are shown in a manner to indicate the sequence in which they would be expected to occur, thus suggesting primary failure detection methods which allow the most time for reaction.

Conventional instrumentation (i.e., pressure and temperature sensors, flowmeters, etc.) can satisfactorily be employed for detecting most system failures. However, detection of flow restriction of individual tubes within a panel by these methods presents significant practical problems because of the large numbers (over 400 - 1.2 m by 6.1 m (4 ft by 20 ft)) of panels.

However, this type of failure would essentially have no effect on any other measurable system parameters (i.e., coolant flowrate, ΔP, or temperatures of the overall coolant system or even of an individual panel). Thus, some type of conventional failure detection device is required. The failure must be isolated to one panel, or even to a part of a panel, without producing a discernible effect on the remainder of the system.

Preflight detection of clogged tubes might be achieved by visual inspection for dents or use of some method such as Thermovision (infrared scanning) for identifying internal restrictions. However, detecting a restricted coolant tube or a debonding of the tube from the skin requires sensing the panel local skin temperature either directly or indirectly.

Figure 25 illustrates a number of approaches to in-flight sensing of panel "hot spots". The problem requires both fast response time and the capability to survey a large surface area with a small number of sensors. Sensors in contact with the panel skin are subjected to all of the practical problems associated with the use of more conventional temperature sensors. A vast network would be required and would result in a highly complex system.

One of the study guidelines was to consider detection of local "hot spots" a primary concern. Therefore, the list of schemes shown in Figure 25 was expanded to include as many approaches as possible. These approaches were grouped into three major categories: Contact Thermometry, Radiation Thermometry, and Released Mass Sensing.

a. Contact Thermometry - Discrete point sensors and area coverage sensors were both considered for contact thermometry. Discrete point sensing involves the use of a large number of sensors. The fast detection of a

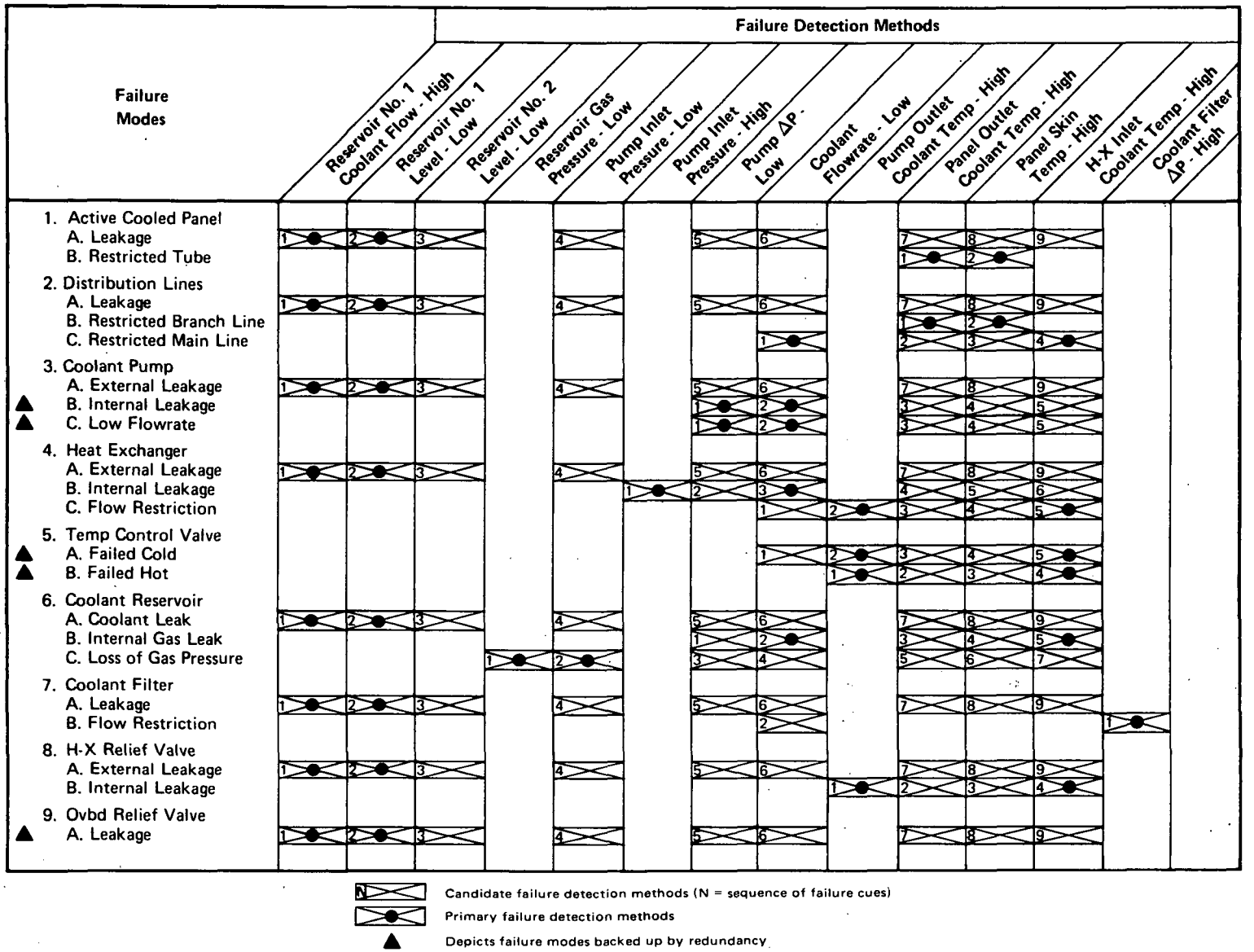

FIGURE 24
METHODS OF ACTIVE COOLING SYSTEM FAILURE DETECTION

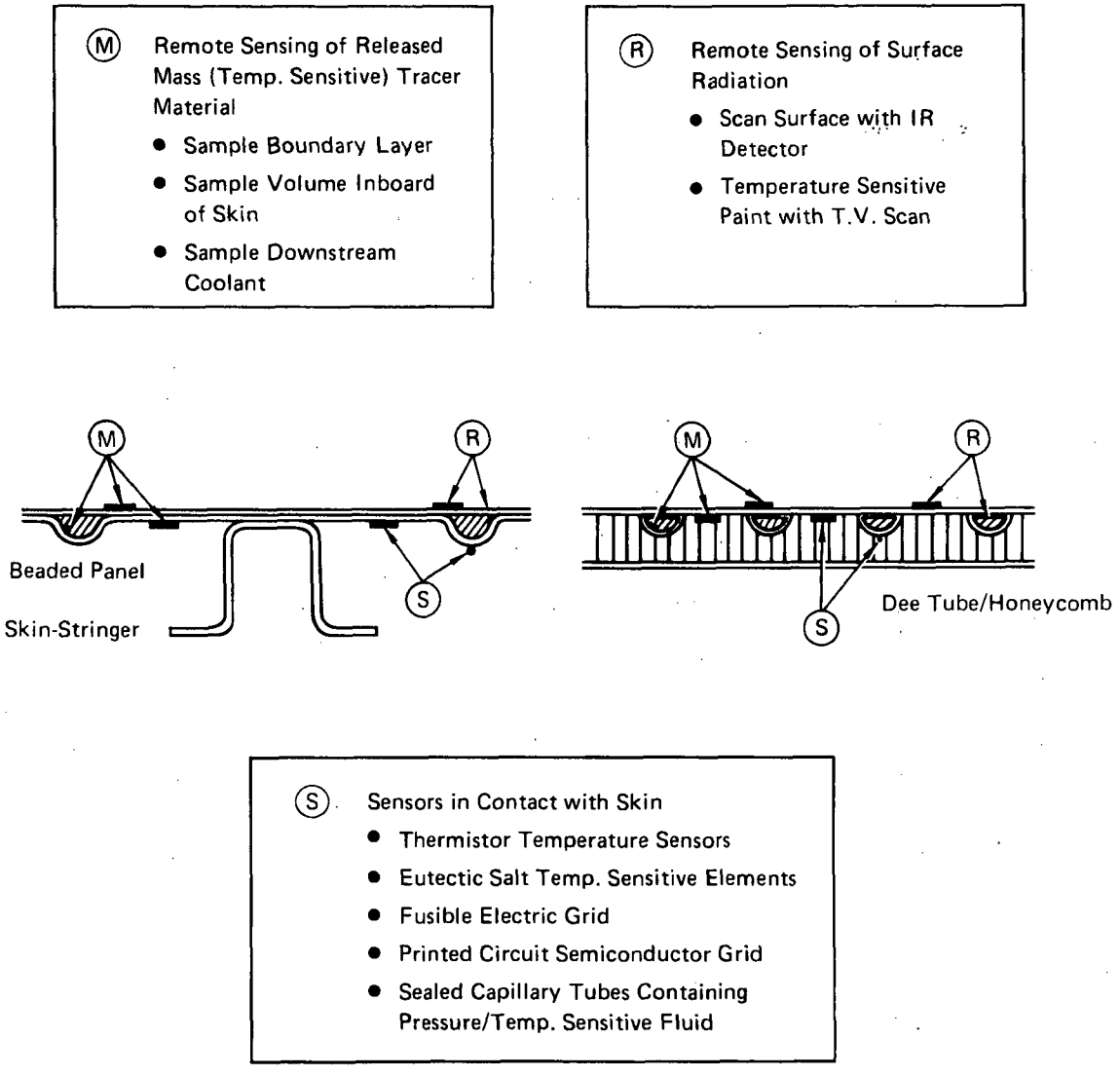

FIGURE 25
ACTIVELY COOLED PANEL SKIN TEMPERATURE SENSING METHODS

critical out-of-tolerance overtemperature condition requires spacing the sensors on the order of one half of the coolant tube pitch. Thus, for a typical 1.2 m by 6.1 m (4 ft by 20 ft) panel, and coolant tubes running lengthwise with a 10.2 cm (4 inch) pitch, 12 rows of sensors, or 1440 sensors per panel, would be required.

Thermistors, thermocouples, thermal fuses, bimetal actuators, thin-film capacitors, thin-film resistors, paired transistors, etc., all have the

potential for use as discrete point sensors. However, solid state, integrated circuit, electronic devices also have the potential for detection of temperature change. The use of printed circuits and semiconductor technology could result in fast response, low weight systems. For example, chips containing a circuit that gives a repeatable, and predictable, change in signal output with change in temperature would be a viable candidate.

Surface contact sensors that can provide coverage of a large area, such as an individual panel, include eutectic salt temperature sensitive elements, fusible metal alloy electrical circuit grids, and sealed tube elements containing fluids.

The eutectic salt temperature sensitive elements are used in current aircraft for engine compartment fire warning and engine bleed air leak detection. Melting of the eutectic, changes the resistance of the element and the magnitude of the voltage signal. Dual sensing elements are normally used, to prevent false warnings due to shorts. Elements are available with a set point temperature of 403 K (265°F).

Temperature sensitive elements based on thermistor technology are also used as fire detection systems. These consist of a metal tube sheath containing a ceramic-like thermistor material in which are embedded the electrical conductors. The thermistor changes its electrical resistance between conductors as a function of temperature. These sensors are averaging devices, however, and do not appear to have high potential to detect "hot spots".

Fusible metal alloys may be used as discrete point fuses or as area coverage grids. A number of eutectic alloys with melting points in the range of interest are available. For example, an alloy with a composition of 55.5% bismuth 44.5% lead (by weight) melts at 397 K (255°F). A composition of 58% bismuth and 42% tin melts at 411 K (281°F). The eutectic alloy of 30.6% lead, 51.2% tin, and 18.2% cadmium melts at 415 K (288°F). Other alloys are available that melt in the range from 417 K (291°F) up to 472 K (390°F).

Sealed tube elements containing fluids offer some interesting possibilities. Thermal expansion of a liquid in a small diameter tube is one such approach. The tube must be small enough to exhibit a significant change in the length of the liquid mass. The change in length could be detected by a transducer. The phase change of a high vapor pressure liquid contained in a tube element could also be utilized to provide detection of overtemperature

conditions. Small diameter tubing, containing the liquid at constant pressure in a subcooled or saturated liquid state, would be installed with good thermal contact to the panel skin. If the heat input is greater than heat loss due to conduction and convection, the liquid would boil, raising the pressure. A transducer would provide a signal of the pressure change. A liquid reservoir would be required to accommodate thermal expansion of the liquid and maintain constant system pressure during operation at normal conditions.

b. Radiation Thermometry - The change in the electromagnetic emission of a panel with a change in surface temperature could also be used to detect "hot spots". Infrared scanning of the aircraft surfaces to detect these changes is a possible approach.

Another approach is the use of a surface coating which changes reflectance with changes in temperature. This surface, if illuminated and optically scanned to provide input to a photocell, would clue the location and magnitude of an out-of-tolerance temperature.

A third technique would be use of thermographic phosphor surface coatings illuminated with ultraviolet radiation. The phosphor brightness is dependent upon the surface temperature. Optical scanning and photocells could detect changes in phosphor brightness.

c. Released Mass Sensing - Remote sensing of a released mass (i.e., a temperature sensitive release of a tracer material is another possibility. This can be approached in several ways. A tracer material released from a temperature sensitive surface coating and seeding the external boundary layer is one approach. Sampling probes for mass spectrometers would be located downstream of the areas to be monitored.

Another scheme is the use of a temperature sensitive release of a detectable material within the coolant. Radioisotopes are a possibility. A thin coating of radioactive material would be used on the internal surface of the coolant tubes. Localized overtemperature would release the tracer which would be detected by geiger counters or ionization cells.

4.1.4 Evaluation of Failure Detection Methods - A wide range of failure detection methods was evaluated to determine the best overall approaches, based on system characteristics. The study of the baseline cooling system (Section 4.1.1 through 4.1.3) did not result in any unique instrumentation

requirements. Figure 26 lists failure detection system discrete parameters and onboard crew display parameters for active cooling system monitoring. It was judged that conventional instrumentation can be used to obtain these parameters with minute impact on cooling system weight and no significant impact on cooling system cost. Therefore, the primary effort was directed toward methods for detecting "hot spots" in individual panels.

o Evaluation of Panel "Hot Spot" Detection Methods - The evaluation criteria were cost (complexity and ease of integration and installation), reliability (complexity), relative weight, and response time. The first step in the evaluation was to screen the available approaches within the three general method categories (contact thermometry, radiation thermometry, and released mass sensing) to identify the more promising approaches.

Two levels of screening were conducted. The first level considered basic feasibility. In the second level the development status, integration and installation complexity, and the risk and expected payoff were assessed.

a. Contact Thermometry - First Level Screening

o Thermistors - State-of-art metallic oxide "thermal resistors" are in widespread use in temperature control and overheat detection applications. Their resistance coefficient is generally negative (resistance decreases with increasing temperature). They are available as beads, disks, or rod type elements. Their hard ceramic-like structure will be subject to severe thermal stress, vibration and shock and may not be rugged enough for application to aircraft skin. This approach was considered marginal, but was retained for second level screening.

o Thermocouples - These devices are state-of-art instrumentation and are in widespread use in temperature measurement and control applications. Generally, they are more rugged than thermistors. Their EMF characteristics are subject to change due to oxidation or alloying with environmental contaminants. They will require a reference junction to obtain accurate temperature measurements. This method was retained for second level screening.

o Thermal Fuse - Thermal fuses are state-of-art and in use as fire detection and overheat protection devices. The sensor is destroyed by the detection process. They could be configured as an electrical grid over panel skin, with the most likely application to skin-stringer structure. They are not practical for honeycomb panels. Marginal, but retained.

SYSTEM FAILURE DISCRETE PARAMETERS (1)	ONBOARD DISPLAY INSTRUMENTATION PARAMETERS (2)
H-X INLET COOLANT TEMP - HIGH	H-X INLET COOLANT TEMP
	H-X OUTLET COOLANT TEMP
	AUX. EQUIP. INLET COOLANT TEMP
	PUMP INLET COOLANT TEMP
PUMP OUTLET COOLANT TEMP - HIGH	PUMP OUTLET COOLANT TEMP
PANEL OUTLET COOLANT TEMP - HIGH	PANEL OUTLET COOLANT TEMP
PANEL SKIN TEMP - HIGH	PANEL SKIN TEMP
PUMP INLET PRESSURE - LOW	PUMP INLET PRESSURE
PUMP INLET PRESSURE - HIGH	H-X OUTLET H_2 TEMP PUMP INLET FILTER ΔP PUMP OUTLET FILTER ΔP
PUMP ΔP - LOW	COOLANT PUMP ΔP
RESERVOIR #1 FLOW RESTRICTOR ΔP - HIGH (HI-FLOW) RESERVOIR #1 GAS PRESSURE - LOW	RESERVOIR #1 FLOW RESTRICTOR ΔP RESERVOIR #1 GAS PRESSURE RESERVOIR #2 GAS PRESSURE RESERVOIR GAS SUPPLY REGULATOR INLET PRESSURE
	H_2 PUMP ΔP
COOLANT FLOWRATE - LOW RESERVOIR #1 LEVEL - LOW RESERVOIR #2 LEVEL - LOW	COOLANT FLOWRATE RESERVOIR #1 LEVEL RESERVOIR #2 LEVEL
	H-X BYPASS RELIEF VALVE POSITION H_2 FLOW SELECTOR VALVE POSITION COOLANT PUMP 1 RPM COOLANT PUMP 2 RPM H_2 FLOWRATE

(1) DISCRETE PARAMETERS INPUT TO FAILURE DETECTION SYSTEM
(2) ONBOARD CREW DISPLAY FOR SYSTEM MONITORING AS BACKUP TO FAILURE DETECTION SYSTEM. HELPFUL IN FAULT ISOLATION.

FIGURE 26
ACTIVE COOLING SYSTEM INSTRUMENTATION

o Bimetal Actuators - State-of-art devices which are rugged but heavy. Retained.

o Thin-Film Resistors - State-of-art devices which provide a fast response to temperature change. Retained.

o Thin-Film Capacitors - These sensors showed no apparent advantage over thin-film resistors and were rejected.

o Paired Transistors - A new technique which changes EMF output as a function of temperature. They offer high accuracy and fast response to temperature change. Reliability is questionable in the considered application due to the high temperature environment (394 K (250°F) normal operation to as high as 478 K (400°F)). Marginal, but retained.

o Advanced Semiconductor Integrated Circuit Devices - This approach would require a chip circuit that changes EMF characteristics as a function of temperature. Reliability is questionable due to the high temperature environment (394 K (250°F) normal operation to as high as 478 K (400°F)). They must be able to cope with thermal stresses, vibration, and shock environments. The approach was considered very marginal and rejected until paired transistors were further screened. The paired transistor technique uses an integrated circuit and the application would be equivalent.

o Eutectic Salt Elements - These are state-of-the-art devices. The elements are rugged but subject to electrical shorts in some installations. Retained for additional evaluation.

o Fluid Filled Tube Elements - This is a new application of vapor pressure thermometry and fluid thermal expansion thermometry. This approach has the potential for a rugged system, with the capability for continuous readout of panel temperature. Retained for additional evaluation.

b. Radiation Thermometry - First Level Screening

o Infrared Scanning - A state-of-art technique which has high sensitivity and fast response. Retained.

o Visible Wave Length Scanning - A state-of-art technique which is in use in a number of pattern recognition applications such as fingerprint identification, food packaging, pricing and inventory control, scan of temperature sensitive coatings on wind tunnel models, etc. Retained for additional screening, but considered marginal due to requirement for illumination.

o Ultraviolet Scanning - A state-of-art technique used in temperature distribution detection for wind tunnel models. The technique is based on ultraviolet illumination of thermographic phosphor coating. Retained for additional screening.

c. Release Mass Sensing - First Level Screening

o Tracer Material Release from Surface Coat - This is a very marginal technique due to material availability, and the inherent complexity of the aircraft flow field. This method was carried to second level screening but was not considered a prime candidate.

o Tracer Material Release Within Coolant Tube - This approach appeared to have more potential than the release of tracer material into the aircraft boundary layer or into the internal volume behind a panel. Therefore, it was retained.

d. Contact Thermometry - Second Level Screening - Figure 27 presents the results of additional screening for discrete point sensors. As shown, all discrete point sensors were rejected during the second level screening, even though the sensors were state-of-the-art, and would provide fast response to failure (the majority would provide real time continuous monitoring of panel temperatures). The method was judged impractical because of the vast number of sensors required. For example, the requirement for a discrete point sensor at the critical spacing of one half the typical tube pitch results in 18 sensors per square foot of cooled area, or 578,412 sensors for the baseline aircraft. Even if the number of sensors could be reduced to one third of this requirement, nearly 200,000 sensors and 400,000 wiring connections are still required. Each sensor and wiring connection is absolutely vital to insure detection of an actively cooled panel "hot spot" which could lead to structural failure. The sheer numbers of sensors and electrical connections required (coupled with the requirement for extremely high reliability and long life in a severe shock, vibration, temperature cycling and stress environment) cannot be ignored. The number of opportunities for failure of a discrete point sensor system is enormous and therefore this approach was rejected.

Figure 28 presents the results of a screening of area coverage sensors useful for contact thermometry. The probability of success is more favorable

APPROACH	DEVELOPMENT STATUS	INTEGRATION - INSTALLATION COMPLEXITY	APPROACH RISK/PAYOFF	RETAIN/ REJECT
(A) THERMISTORS	(A) STATE OF ART	(A) HIGH COMPLEXITY DUE TO LARGE NUMBER OF SENSORS AND LARGE NUMBER OF PARALLEL CIRCUITS. TYPICAL 1.2M X 6.1M (4 FT X 20 FT) PANEL REQUIRES 1440 SENSORS FOR COOLANT TUBE PITCH OF 10.2 CM (4 INCHES). WOULD RESULT IN SIGNIFICANT INCREASE IN PANEL FABRICATION COST.	(A) HIGH RISK DUE CRITICAL NATURE OF LARGE NUMBER OF SENSORS. LOSS OF ANY ONE SENSOR COULD VOID CAPABILITY TO DETECT "HOT SPOT" OR SLOW RESPONSE TIME. PAYOFF IN CAPABILITY HIGH IF HIGH RELIABILITY COULD BE OBTAINED. WITH THIS NUMBER OF SENSORS IT IS EXTREMELY UNLIKELY TO ACHIEVE DESIRED RELIABILITY.	(A) REJECT
(B) THERMO-COUPLES	(B) STATE OF ART	(B) SAME AS ABOVE.	(B) SAME AS ABOVE.	(B) REJECT
(C) THIN-FILM METALLIC RESISTANCE THERMOMETERS	(C) STATE OF ART	(C) SAME AS ABOVE.	(C) SAME AS ABOVE.	(C) REJECT
(D) PAIRED TRANSISTORS	(D) STATE OF ART	(D) HIGH COMPLEXITY. REQUIRES PAIR OF HIGHLY MATCHED MONOLITHIC TRANSISTORS FOR EACH SENSING POINT. ELIMINATES NEED FOR LINEARIZING CIRCUITS OR REFERENCE JUNCTIONS. WOULD RESULT IN SIGNIFICANT INCREASE IN PANEL FABRICATION COST.	(D) SAME AS ABOVE.	(D) REJECT
(E) BIMETAL ACTUATORS OR	(E) STATE OF ART	(E) MODERATE COMPLEXITY. SERIES CIRCUITS. STILL REQUIRES 1440 SENSORS. HIGH FABRICATION COST. HIGHER WEIGHT THAN (A),(B),(C),(D).	(E) RISK SAME AS ABOVE. PAYOFF LESS THAN ABOVE.	(E) REJECT
(F) THERMAL FUSES (FUSIBLE ALLOY)	(F) STATE OF ART	(F) MODERATE COMPLEXITY. SERIES CIRCUITS. 1440 SENSORS. HIGH FABRICATION COST. SENSOR DESTROYED BY OVERTEMP.	(F) SAME AS (E)	(F) REJECT

FIGURE 27
ACTIVELY COOLED PANEL "HOT SPOT" DETECTION METHOD SCREENING
Contact Thermometry - Discrete Point Sensors

APPROACH	DEVELOPMENT STATUS	INTEGRATION - INSTALLATION COMPLEXITY	APPROACH RISK/PAYOFF	RETAIN/REJECT
(A) EUTECTIC SALT ELEMENTS	(A) STATE OF ART	(A) DUAL SENSING ELEMENTS CONNECTED TO PANEL SKIN. TWO SERIES CIRCUITS. TYPICAL PANEL REQUIRES 149.4 m (490 ft) OF ⚠1 SENSING ELEMENTS. ELEMENTS RELATIVELY HEAVY COMPARED TO DISCRETE POINT SENSORS. MODERATE INCREASE IN PANEL COST.	(A) LOW RISK. MODERATE PAYOFF. RUGGED SYSTEM. SYSTEM CAN ONLY GIVE FAILURE INDICATION. CAN NOT PROVIDE CONTINUOUS RECORD OF PANEL TEMP. OR AID IN GROUND CHECKOUT.	(A) RETAIN FOR COMPARISON
(B) FUSIBLE METAL ALLOY ELEMENTS	(B) STATE OF ART	(B) 74.4 m (244 ft) OF SERIES ELECTRICAL GRID. SENSOR DESTROYED BY OVERTEMP. MODERATE INCREASE IN PANEL FABRI- ⚠2 CATION COST. WOULD REQUIRE REPLACEMENT OF PANEL IN CASE OF FAILURE	(B) LOW RISK. LOW PAYOFF.	(B) REJECT ⚠2
(C) FLUID FILLED TUBES (THERMAL EXPANSION OF FLUID)	(C) MODERATE DEVELOPMENT REQUIRED	(C) MORE COMPLEX THAN (A) OR (B) ABOVE. TYPICAL PANEL REQUIRES 240 SENSOR ELEMENTS. PANEL WEIGHT INCREASE MAY APPROACH (A) ABOVE. PANEL FABRICATION COST HIGHER THAN (A) OR (B) ABOVE. COULD RESULT IN CAPABILITY FOR CONTINUOUS MONITORING OF MAXIMUM PANEL TEMPERATURE.	(C) MODERATE RISK. HIGH POTENTIAL PAYOFF. CONTINUOUS RECORD OF PANEL TEMPERATURE AND AID IN GROUND CHECKOUT OF SYSTEM.	(C) RETAIN FOR COMPARISON
(D) FLUID FILLED TUBES (PHASE CHANGE)	(D) MODERATE DEVELOPMENT REQUIRED	(D) ONE SENSOR ELEMENT COVERS PANEL. LOW WEIGHT INCREASE COMPARED TO (A) AND (C) ABOVE. COULD RESULT IN CAPABILITY FOR CONTINUOUS MONITORING OF MAXIMUM PANEL TEMPERATURE.	(D) MODERATE RISK. HIGH POTENTIAL PAYOFF. SAME AS (C).	(D) RETAIN FOR COMPARISON

NOTE: ⚠1 ALL ESTIMATES OF SENSOR NUMBER OR LENGTH REQUIREMENTS BASED ON TYPICAL 1.2 m X 6.1 m (4 ft X 20 ft) PANEL.

⚠2 HONEYCOMB PANEL WOULD REQUIRE REPLACEMENT. SKIN/STRINGER PANEL DESIGN COULD BE REFURBISHED.

FIGURE 28
ACTIVELY COOLED PANEL "HOT SPOT" DETECTION METHOD SCREENING
Contact Thermometry - Area Coverage

than for the discrete point sensors. As shown in Figure 28, three approaches were retained for additional comparison.

During the initial screening, fusible metal alloy elements had been rejected. Overtemperatures in a honeycomb panel would destroy the fusible element and require replacement of the panel. These elements could be used with a skin-stringer panel design. If melted during an overtemperature condition, they could be replaced by removing the panel from the aircraft. The panel would be reusable. However, any failure which resulted in reduction of coolant flow, or in higher than normal coolant temperatures would require replacement of the fusible elements over large areas, or even over all of the cooled area of the aircraft. On this basis the fusible metal elements were rejected.

The eutectic salt elements and both types of fluid filled tube elements were retained. The eutectic salt elements offer a modest weight system with low risk. The fluid filled tube elements offer the lowest weight system. However, some development risk and cost is incurred.

e. Radiation Thermometry - Second Level Screening - Figure 29 presents the results of screening the radiation thermometry approaches. Infrared scanning was retained for additional comparison. Visible wavelength scanning was rejected because it was judged that present state-of-art temperature sensitive coatings do not have the durability required. Extensive research and development would be required, with no assurance of success. The aircraft surface monitored would require illumination and would therefore result in a more complex installation than for infrared scanning.

Ultraviolet scanning was rejected for the same reasons.

f. Released Mass Sensing - Second Level Screening - Figure 30 presents the results of screening the category of released mass sensing. As shown, all are rejected. First, extensive research and development would be required to determine surface coatings with the desired characteristics. A wide range of operating temperatures would have to be considered, due to basic differences in thermo-structural concepts (bare panels, overcoated panels, heat shielded panels, etc.). Extensive research and development would also be required to determine the location, number, and type of tracer material sampling probes. The probability of success appears extremely low.

APPROACH	DEVELOPMENT STATUS	INTEGRATION - INSTALLATION COMPLEXITY	APPROACH RISK/PAYOFF	RETAIN/ REJECT
(A) INFRARED SCANNING	(A) STATE OF ART FOR DETECTOR AND ELECTRONICS. EXTENSIVE DEVELOPMENT REQUIRED FOR OPTICS WITHIN HYPERSONIC ENVIRONMENT.	(A) REQUIRES MULTI-OPTICAL WINDOW LOCATIONS (FOUR WINDOWS TO SCAN APPROXIMATELY 47 PERCENT OF AIRCRAFT SURFACE). DUE TO LINE-OF-SIGHT PROBLEMS AND SURFACE TEMPERATURES RESPONSE-TO-FAILURE PROBLEMS CAN NOT BE USED TO MONITOR ALL SURFACE AREAS. NO INCREASE IN PANEL COMPLEXITY OR COST. SYSTEM USEFUL FOR GROUND CHECKOUT OF PANELS/ COOLING SYSTEM.	(A) HIGH RISK. MOUNTING OF WINDOWS REQUIRES EXTENSIVE DEVELOPMENT. HIGH POTENTIAL PAYOFF-POTENTIALLY HIGH ACCURACY AND SENSITIVITY, LOW WEIGHT.	(A) RETAIN FOR COMPARISON
(B) VISIBLE WAVELENGTH SCANNING (TEMPERATURE SENSITIVE COATING)	(B) STATE OF ART FOR DETECTORS (PHOTOCELLS) AND ELECTRONICS. EXTENSIVE DEVELOPMENT FOR DURABLE COATING AND WINDOWS FOR OPTICS WITHIN HYPERSONIC ENVIRONMENT.	(B) SAME TYPE OF LIMITATIONS AS ABOVE, EXCEPT BOUNDARY LAYER RADIATION NOT A PROBLEM. SURFACE COATING MUST BE REVERSIBLE AND REUSABLE. REQUIRES ILLUMINATION OF SURFACE FOR NIGHT OPERATION. MORE COMPLEX THAN (A).	(B) HIGH RISK. PAYOFF IN TERMS OF CAPABILITY NOT AS HIGH AS (A) ABOVE.	(B) REJECT
(C) ULTRAVIOLET SCANNING (ULTRAVIOLET ILLUMINATION OF THERMOGRAPHIC PHOSPHOR)	(C) SAME AS (B)	(C) MORE COMPLEX THAN (A) DUE TO REQUIREMENT TO ILLUMINATE SURFACE. SAME TYPE PROBLEMS AS (A) AND (B) IN REGARD TO LINE-OF-SIGHT AND TEMPERATURE RESPONSE OF MONITORED SURFACES. PANEL SURFACES REQUIRE COATING.	(C) HIGH RISK. PAYOFF SAME AS (B).	(C) REJECT

FIGURE 29
ACTIVELY COOLED PANEL "HOT SPOT" DETECTION METHOD SCREENING
Radiation Thermometry

APPROACH	DEVELOPMENT STATUS	INTEGRATION - INSTALLATION COMPLEXITY	APPROACH RISK/ PAYOFF	RETAIN/ REJECT
(A) TRACER MATERIAL RELEASE FROM SURFACE COATING	(A) EXTENSIVE RESEARCH AND DEVELOPMENT REQUIRED	(A) HIGH COMPLEXITY. MASS SPECTROMETERS UTILIZING SAMPLING PROBES TO DETECT TRACER. MAJOR DEVELOPMENT PROBLEMS KEYED TO SURFACE COAT MATERIAL SENSITIVITY TO TEMPERATURE (RATE OF TRACER RELEASE) AND LOCATION OF SENSOR PROBES. SURFACE COAT MATERIAL AND IMPACT ON PANEL WEIGHT AND COST UNKNOWN.	(A) EXTREMELY HIGH RISK. R&D COSTS EXPECTED TO BE HIGH WITH LOW PROBABILITY OF PAYOFF.	(A) REJECT
(B) TRACER MATERIAL RELEASE WITHIN COOLANT TUBE	(B) SAME AS (A)	(B) COMPLEXITY LESS THAN (A). POSSIBLE DEGRADATION OF HEAT TRANSFER TO COOLANT - SYSTEM WEIGHT PENALTY. CAN NOT DETECT TUBE DEBOND FROM PANEL EXTERNAL SKIN. CAN NOT DETECT PANEL OVERTEMP. DUE TO LOSS OF COOLANT. COULD DETECT REDUCTION IN COOLANT FLOW.	(B) HIGH RISK - LOW PAYOFF.	(B) REJECT

FIGURE 30
ACTIVELY COOLED PANEL "HOT SPOT" DETECTION METHOD SCREENING
Released Mass Sensing

Releasing a tracer material within the coolant tubes cannot detect all failure modes and would also require extensive research and development of materials. Degradation of heat transfer characteristics during normal operation due to the coating of the internal tube walls, is also highly probable, and would result in weight penalties. Thus, this approach is not considered a viable candidate.

g. Evaluation of Final Candidate Panel "Hot Spot" Detection Methods - The promising approaches surviving the two levels of screening were:

- o Eutectic salt elements (resistance change)
- o Fluid filled tube elements (thermal expansion)
- o Fluid filled tube elements (phase change)
- o Infrared Scanning (surface IR emission)

Figures 31 through 34 illustrate the candidate approaches. The eutectic salt elements can be installed as dual elements, as shown in Figure 31, or as single elements. Dual elements are normally used in present aircraft, to prevent false warnings due to element shorts. A signal from both elements is required before a warning signal is provided. The control unit can be reconfigured to operate with a single element signal. With proper quality control during manufacture and installation, the single element design should prove to have adequate reliability. A single element design would have faster response time due to the decrease in mass along the sensor routing.

Verification of the electronic circuitry by built-in-test (BIT) and press-to-test techniques is state-of-the-art and would be used for all the candidate systems to provide ground and in-flight checkout of the failure detection systems.

The four candidates were evaluated on the basis of cost (complexity and ease of integration and installation), reliability, relative weight, and response time. The cost factor was further broken down into initial and operating cost. Initial cost included panel fabrication cost and failure detection system cost (including research and development). Operating cost includes weight, damage resistance, inspectability, and maintainability. The reliability criterion was expanded to consider not only complexity, but also damage tolerance and inspectability. The response time criterion considered sensor characteristics such as the capability to continuously monitor panel temperature and the time required to respond to temperature change. Each evaluation criterion was assigned an importance factor and the concepts rated.

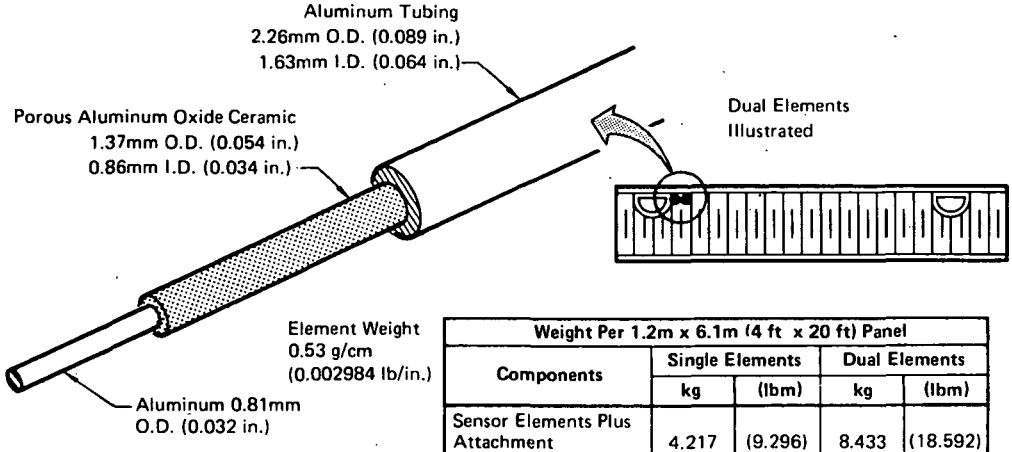

Voids Between Tubing, Ceramic and Wire and Porosity of Ceramic are Saturated with a Eutectic Salt Mixture.

Weight Per 1.2m x 6.1m (4 ft x 20 ft) Panel				
Components	Single Elements		Dual Elements	
	kg	(lbm)	kg	(lbm)
Sensor Elements Plus Attachment	4.217	(9.296)	8.433	(18.592)
Signal Processor	0.091	(0.200)	0.113	(0.250)
Connectors and Element End Fittings	0.045	(0.100)	0.091	(0.200)
Wiring and Display Electronics	0.109	(0.240)	0.109	(0.240)
Totals	4.462	(9.836)	8.746	(19.282)
Unit Weight - kg/m^2 (lbm/ft^2)	0.602	(0.123)	1.18	(0.241)

FIGURE 31
EUTECTIC SALT TEMPERATURE SENSING ELEMENT

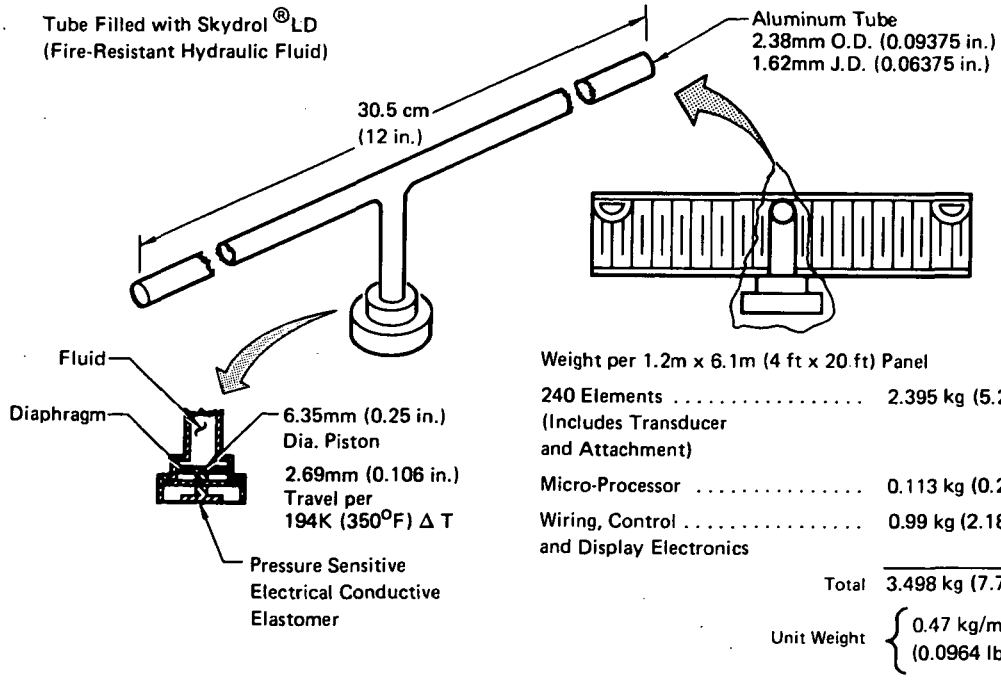

Weight per 1.2m x 6.1m (4 ft x 20 ft) Panel

240 Elements (Includes Transducer and Attachment)	2.395 kg (5.28 lbm)
Micro-Processor	0.113 kg (0.25 lbm)
Wiring, Control and Display Electronics	0.99 kg (2.182 lbm)
Total	3.498 kg (7.712 lbm)
Unit Weight	0.47 kg/m^2 (0.0964 lbm/ft^2)

FIGURE 32
FLUID FILLED TUBE ELEMENT (THERMAL EXPANSION)

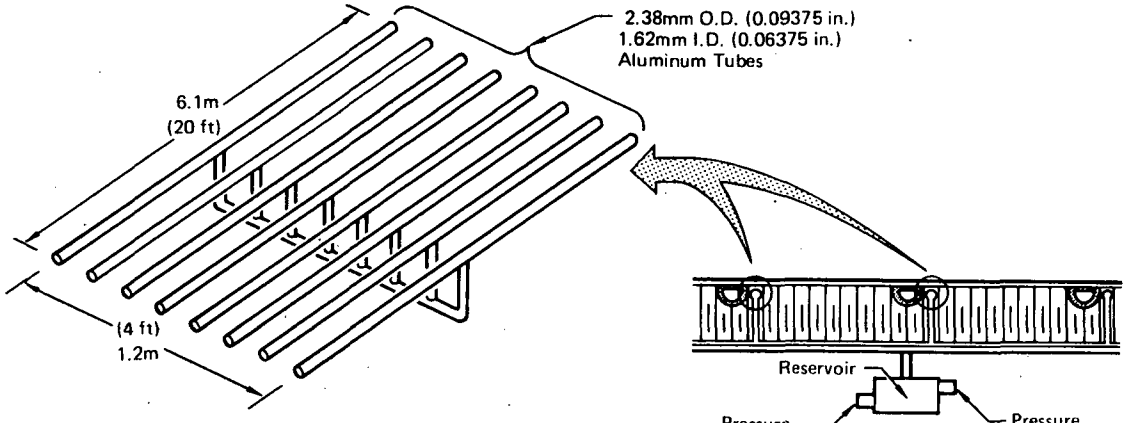

Network of Tube Elements Manifolded Together. Tubes Filled with Freon 21.

Weight per 1.2m x 6.1m (4 ft x 20 ft) Panel

75m (246 ft) of Filled Elements and Attachment	0.79 kg (1.75 lbm)
Pressure Transducer, Relief Valve and Reservoir	0.23 kg (0.50 lbm)
Wiring, Control and Display Electronics	0.23 kg (0.51 lbm)
Total	1.25 kg (2.76 lbm)
Unit Weight	0.55 kg/m^2 (0.0345 lbm/ft^2)

FIGURE 33
FLUID FILLED TUBE ELEMENTS (PHASE CHANGE)

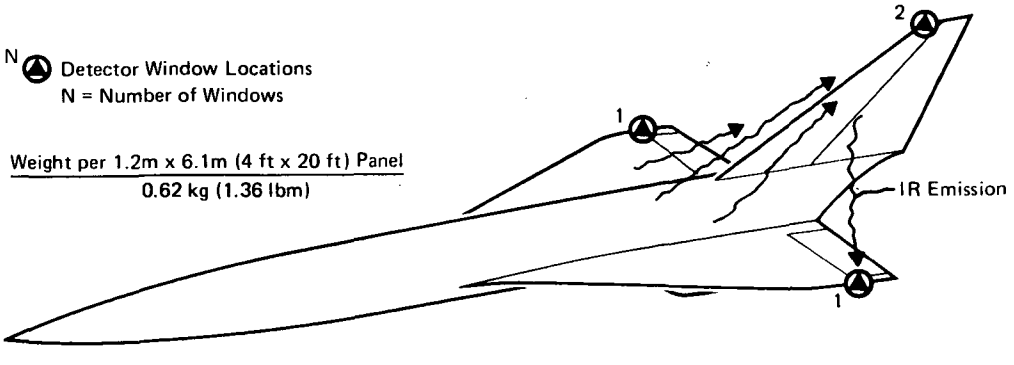

Weight per 1.2m x 6.1m (4 ft x 20 ft) Panel
0.62 kg (1.36 lbm)

Four Detector Windows at Illustrated Locations Scanning 70% of Upper Fuselage, Vertical Tail, and Upper Wing Surfaces.

70% Upper Fuselage Area	=	590 m^2 (6346 ft^2)
Upper Wing Surfaces	=	541m^2 (5827 ft^2)
Vertical Surfaces	=	285m^2 (3070 ft^2)
		1416m^2 (15,243 ft^2)

4 Detector Windows, Detectors, Installation, Electronics, Cooling	90.7 kg (200 lbm)
Wiring, Processor and Display Electronics	26.8 kg (59 lbm)
Total	117.5 kg (259 lbm)
Unit Weight	0.27 kg/m^2 (0.017 lbm/ft^2)

FIGURE 34
INFRARED SCANNING

Figure 35 presents the ranking results of the panel "hot spot" detection methods. As shown, the infrared scanning and liquid phase change methods were rated the two most promising approaches. Infrared scanning, due to low weight per unit area monitored and its high overall rating, must be considered a candidate system. However, all surfaces of the aircraft cannot be monitored. Also, its use would be limited to panel concepts with fast temperature response to failure, thus negating its use for shielded or overcoated areas. The concept utilizing the phase change of a fluid contained in tube elements was found to be applicable to all thermo-structural concepts.

The single element eutectic salt approach is rated a strong third. This approach represents a minimum development risk. However, the elements are heavy and do not offer the potential monitoring capability of the infrared scan or the liquid to vapor phase change sensors.

On the basis of weight and potential overall capability, it is recommended that the phase change (fluid filled tube elements) approach be considered the prime candidate. This approach can be used with both honeycomb and skin-stringer type structure and is applicable to all areas of the aircraft.

The infrared scanning approach was considered as an alternate due to its potential low weight per unit area scanned. With development, this technique could possibly be used to monitor about half of the aircraft cooled area. The remaining area could be monitored with the liquid filled phase change elements.

On the basis of the foregoing analysis, the weight increment chargeable to the phase change (fluid filled tube element) approach has been used for determining total fail-safe system weights.

4.1.5 Integration of Failure Detection Methods - The integration of the failure detection methods identified in Sections 4.1.3 and 4.1.4 into an overall failure detection system is portrayed in Figure 36. The failure detection system includes instrumentation and crew displays for failure detection as well as for system monitoring.

The total cooled aircraft surface, 2980 m^2 (32,134 ft^2), was divided into failure detection system control zones to illustrate how a detection system utilizing the fluid filled elements (phase change) would be configured. Figure 37 presents a schematic of the system. Each output signal from a control zone represents the sensor output signal from an individual panel. The signal from the panel sensors would be transmitted, by pressure trans-

CANDIDATE "HOT SPOT" DETECTION APPROACH	UNIT WEIGHT kg/m² (lbm/ft²) (1)	(A) OPERATING COST: WEIGHT (.75) (3) (4)	DAMAGE RESISTANCE (.05) (5)	INSPECTABILITY (.1)	MAINTAINABILITY (.1)	SUBSCORE	(B) INITIAL COST: FABRICATION COST (.67)	DETECTION SYSTEM COST (.33)	SUBSCORE	(C) RELIABILITY: DAMAGE TOLERANCE (.2) (6)	COMPLEXITY (.6)	INSPECTABILITY (.2)	SUBSCORE	(D) RESPONSE: CONTINUOUS RECORD (.6)	SENSITIVITY (.4)	SUBSCORE	APPROACH RATING: TOTAL SCORE = $.9\sum\frac{A,B,C}{3} + .1D$	RELATIVE RATING
FLUID FILLED TUBE (THERMAL EXPANSION)	0.471 (0.0964)	7	9	8	8	7.15	5	7	5.66	10	1	2	3.0	10	8	9.2	5.66	4
FLUID FILLED TUBE (PHASE CHANGE)	0.168 (0.0345)	9	9	8	8	8.95	7	8	7.33	5	5	5	5.0	10	8	9.2	7.3	2
INFRARED SCANNING (7)	0.083 (0.017) (2)	10	8	10	10	9.9	10	1	7.03	1	5	10	5.2	10	10	10	7.64	1
EUTECTIC SALT ELEMENTS																		
SINGLE ELEMENT	0.601 (0.123)	5	10	5	5	5.25	7	10	7.91	7	10	5	8.4	1	3	1.8	6.67	3
DUAL ELEMENTS	1.18 (0.241)	1	10	5	5	2.25	6	9	6.99	7	9	5	7.8	1	3	1.8	5.29	5

NOTES:

(1) BASED ON WEIGHT OF SENSORS, INSTALLATION, WIRING, PROCESSOR AND DISPLAY ELECTRONICS FOR 2985 m² (32,134 ft²) OF COOLED AREA.

(2) BASED ON INSTALLATION OF 4 DETECTOR UNIT WINDOWS SCANNING 1416 m² (15,243 ft²) OF COOLED AREA PLUS WIRING, PROCESSOR AND DISPLAY ELECTRONICS.

(3) NUMBER IN PARENTHESIS IS IMPORTANCE FACTOR.

(4) TEN IS MOST DESIRABLE, ONE IS LEAST DESIRABLE.

(5) DAMAGE RESISTANCE - ABILITY TO RESIST DAMAGE DUE TO HANDLING OR FOREING OBJECT IMPACT.

(6) DAMAGE TOLERANCE - ABILITY TO FUNCTION, OR PARTIALLY FUNCTION AFTER PANEL (OR IR WINDOW) SUSTAINS DAMAGE.

(7) LIMITED AREA COVERAGE. APPLICABLE ONLY TO COMPATIBLE THERMO-STRUCTURAL TECHNIQUES. MUST BE USED IN CONJUNCTION WITH SECONDARY APPROACH.

FIGURE 35
PANEL "HOT SPOT" DETECTION APPROACH RANKING

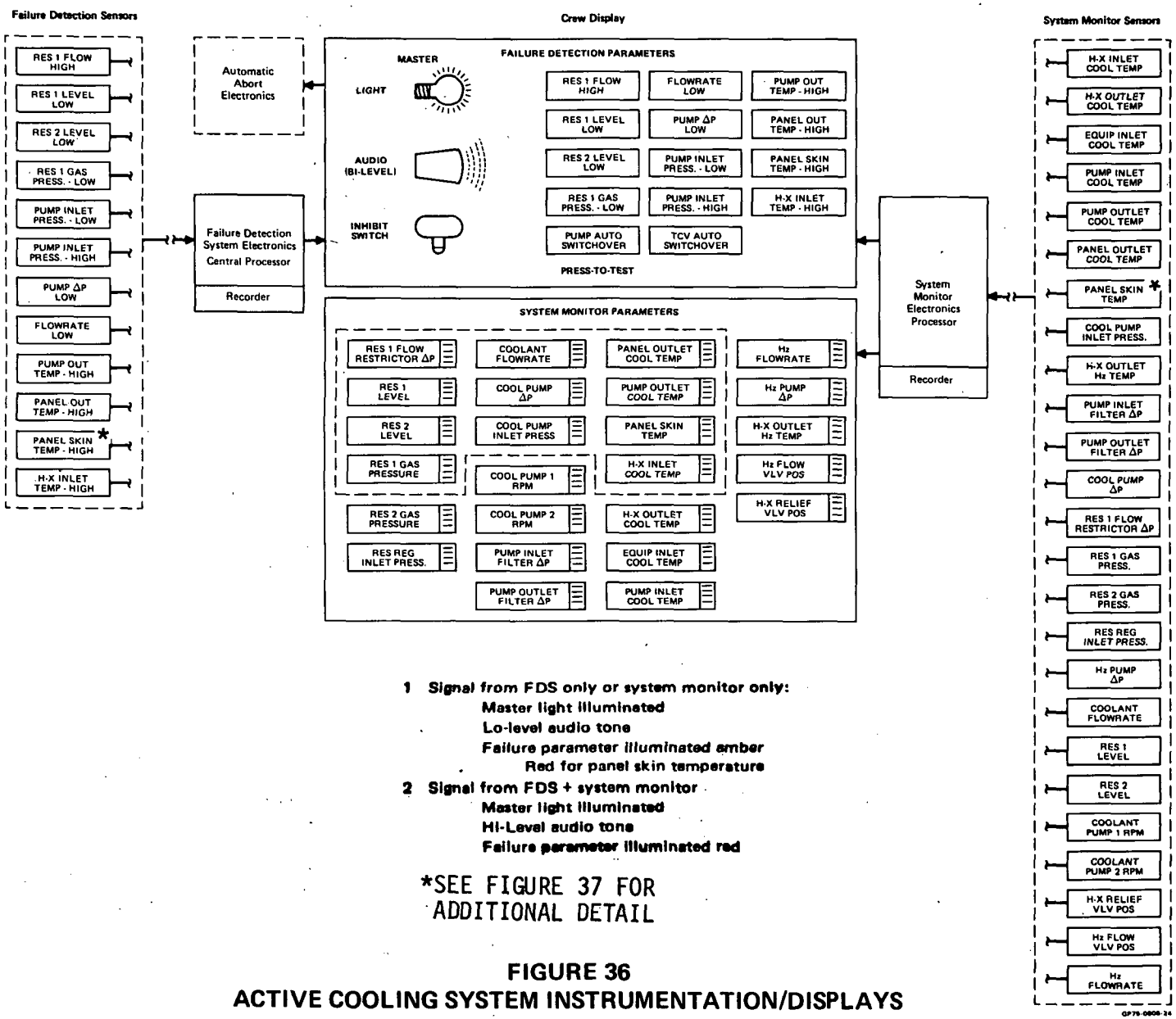

1 Signal from FDS only or system monitor only:
- **Master light illuminated**
- **Lo-level audio tone**
- **Failure parameter illuminated amber**
  - **Red for panel skin temperature**

2 Signal from FDS + system monitor
- **Master light illuminated**
- **Hi-Level audio tone**
- **Failure parameter illuminated red**

*SEE FIGURE 37 FOR ADDITIONAL DETAIL

FIGURE 36
ACTIVE COOLING SYSTEM INSTRUMENTATION/DISPLAYS

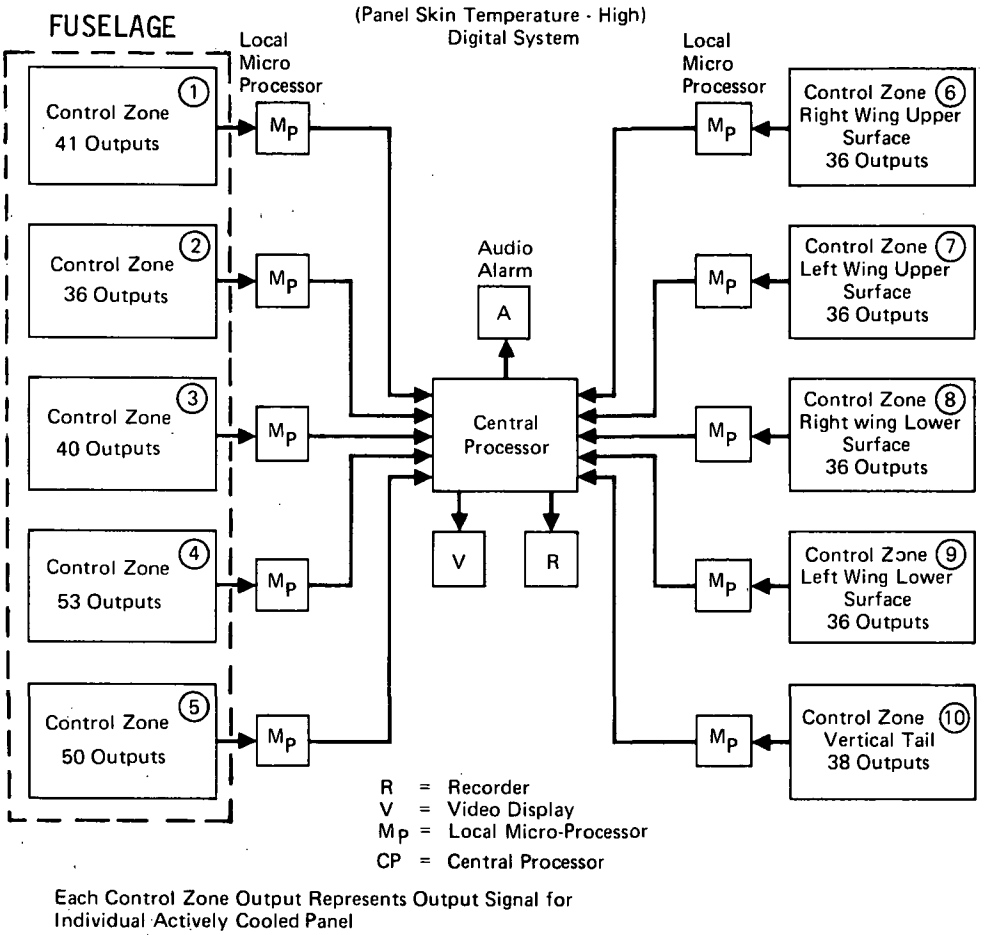

FIGURE 37
FAILURE DETECTION SYSTEM CONTROL AND DISPLAY ELECTRONICS

ducers, to the local control zone micro-processor. This processor would, using memory, digital logic and computation, make decisions and issue commands to a central processor. The central processor monitors input data from all local micro-processors and provides the data to a video monitor, an audio monitor, and to a continuous recorder of panel temperature status. The use of semiconductor technology and large scale integration (LSI) devices for the local micro-processors and central control and display electronics will result in reliable low weight components.

A signal from any of the failure detection sensors indicating a failure condition is routed through system electronics to a crew display panel, resulting in illumination of the master light, an audio tone, and illumination of that particular parameter displayed on the panel. The system monitor

sensors shown in Figure 36 detect the same parameters as the failure detection sensors plus other instrumentation considered to be of value for system monitoring. Outputs from these sensors provide a read-out of the parameter on the display panel. A discrete failure signal from either a failure detection sensor or its corresponding monitor sensor will alert the crew by master light illumination, an audio tone, and illumination of the failure detection parameter display. In-flight verification of the electronics and circuitry associated with each failure detection sensor would be provided by built-in-test (BIT) or press-to-test provisions.

Figure 36 also illustrates an output from the master panel to automatic abort mode electronics. In the case of a cooling system malfunction judged (by the central data processors, if crew reaction is not within an established time limit) to warrant abort, the automatic abort mode electronics would take command of the flight control system and initiate the abort maneuver.

Section 4.3 will show that, unless the reaction to a failure requiring abort takes place within a certain time, the weight penalty to maintain panel temperatures within the desired limits will become excessive. Therefore, the central processor will have the capability to make decisions on the basis of input data and initiate the aircraft abort, if the situation demands.

Example detection system failure parameter limits are shown in Figure 38. These values are based on system studies applicable to the Mach 6 baseline aircraft and cooling system.

A summary of system characteristics, viewed from the standpoint of response and reliability, is shown in Figure 39. Although some protection from false alarms is provided, further consideration of reliability might lead one to quad-redundant sensors in certain critical locations.

4.2 ABORT TRAJECTORIES

Once a failure of the active cooling system, or an individual panel is detected, an abort maneuver is initiated. The manner in which the aircraft is maneuvered can result in significant effects on the total heat load that must be absorbed.

Detailed studies were made of abort from the selected cruise altitudes and Mach numbers. The limits of aircraft maneuvers during abort, such as

PARAMETER	LIMIT	RATIONALE FOR LIMIT
1. Res #1 Flow-High	> 0.8 kg/s (1.77 lb/sec) (Mach 6 System)	Flowrate > flow required for system coolant cool-down corresponding to $dT/d\tau$ = 0.093 K/s (10°F/min)
2. Res #1 Level-Low	Res #1 Empty	Res #1 Empty
3. Res #2 Level-Low	Res #2 Empty	Res #2 Empty
4. Res #1 Gas Press-Low	<25 psia	103 kPa (15 psi) below normal
5. Coolant Flowrate-Low	<75% of normal	25% below normal
6. Pump ΔP--Low	ΔP corresponding to <75% normal flowrate	25% below normal
7. Pump Inlet Press-Low	<172 kPa (25 psia)	103 kPa (15 psi) below normal
8. Pump Inlet Press-High	>414 kPa (60 psia)	138 kPa (20 psi) above normal
9. Pump Out Temp-High	>266 K (20°F)	11 K (20°F) above normal
10. Panel Out Temp-High	>311 K (100°F)	17 K (30°F) above normal
11. Panel Skin Temp-High	>(Normal max + 28 K (50°F)	28 K (50°F) above normal
12. H-X Inlet Temp-High	>311 K (100°F)	17 K (30°F) above normal
13. Pump Auto Switchover o Flowrate < 75% Normal o Pump ΔP<ΔP Corresponding to 75% Normal Flowrate	After Event	Pump Failure Has Occurred
14. TCV Auto Switchover o H-X Outlet Coolant Temp >264 K (15°F) o H-X Outlet Coolant Temp <247 K (-15°F)	After Event	TCV Failure Has Occurred

FIGURE 38
EXAMPLE FAILURE DETECTION SYSTEM FAILURE LIMITS
(FOR TYPICAL BASELINE SYSTEM)

- **Response**
  - Instrumentation Selected to Respond to Earliest Positive Failure Cues
  - Most Significant Failures Provide Multiple Cues Which are Also Detected
  - Visual and Audio Failure Signals Provided to Crew
  - Quantitative Response Times Dependent on Detailed System Characteristics and Specific Failure Modes
- **Reliability**
  - Proven Reliable Instrumentation Used Where Possible
  - FDS Instrumentation Electronics and Circuitry Checked Periodically Before and During Sustained Cruise by Crew via Press-to-Test Capability
  - System Monitor Parameters Checked by Crew to Verify System Parameters are Within Tolerance
  - For Each Failure Parameter, a Cue is Available from Either the FDS Display or the System Monitor Display

    ∴ A Double Failure Would Have to Occur to Prevent the Crew from Being Alerted to Out-of-Tolerance Condition for Each Parameter
  - One Failure Generally Results in Another Secondary Failure Cue Which is also Monitored by the Failure Detection System

    ∴ Redundancy is also Provided by Detection of Secondary Failure Cues
  - Protection from False Alarms Provided by Requirement that Failure Signals from Both the FDS and the System Monitor Sensors Must Occur Before Failure Confirmation (Except for Skin Temperature)

    Failure Confirmation by:
    - Hi-Level Audio Signal
    - FDS Display Illuminated Red

FIGURE 39
FAILURE DETECTION SYSTEM DESIGN FEATURES/CONSIDERATIONS

maximum allowable "g" and maximum allowable angle of attack, were examined. The abort maneuvers were constrained to the allowable structural-aerodynamic-crew/passenger limitations.

All initial abort trajectories were based on the assumption that start-of-abort descent occurred from a nominal cruise dynamic pressure of 24.1 kPa (504 lbf/ft^2). This was later modified by revising start of cruise altitudes during the optimization of abort trajectories. This was done to provide results more consistent with the design of aircraft optimized to operate not only at Mach 6, but at Mach 4.5 and Mach 3. In addition, all abort descents were assumed to occur with start-of-cruise fuel load. This results in maximum cruise wing loading and maximum descent heat load for any given type of descent.

Abort from mid-cruise or end of cruise flight conditions results in a reduction in abort heat load.

4.2.1 Trajectory Constraints - Several basic limitations were applied to the type of trajectory utilized for descent from cruise altitude and Mach number. These were airframe structural constraints, the configuration aerodynamic characteristics, and physical limitations of the crew and passengers.

a. Airframe Structural Constraints - The airframe structural constraints utilized to define the initial abort trajectory limits were the maximum allowable inflight load factors defined for the Reference (5) Concept 3 aircraft. Concept 3 was designed for a limit load factor (n_Z) of +2.5, -1.0 (Z direction positive upward) at maximum normal operating temperature of 399 K (250°F).

Ultimate shear and bending moment curves for Concept 3, for the +2.5g flight condition, are available in Reference (5). Combined loads, temperature effects, etc., were not considered until final optimization of aircraft thermostructural concepts.

b. Configuration Aerodynamic Characteristics - An examination of the Reference (4) Concept 3 aircraft aerodynamic characteristics identified the following maneuver limits:

o Maximum permissible angle of attack at Mach 3 was limited to 13 degrees due to control limits at nominal c.g. position.

o Maximum permissible angle of attack at Mach 4.5 was limited to 14 degrees due to control limits at nominal c.g. position.

o Initial maximum permissible angle of attack at Mach 6 was limited to 10 degrees due to control limits at forward c.g. position. Aft fuel was used to accelerate to cruise conditions. This angle of attack limit was modified by assuming remanagement of onboard fuel. A limit on angle of attack due to a loss in directional stability did not materialize, since dynamic C_{N_β} was always greater than 0.002. A flared rudder on the vertical fin was used to provide control at the higher angles of attack and to provide larger deceleration forces. Thus, the maximum permissible angle of attack at Mach 6 was set at 20 degrees.

o Minimum flight dynamic pressure was limited to 5.6 kPa (117 lbf/ft^2) due to a requirement for adequate rolling moment generation at the apogee of a maximum g-load zoom climb, to prevent the buildup of an excessive sink rate when the aircraft is banked to modulate the vertical load factor.

The above aerodynamic constraints were used in all initial abort maneuver studies. The constraints on angle of attack at Mach 3 and Mach 4.5 were modified for the final trajectory studies. This modification was the increase of maximum allowable angle of attack to a value of 20 degrees. Aircraft designed for Mach 3 and Mach 4.5 operation should have the capability of reaching this value without undue problems.

c. Physiological Limitations - These limitations were found to be the most nebulous of the trajectory constraints. The spectrum of acceleration environments is extremely large and may vary in duration, magnitude, rate of onset and decline, and direction. Physiological, and psychophysiological tolerance is a function of these variables plus a host of other variables. Discussions with MDC aerospace medicine personnel resulted in recommendations for limits and these are presented as Figure 40. These limits were derived by reducing tolerance limits from Reference (8) (Page 574 for positive g and Page 691 for negative g) by 50 percent. These limits, depending upon time to end point of acceleration, could exceed the structural limits of the airframe. Therefore, the limits used to define the trajectory constraints were the smaller value of absolute acceleration, comparing airframe limit load factor and personnel acceleration limits.

Discussions with airline pilots in regard to limitations on crew/passenger absolute accelerations during an abort brought forth some pertinent comments. After hearing an explanation of why abort maneuvers are a requirement for the study aircraft, three out of three pilots related these maneuvers to collision avoidance maneuvers. In all cases the feeling was that the pilot would "pull the wings off," if required to avoid a mid-air collision. The abort from high speed cruise was placed in the same category, with the aircraft maneuvered to its maximum g-load capability. Passenger safety during the maneuver would be a major concern. However, the prime concern is to save the majority.

4.2.2 Minimum Heat Load Trajectories - The parameters that influence the aircraft heating during abort were studied in order to minimize the abort heat loads. Vehicle aerodynamic characteristics used were those of aircraft Concept 3, Reference (4). Mach 6 descents were investigated first, followed by Mach 4.5 and Mach 3. In all cases, the abort trajectories were assumed to occur with zero engine thrust. In addition, the use of a drag brake was investigated.

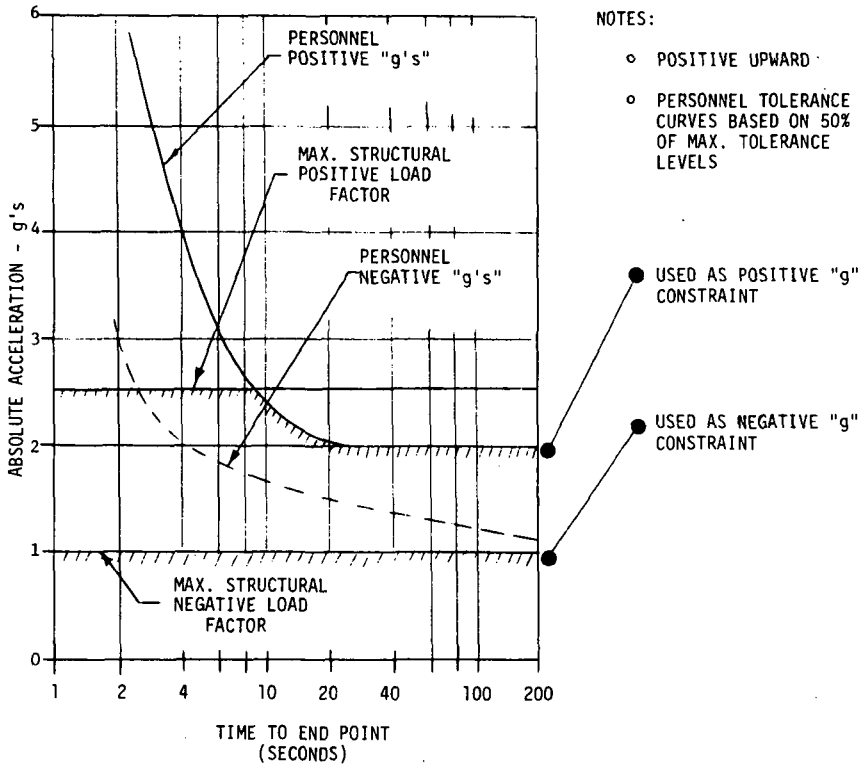

FIGURE 40
ACCELERATION CONSTRAINTS DURING ABORT

A typical location on the centerline 27.4 m (90 ft) aft of the nose tip was selected as being representative of the average heating location for the lower surface of the aircraft. The typical average heating location for the upper surfaces was on the centerline 15.2 m (50 ft) aft of the nose tip. These locations were used throughout the trajectory studies to determine abort heating rates and total heat loads. The locations were selected in the following manner.

The aircraft surface was divided into 43 heating zones, (Figure 10), and the total aircraft cruise heat load determined. The total cruise heat load was 90.20 MW (3.08×10^8 Btu/hr) with an average heating rate of 30.188 kW/m^2 (2.66 Btu/ft^2 sec). The average heating rate to the upper surfaces during cruise was found to be 17.93 kW/m^2 (1.58 Btu/ft^2 sec). Heating Zone 7, with an average heating rate of 18.16 kW/m^2 (1.6 Btu/ft^2 sec), as shown on Figure 10, was selected as being representative of the average upper surface. Heat transfer to aircraft lower surfaces during cruise indicated an average heating rate of 44.94 kW/m^2 (3.96 Btu/ft^2 sec). Heating Zone 15 (Figure 10), with an

average heating rate of 45.4 kW/m^2 (4 Btu/ft^2 sec), was selected as being representative of the average lower surface. Figure 41 illustrates the heating rates for various locations on the aircraft.

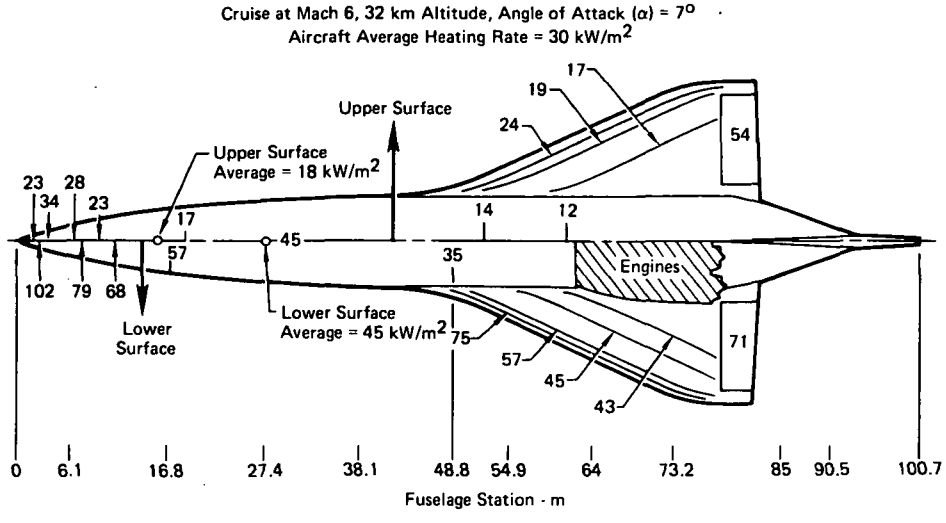

FIGURE 41a
AIRCRAFT CONCEPT 3 DESIGN HEATING RATES
Aircraft Design per Reference (4)

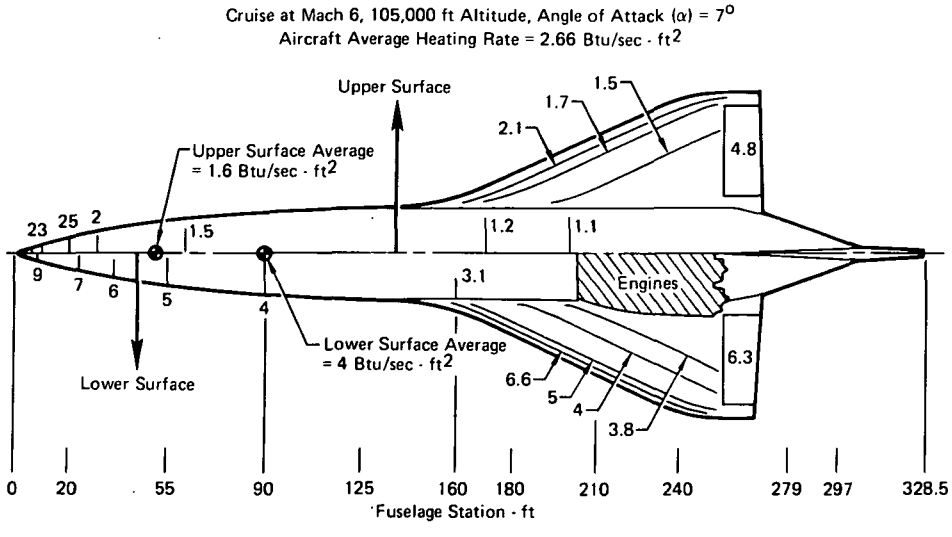

FIGURE 41b
AIRCRAFT CONCEPT 3 DESIGN HEATING RATES
Aircraft Design per Reference (4)

a. Mach 6 Abort Heat Loads - Figures 42 and 43 present comparisons of the altitude and Mach number histories of six early Mach 6 abort trajectories. All of these trajectories were tailored to stay within the load factor, angle of attack, and dynamic pressure constraints. The angle of attack during these trajectories was held constant. This descent mode results in a phugoid oscillation. The oscillation could be prevented by modulating the angle of attack so that the equilibrium altitude corresponding to the lift coefficient is maintained. However, this type of trajectory does not reduce the Mach number as rapidly as the oscillating trajectory. Maximum load factor experienced was 1.85g (2.5 limit). All trajectories were for start-of-cruise aircraft weight 257.43 Mg (567,529 lbm).

As shown in Figures 42 and 43, drag brakes were investigated as a means of reducing L/D, and thus descent time. However, the 70.7 m^2 (761 ft^2) of split rudder at 45° flare, utilized as a drag brake, was not effective at the higher angles of attack (see Trajectories (4) and (6) on Figures 42 and 43). The kinetic energy of the aircraft at cruise completely overpowers the available drag brake area. It is highly doubtful if it is practical to install a large enough drag brake area on the aircraft to make any significant difference in descent time.

Figures 44 and 45 present abort heating rate histories for Trajectories (1) and (3), and (5) and (6), respectively. Heating rates were not calculated for Trajectories (2) and (4) because of the similarity between (2) and (3) and between (4) and (6).

Trajectory (6), the high angle of attack zoom, was the most effective in reducing the heat load. However, the typical lower surface heat load is still quite high, 6.55 MJ/m^2 (576 Btu/ft^2). For example, approximately 48.82 kg/m^2 (10 lbm/ft^2) of aluminum with a 139 K ΔT (250°F) would be required to absorb this heat load.

Two additional abort trajectories were evaluated to determine if the heat loads could be reduced by trajectory tailoring. Figures 46 and 47 present comparisons of these trajectories (Trajectories (7) and (8)) in terms of altitude, angle of attack, bank angle and Mach number histories. Trajectory (7), a high α zoom, exceeds the basic trajectory constraints. Angle of attack is allowed to go to 45 degrees, and the minimum dynamic pressure goes as low as 1.96 kPa (41 lbf/ft^2). This type of trajectory would generate a requirement

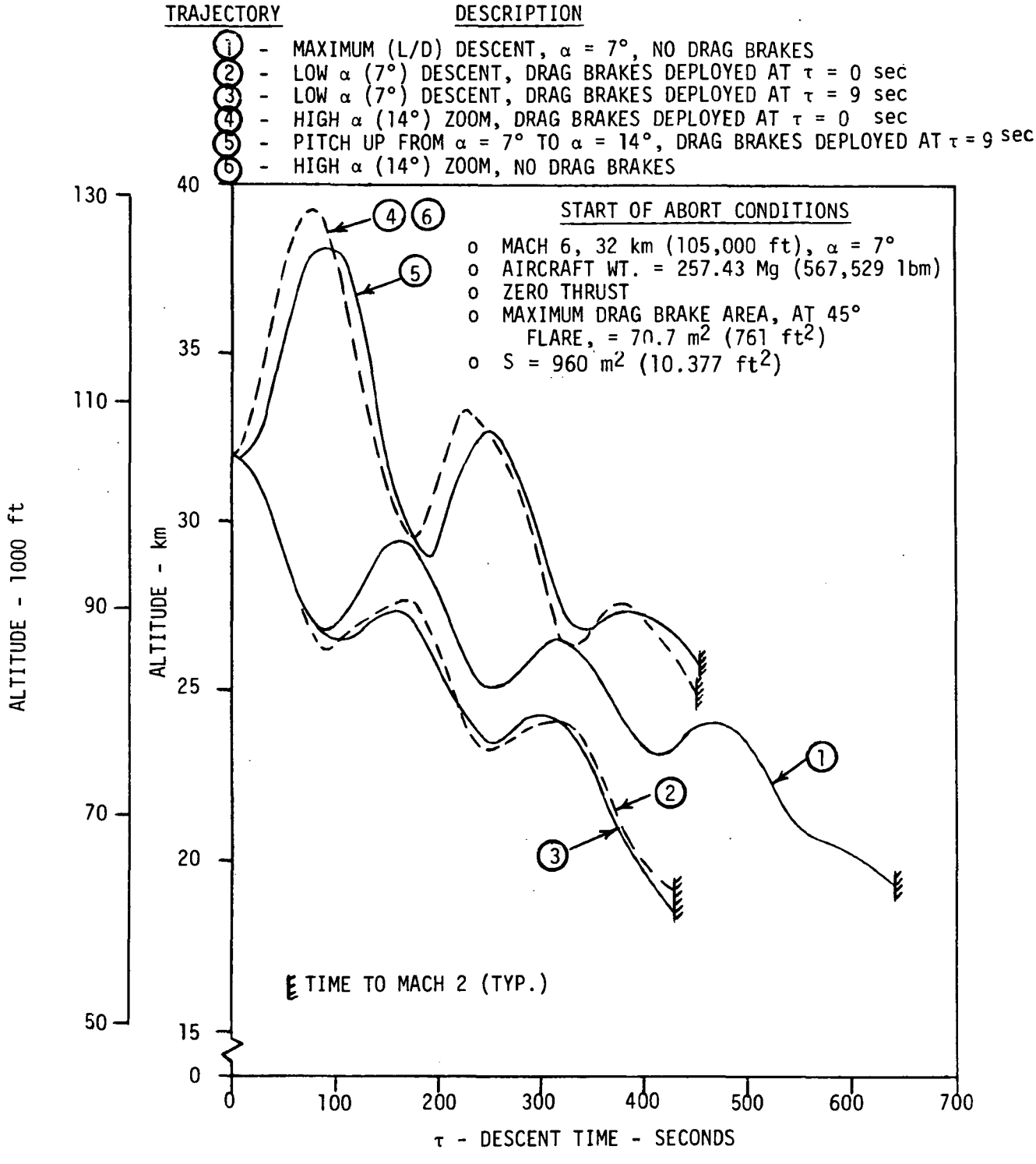

FIGURE 42
COMPARISON OF ALTITUDE HISTORIES

TRAJECTORY	DESCRIPTION
①	= MAXIMUM (L/D) DESCENT, α = 7°
②	= LOW α (7°) DESCENT, DRAG BRAKES DEPLOYED AT τ = 0 sec
③	= LOW α (7°) DESCENT, DRAG BRAKES DEPLOYED AT τ = 9 sec
④	= HIGH α (14°) ZOOM, DRAG BRAKES DEPLOYED AT τ = 0 sec
⑤	= PITCH UP FROM α = 7° TO α = 14°, DRAG BRAKES DEPLOYED AT τ = 9 sec
⑥	= HIGH α (14°) ZOOM o MAXIMUM DRAG BRAKE AREA, AT 45° FLARE, = 70.7 m^2 (761 ft^2)

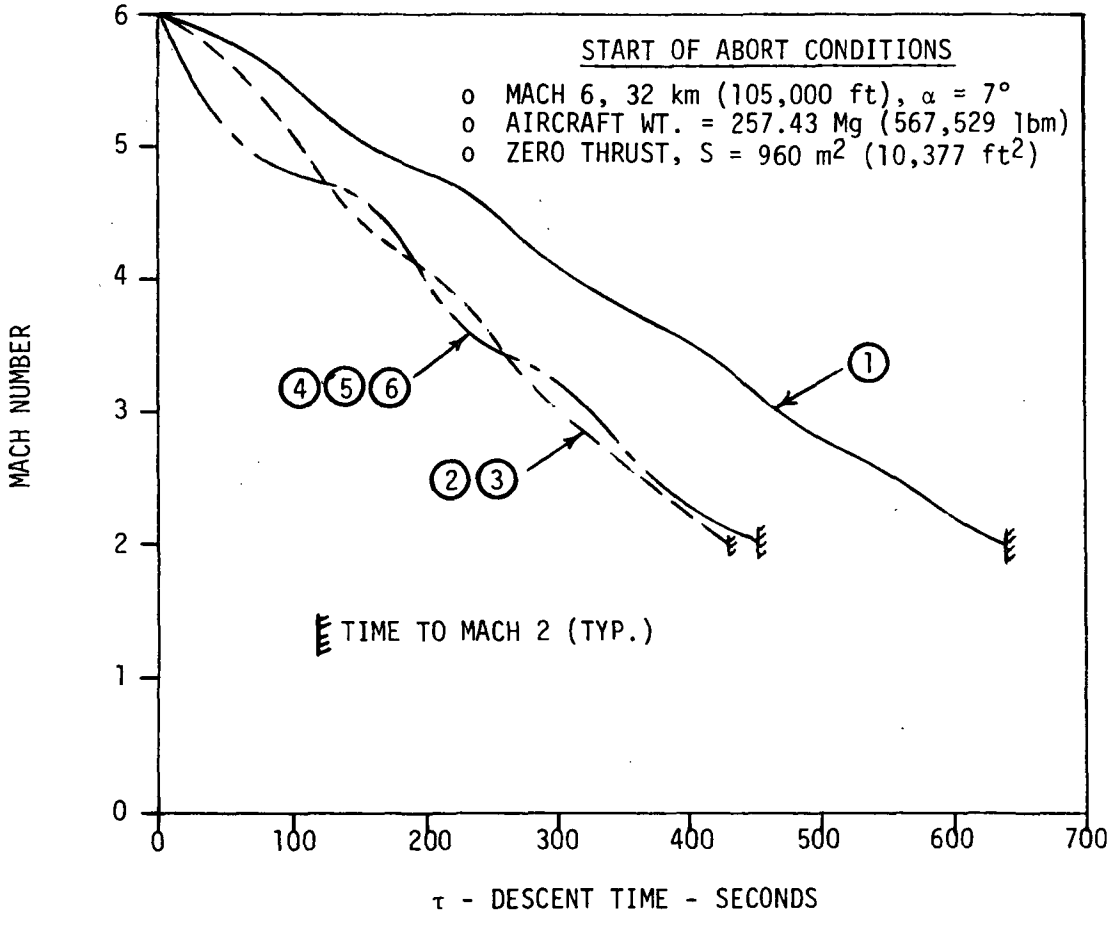

FIGURE 43
COMPARISON OF MACH NUMBER HISTORIES FOR MACH 6 ABORT TRAJECTORIES 1 THROUGH 6

START OF ABORT CONDITIONS

- o MACH 6, 32 km (105,000 ft), α = 7°
- o AIRCRAFT WT. = 257.43 Mg (567,529 lbm)
- o ZERO THRUST
- o S= 960 m^2 (10,377 ft^2)

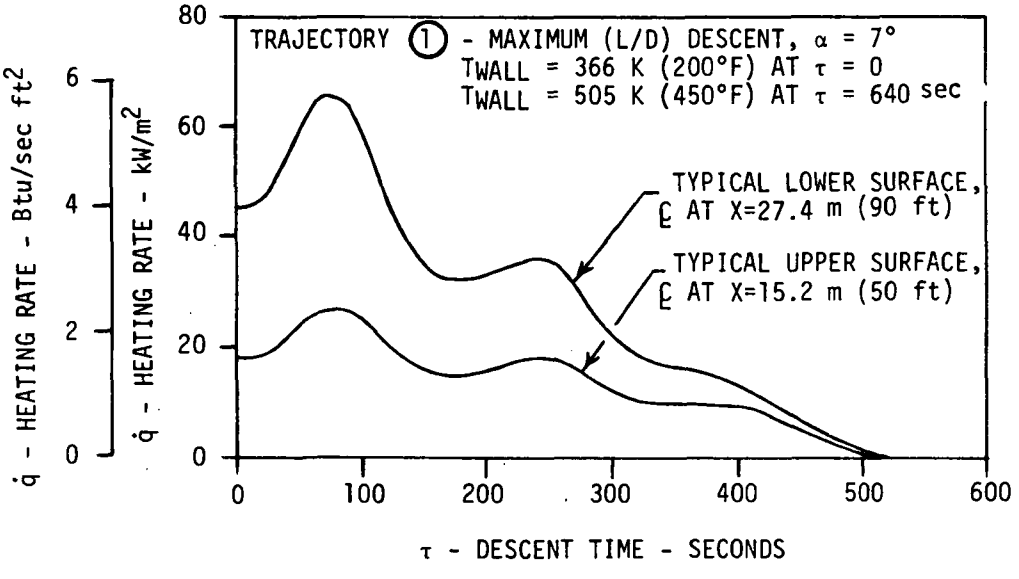

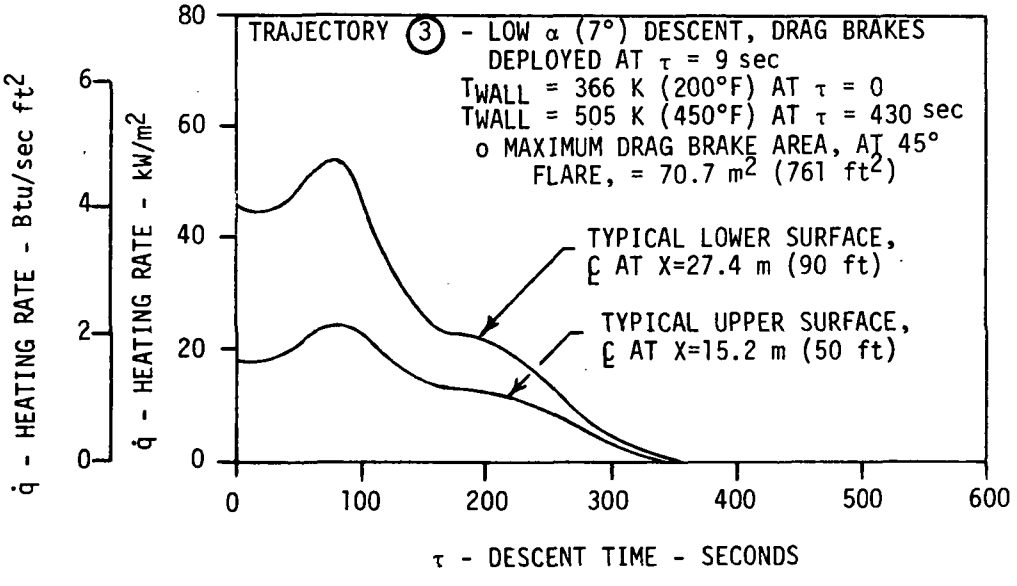

FIGURE 44
TYPICAL SURFACE HEATING RATES FOR MACH 6 ABORT TRAJECTORIES 1 AND 3

START OF ABORT CONDITIONS

- o MACH 6, 32 km (105,000 ft), α = 7°
- o AIRCRAFT WT. = 257.43 Mg (567,529 lbm)
- o ZERO THRUST
- o S = 960 m^2 (10,377 ft^2)

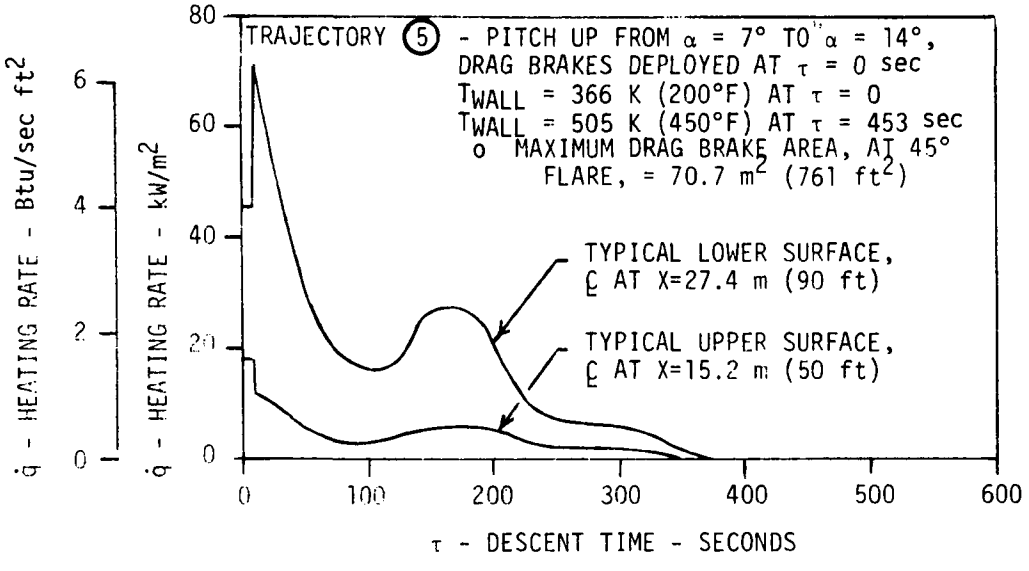

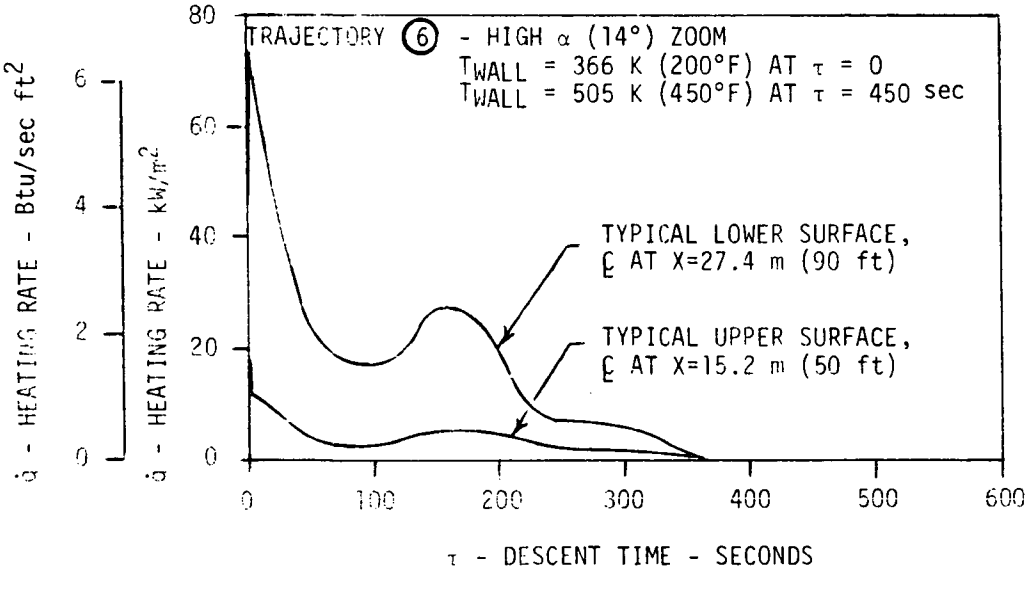

FIGURE 45
TYPICAL SURFACE HEATING RATES
FOR MACH 6 ABORT TRAJECTORIES 5 AND 6

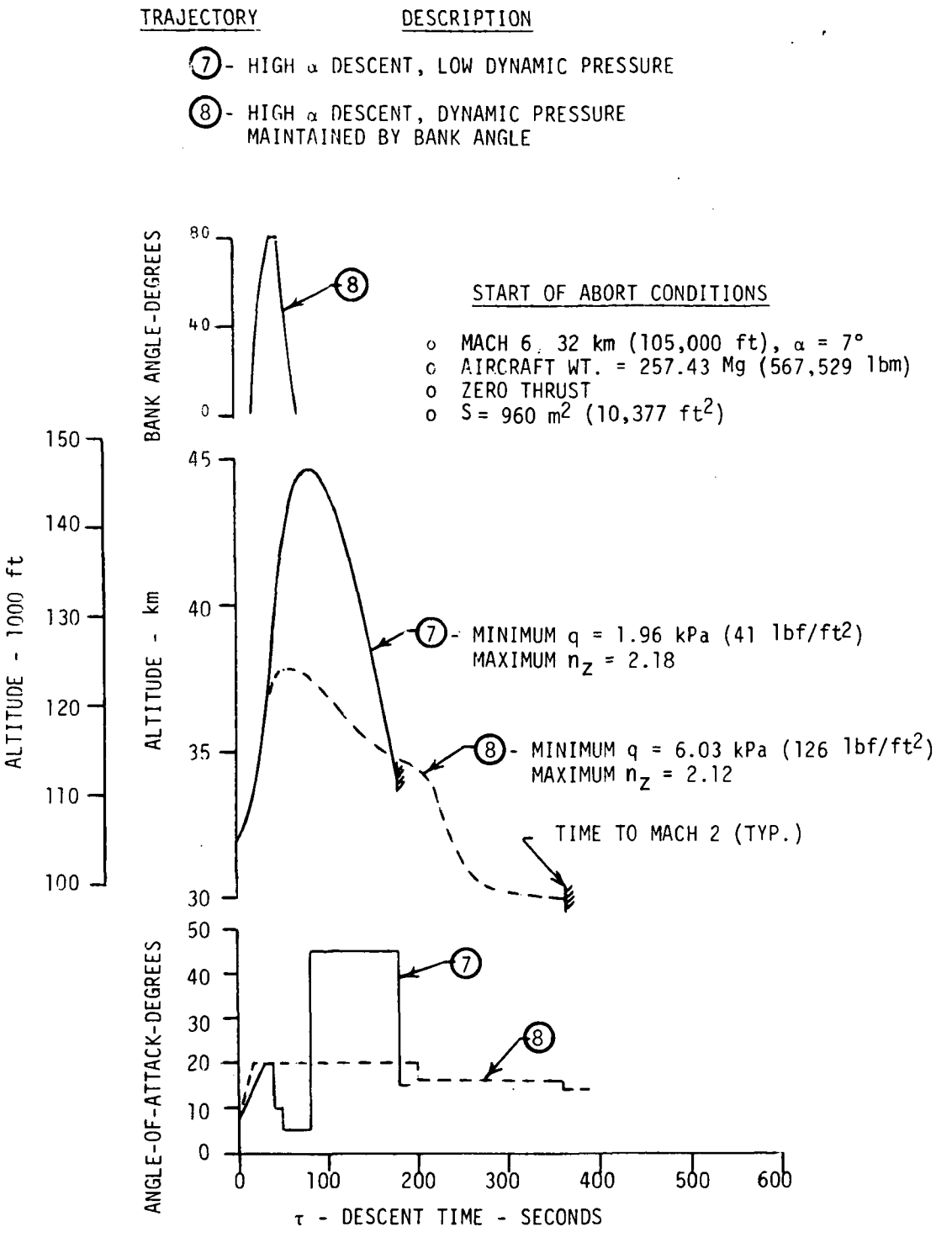

FIGURE 46
COMPARISON OF ALTITUDE, ANGLE-OF-ATTACK, AND BANK ANGLE HISTORIES FOR MACH 6 ABORT TRAJECTORIES 7 AND 8

TRAJECTORY DESCRIPTION

⑦ - HIGH α DESCENT, LOW DYNAMIC PRESSURE

⑧ - HIGH α DESCENT, DYNAMIC PRESSURE MAINTAINED BY BANK ANGLE

START OF ABORT CONDITIONS

- MACH 6, 32 km (105,000 ft), α = 7°
- AIRCRAFT WT. = 257.43 Mg (567,529 lbm)
- ZERO THRUST
- S= 960 m^2 (10,377 ft^2)

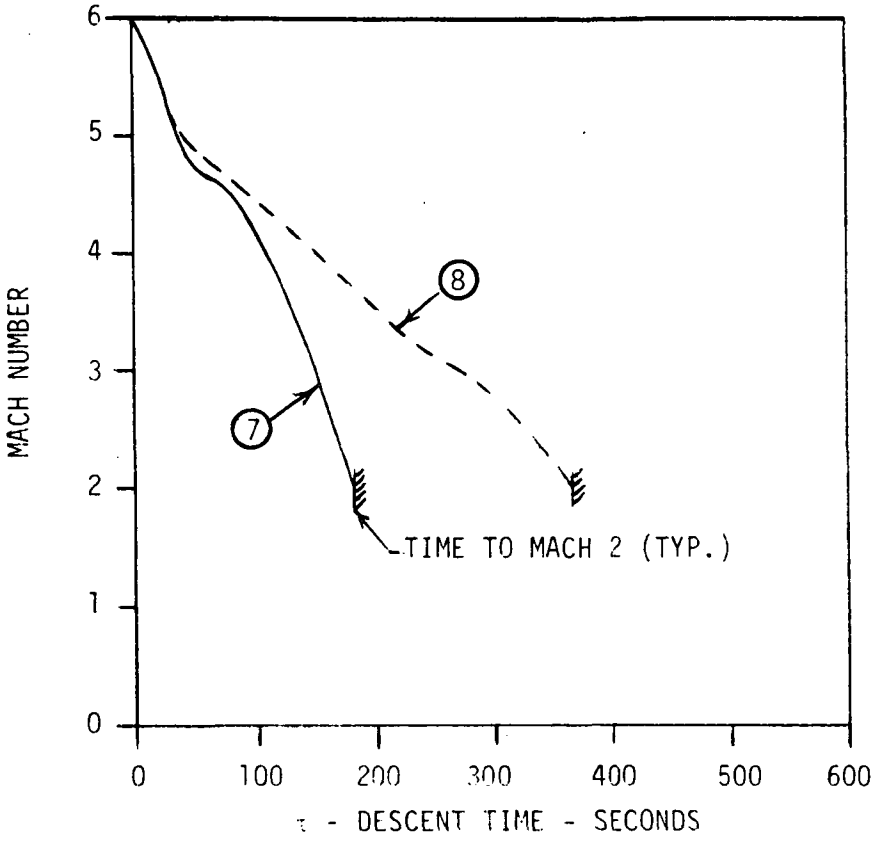

FIGURE 47
COMPARISON OF MACH NUMBER HISTORIES FOR MACH 6 ABORT TRAJECTORIES 7 AND 8

for a reaction control system to maintain adequate handling qualities and stability levels. Addition of a reaction control system would add to normal maintainability requirements and reduce payload. Thus, reaction control was not considered further. Trajectory (8), a high α (20°) zoom with bank to maintain dynamic pressure, is within all trajectory constraints.

Figure 48 presents a comparison of the heating rate histories for trajectories (7) and (8). Figure 49 compares the abort heat loads for all evaluated Mach 6 trajectories. As mentioned earlier, Trajectories (2) and (4) are not shown and Trajectory (7) was rejected as a viable approach due to the reaction control requirement. Trajectory (8), the modulated angle of attack (20° max) with bank angle, was selected as being representative of Mach 6 minimum heat load trajectories.

b. Mach 4.5 Abort Heat Loads - The abort descent from cruise at Mach 4.5 was assumed to start at a cruise dynamic pressure of 24.1 kPa (504 lbf/ft^2) and with a start-of-cruise fuel load. Only one Mach 4.5 abort trajectory was initially evaluated. However, this trajectory, Number (9) (Figure 50), was tailored using the minimum heating characteristics (high g-load pull-up) derived from the Mach 6 studies. The heating rate histories (Figure 50) were integrated to determine abort heat load.

c. Mach 3 Abort Heat Loads - The abort descent from cruise at Mach 3 was assumed to start at a cruise dynamic pressure of 24.1 kPa (504 lbf/ft^2) and with a start-of-cruise fuel load. Figures 51 and 52 present comparisons of the Mach number, angle of attack, bank angle and altitude histories for the three initial Mach 3 trajectories evaluated. Figure 53 shows the heating rate histories. All trajectories are within, or near, the constraints. As shown, although the descent time is less for Trajectory (12) compared to (11), the average heating rate is higher (higher average dynamic pressure), and results in a larger abort heat load.

This is illustrated in Figure 54, which compares abort heat loads. A bare uninsulated aluminum (0.040 inch) skin could survive (without exceeding 505 K (450°F)) a trajectory such as (11). Such a skin has the capacity to absorb about 0.3 MJ/m^2 (26 Btu/ft^2) with a temperature rise from 366 K to 478 K (200°F ΔT). Thus, Trajectory (11) was selected as being representative of Mach 3 minimum heat load trajectories.

START OF ABORT CONDITIONS

- MACH 6, 32 km (105,000 ft), α = 7°
- AIRCRAFT WT. = 257.43 Mg (567,529 lbm)
- ZERO THRUST
- S = 960 m^2 (10,377 ft^2)

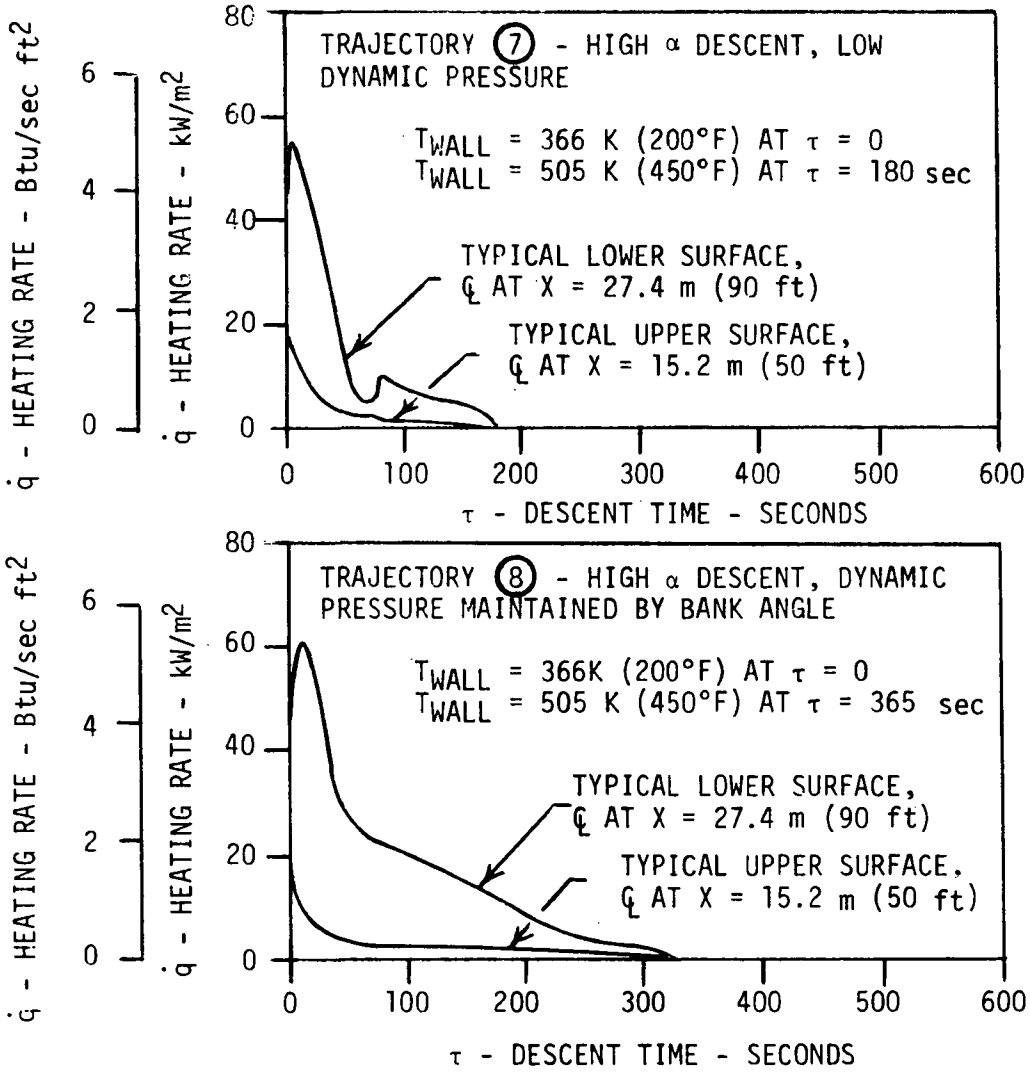

FIGURE 48
TYPICAL SURFACE HEATING RATES FOR MACH 6 ABORT TRAJECTORIES 7 AND 8

TRAJECTORY	TYPICAL HEAT LOADS - MJ/m² (Btu/ft²) (1)					
	LOWER SURFACE, Q_L		UPPER SURFACE, Q_U		AVERAGE, Q_A (2)	
①	15.22	(1341)	7.42	(654)	11.07	(975)
③	9.10	(802)	4.61	(406)	6.71	(591)
⑤	6.92	(610)	1.52	(134)	4.04	(356)
⑥	6.54	(576)	1.49	(131)	3.85	(339)
⑦	2.56	(226)	0.52	(46)	1.48	(130)
⑧	5.22	(460)	0.74	(65)	2.83	(249)

(1) HEAT LOAD = $\int \dot{q} d\tau$ FROM FIGURES 44, 45, AND 48

(2) Q_A (AREA WEIGHTED AVERAGE) = 0.457 Q_L + 0.543 Q_U

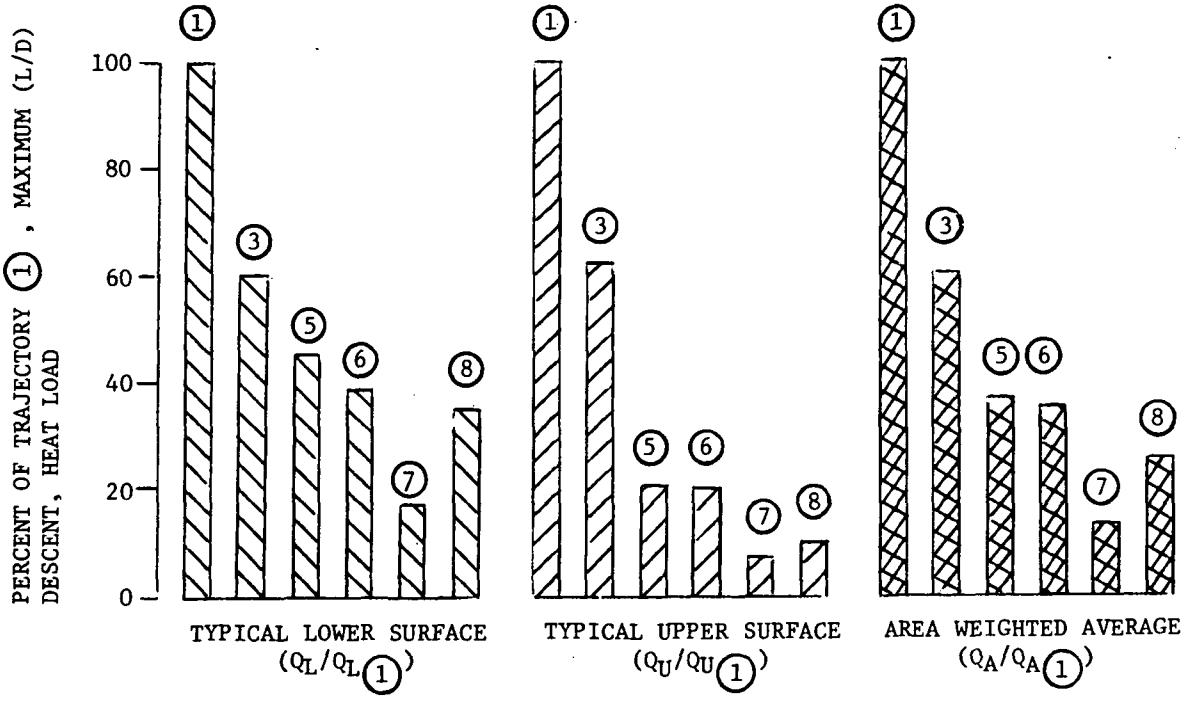

FIGURE 49
COMPARISON OF MACH 6 ABORT DESCENT TRAJECTORY HEAT LOADS

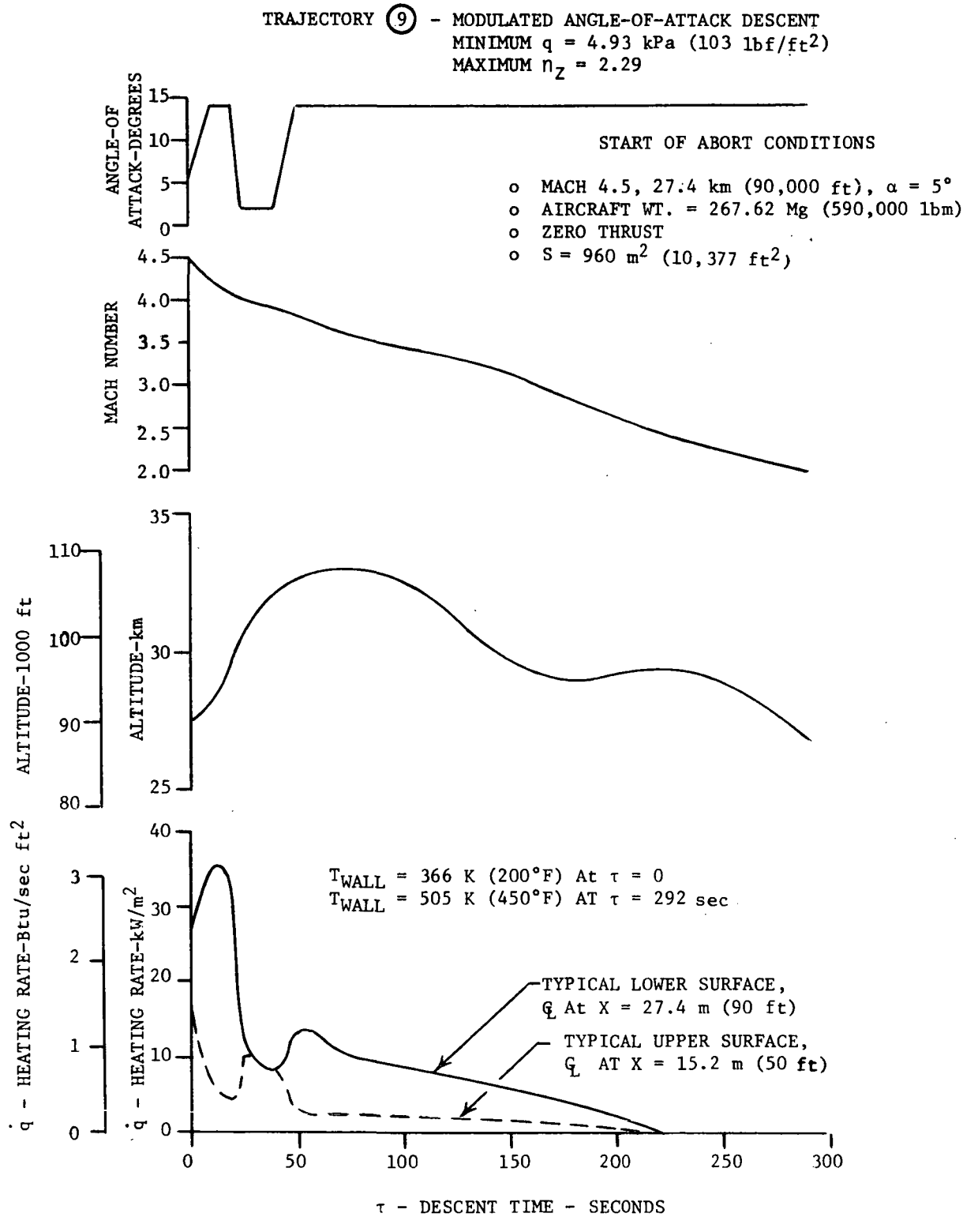

FIGURE 50
MACH 4.5 ABORT TRAJECTORY

TRAJECTORY	DESCRIPTION
⑩	MAXIMUM (L/D) DESCENT AT $\alpha \doteq 4°$
⑪	MODULATED α DESCENT, MAX. n_z = 2.5, MIN. q = 5.1 kPa (106 lbf/ft^2)
⑫	MODULATED α WITH BANK, MAX. n_z = 2.5, MIN. q = 17.3 kPa (362 lbf/ft^2)

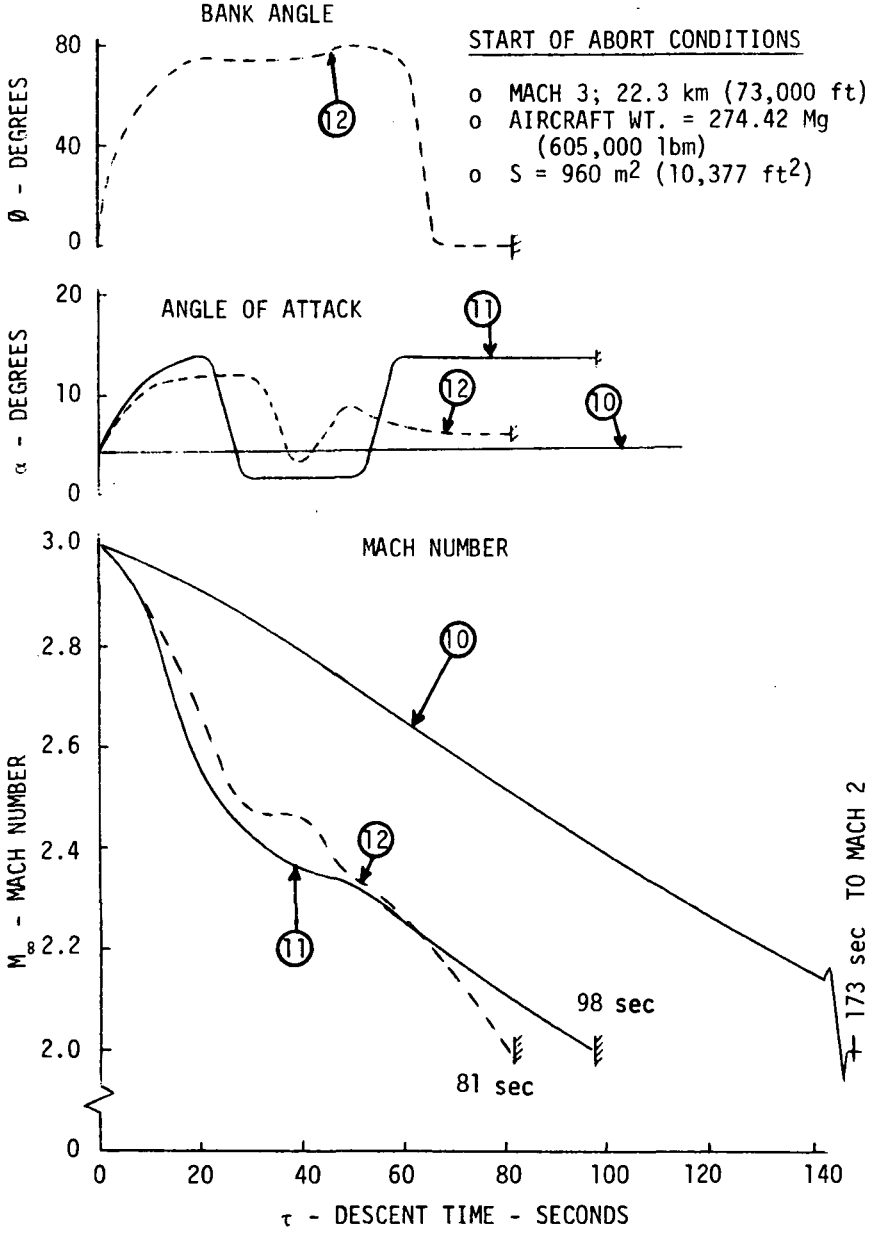

FIGURE 51
COMPARISON OF MACH NUMBER, ANGLE OF ATTACK, AND BANK ANGLE HISTORIES FOR MACH 3 ABORT TRAJECTORIES 10, 11, AND 12

TRAJECTORY	DESCRIPTION
⑩	MAXIMUM (L/D) DESCENT AT α = 4°
⑪	MODULATED α_2(MAX. 14°) DESCENT, MAX n_z = 2.5, MIN. q = 5.1 kPa (106 lbf/ft^2)
⑫	MODULATED α (MAX. 12.2°) DESCENT WITH BANK (MAX. 60°), MAX n_z = 2.5, MIN. q = 17.3 kPa (362 lbf/ft^2)

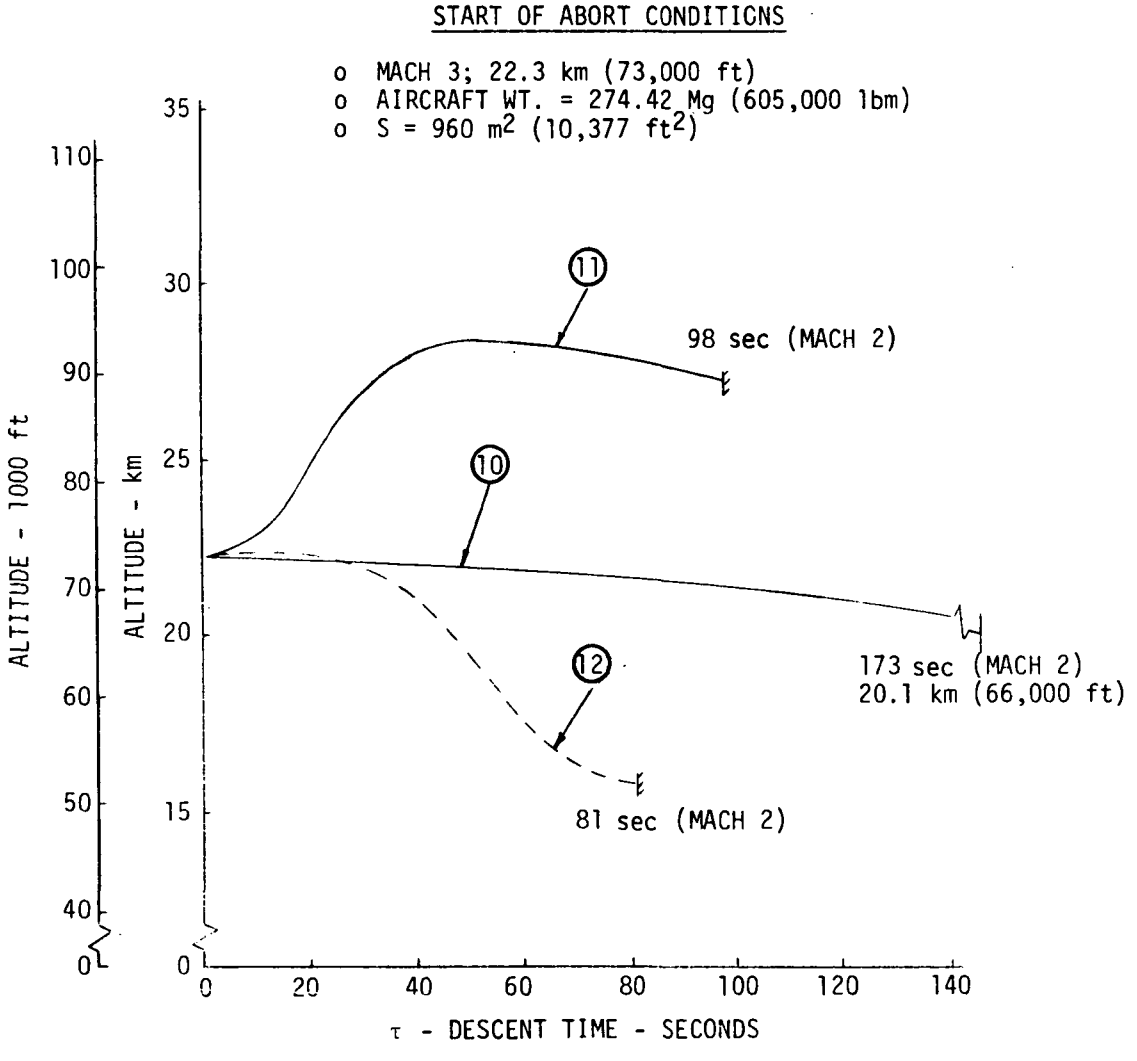

FIGURE 52
COMPARISON OF ALTITUDE HISTORIES FOR MACH 3 ABORT TRAJECTORIES 10, 11, AND 12

START OF ABORT CONDITIONS

- o MACH 3; 22.3 km (73,000 ft)
- o AIRCRAFT WT. = 274.42 Mg (605,000 lbm)
- o S_r = 960 m^2 (10,377 ft^2)
- o T_{WALL} = 366K (200°F)

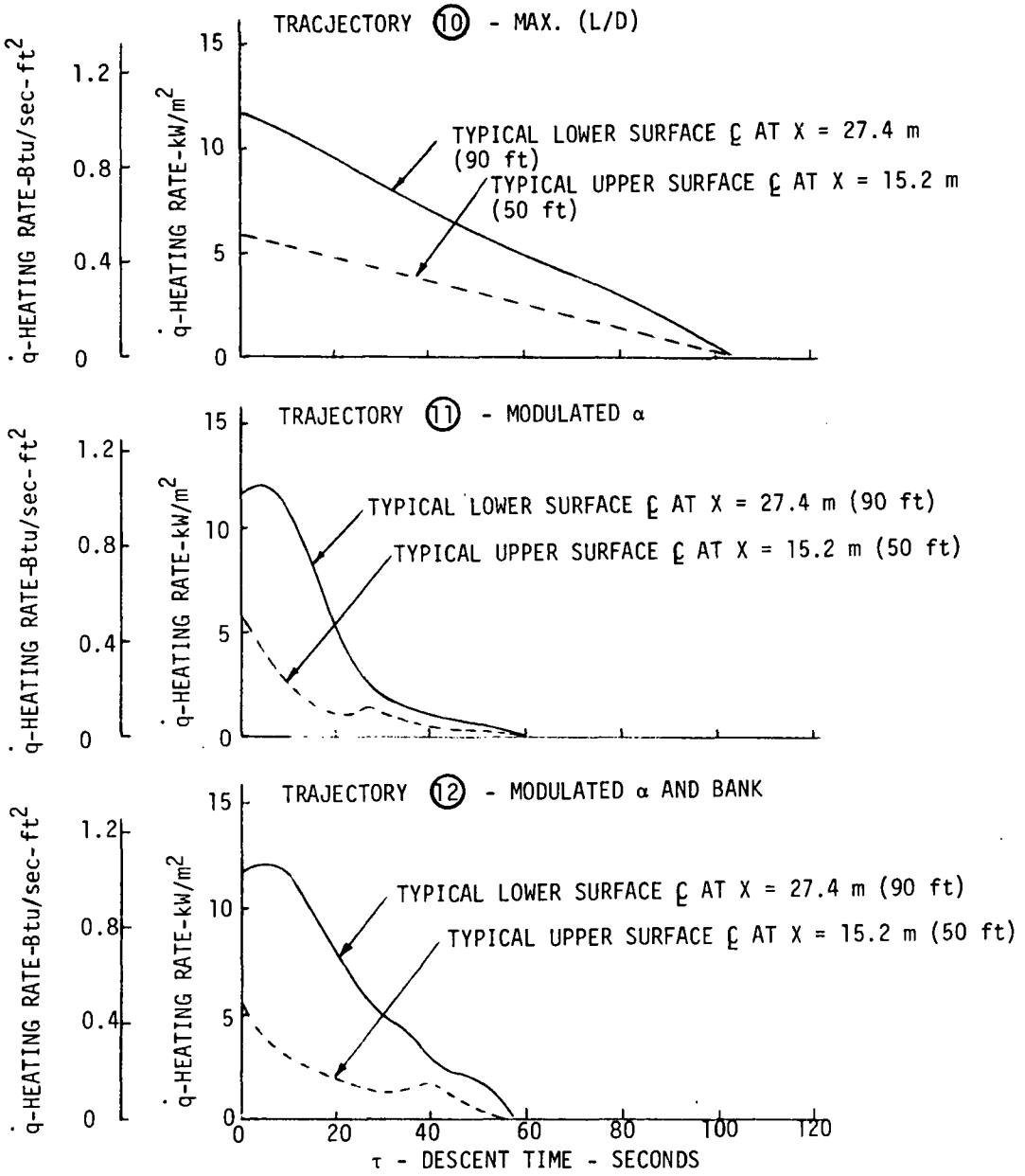

FIGURE 53
COMPARISON OF HEATING RATE HISTORIES FOR MACH 3 ABORT TRAJECTORIES 10, 11, AND 12

TRAJECTORY	TYPICAL HEAT LOADS - KJ/m^2 (Btu/ft^2) (1) LOWER SURFACE, Q_L	UPPER SURFACE, Q_U	WEIGHTED AVERAGE, Q_A (2)
(10)	613 (54)	182 (16)	379 (33.4)
(11)	250 (22)	79 (7)	159 (14)
(12)	340 (30)	113 (10)	216 (19)

(1) HEAT LOAD = $\int \dot{q} d\tau$ FROM FIGURE 53

(2) Q_A (AREA WEIGHTED AVERAGE) = 0.457 Q_L + 0.543 Q_U

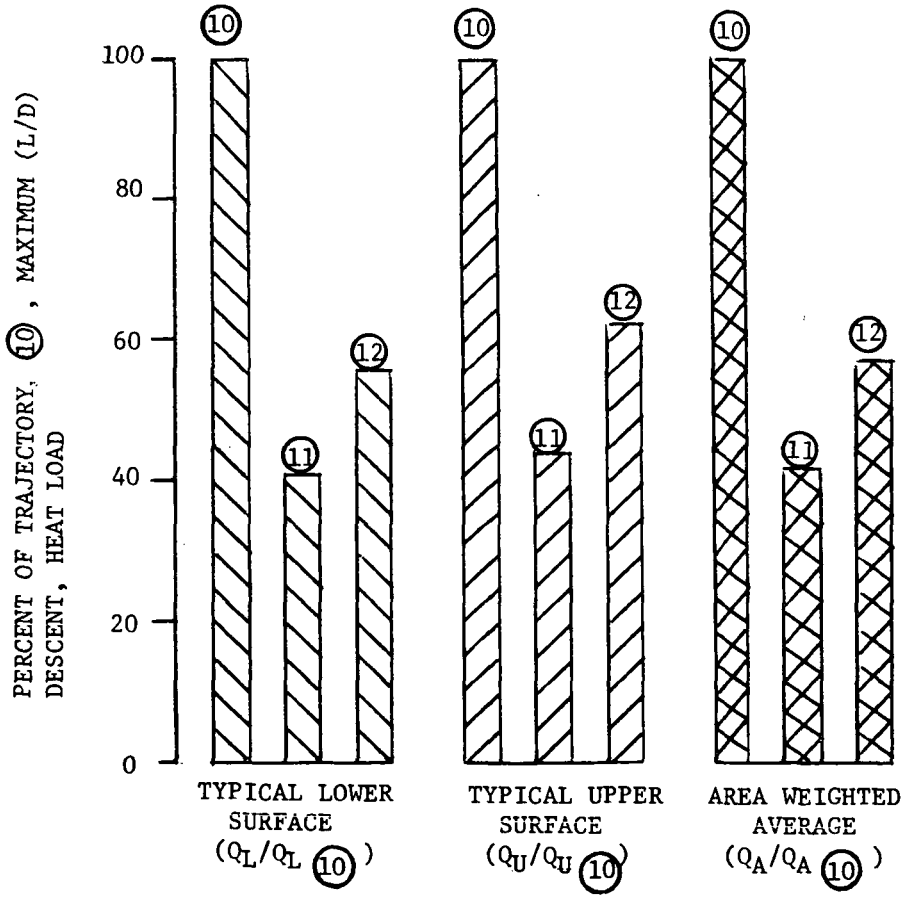

FIGURE 54
COMPARISON OF MACH 3 ABORT DESCENT TRAJECTORY HEAT LOADS

d. Summary of Initial Minimum Heat Load Trajectories - This section summarizes results of the initial abort trajectory studies. These results were utilized in all initial evaluations and screening of potential abort heat protection concepts.

A total of 12 abort trajectories were evaluated, considering a typical lower aircraft surface and a typical upper surface. Mach 6 studies (8 trajectories) resulted in a trajectory producing low abort heat loads. The Mach 3 studies (3 trajectories) resulted in an abort trajectory giving a near minimum head load. Only one trajectory was evaluated for Mach 4.5 abort. However, this trajectory was tailored to produce near minimum abort heating, based on Mach 6 results.

The results of these trajectory studies are summarized below:

	ABORT HEAT LOADS TO TYPICAL SURFACES		
ABORT MACH NUMBER	LOWER MJ/m^2 (Btu/ft^2)	UPPER MJ/m^2 (Btu/ft^2)	AVERAGE* MJ/m^2 (Btu/ft^2)
6	5.23 (460)	0.74 (65)	2.83 (249)
4.5	2.11 (186)	0.63 (55)	1.32 (116)
3	0.25 (22)	0.08 (7)	0.16 (14)

Note: *The area weighted average heat load was based on the following: $Q_{avg} = \frac{A_L Q_L + A_U Q_U}{A_T} = 0.457 Q_L + 0.543 Q_U$, and was considered as representative of average heat load to the aircraft.

Figure 55 illustrates the effect of start-of-abort Mach number on abort heat load. Based on these results, it was concluded that any start-of-abort Mach number above 3 will result in exceeding the heat absorption capacity of bare uninsulated aluminum skin with a typical thickness of 1.02 mm (0.040 in.) as utilized for lower surface coverage.

4.2.3 Optimized Trajectories - The abort trajectories for descent from Mach 3, 4.5, and 6 cruise were reevaluated and refined where required. These trajectories utilized the following constraints. The maximum allowable load factor was 2.5 g's. The minimum flight dynamic pressure was limited to 4.79 kPa (100 lbf/ft^2) to insure adequate control at apogee. The maximum permissible angle of attack was set at 20 degrees for all abort Mach numbers. Aircraft

START OF ABORT CONDITIONS

- CRUISE DYNAMIC PRESSURE = 24.1 kPa (504 lbf/ft^2)
- START OF CRUISE FUEL LOAD

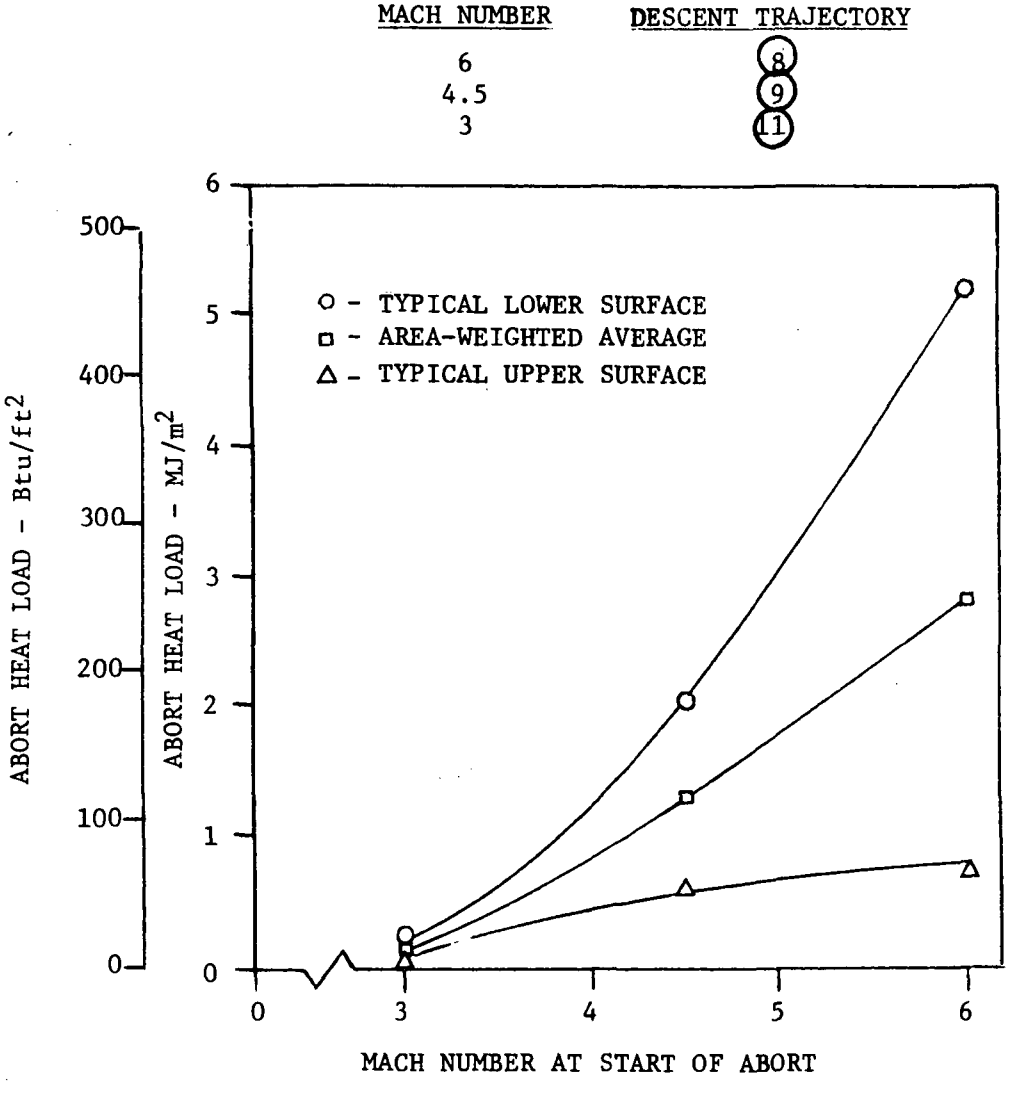

FIGURE 55
EFFECT OF MACH NUMBER ON INITIAL ABORT HEAT LOADS

designed to operate at these Mach numbers can be expected to have adequate control at 20 degrees angle of attack.

Additional study of the baseline aircraft configuration, a Mach 6 design, indicated that the characteristics of this aircraft are not representative of aircraft designed for cruise at Mach 4.5, or Mach 3. For example, a representative lift-to-drag ratio (L/D) for a Mach 3 transport would be on order of 7. The baseline aircraft L/D at Mach 3 was about 5.3. Reference (9) indicated that transport designs optimized for cruise in the Mach number range of 2.7 to 3.2 have wing loadings (W/S) of about 0.22 Mg/m^2 (45 lbm/ft^2). The baseline aircraft, at start of Mach 6 cruise, has a wing loading of 0.27 Mg/m^2 (54.7 lbm/ft^2). The W/S was 0.28 Mg/m^2 (56.9 lbm/ft^2) at start of Mach 4.5 cruise and 0.28 Mg/m^2 (58.3 (lbm/ft^2) at start of Mach 3 cruise.

These differences in aircraft characteristics can result in significant differences in cruise heating rates and total heat loads. Therefore, a decision was made to modify the Mach 6 baseline aircraft characteristics for the Mach 3 and Mach 4.5 cases. Reference (9) was used as a guide to typical LH_2 fueled Mach 3 cruise aircraft wing-loading. The selected W/S value was 0.22 Mg/m^2 (45.5 lbm/ft^2). In the absence of any other guide for a Mach 4.5 transport design, the W/S chosen for the Mach 4.5 cruise aircraft was the average of the Mach 3 and Mach 6 values, a W/S of 0.24 Mg/m^2 (50.1 lbm/ft^2).

a. Mach 6 Abort Heat Loads - Descent Trajectory (8) of Section 4.2.2, the modulated angle of attack (20° max.), with bank angle, stays within trajectory constraints and was representative of a Mach 6 aircraft minimum descent heat load trajectory. Therefore, this trajectory remained unchanged and was considered the final Mach 6 abort trajectory.

b. Mach 4.5 Abort Heat Loads - The abort trajectory for descent from Mach 4.5 cruise was modified from the Trajectory (9) presented in Section 4.2.2. The refined trajectory, using the wing loading value of 0.29 Mg/m^2 (50.1 lbm/ft^2, required substantial bank angle (47 degrees maximum) during the initial 76 seconds of descent to maintain dynamic pressure at 4.79 kPa (100 lbf/ft^2) at apogee. A full 20 degree angle of attack could not be developed at initiation of the pull-up maneuver due to the 2.5g load factor constraint. Therefore, angle of attack was modulated from 5 degrees up to 20 degrees during the initial 16 seconds of descent. Figure 56 presents the modified descent from Mach 4.5 cruise.

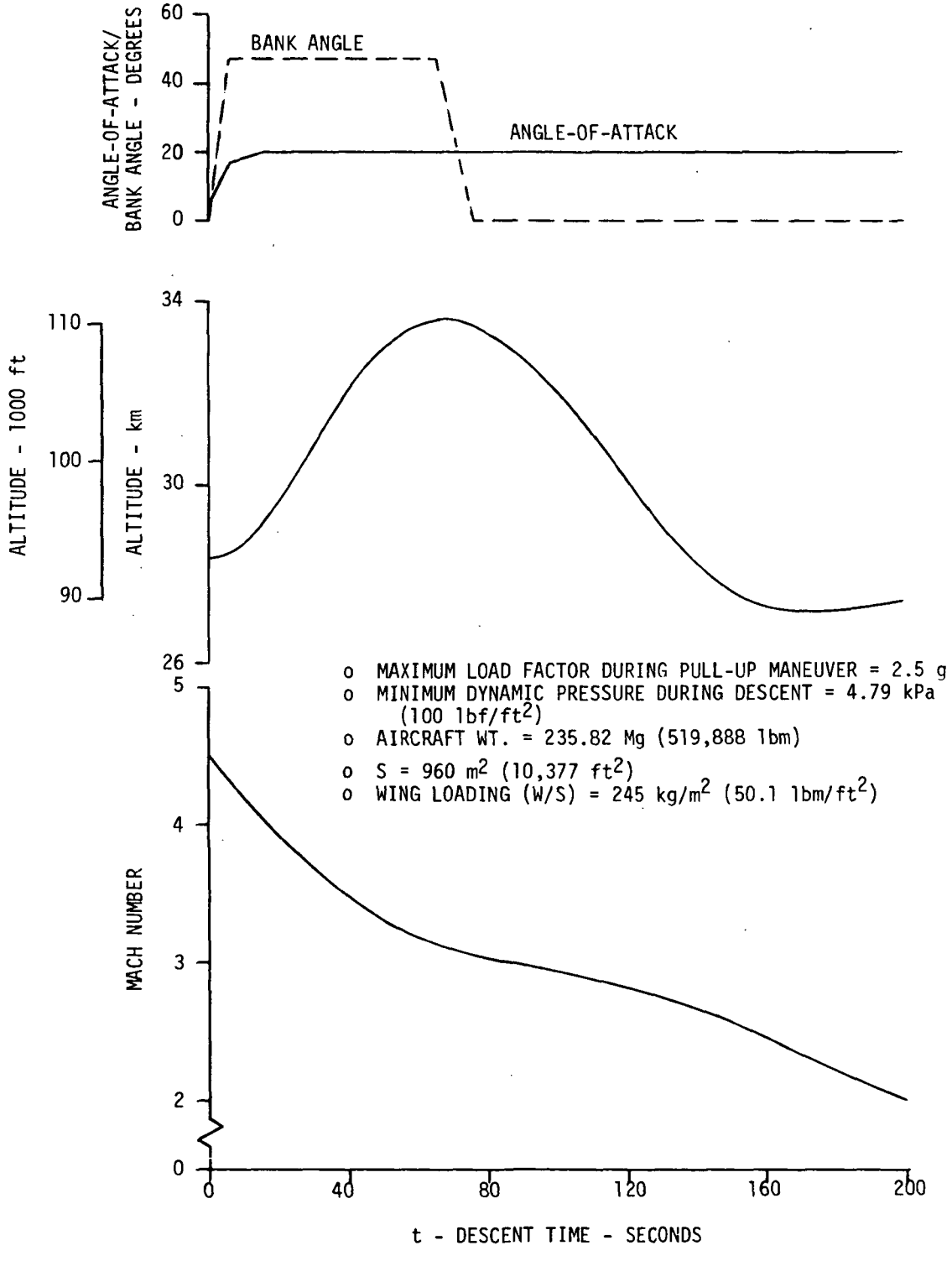

FIGURE 56
REFINED MACH 4.5 ABORT DESCENT TRAJECTORY

c. Mach 3 Abort Heat Loads - The abort trajectory for descent from Mach 3 cruise was modified from the Trajectory (11) presented in Section 4.2.2. The refined trajectory, a load factor limited pull-up, was similar to the Mach 4.5 trajectory in that bank angle was required to maintain dynamic pressure at apogee, and angle of attack required modulation during the pull-up to keep from exceeding the 2.5g limit. Maximum angle of attack during glide was 20 degrees. Figure 57 shows the modified Mach 3 descent trajectory.

d. Heating Rate and Heat Load Comparisons - Figure 58 presents a comparison of the cruise heating rates from Section 4.2.2 (initial trajectories) and the refined trajectories. The modification in aircraft wing loading resulted in slight changes in aircraft altitude, and attitude, for the Mach 3 and Mach 4.5 cases, and a corresponding change in heating rate. As shown, the significant change was at Mach 4.5.

Figure 59 compares the abort heat loads for the refined trajectories with those from Section 4.2.2. The difference in magnitude of the heat load for Mach numbers less than 6 was significant and resulted in weight reductions for the candidate thermo-structural concepts configured to survive the abort heating. The reduction in heat load was due to the use of the high (20° versus 14°) angle of attack and the reduction in wing loading. The increased angle of attack resulted in high lift coefficients (higher glide altitude) leading to reduced heating rates, and lower lift-to-drag ratio (reduced glide time).

Reference (10) presented a detailed examination of the envelope of probable descent operating conditions for a hypersonic air-breathing research airplane. Trends in total heat load as a function of cruise Mach number, cruise dynamic pressure, angle-of-attack limitations, pull-up "g" loads, etc., were presented. The Reference (10) findings were compared with those presented herein as a check on the validity of our results. Reference (3), which presented estimates of the reductions in total descent heat loads available from a pull-up maneuver, is included in the comparison. Figure 60 presents the comparison of abort maneuver heat loads.

The trends for the Reference (10) data and the data of this study are about the same and show an increase in the ratio of abort heat load-to-maximum L/D descent heat load with decreasing Mach number. The trend of the Reference (3) data shown by Figure 60 may be due to the difference in techniques used

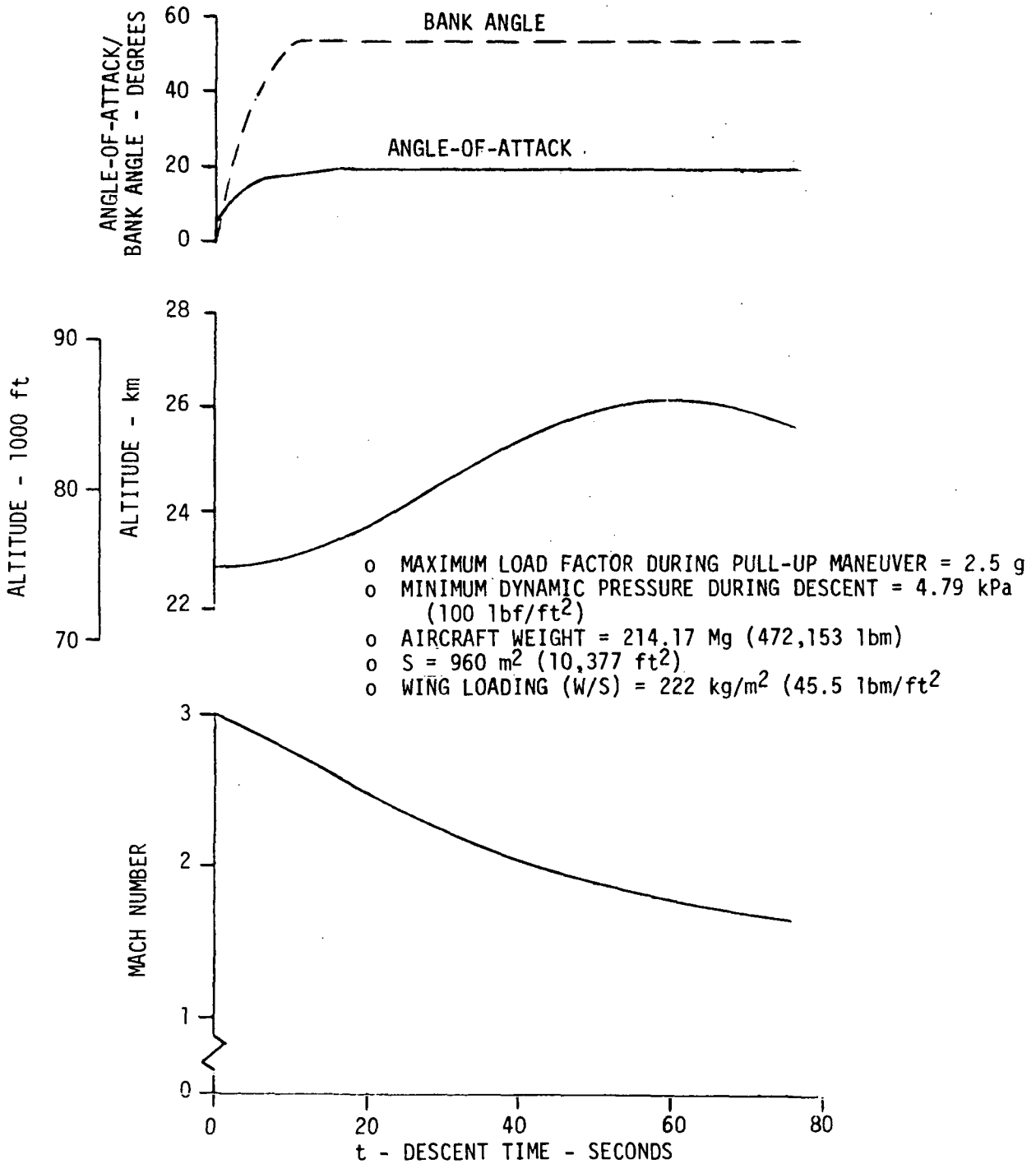

FIGURE 57
REFINED MACH 3 ABORT DESCENT TRAJECTORY

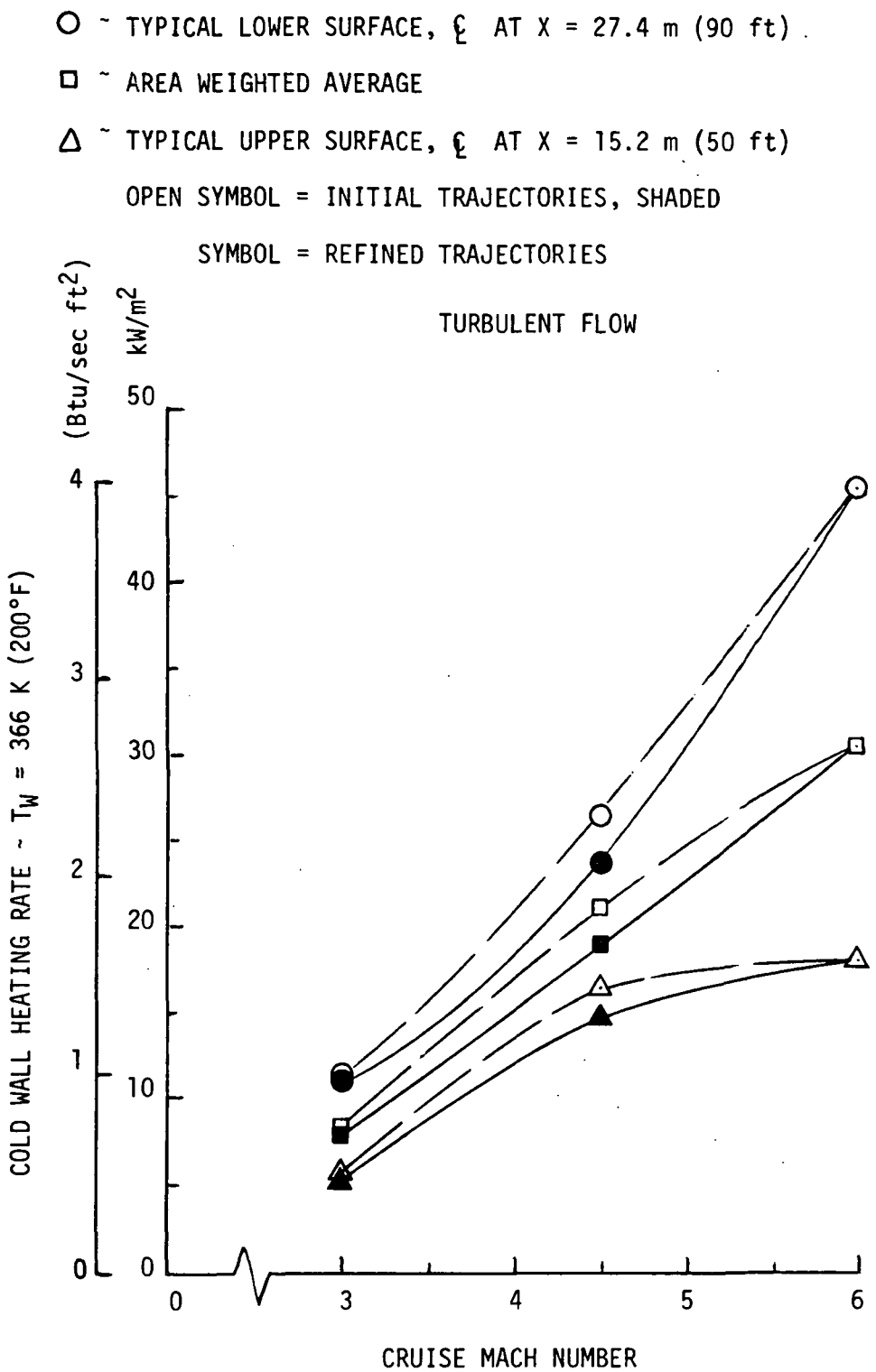

FIGURE 58
AIRCRAFT HEATING RATES AT CRUISE

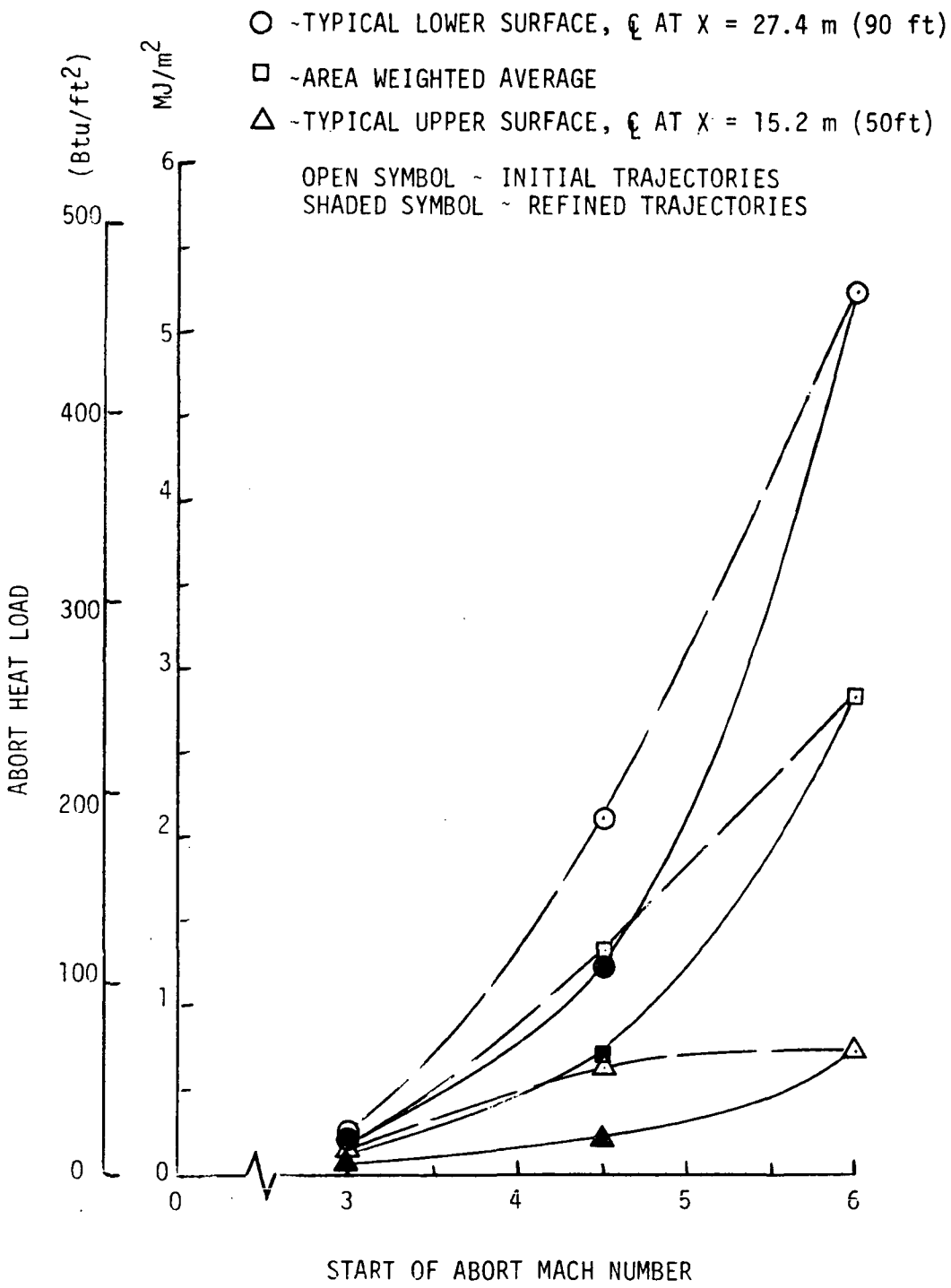

FIGURE 59
REFINED TRAJECTORIES REDUCE ABORT HEAT LOADS

□ - REFERENCE (10) 2.5g PULL-UP FROM CRUISE AT q = 23.94 kPa (500 lbf/ft^2), α = 20° GLIDE.

△ - REFERENCE (3) 2.0g PULL-UP FROM CRUISE AT q = 19.15 kPa (400 lbf/ft^2), α = 20° GLIDE.

○ - THIS STUDY, REFINED TRAJECTORIES, 2.5g PULL-UP FROM CRUISE AT q SHOWN, α = 20° GLIDE. ABORT q MINIMUM LIMITED TO 4.79 kPa (100 lbf/ft^2)

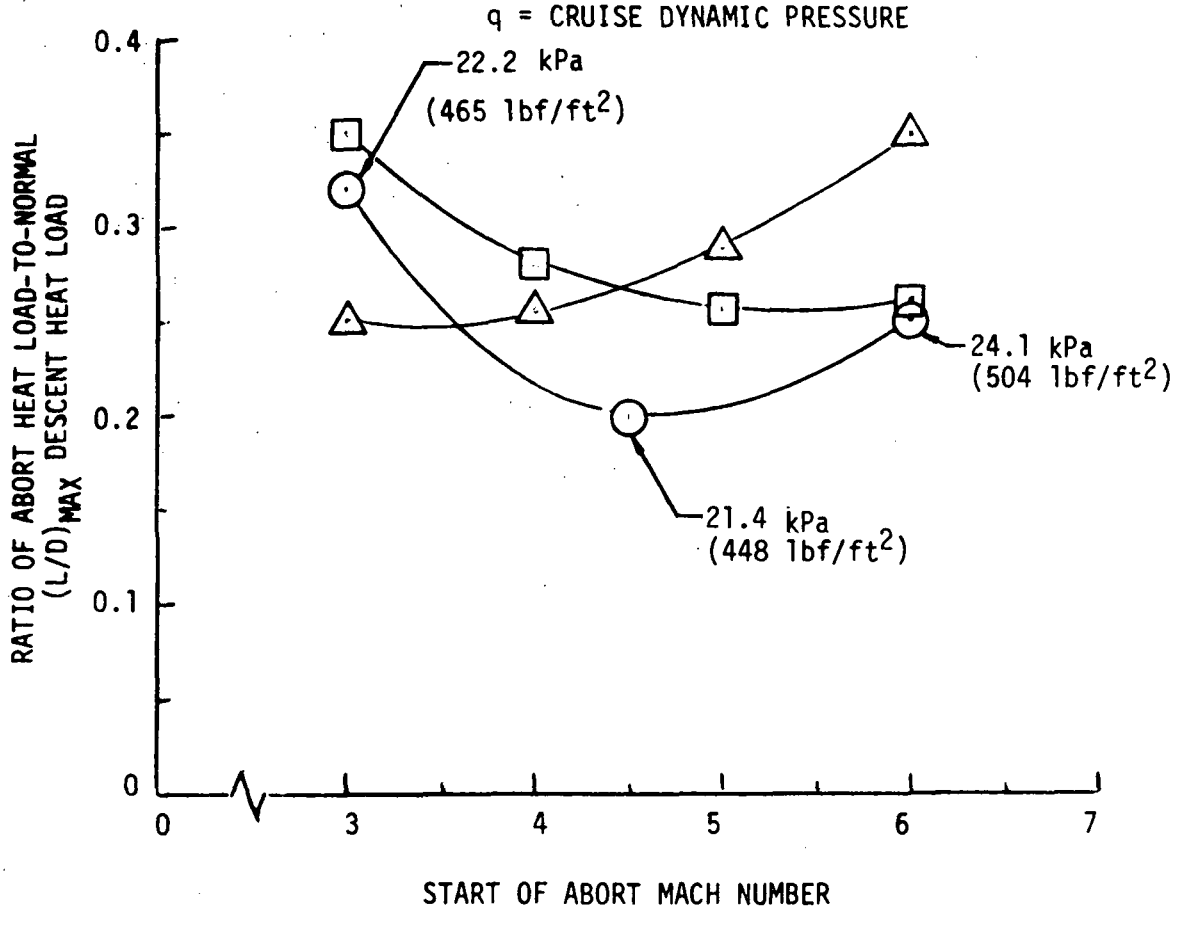

FIGURE 60
COMPARISON OF ABORT MANEUVER HEAT LOADS

during the pull-up maneuver. Both the Reference (10) and the MCAIR abort maneuvers utilized lift reduction at apogee prior to reaching the constant angle of attack equilibrium glide path. The Reference (10) investigation used a reduction in angle of attack to kill lift. Our evaluation used bank angle to reduce lift.

The Reference (3) study maintained maximum angle of attack (and lift) through apogee without an attempt to control minimum dynamic pressure at apogee, or sink rate after apogee. The current study data shows somewhat lower ratios of abort heat load-to-maximum (L/D) descent heat load than the Reference (10) data. This is due to the significant difference in wetted area of the aircraft compared. The much larger transport design, compared to the small research aircraft, would be expected to have a lower average heating rate at any given flight condition.

The refined abort trajectories discussed above were used to determine the cruise and abort thermal protection requirements for each of the candidate concepts selected for concept optimization.

4.3 FAIL-SAFE THERMOSTRUCTURAL CONCEPTS

A number of studies, References (11), (12), (13), (14), and (15), have shown that actively cooled structure has the potential for lower weight than hot structure for hydrogen fueled high speed aircraft. Because of its high thermal conductivity, high structural efficiency, and low cost, aluminum is presently the preferred material for actively cooled structure. However, in the event of inactivity following a cooling system failure, unprotected aluminum would rapidly overheat, resulting in catastrophic failure.

Providing a redundant cooling system may not in all instances ensure against such a failure. Therefore, the objective of this portion of the study was to define and evaluate thermostructural concepts for actively cooled structure which will absorb an abort heat load in case of cooling system failure.

4.3.1 Baseline Actively Cooled Structure - A baseline actively cooled structural system was defined for each of the three Mach/altitude cruise conditions and weights were determined. The baseline weights were derived to ensure a consistent basis of comparison for evaluating candidate fail-safe abort concepts. Analytical methods included approximate expressions and

correlations for active cooling system weight estimates and simplified thermal analyses for actively cooled panel designs. Typical upper and lower surface locations representative of average external heating rates were used, with total system heat loads being determined by area-averaging these typical values over the entire aircraft surface. The actively cooled panel design analyses were then verified by a more detailed computer analysis.

Major design parameters are summarized on Figure 61 for baseline designs applicable to Mach 3, 4.5 and 6 using cruise altitudes corresponding to a freestream dynamic pressure of approximately 24.1 kPa (500 lb_f/ft^2). Each baseline includes a nonredundant active cooling system, employing 60/40 methanol/water coolant which exits the actively cooled panels at 322 K (120°F) and is cooled to 255 K (0°F) for return to the inlets.

The active cooling systems were assumed to contain only a single coolant loop. However, some selected components, such as coolant pumps and temperature control valves were assumed to be redundant, as shown by Figure 14. The actively cooled panels consist of uninsulated 1.02 mm (0.040 in.) aluminum skins, to which 8.64 mm (0.34 in) I.D. dee-tubes are attached and spaced to limit aluminum skin temperature to 394 K (250°F) during sustained cruise. No additional heat protection was provided for an abort trajectory. Designs of actively cooled panels were based on typical average values of upper and lower surface cold wall heating rates (T_{wall} = 366K (200°F)) defined by Figure 41. As such, the design parameters are typical of only upper and lower surface configurations. A considerable variation in heating rates will occur at various locations on the aircraft, as shown in Figure 41. In-depth analysis of other locations was not considered necessary for this portion of the study. However, maximum heating rate locations are addressed in the evaluation of passive abort heat protection concepts.

a. Baseline Weight Parametrics - Figures (62), (63) and (64) present the effects of system coolant pressure drop and panel coolant outlet temperature on system weight for cruise Mach numbers of 3, 4.5 and 6, respectively. A coolant outlet temperature of 322 K (120°F) and a system pressure drop of 1.17 MPa (170 lb_f/in^2) were selected for the baseline systems for all three baseline cruise Mach numbers. Designing the system for coolant pressure drops greater than 1.17 MPa (170 lb_f/in^2) appears to offer diminishing returns in terms of total weight.

	MACH 3 @ 22.3 km		MACH 4.5 @ 27.5 km		MACH 6 @ 32 km	
ACTIVELY COOLED PANELS	UPPER	LOWER	UPPER	LOWER	UPPER	LOWER
HEATING RATE - kW/m^2 (Tw = 366 K)	5.8	11.6	16.8	26.6	18.2	45.4
ALUM. SKIN THICKNESS - mm	1.02	1.02	1.02	1.02	1.02	1.02
COOLANT TUBE SPACING - cm	10.7	7.5	6.2	4.9	6.0	3.8
COOLANT INLET TEMP - K	273	273	273	273	273	273
COOLANT OUTLET TEMP - K	322	322	322	322	322	322
MAX. SKIN TEMP - K	394	394	394	394	394	394
MAX. SKIN LOCAL ΔT - K	49	46	43	39	42	34
COOLANT FLOWRATE PER TUBE - g/s	16.9	23.8	28.8	35.8	29.5	46.5
COOLANT TUBE ΔP - kPa	14	21	28	41	30	66
PANEL UNIT WEIGHT - kg/m^2 ⚠1	3.47	3.75	3.94	4.24	3.98	4.67
TOTAL PANEL WEIGHT - Mg ⚠1	10.748		12.173		12.83	
ACTIVE COOLING SYSTEM						
HEAT LOAD - MW	25.2		63.6		90.2	
COOLANT FLOWRATE - kg/s	113		286		407	
SYSTEM ΔP - MPa	1.17		1.17		1.17	
SYSTEM WEIGHT - Mg						
COOLANT IN LINES	1.153		2.298		3.011	
COOLANT IN PANELS	1.036		1.663		1.954	
DISTRIBUTION LINES	0.216		0.431		0.565	
DUAL PUMPS	0.064		0.132		0.227	
HEAT EXCHANGER	0.265		0.667		0.947	
RESERVOIR	0.142		0.254		0.318	
TOTAL	2.876		5.445		7.022	
APU FUEL PENALTY - Mg (0.338 g/kW•s)	0.429		0.720		0.768	
TOTAL WEIGHT (PANELS, ACS, APU FUEL) - Mg	14.053		18.338		20.62	
H_2 FLOWRATES - kg/s REQUIRED FOR COOLING	6.76		17.0		24.1	

⚠1 ALUM. SKIN, DRY COOLANT TUBES, INTERFACIAL ADHESIVE ONLY

FIGURE 61a
BASELINE SYSTEM DESCRIPTIONS

	MACH 3 @ 73,000 ft		MACH 4.5 @ 90,000 ft		MACH 6 @ 105,000 ft	
ACTIVELY COOLED PANELS	UPPER	LOWER	UPPER	LOWER	UPPER	LOWER
HEATING RATE - Btu/sec ft^2 (T_w = 200°F)	0.508	1.026	1.48	2.34	1.6	4.0
ALUM. SKIN THICKNESS - in	0.040	0.040	0.040	0.040	0.040	0.040
COOLANT TUBE SPACING - in	4.2	2.95	2.46	1.94	2.37	1.49
COOLANT INLET TEMP - °F	0	0	0	0	0	0
COOLANT OUTLET TEMP - °F	120	120	120	120	120	120
MAX. SKIN TEMP - °F	250	250	250	250	250	250
MAX. SKIN LOCAL ΔT - °F	89	82	78	70	76	61
COOLANT FLOWRATE PER TUBE - lbm/hr	134	189	228	284	234	369
COOLANT TUBE ΔP - psi	2	3	4	6	4.3	9.5
PANEL UNIT WEIGHT - lbm/ft^2 (1)	0.7112	0.7685	0.8069	0.8687	0.8156	0.9571
TOTAL PANEL WEIGHT - lbm (1)	23,695		26,836		28,286	
ACTIVE COOLING SYSTEM						
HEAT LOAD - Btu/hr	86×10^6		217×10^6		308×10^6	
COOLANT FLOWRATE - lbm/hr	0.9×10^6		2.27×10^6		3.23×10^6	
SYSTEM ΔP - psid	170		170		170	
SYSTEM WEIGHT - lbm						
COOLANT IN LINES	2542		5066		6638	
COOLANT IN PANELS	2284		3666		4308	
DISTRIBUTION LINES	477		951		1246	
DUAL PUMPS	140		290		500	
HEAT EXCHANGER	584		1471		2088	
RESERVOIR	313		559		699	
TOTAL	6340		12003		15479	
APU FUEL PENALTY - lbm (2 lbm/hp•hr)	945		1587		1694	
TOTAL WEIGHT (PANELS, ACS, APU FUEL) - lbm	30,980		40,426		45,459	
H_2 FLOWRATES - lbm/sec REQUIRED FOR COOLING	14.9		37.4		53.2	

(1) ALUM. SKIN, DRY COOLANT TUBES, INTERFACIAL ADHESIVE ONLY

FIGURE 61b
BASELINE SYSTEMS DESCRIPTIONS

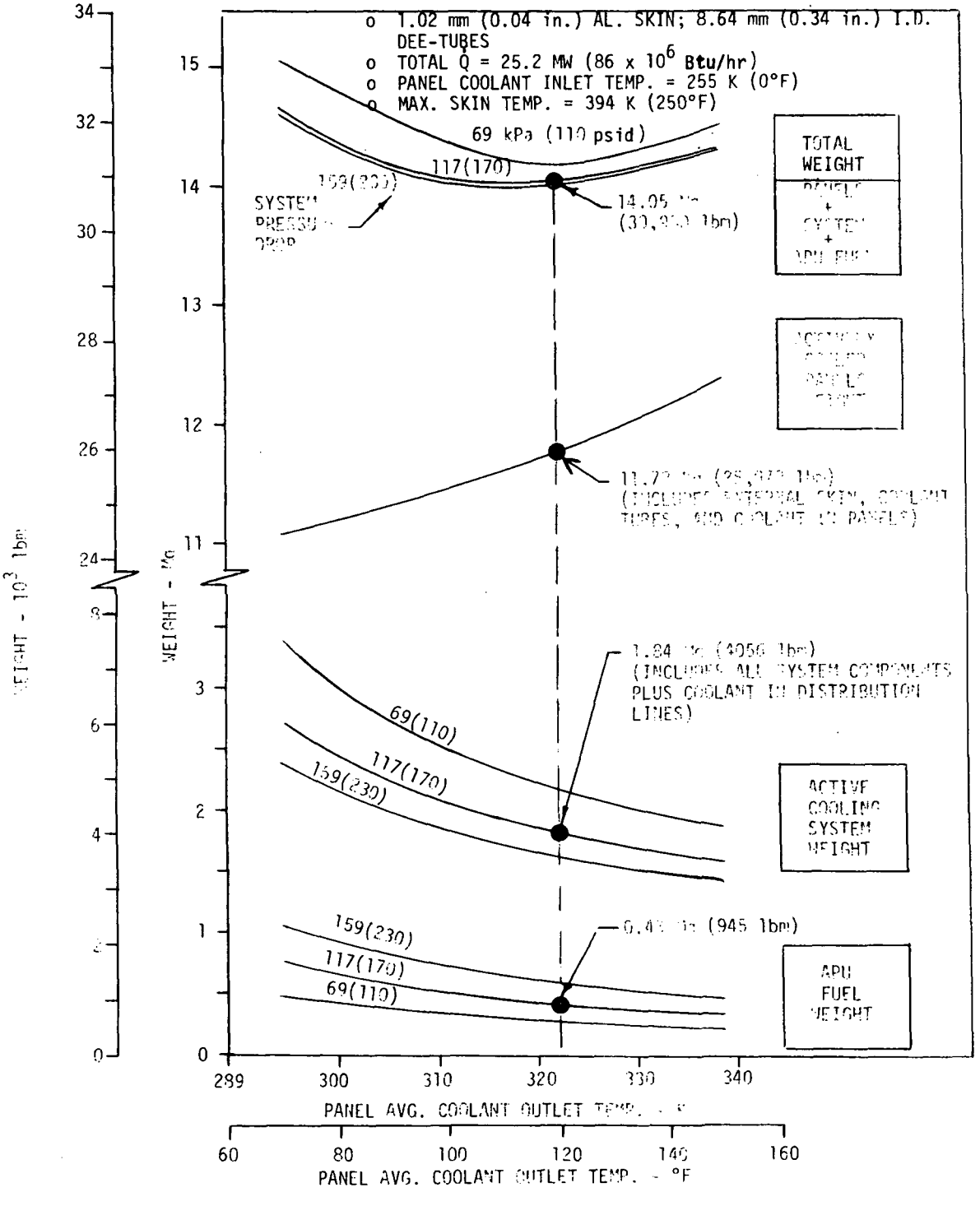

FIGURE 62
MACH 3 BASELINE SYSTEM WEIGHT PARAMETRICS

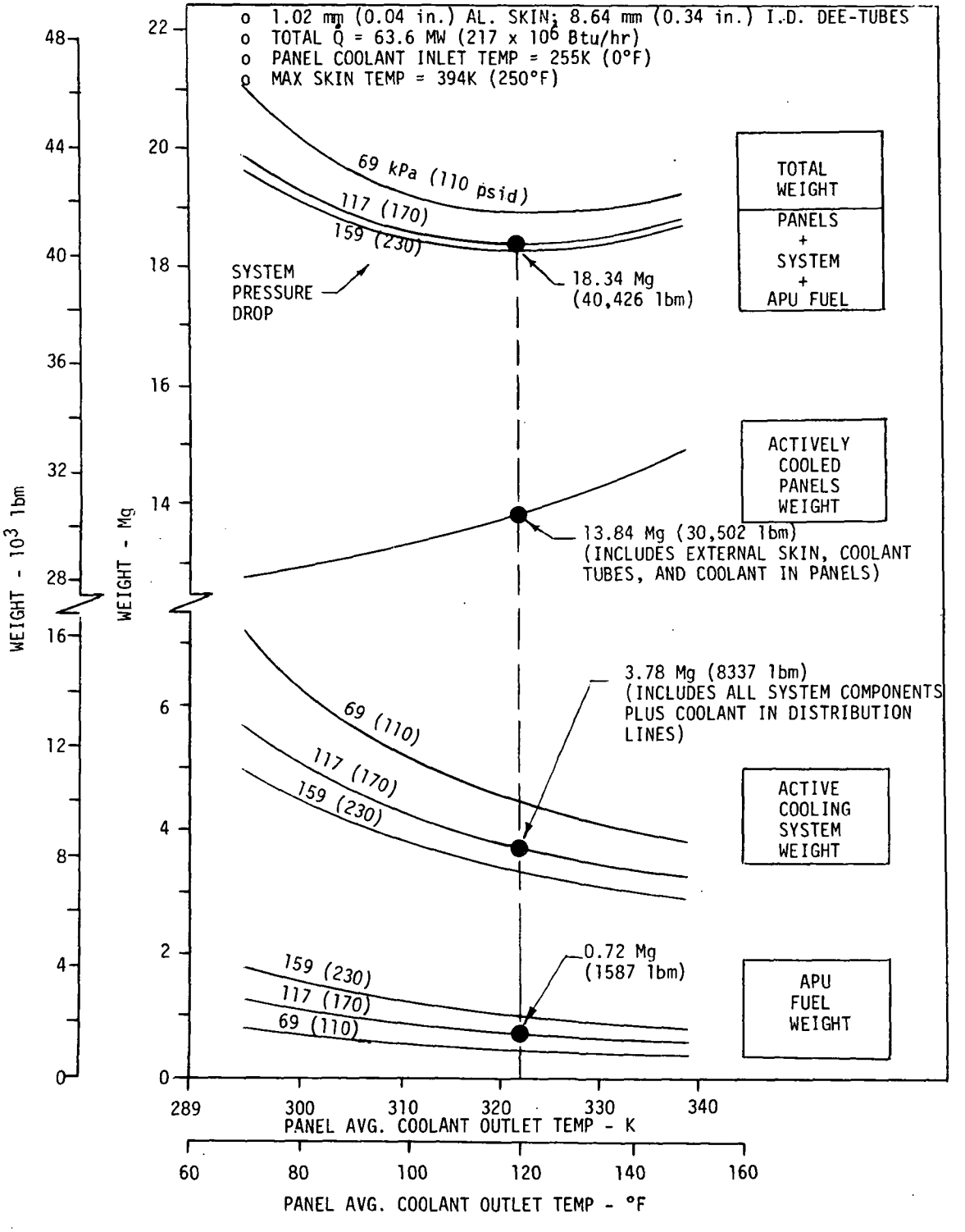

FIGURE 63
MACH 4.5 BASELINE SYSTEM WEIGHT PARAMETRICS

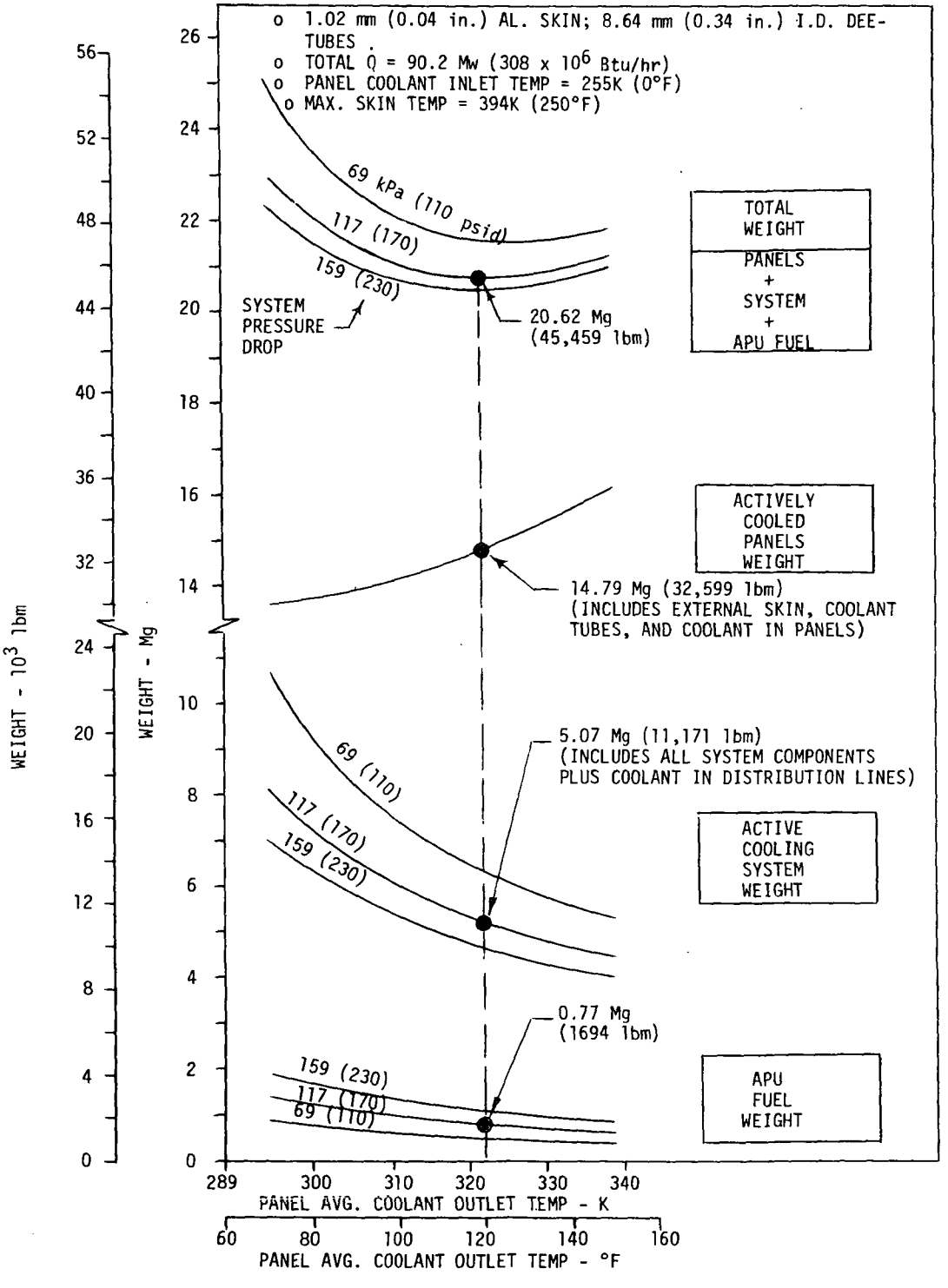

FIGURE 64
MACH 6 BASELINE SYSTEM WEIGHT PARAMETRICS

o Actively Cooled Panels - In assessing actively cooled panel requirements, initial configurations were based on the preliminary design relations shown by Figure 65. These simplified expressions provided an initial determination of required coolant tube spacing (pitch) and coolant flow rate to limit peak panel skin temperature to 394 K (250°F) during sustained cruise for each Mach/altitude design condition. A number of common assumptions were made based on the results of MCAIR work on actively cooled panel designs (Reference (2) and (6)), in order to minimize the number of variables in the analysis. The more important ones include: (1) 1.02 mm (0.04 in) aluminum panel skins, (2) 8.14 mm (0.34 in) I.D. dee-shaped coolant tubes adhesively bonded to the skins, and (3) the use of a 60/40 mixture of methanol/water coolant entering the panels at 255 K (0°F).

Once the actively cooled panels were initially sized, a detailed thermal model was employed to verify the baseline designs. Salient features of this model are summarized by Figure 66.

The model represented a cooled panel one pitch (distance between tube centers) wide and 6.1 m (20 ft) long (the nominal panel length). Ten fluid nodes and 54 structural nodes were incorporated to accommodate both lengthwise and spanwise temperature gradients. Heat transfer coefficients between the coolant and tube wall, as well as pressure drop down the length of the coolant tube, were based on conventional laminar and turbulent flow expressions. Figure 67 shows results of a typical analysis applicable to the Mach 6 aircraft lower surface baseline configuration.

o Active Cooling System - Active cooling system weight sensitivities to heat load, coolant pressure drop, and actively cooled panel outlet coolant temperature were derived to provide a more reliable weight baseline, and also to provide a data base for subsequent comparative analyses of candidate fail-safe abort concepts which employ insulated exterior surfaces (i.e., overcoats or heat shields).

Basis of System Weights - The weight parameters shown below are based upon first approximation type expressions, which utilize or correlate results of more in-depth studies on the baseline cooling system per Reference (2) and Figure 68. Further iterations were not deemed necessary, since the primary objective was to obtain trends and more insight for conduct of subsequent analyses.

INPUT PARAMETERS:

- $\dot{q}$ ~ DESIGN HEATING RATE ~ kW/m^2 (Btu/sec~ft^2) ~ VARIABLE
- t_s ~ PANEL SKIN THICKNESS ~ 1.02 mm (0.04 in.)
- D ~ COOLANT TUBE DIAMETER 0.864 cm (0.34 in.)
- T_{ci} ~ COOLANT TEMPERATURE @ PANEL INLET ~ 255 K (0°F)
- T_{co} ~ COOLANT TEMPERATURE @ PANEL EXIT ~ K (°F) ~ VARIABLE

DERIVED PARAMETERS:

- P ~ TUBE SPACING (PITCH) ~ cm (in.)
- $\dot{m}_t$ ~ COOLANT FLOWRATE PER TUBE ~ g/s (lbm/hr)
- ΔP ~ COOLANT PRESSURE DROP ~ kPa (psid)
- T_m ~ MAXIMUM SKIN TEMPERATURE ~ K (°F)

WHERE:

$$\dot{m}_t = \frac{C_1 \dot{q} P}{T_{co} - T_{ci}}$$

$$C_1 = 18.23\ (7500)$$

$$T_m = T_c + (T_r - T_c) + (T_m - T_r)$$

$$T_m = T_c + \frac{C_2 \dot{q} P}{(UA)_{c-r}} + \frac{C_3 (P-D)^2 \dot{q}}{t_s}$$

$$C_2 = 10\ (300)$$
$$C_3 = 0.0904\ (0.469)$$

$$\Delta P = C_4\ (\dot{m}_t)^{1.75}$$

$C_4 = 8.27 \times 10^{-2}\ (3.2 \times 10^{-4})$ FOR T_{co} = 294 K (70°F)

$C_4 = 7.75 \times 10^{-2}\ (3.0 \times 10^{-4})$ FOR T_{co} = 322 K (120°F)

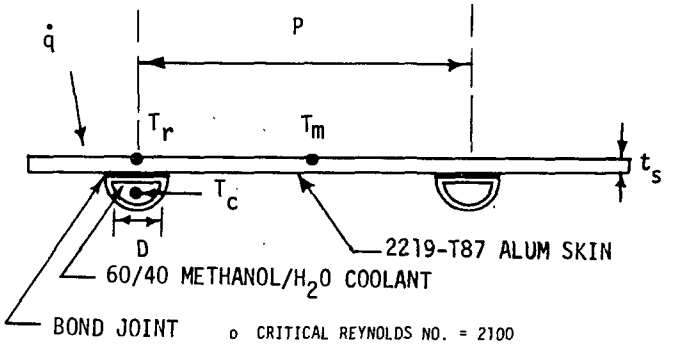

- CRITICAL REYNOLDS NO. = 2100
- BOND JOINT CONDUCTANCE = 5.76 kW/K PER m (3333 Btu/hr °F per ft)

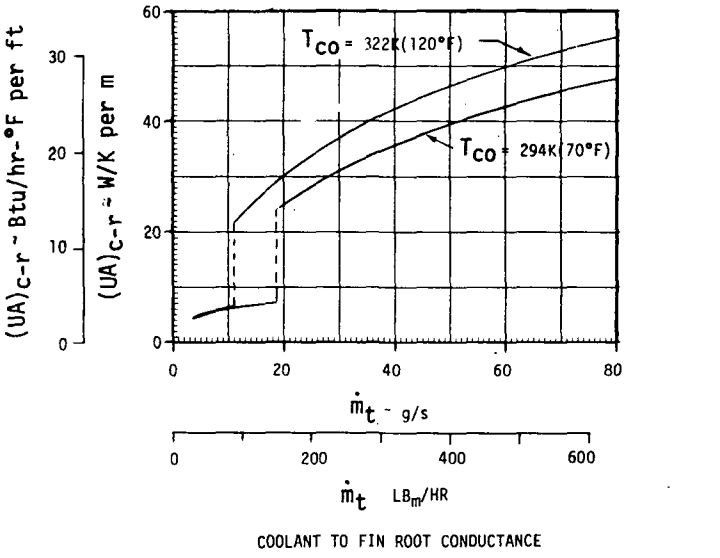

COOLANT TO FIN ROOT CONDUCTANCE

FIGURE 65
ACTIVELY COOLED PANEL PRELIMINARY THERMAL DESIGN PARAMETERS

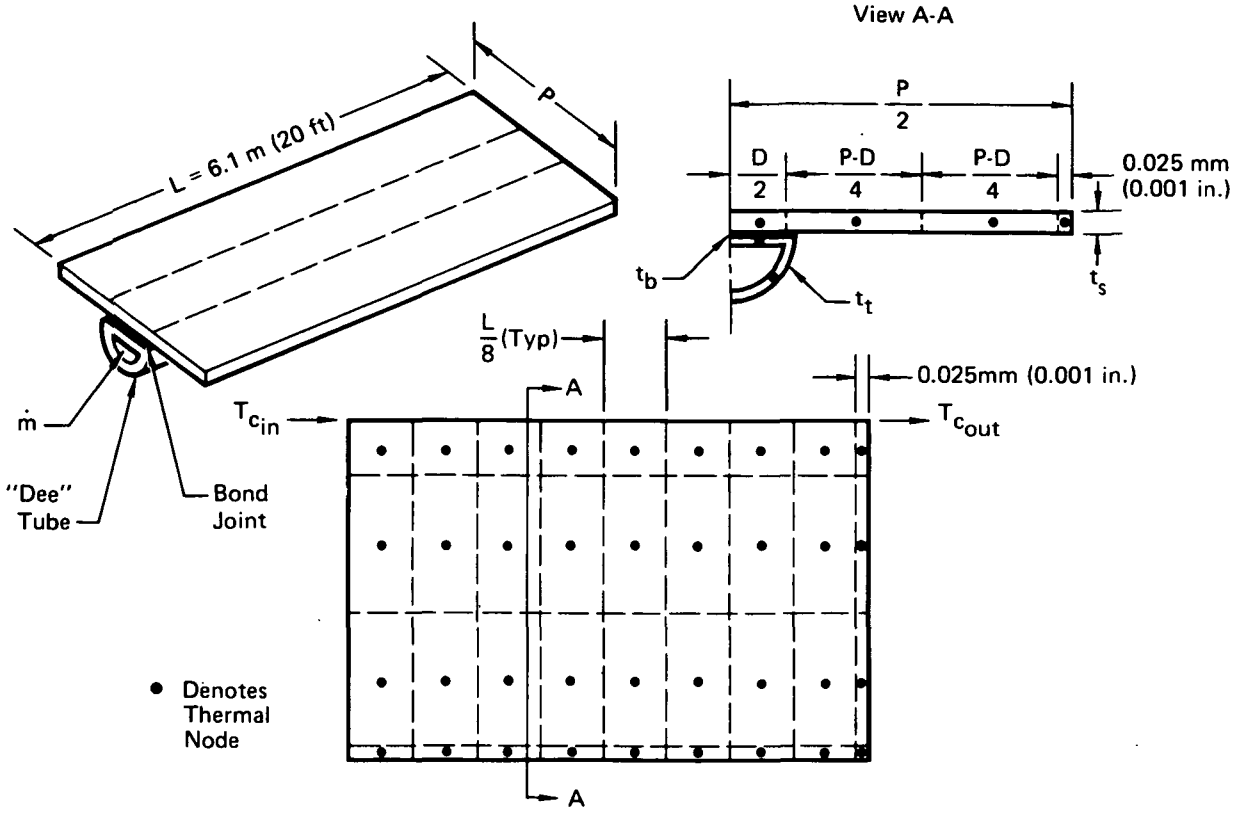

Constant Inputs:

- Material Properties vs Temperature, 60% Methanol/40% Water Solution 2219-T87 Aluminum
- Adhesive Bond Characteristics
- L = 6.1 m (20 ft)
- D = 8.64mm (0.34 in.)
- t_t = 0.89mm (0.035 in.)
- t_b = 0.13mm (0.005 in.)
- $T_{c_{in}}$ = 256K (0°F)

Variable Inputs:

- Surface Heating Rate ($\dot{q}$)
- External Heat Transfer Coefficient (h)
- Adibatic Wall Temperature ($T_{\alpha\omega}$)
- Outer Skin Thickness (t_s)
- Pitch (P)
- Coolant Flowrate ($\dot{m}$)

Output:

- 10 Fluid Node Temperatures
- 54 Structural Node Temperatures
- Coolant Pressure Drop

GP75-0805-28

FIGURE 66
COOLED PANEL THERMAL MODEL

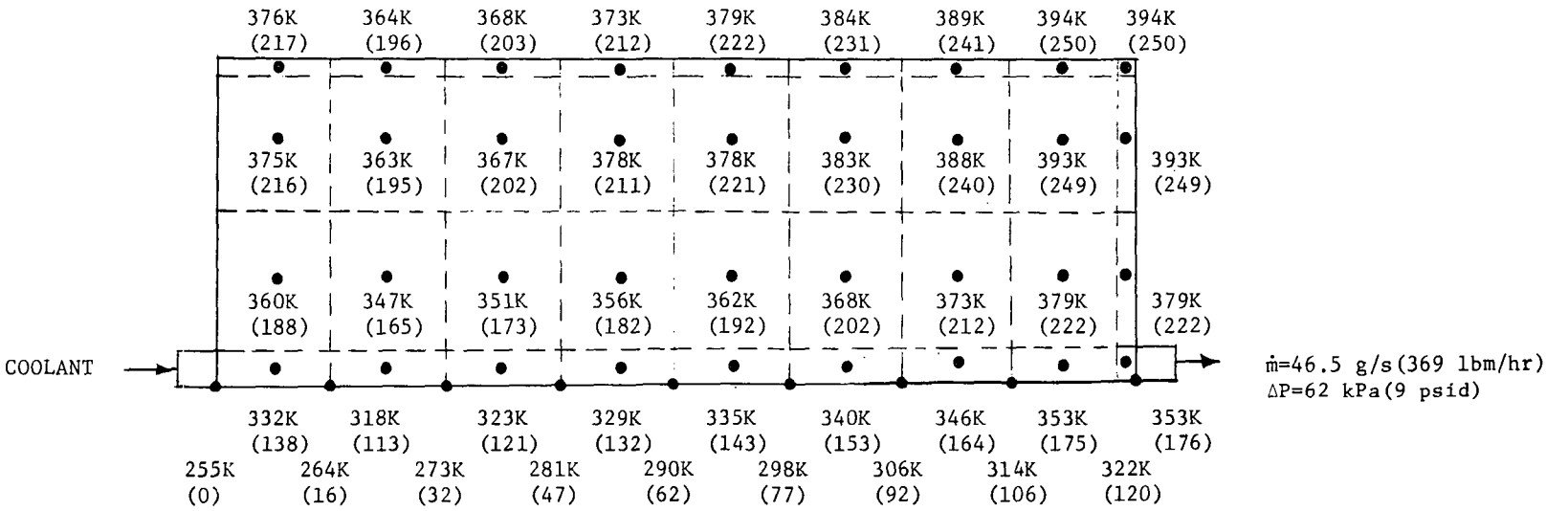

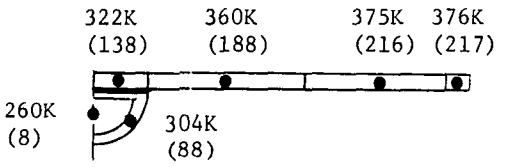

INLET PANEL SEGMENT

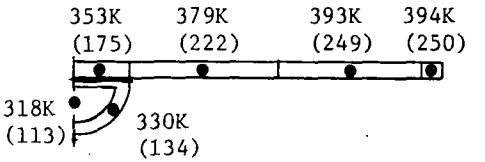

OUTLET PANEL SEGMENT

NOTE: TEMPERATURES IN PARENTHESES ARE °F

FIGURE 67
TYPICAL BASELINE PANEL TEMPERATURES DURING CRUISE
(MACH 6 LOWER SURFACE)

SYMBOL	REFERENCE	DESIGN MACH NUMBER	HEAT LOAD MW (10^6 Btu/hr)	WEIGHT* Mg (lbm)
▲	9	2.7	8.67 (29.6)	1.344 (2,962)
△		3.2	17.5 (59.7)	2.308 (5,083)
■	15	6	67.9 (232)	5.679 (12,520)
□		6	105 (357)	8.518 (18,780)
◓	CURRENT	3	25 (86)	3.304 (7,285)
●	STUDY	4.5	63.5 (217)	6.164 (13,590)
◒	BASELINES	6	90.2 (308)	7.79 (17,173)

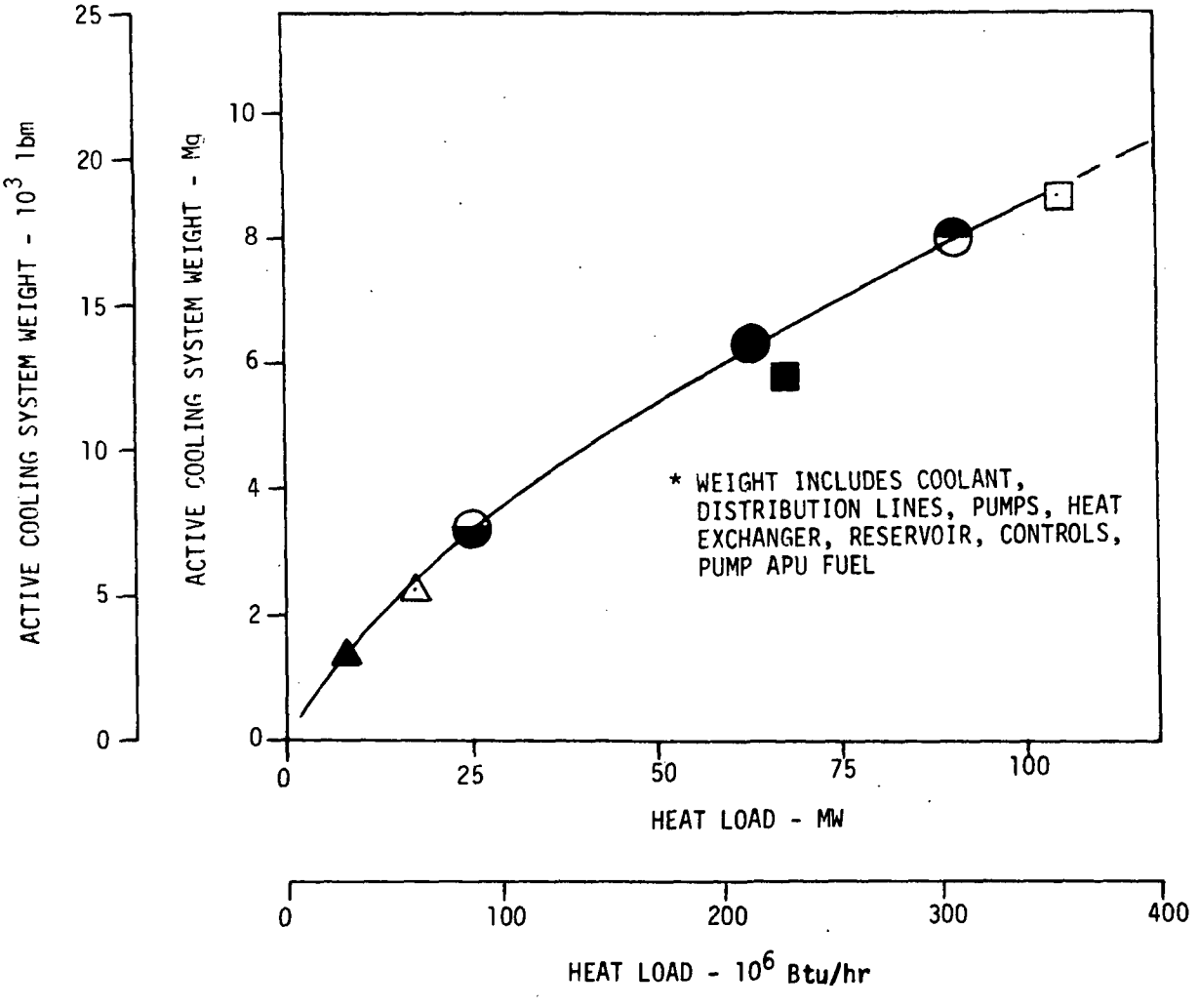

FIGURE 68
ACTIVE COOLING SYSTEM WEIGHT TRENDS

Residual Coolant in Distribution Lines - The coolant distribution system layout and line lengths are, by definition, identical to those of the baseline aircraft. With this ground rule and the further assumption, employed in Reference (2), that all lines are sized on the basis of a constant pressure drop per unit length, the resultant residual coolant weight (W_{Cl}) is dependent upon system flow rate ($\dot{m}_l$), line pressure drop (ΔP_{Ll}), and coolant viscosity (μ), according to the following expression:

$$\frac{W_{Cl}}{W_{CB}} = \left(\frac{\dot{m}_l}{\dot{m}_B}\right)^{0.7368} \left(\frac{\Delta P_{Ll}}{\Delta P_{LB}}\right)^{-0.421} \left(\frac{\mu_l}{\mu_B}\right)^{0.1053}$$

where: W_{CB} = Baseline system line residual coolant = 7.17Mg(15807 lb_m)

$\dot{m}_B$ = Baseline system coolant flow rate = 712 kg/s(5.65 x 10^6 lb/hr)

ΔP_{LB} = Baseline system line ΔP = 395kPa (50 lb_f/in^2)

μ_B = Coolant viscosity at baseline system temperature

Distribution Line Hardware - Dry weight of the distribution system (W_{Ll}) was assumed to vary linearly with residual coolant weight (W_{Cl}) and pump outlet pressure (i.e. system or pump ΔP_l + 276 kPa (40 lb_f/in^2) pump inlet pressure P_i):

$$\frac{W_{Ll}}{W_{LB}} = \frac{W_{Cl}}{W_{CB}} \times \left(\frac{\Delta P_l + P_i}{\Delta P_B + P_i}\right)$$

where: W_{LB} = Baseline system distribution line weight = 1.35Mg (2967 lbm)

ΔP_B = Baseline system total ΔP = 759kPa (110 lb_f/in^2)

Heat Exchanger - Heat exchanger total weight ($W_{T_{H-X}}$) was assumed to vary linearly with heat load, using the baseline heat exchanger weight ($W_{B_{H-X}}$) as a reference point. Coolant contained within the heat exchanger ($W_{C_{H-X}}$) was assumed equal to 40% of the total heat exchanger weight.

$$W_{T_{H-X}} = W_{B_{H-X}}\left(\frac{Q_l}{Q_B}\right)$$

$$W_{C_{H-X}} = 0.4\ W_{T_{H-X}} \quad \text{(Coolant wt.)}$$

where: Q_B = Baseline system heat load = 90.6 MW (308 x 10^6 Btu/hr).

$W_{B_{H-X}}$ = Baseline heat exchanger weight = 950 kg (2088 LBm)

Coolant Pumps - Redundant coolant pumps were assumed for the baseline and the weights determined from Reference (15) data.

Coolant Reservoirs - The following relation was used:

$$\text{Reservoir Wt} = 0.05152\ W_{cs} + 0.1782\ (W_{cs})^{2/3}$$

where: W_{cs} = Coolant in system

$W_{cs} = W_{cl} + W_p + W_{C_{H-X}}$

W_{cl} = Weight of coolant in distribution lines

$W_{C_{H-X}}$ = Weight of coolant in heat exchanger

W_p = Weight of coolant in actively cooled panels

The first term of the reservoir weight expression represents coolant weight in the reservoirs during ground fill at 299K (70°F), while the second is the dry weight of the reservoirs. Reservoir sizing was based on minimum and maximum bulk coolant temperatures of 241K (-25°F) and 325K (+125°F) (i.e. empty at 241K (-25°F) and full at 325K (+125°F).

APU Fuel - For equivalent weight of power required to drive the coolant pump, a value of 0.338 g/kW·s (2.0 lbm/HP hr) was assumed. The specific relationship used is:

$$\text{APU Fuel Wt.} = C\ \dot{m}_1 \Delta P_1 \theta$$

where: C = constant = 1.32 x 10^{-6} (2.53 x 10^{-6})

$\dot{m}_1$ = coolant flow rate ~ g/s (lbm/hr)

ΔP_1 = system pressure drop ~ kPa (psid)

θ = operating time ~ hrs

θ = 1.22 for Mach 6

θ = 1.63 for Mach 4.5

θ = 2.44 for Mach 3

Figure 68 exhibits a comparison of active cooling system weights per References (9) and (15) and the current study. The correlation, in terms of the weight versus heat load, appears good.

For subsequent thermostructural concept evaluation, a general correlation of cooling system weight was derived as a function of system heat load, to provide cooling system weight sensitivity relationships. This correlation is

shown in Figure 69. As a check on the validity of the derived cooling system weight sensitivity factors, a comparison was made for the baseline systems summarized on Figure 61. Figure 70 presents the results of this weight comparison. As shown, the active cooling system weights determined using the weight sensitivity factors are in good agreement with the detailed calculated weights.

Heating Rate Range ($\dot{q}$) (1)	Cooling System Weight			
	Unit Area Panel	Typical Panel (2)	Baseline Aircraft Total Panels (3)	
			Upper Surface	Lower Surface
kW/m^2 ($Btu/sec\ ft^2$)	kg/m^2 (lbm/ft^2)	kg (lbm)	kg (lbm)	kg (lbm)
0 to 2.94 (0 to 0.2593)	$0.1704\dot{q}$ ($0.3961\dot{q}$)	$1.266\dot{q}$ ($31.68\dot{q}$)	$276.2\dot{q}$ ($6910\dot{q}$)	$232.5\dot{q}$ ($5816\dot{q}$)
2.94 to 7.85 (0.2593 to 0.6915	$0.1977 + 0.108\dot{q}$ ($0.0405 + 0.252\dot{q}$)	$1.5 + 0.8057\dot{q}$ ($3.24 + 20.16\dot{q}$)	$320 + 175.7\dot{q}$ ($706 + 4397\dot{q}$)	$269 + 147.9\dot{q}$ ($594 + 3701\dot{q}$)
7.85 to 17.7 (0.6915 to 1.556)	$0.4409 + 0.0792\dot{q}$ ($0.9093 + 0.184\dot{q}$)	$3.27 + 0.5883\dot{q}$ ($7.22 + 14.72\dot{q}$)	$71.4 + 128.3\dot{q}$ ($1575 + 3211\dot{q}$)	$616 + 108.0\dot{q}$ $1358 + 2702\dot{q}$)
> 17.7 (> 1.556)	$0.7446 + 0.0613\dot{q}$ ($0.1525 + 0.1425\dot{q}$)	$5.53 + 0.456\dot{q}$ ($12.2 + 11.41\dot{q}$)	$1207 + 99.44\dot{q}$ ($2661 + 2488\dot{q}$)	$1016 + 83.69\dot{q}$ ($2239 + 2094\dot{q}$)

NOTES: (1) $\dot{q}$ is panel average heating rate absorbed by coolant.
(2) Area of typical panel = 7.43 m^2 (80 ft^2).
(3) Total aircraft cooling system weight = Σ (upper + lower).

FIGURE 69
EMPIRICAL ESTIMATION OF COOLING SYSTEM WEIGHT SENSITIVITY TO PANEL HEATING RATE

Baseline Uninsulated Systems	Average $\dot{q}$ kW/m^2 ($Btu/sec\ ft^2$)	System Weight kg (lbm)*	Total Cooling System Weight kg (lbm)*	Detailed Cooling System Weight kg (lbm)
Mach 3 Upper Surface	5.76 (0.508)	1334 (2,940)	3207 (7,070)	3304 (7,285)
Mach 3 Lower Surface	11.64 (1.026)	1873 (4,130)		
Mach 4.5 Upper Surface	16.8 (1.48)	2870 (6,327)	6108 (13,466)	6164 (13,590)
Mach 4.5 Lower Surface	26.6 (2.34)	3238 (7,139)		
Mach 6 Upper Surface	17.9 (1.58)	2990 (6,592)	7767 (17,123)	7790 (17,173)
Mach 6 Lower Surface	44.9 (3.96)	4777 (10,531)		

* Based on Figure 69 Sensitivity factors.

FIGURE 70
COMPARISON OF ESTIMATED WITH CALCULATED COOLING SYSTEM WEIGHT

b. Baseline Panel Abort Temperatures - Transient temperature analyses were performed to provide an indication of the temperatures which the typical upper and lower surface baseline configurations would experience during abort following a system failure. Results are shown on Figures 71, 72 and 73. For all cases, a failure resulting in total coolant flow cessation was assumed 15 seconds prior to abort initiation. Local external heat transfer coefficients and adiabatic wall temperatures corresponding to the typical upper and lower surface locations for the trajectories defined in Section 4.2.2 were used in the analyses. It was assumed that a structural failure had occurred which depleted the coolant fluid in the tubes at the time of failure. This, combined with the further assumption that the structure was typical of a skin/stringer configuration and offered very little heat capacity for portions of the panel between stringers, represents a worst-case failure situation.

Figure 74 presents the results of similar analyses, comparing maximum panel skin temperatures with and without contained coolant, for all three design Mach numbers. As shown, the availability of the coolant as a heat sink results in a significant reduction in maximum skin temperature during the abort. Likewise, the additional heat capacity of a honeycomb type structure produces a fairly significant reduction in peak skin temperatures during abort, as will be shown in Section 4.4, although it has little effect on external skin gradients during cruise.

The maximum panel skin temperatures, without coolant in the panel indicate the degree of abort heat protection required. These data, using a maximum allowable aluminum skin temperature during abort of 478 K (400°F), indicated that the major abort heat protection requirements will be for the lower surface panels of Mach 4.5 and 6 concepts.

4.3.2 Thermostructural Concepts - Candidate fail-safe thermostructural concepts capable of passively absorbing the abort heat load were identified for each of the three cruise Mach numbers. Expected heating rates, total heat load, type of structural skin panels, and panel location (lower or upper aircraft surface) were used in the initial concept definition.

a. Classes of Concepts - The basic concepts investigated included thickened outer skin, precooled skin, overcoats, undercoats, and phase-change materials. These are illustrated by Figure 75, which shows typical candidate materials and the arrangements.

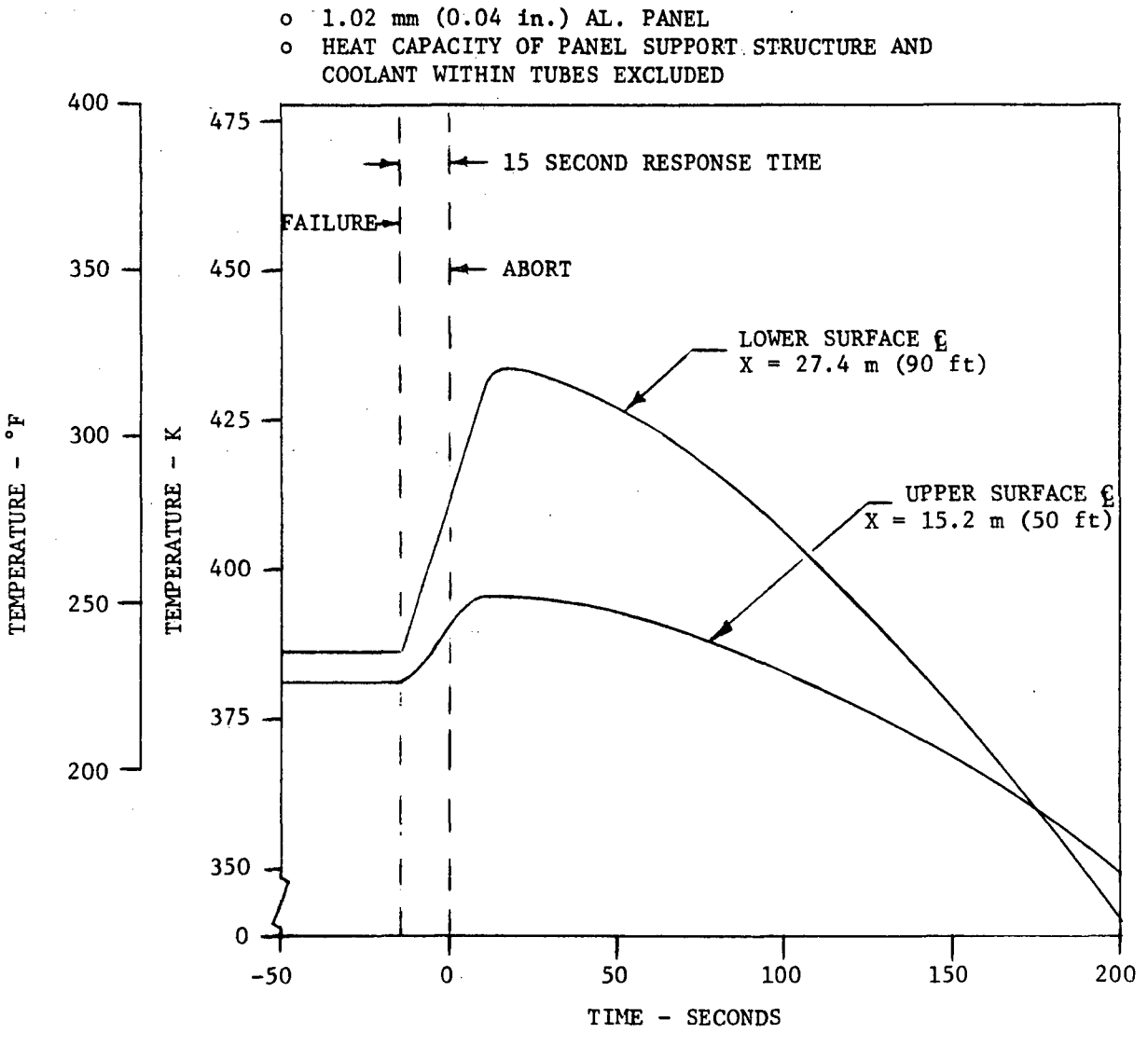

FIGURE 71
BASELINE PANEL SKIN TEMPERATURES DURING MACH 3 ABORT

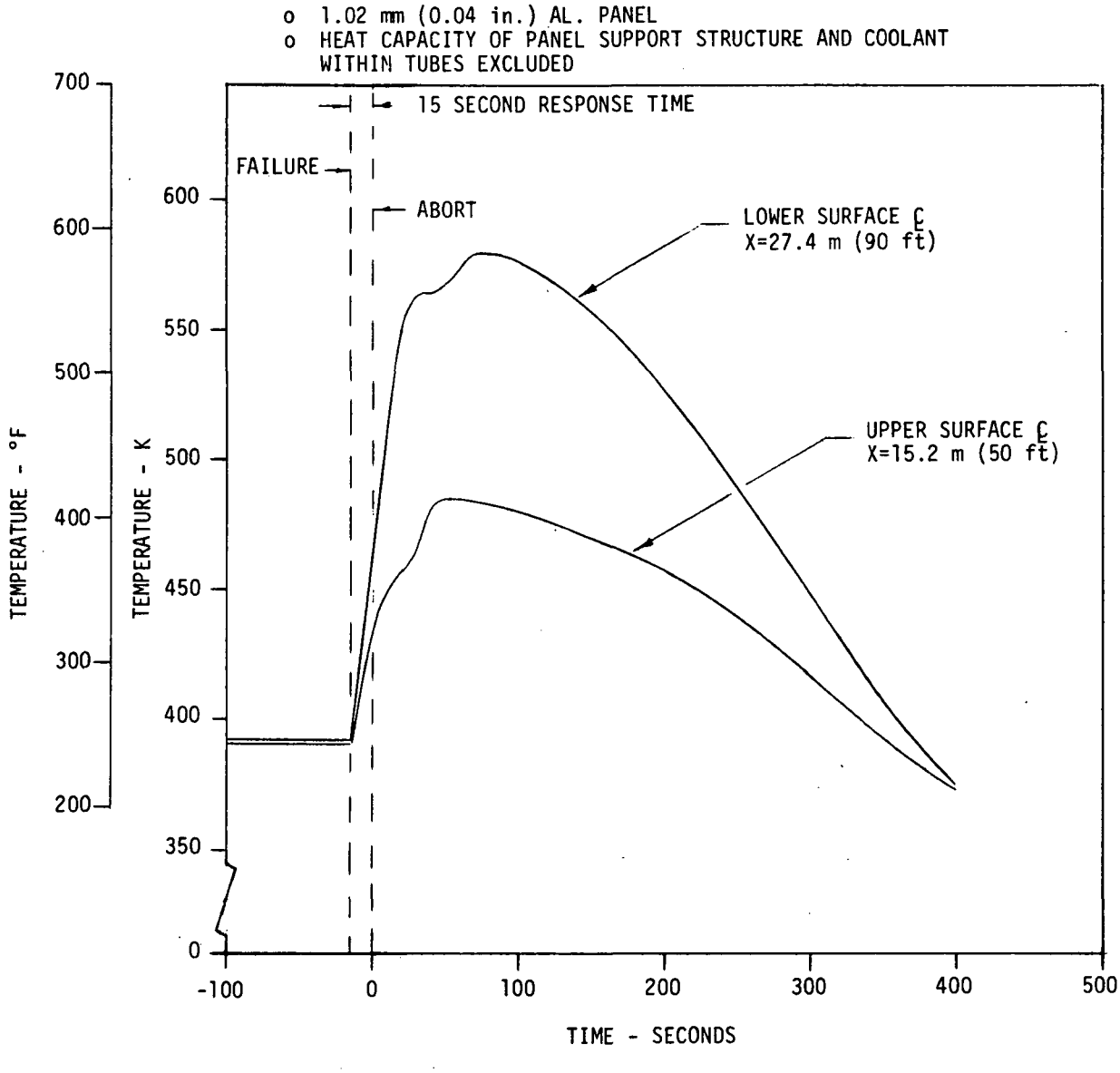

FIGURE 72
BASELINE PANEL SKIN TEMPERATURES DURING MACH 4.5 ABORT

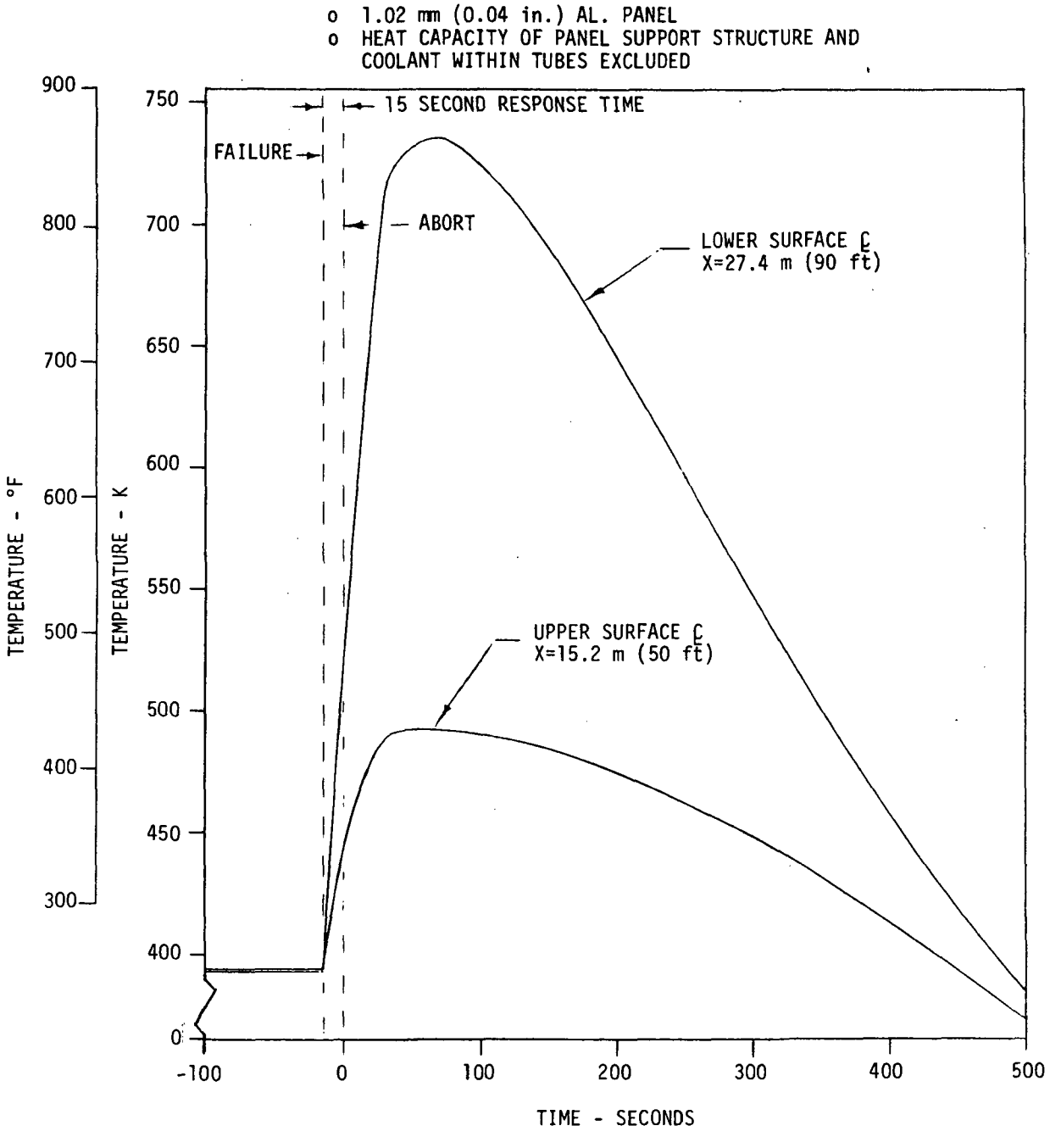

FIGURE 73
BASELINE PANEL TEMPERATURES DURING MACH 6 ABORT

ABORT MACH NUMBER	SURFACE LOCATION (1)	PANEL SKIN TEMPERATURE (2)			TIME TO MAX. SKIN TEMP.	
		INITIAL K (°F)	MAX. WITH COOLANT K (°F)	MAX. WITHOUT COOLANT K (°F)	WITH COOLANT (3) (sec)	WITHOUT COOLANT (3) (sec)
6	LOWER	394 (250)	683 (769)	736 (865)	55	76
6	UPPER	390 (243)	468 (383)	493 (428)	45	71
4.5	LOWER	391 (244)	541 (514)	579 (582)	95	96
4.5	UPPER	390 (242)	463 (374)	485 (414)	60	61
3	LOWER	385 (234)	427 (309)	433 (320)	31	36
3	UPPER	381 (226)	392 (246)	395 (251)	22	31

NOTES:

(1) SURFACE LOCATIONS ARE LOWER SURFACE CENTERLINE 27.4 m (90 ft) AFT OF NOSE TIP AND UPPER SURFACE CENTERLINE 15.2 m (50 ft) AFT OF NOSE TIP.

(2) INITIAL SKIN TEMP. IS MAX. DURING NORMAL OPERATION. MAX. WITH COOLANT IS MAX. TEMP. DURING ABORT WITH COOLANT CONTAINED IN COOLANT TUBES. MAX. WITHOUT COOLANT IS MAX. TEMP. DURING ABORT WITHOUT COOLANT IN TUBES. SKIN IS 1.02 mm (0.040 in.) THICK ALUMINUM. COOLANT IS METHANOL/WATER.

(3) TIME TO MAX. SKIN TEMP. IS TIME MEASURED FROM TIME OF FAILURE. START OF ABORT IS 15 SECONDS AFTER FAILURE.

FIGURE 74
MAXIMUM PANEL SKIN TEMPERATURES DURING ABORT

Concept	Typical Thermostructural Arrangement	Primary Thermal Protection Mode	Typical Candidate Materials
① Thickened Outer Skin	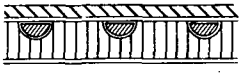	• Heat Sink of Additional Mass	Aluminum, Boron Aluminum, Beryllium, Lockalloy
② Precooled Skin	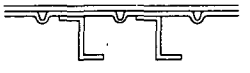	• Heat Sink of Additional ΔT	Aluminum, Boron Aluminum, Beryllium, Lockalloy
③ Overcoats	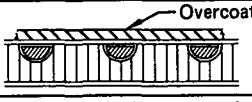	• Heat Sink • Insulation	Teflon, Kapton, Silicone Rubber, Insulative Heat Shields
④ Undercoats	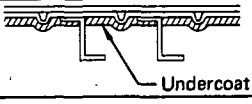	• Heat Sink	Beryllium, Lockalloy, Silicones with Lithium Additives
⑤ Phase-Change		• Heat of Fusion	Paraffins, Waxes, Polymers

FIGURE 75
BASIC THERMOSTRUCTURAL CONCEPTS

o Thickened Outer Skin - This approach offered a relatively simple method for providing the necessary heat capacity. At lower speeds, a thickened aluminum skin is attractive because of design simplicity. In addition, the thicker skin permits wider tube spacing, thus lowering residual coolant weights and minimizing potential leak points. But, as cruise velocity increases, increasing the skin thickness imposes a significant weight penalty. Boron-aluminum, beryllium, and Lockalloy were considered as candidate skin materials, in addition to aluminum, because of their favorable strength, weight, and thermal characteristics.

o Precooled Skin - Precooling the skin to a level further below material temperature limits provides additional heat capacity and would result in higher material allowables. However, the added weight of the cooling system required tends to offset these benefits. Assuming the same coolant temperature, the required flow rates would increase, resulting in larger weights for pumps, heat exchanger, distribution lines, residual coolant, pumping power, etc. Due to the higher allowable temperature limits of boron-aluminum composite, beryllium, and Lockalloy, as compared to aluminum, they were considered prime candidate materials for this concept.

o Undercoats - A material with a higher effective specific heat than aluminum could be employed as an undercoating to the basic skin, thus providing a weight savings over the thickened aluminum skin approach. Undercoats, however, are applicable only to a skin/stringer panel. They also provide no thermal shielding benefits, as do overcoats; however they are less susceptible to damage.

The desirable properties of undercoats include high values of specific heat, thermal conductivity, and thermal diffusivity. To be effective, they must be placed in contact with the skin with minimal thermal resistance. Adhesive bonding is one method of attachment.

Properties of several candidate undercoats, compared to aluminum, are shown on Figure 76. The specific heat of the material relative to aluminum is an indication of the weight saving potential. However, the generally low thermal conductivity and thermal diffusivity of the nonmetallics make them less efficient, except in small thicknesses at low heat pulses. Materials such as lithium compounds possess favorable thermal characteristics, but

Candidate Materials	Property Ratio (Re Aluminum)			
	Specific Heat	Density x Specific Heat	Thermal Conductivity	Thermal Diffusivity
Desirable Ratio	High	High	High	High
Metals				
o Aluminum	1	1	1	1
o Beryllium	2.0	1.36	1.3	0.96
o Lockalloy	1.8	1.35	1.54	1.14
Nonmetals:				
o Kapton	1.2	0.61	0.0026	0.004
o Silicone (40% LiO_2)	3.1	1.16	0.0026	0.0023

FIGURE 76
UNDERCOAT PROPERTIES RELATIVE TO ALUMINUM

require a means of containment, to avoid reactions with moisture. Metallic undercoats (boron-aluminum, beryllium and Lockalloy) have higher useful temperature capability than aluminum, however the maximum temperature capability of the aluminum skin is still the limiting factor.

o Overcoats - Certain nonmetallic materials applied to the external skin offer potential for overall weight reductions, because of their combined heat sink and insulative qualities. The more promising ones, tabulated in Figure 77 have a higher specific heat, lower density and thermal conductivity, and higher allowable operating temperature than aluminum. They are applied by bonding or spraying. The main advantage of overcoats is their potential for reducing heat transfer, during both normal cruise and abort. The reduced heating also allows the use of smaller tubes and a wider tube spacing, resulting in lower weight and fewer potential leakage points.

The maximum temperature recommended for the overcoat materials, shown on Figure 77 is approximately 533K to 561K (500° to 550°F) for long term operation, such as cruise, and 644K to 672K (700° to 750°F) for short term situations such as abort. Higher temperatures can be tolerated but would result in some degree of pyrolysis, with life/maintenance implications. The exception is Kapton (polyimide) which can tolerate temperatures several hundreds of degrees higher. Kapton begins to char at 1073K (1472°F).

Property	Aluminum	Teflon	Silicone (Unmodified)	Silicone (40% LiO_2 Additive)	Kapton
Density Mg/m^3	2.77	2.10	0.4	1.04	1.42
Density (lbm/ft^3)	(173)	(131)	(25)	(65)	(89)
Specific Heat J/g•K	0.92	1.05	1.34	2.85	1.09
Specific Heat (Btu/lbm°F)	(0.22)	(0.25)	(0.32)	(0.68)	(0.26)
Thermal Conductivity W/m•K	138	0.246	0.10	0.36	0.16
Thermal Conductivity (Btu/hr ft °F)	(80)	(0.142)	(0.06)	(0.21)	(0.09)
Allowable Temperature K					
o Cruise	394	533	533	533	589
(°F)	(250)	(500)	(500)	(500)	(600)
o Failure	478	589	589	589	644
	(400)	(600)	(600)	(600)	(700)

FIGURE 77
OVERCOAT NOMINAL PROPERTIES RELATIVE TO ALUMINUM

Insulative metallic heat shields were also included in the overcoat thermostructural concept class. The heat shield approach has primary application for very high heat loads. External radiation shields fabricated of titanium, Inconel, Rene' 41, etc., combined with fibrous insulations, were considered for this application.

In all cases, the insulative heat shield concepts were applied without gaps between the heat shield and insulation package or between the insulation and aluminum panel. This was done to eliminate degradation of thermal performance due to boundary layer leakage into, and through, the insulative system. Boundary layer leakage can increase the heat transfer rate to the insulated structure by significant amounts.

o Phase Change Materials - Phase change materials (PCM) that absorb heat through changes of molecular structure or melting are readily available. These materials accomplish phase change at a known and reproducible temperature with a low volumetric change and possess high thermal conductivity, materials compatibility, and low cost. Reference (16) describes some of these characteristics for various PCM's.

In order to be effective the PCM must be below the melting point during normal cruise. In addition, a relatively high heat transfer path must be pro-

vided. This can be accommodated by packaging the PCM in the cells of the honeycomb core, as depicted in Figure 75.

Figure 78 shows representative properties of classes of phase change materials. Most of the materials have heat of fusion values in the range of 163 to 303 J/g (70 to 130 Btu/lbm). Lithium provides a heat of fusion of 661 J/g (284 Btu/lbm). However, it is a hazardous material, being combustible in air near the melting point. Water is not considered a viable PCM and is shown for comparison only.

Material and (Class)	Melting Point K (°F)	Latent Heat of Fusion J/g (Btu/lbm)	Density $\frac{Mg}{m^3}$ (lbm/ft^3)
n - Octacosane (Paraffin)	335(142.9)	254(109)	0.78(48.6)
Hydroquinone (Nonparaffin Organic)	446(342.3)	258(111)	1.36(84.78)
Sodium Hydroxide Monohydrate (Salt Hydrate)	410(279)	172(74)	1.45(90.5)
Lithium (Metallic)	452(354)	661(284)	0.53(33.3)
duPont HTS (Fused Salt Eutectic 60 $AlCi_3$/26NaCl/14KCl	366(199)	214(92)	-
Polyethylene (Polymer) √	408(274)	244(105)	0.96(60.2)
Polypropylene (Polymer)	449(349)	237(102)	-
Transit HEET(R) (Inorganic Salt)			
Series 450	450(350)	298(128)	2.69(168)
Series 505	505(450)	300(129)	1.6 (100)
Aluminum Chloride (Salt)	465(378)	272(117)	2.43(152)
Solid-Solid Transition			
Material 2.2-Bis (Hydroxymethyl) Propionic Acid	425(306) △1 428(311) △2	289(124) △1 27 (11.5) △2	
Water			
Solid-to-Liquid	273(32)	333(143.1)	1.0(62.42)
Liquid-to-Gas (at 14.7 psia)	373(212) △3	2259(970.3) △4	

Notes:
△1 Temperature and Heat of Transition
△2 Melting Temperature and Heat of Fusion
△3 Boiling Point
△4 Heat of Vaporization
√ Selected PCM

FIGURE 78
PHASE CHANGE MATERIAL CHARACTERISTICS

The primary candidate material considered for this application was deemed to be polyethylene. This choice was made through consideration of: (1) the compatibility of the melting point, (408 K (274°F), with the baseline panel maximum design temperature during cruise (<399K(<250°F)), and (2) its relatively high latent heat.

b. Initial Screening - A matrix of applicable concepts was devised for initial screening purposes. This matrix included the basic thermostructural arrangements and materials shown on Figure 77, and combinations of these. After preliminary screening, over 300 possible arrangements still remained. Therefore, an additional screening process was used to reduce the total to a manageable number. This was done in the following manner:

First, the transient temperature characteristics of the baseline panels during abort were examined. It was shown that during Mach 3 abort, maximum baseline panel temperatures, were below the allowable 478K (400°F) level, and that the upper surfaces required only a slight amount of additional heat protection even during Mach 4.5 and Mach 6 abort. This eliminated the need for considering large numbers of concepts for the upper surfaces. However, insulative overcoats on upper surfaces were retained for further trade studies, because of the potential reduction in cooling system heat load and weight and the flow rates required during cruise.

Second, the thermodynamic and physical property characteristics of possible materials were compared. For example, Lockalloy and beryllium were both considered for use as thickened skin and precooled skin concepts. Lockalloy and beryllium have similar characteristics, with Lockalloy being somewhat easier to fabricate. Thus, Lockalloy was selected as being representative of this class material.

The materials considered for overcoats included Teflon, Kapton, silicone elastomer, and silicone with lithium compound additives. Insulative heat shields were also considered. A comparison of Teflon (fluorocarbon) and Kapton (polyimide) properties indicated very similar thermal conductivity and specific heat. The specific gravity of Kapton is 1.42, compared to 2.1 to 2.2 for Teflon. Teflon also has a maximum continuous service temperature of 533K (500°F), compared to the range of 644K to 672K (700° to 750°F) assumed for Kapton. Kapton will actually withstand higher temperatures than the assumed range. Therefore, Teflon was deleted.

During evaluation of PCM heat sinks, all but polyethylene were eliminated. No suitable paraffin or wax was found because of their low melting points.

Nonmetallic undercoat material candidates were narrowed down to lithium oxide enriched silicone, because of its higher heat capacity. Also, it was judged that materials such as boron-aluminum composite, beryllium, or Lockalloy would realistically be more suitable for the primary cooled panel skin rather than as an undercoat.

c. Candidate Concepts - Figure 79 presents a matrix of the basic thermostructural concepts which remain after initial screening. A total of 38 candidate concepts, plus the 6 baseline (aluminum) concepts were selected for further comparison.

Thermo-Structural Concept	Cruise (Abort) Flight Condition/Panel Location					
	Mach 3 22.3 km (73,000 ft)		Mach 4.5 27.4 km (90,000 ft)		Mach 6 32 km (105,000 ft)	
	Upper Surface	Lower Surface	Upper Surface	Lower Surface	Upper Surface	Lower Surface
1. Thickened Skin						
a) Aluminum	●	●	●	●	●	●
b) Boron-Alum.	–	–	–	●	–	●
c) Lockalloy	–	–	–	●	–	●
2. Precooled Skin						
a) Aluminum	–	–	●	●	●	–
b) Boron-Alum.	–	–	–	●	–	●
c) Lockalloy	–	–	–	●	–	●
3. Overcoated Aluminum Skin						
a) Kapton	●	●	●	●	●	●
b) Silicone	●	●	●	●	●	●
c) Silicone (40% $Li0_2$)	–	–	●	●	–	–
d) Insulative Heat Shield	–	–	–	●	–	●
4. Undercoated Aluminum Skin						
a) Silicone (40% $Li0_2$)	–	–	–	●	●	●
5. Phase Change Material (PCM)						
{Aluminum Skin, Alum. Honeycomb, Polyethylene PCM}	–	–	–	●	–	●
6. Baseline Aluminum Skin (Unprotected)	●	●	●	●	●	●

● Selected for further evaluation

FIGURE 79
MATRIX OF THERMOSTRUCTURAL CONCEPTS

4.3.3 Thermostructural Concept Evaluation - The capability of the thermostructural concepts was evaluated on the basis of weight, considering maximum structural temperatures during abort, abort heating rates, and total heat load. An additional consideration was the structural cooling requirements during cruise, since some of the concepts could exceed the available heat sink capacity during cruise operation.

a. Evaluation Methods/Criteria - Certain ground-rules and assumptions were established in order to provide consistency.

The candidate thermostructural concepts were compared on the basis of the typical panel weight plus the cooling system weight chargeable to the panel. The typical panel, for both upper and lower surfaces, has 7.43 m^2 (80 ft^2) of surface area. The correlation of cooling system weight as a function system heat load, shown on Figure 69, was used to provide the cooling system weight sensitivity relationships.

Minimum panel skin thickness was assumed to be 1.02 mm (0.04 in.). Although it was realized the skin thickness on some portions of the aircraft could likely be lower than this value, 1.02 mm (0.04 in.) was considered a realistic nominal minimum, based on results of the Reference (2) study.

A simple one-dimensional transient thermal analysis was judged to be adequate for this initial evaluation. The one-dimensional analysis used an effective specific heat of the skin material to account for the heat capacity of the dry coolant tubes. Results were compared with those obtained from a more sophisticated analysis which incorporated heat conduction to the tubes. The transient temperature characteristics were nearly identical for the baseline 1.02 mm (0.04 inch) aluminum skin panel model used as a check case. The one-dimensional analysis was therefore utilized at this point, with the more sophisticated thermal analysis being utilized later for refinement of selected concepts.

The inherent heat capacity of the panel back-up structure was not included at this early point. This led to some conservatism of results. Subsequent analyses incorporating the honeycomb back-up structure showed significantly lower peak skin temperatures, particularly for the overcoat and insulated heat shield concepts. A skin/stringer type structure does not have as much heat capacity because of lower interface conductance between the stringers and skin.

The response time between failure occurrence and initiation of abort was selected as 15 seconds. It was further assumed that the coolant in the tubes was depleted at the time of failure, thus providing no heat capacity during abort. Average cooled panel skin temperatures at the time of failure were assumed to be 366 K (200°F), except in the evaluation of the pre-cooled outer skin concepts.

b. Hydrogen Fuel Heat Sink Capacity - One of the major parameters in the establishment of a practical thermo-structural concept is the relationship between absorbed cruise heating rate and available heat sink.

In Reference (2) it was noted that the hydrogen fuel flow required to absorb the baseline aircraft cruise heat load exceeded the hydrogen fuel available. The baseline Mach 6 aircraft, with bare uninsulated aluminum skin at an average 366 K (200°F) wall temperature, required 24.13 kg/s (53.2 lbm/sec) of hydrogen heat sink. The engine hydrogen fuel requirement was only 16.78 kg/s (37 lbm/sec) at start of cruise conditions. A fully optimized active cooling system could reduce this difference, but this is basically representative of Mach 6 cruise conditions.

It became apparent that the characteristics of the baseline Mach 6 aircraft would not provide a reasonable guide for establishing heat sink requirements at Mach 4.5 and Mach 3. Aircraft designed to operate at these Mach numbers would have a lower wing loading and higher L/D, and thus, reduced engine fuel flow requirements. In addition, Mach 3 aircraft would be likely to have different types of engines than the turboramjets utilized by the Mach 6 baseline. Therefore, a method was required to provide general guidelines to hydrogen heat sink availability.

References (3), (9), (15), as well as Reference (2) and the current "Fail-Safe Abort System Study" were utilized to define typical flight characteristics of hydrogen fueled aircraft with Mach 3 to 6 capability. In general, the aircraft investigated were large, long range vehicles. The smaller aircraft of Reference (3), a NASA Hypersonic Research Aircraft configuration, was also included because of the useful information available on its average cruise heating rate.

Figure 80 illustrates the cruise altitudes expected for the typical hypersonic cruise aircraft designed to operate within the high supersonic-to-hypersonic Mach number range of 3 to 6. Wing loading, W/S, is in the range

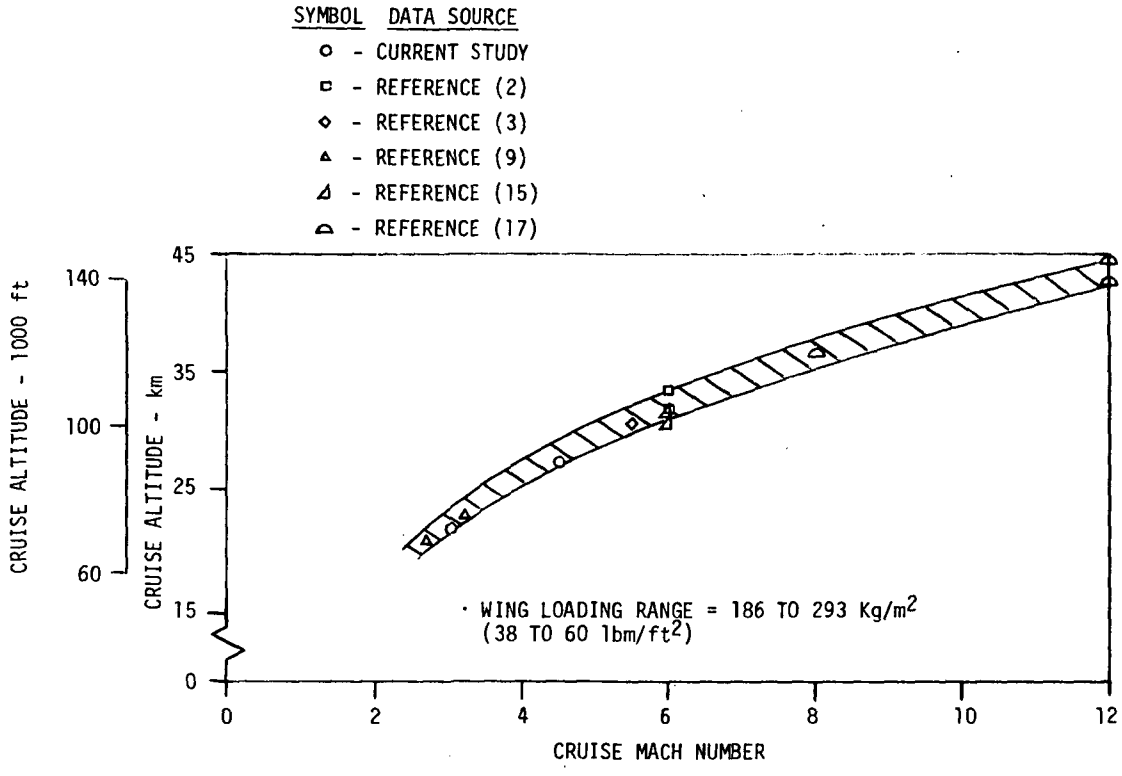

FIGURE 80
TYPICAL FLIGHT REGIMES FOR EFFICIENT HIGH MACH NUMBER CRUISE

of about 195 to 293 kg/m^2 (40 to 60 lbm/ft^2). Figure 81 exhibits typical lift-to-drag ratios. The Reference (2), Concept 3, configuration is known to be far from optimum at Mach 3 and 4.5. Thus, Figure 81 is expected to be a better indicator of typical aircraft L/D's in the Mach 3 to 6 range. Knowledge of reasonable L/D's is important in establishing hydrogen fuel heat sink capacity.

Another extremely important parameter is the aircraft average heating rate. Figure 82 presents average heating rate (to a 366 K (200°F) skin) as a function of cruise Mach number. It can be noted that the average heating rate shown at Mach 4.5 for the "Fail-Safe Abort Study" baseline aircraft appears to be somewhat high. This is due to start-of-cruise at a dynamic pressure of 24.1 kP$_a$ (504 lbf/ft^2) (Mach 4.5 at 27.43 km (90,000 ft.) altitude). It is expected that an aircraft optimized for Mach 4.5 cruise would have a cruise dynamic pressure of about 19.13 kP$_a$ (400 lbf/ft^2) and approximately 28.95 km (95,000 ft.) cruise altitude. This would reduce the start-of-cruise heating rate about 10 to 15 percent and result in better agreement with Figure 82.

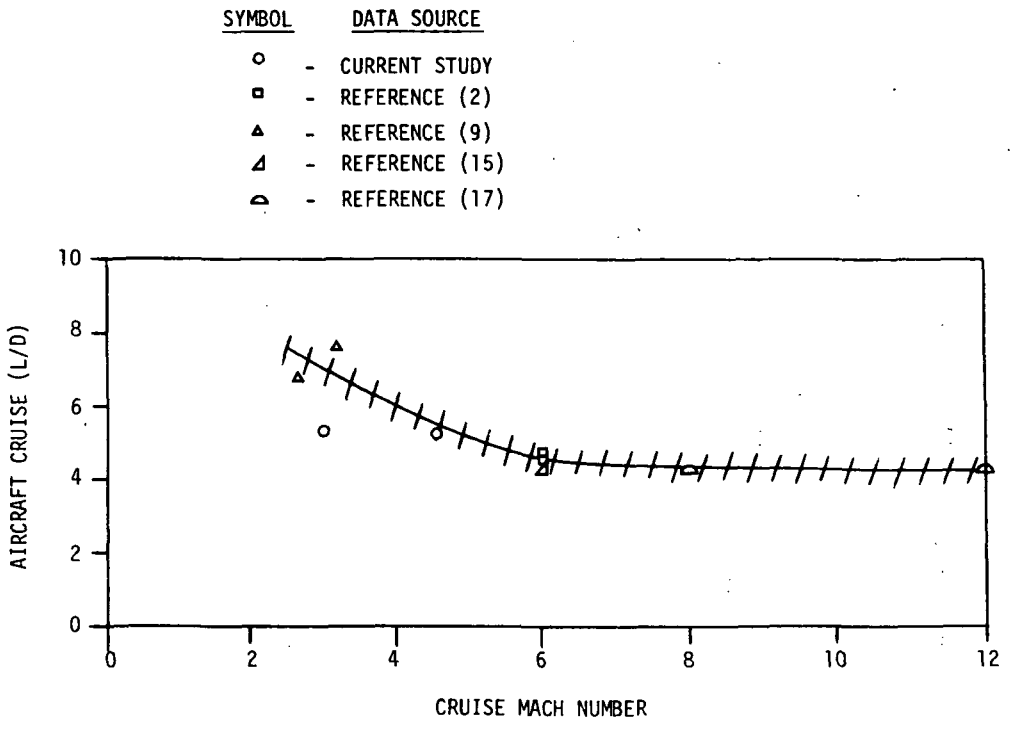

FIGURE 81
TYPICAL CRUISE L/D RATIOS FOR HIGH MACH NUMBER CRUISE AIRCRAFT

It is also noted that the Mach 3.2 data point per Reference (9) appears relatively high. This is due to the method used to assess average heating rate, the aircraft heat load divided by cooled area. Only about 43 percent of the wetted area was cooled on the Reference (9) Mach 3.2 aircraft, and about 71 percent of the cooled area was wing area. This would be expected to result in a higher average heating rate per unit area than if the entire aircraft were cooled.

Overall, Figure 82 is expected to be a good guide to the average heating rates experienced by large actively cooled (366 K (200°F) skin) hypersonic cruise aircraft, and can be utilized to provide reasonable first order estimates of the amount of hydrogen fuel flow required to absorb the heat loads between Mach 3 and Mach 12.

For example, at a cruise Mach number of 10 the average heating rate (per Figure 82) is about 111.22 kW/m^2 (9.8 Btu/ft^2 sec). Cooling structure to 366 K (200°F) limits the maximum achievable hydrogen temperature. The use of an intermediate heat transfer fluid to transport the heat from 366 K (200°F) cooled structure to the heat sink, hydrogen, placed this limit temperature at approximately 311 K (100°F). Thus, the total available temperature rise of

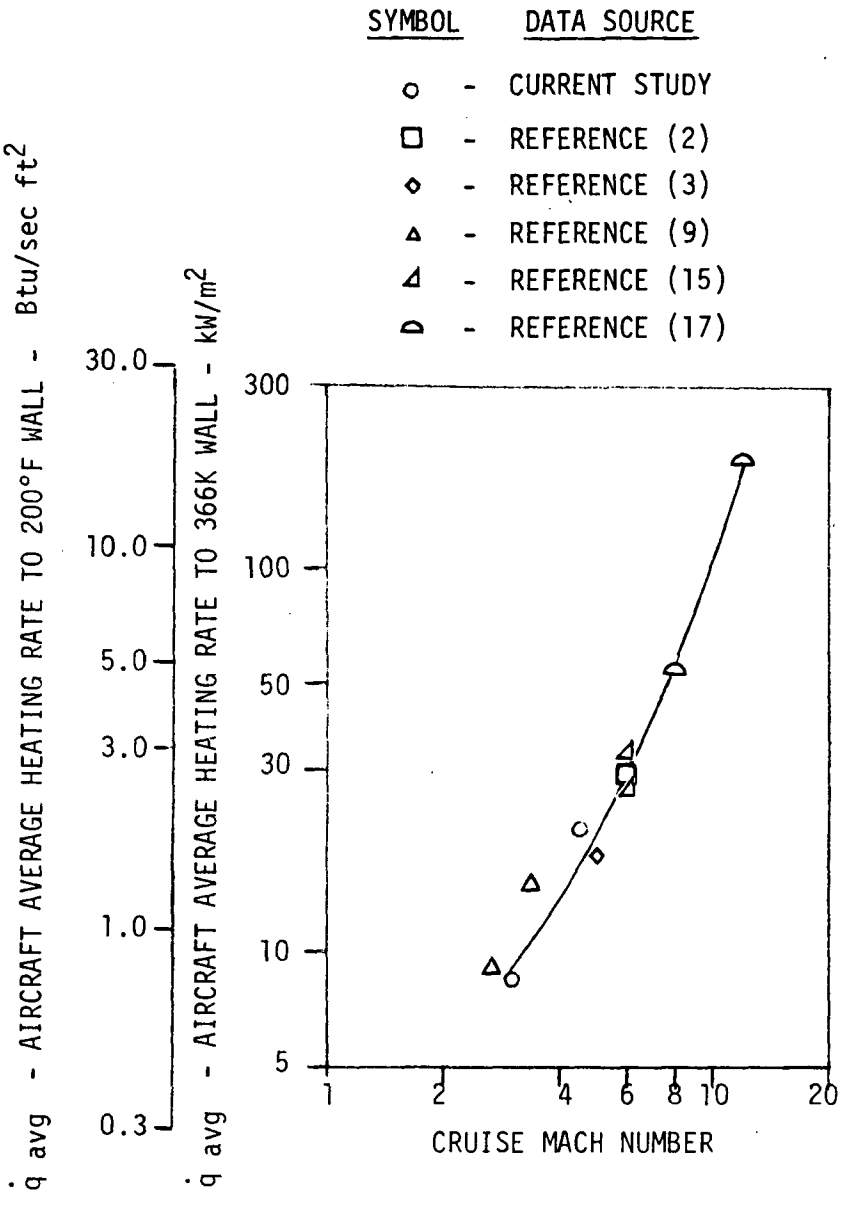

FIGURE 82
TYPICAL AVERAGE HEATING RATES FOR HIGH MACH NUMBER CRUISE AIRCRAFT

the hydrogen is on the order of 278 K ΔT (500°F). With an average specific heat of 14.65 J/g K (3.5 Btu/lbm°F) the hydrogen can absorb 4.07 kJ/g (1750 Btu/lbm). Therefore, for the average heating rate of 111.22 kW/m^2 (9.8 Btu/ft^2 sec), 27.3 g/m^2.s (5.6 x 10^{-3} lbm/sec.ft^2) represents the minimum amount of hydrogen required to maintain the skin at 366 K (200°F).

An assessment of the hydrogen available as heat sink is provided by Figure 83. The parameter of fuel flow per unit wetted area divided by L/D was found to result in a definite trend for estimating the hydrogen available

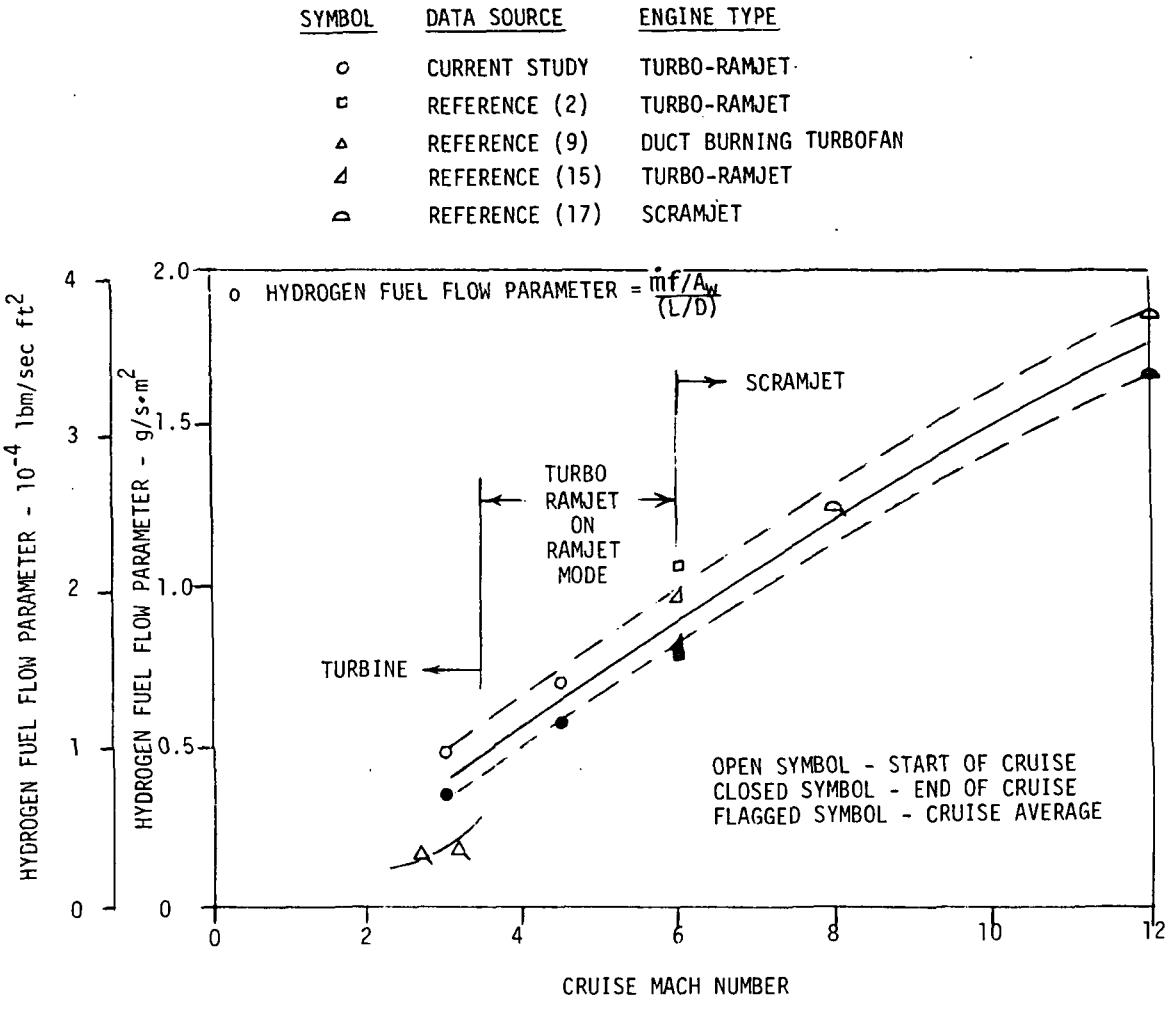

FIGURE 83
HYDROGEN FUEL FLOW PARAMETER FOR HIGH MACH NUMBER CRUISE AIRCRAFT

over the Mach number range of interest. Again, using a hypothetical Mach 10 cruise aircraft, per Figure 81 a typical cruise L/D would be 4.3. Using Figure 83, it can be estimated that at Mach 10 cruise the available hydrogen heat sink is:

$(1.5113)\ (4.3) = 6.498\ g/m^2 s$

$[(3.1 \times 10^{-4}\ lbm/sec.ft^2)\ (4.3) = 1.333 \times 10^{-3}\ lbm/sec.ft^2]$

Thus, the available hydrogen heat sink capacity is only 23.8 percent of that required to maintain the aircraft skin at 366 K (200°F).

Using the typical trends for L/D, average heating rate, and fuel flow parameter per Figures 81, 82, and 83, the heat sink required can be compared to that available for cruise Mach numbers between Mach 3 and 12.

Figure 84 presents estimates of the capability of the hydrogen fuel to provide the required heat sink for structural cooling of typical high Mach cruise aircraft. It should be noted that this approach is expected to be

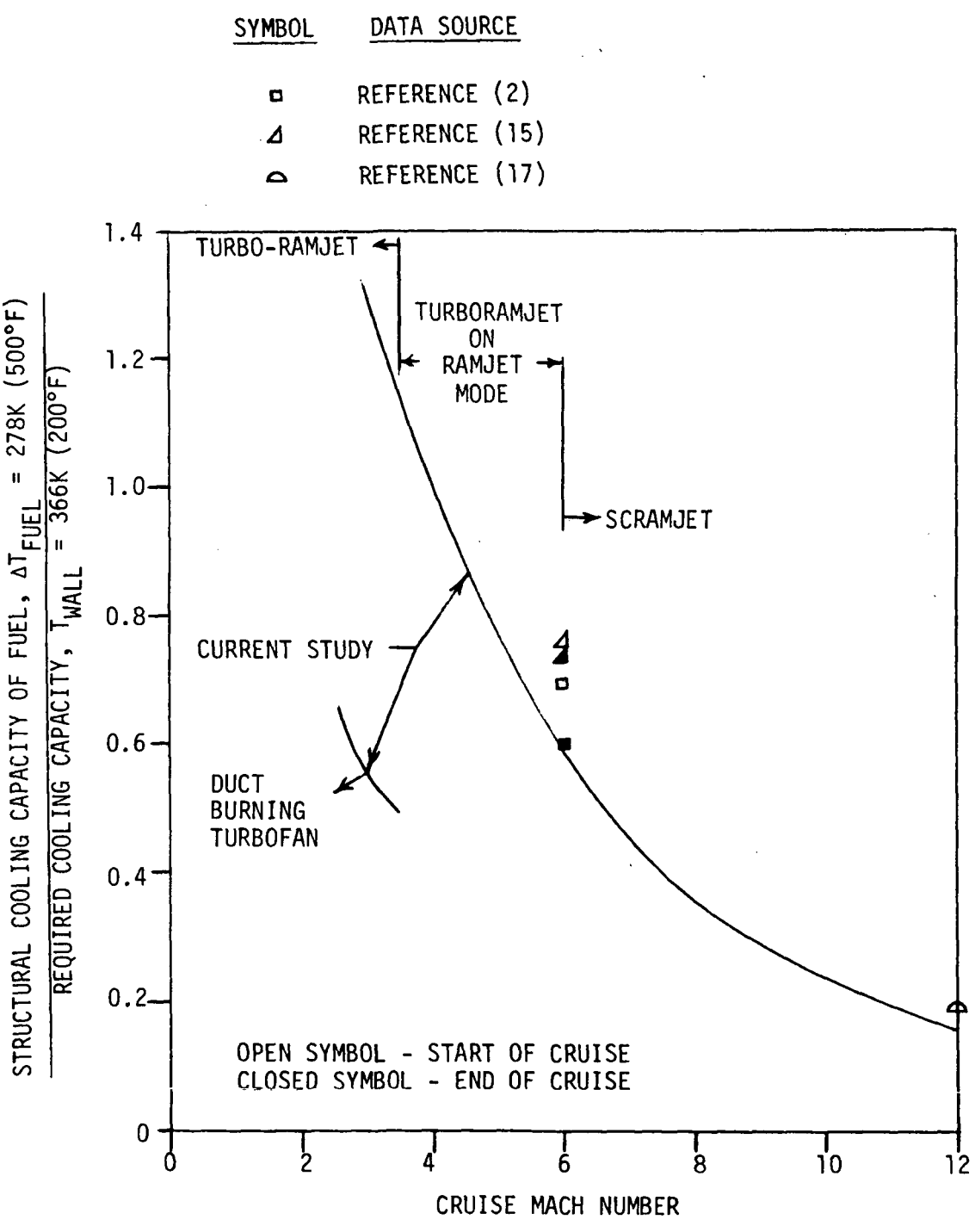

FIGURE 84
ESTIMATE OF STRUCTURAL COOLING CAPACITY FOR HYDROGEN FUELED HIGH MACH NUMBER AIRCRAFT

somewhat optimistic. Any increases in aircraft L/D or specific impulse (reduced specific fuel consumption) experienced in the optimization of a given airframe/propulsion system will decrease the heat sink available. For example, as shown in Figure 84 for Mach 3 aircraft, improvements in propulsion efficiency obtained with the duct burning turbofans, as compared to turbo-ramjet engines would result in much less available heat sink.

Improvements in aircraft L/D would have a similar effect. The fuel flow required would decrease. Also, if payload were not increased, the aircraft size could be reduced. This would lead to a higher average heating rate, due to the smaller aircraft (thinner boundary layer). Thus, a larger mismatch would result between cooling requirements and heat sink availability.

The use of the above method for the Mach 3 to 6 range of interest of the "Fail-Safe Abort System Study" indicates the heat sink availability shown in Figure 85.

Based on the above, the heat sink available for structural cooling (if efficient propulsion modes are utilized and the skin is cooled to temperatures compatible with aluminum) will be less than the heat sink required. Actively cooled, uninsulated aluminum skins may find application for lee surfaces on Mach 3 to 6 aircraft, but only if the overall aircraft-absorbed heat flux can be reduced to match the heat sink capacity of the fuel.

The above method was utilized in the selection of candidate thermostructural concepts for optimization, and provided a reasonable guide to matching cooling requirements to heat sink availability.

Cruise Mach	Engine Type	Average Heating Rate (1) kW/m² (Btu/sec ft²)		Heat Sink Available (2) kW/m² (Btu/sec ft²)		Available Heat Sink / Required Heat Sink
3	Duct Burning Turbo Fan	9.31	(0.82)	5.12	(0.45)	0.55
3	Turboramjet	9.31	(0.82)	12.10	(1.07)	1.30
4.5	Turboramjet	17.02	(1.5)	14.90	(1.31)	0.875
6	Turboramjet	30.19	(2.66)	18.11	(1.60)	0.60

(1) T_w = 366 K (200°F)
(2) Available for structural cooling, ΔT_f = 33 K to 311 K (500°F ΔT_f)

FIGURE 85
HYDROGEN FUEL HEAT SINK AVAILABILITY

c. Generalized Results - Summary results of the Mach 3, 4.5 and 6 thermostructural concept evaluations are presented herein. The results are shown primarily in terms of material type and required thickness, maximum temperature experienced during abort, and total combined weight of a typical 1.2 m x 6.1 m (4 ft by 20 ft) panel and the cooling system weight chargeable to the panel. All concept designs shown are capable of maintaining material temperatures within allowable limits during abort. The bare aluminum baseline skin panel concepts are shown for comparison.

o Mach 3 Concepts - Analyses conducted for the Mach 3 baseline unprotected upper and lower surface typical panels had already indicated that the allowable aluminum skin temperature (478 K (400°F)) would not be exceeded during the abort trajectory. However, because of the limitation of the available hydrogen heat sink, silicone and Kapton overcoats were assumed to be applied to the baseline 1.02 mm (0.04 in) aluminum skin. The spraying of a low density 400.5 kg/m^3 (25 lbm/ft^3) silicone overcoat on the lower surface provide a slight total weight savings (i.e., panel plus active cooling system) (see Figure 86). Applying the silicone overcoat to the upper surface increased weight slightly (Figure 87). A Kapton overcoat is not competitive on a weight basis for either the upper or lower surface.

The overcoat thicknesses were sized to limit the average heat transfer* to the coolant to 4.91 kW/m^2 (0.433 $Btu/ft^2 sec$) versus 7.94 kW/m^2 (0.70 Btu/ft^2 sec) for the bare baseline aluminum skin. An average heat sink capacity of 5.12 kW/m^2 (0.45 Btu/ft^2 sec) is available to absorb the heat transfer to the panel coolant, assuming duct burning turbofan engines for the Mach 3 case. Parametric relationships versus silicone overcoat thickness are shown on Figure 88.

Transient temperature characteristics of the silicone overcoated skin are shown on Figure 89. As shown, both the aluminum skin and silicone overcoat outer surface are well below the material temperature limits.

NOTE: * The average heat transfer to the total cooled area of the baseline aircraft is based on the relationship: $0.543\ \dot{q}_{upper} + 0.457\ \dot{q}_{lower} = \dot{q}_{average}$. This provides the area weighted average value.

Thermo-Structural Concept	Material		Avg. Temp. During Cruise (K)	Max Abort Temp (K) (1)	Cruise Heat Flux (kW/m^2) (2)	Unit Panel Wt. (kg/m^2) (3)	Wt. of 7.43 m^2 Panel		
	Type	Thickness (mm)					Dry Panel (kg)	Cooling System (4) (kg)	Total (5) (kg)
Baseline Skin	Alum	1.02	366	433	11.1	3.72	27.7	9.8	37.5
Overcoated Skin (6)	Alum Silicone	1.02 1.17	366 438	413 453	6.4	3.98	29.6	6.6	36.2
Overcoated Skin (7)	Alum Kapton	1.02 1.96	366 438	410 445	6.4	6.29	46.7	6.6	53.3

NOTES:

(1) Cooling system failure 15 seconds prior to abort. Alum. T_{max} allowable = 478K.
(2) Heat flux absorbed by panel coolant during normal operation at cruise with surface emissivity of 0.8.
(3) Unit panel weight includes skin, dry coolant tubes, and tube attachment (solder, weld, braze, etc.).
(4) Cooling system weight chargeable to typical panel (1.22m x 6.10m panel). Includes all cooling system components, coolant distribution system, and system coolant weights.
(5) Total weight equals summation of dry panel weight plus cooling system weight.
(6) Silicone is low density (400 kg/m^3) sprayable overcoat material. T_{max} allowable = 533K.
(7) Kapton is DuPont polyimide film, type "H". T_{max} allowable = 589K.

FIGURE 86a
MACH 3 THERMO-STRUCTURAL CONCEPT COMPARISON (LOWER SURFACE)

Thermo-Structural Concept	Material		Avg. Temp. During Cruise (°F)	Max. Abort Temp (°F) [1]	Cruise Heat Flux (Btu/sec ft^2) [2]	Unit Panel Wt. (lbm/ft^2) [3]	Wt. of 80 Ft^2 Panel		
	Type	Thickness (in)					Dry Panel (lbm)	Cooling System [4] (lbm)	Total [5] (lbm)
Baseline Skin	Alum	0.040	200	320	0.981	0.762	61.0	21.7	82.7
Overcoated Skin [6]	Alum Silicone	0.040 0.046	200 329	284 355	0.561	0.815	65.2	14.6	79.8
Overcoated Skin [7]	Alum Kapton	0.040 0.077	200 329	278 342	0.561	1.288	103.0	14.6	117.6

NOTES:

1. Cooling system failure 15 seconds prior to abort. Alum T_{max} allowable = 400°F.
2. Heat flux absorbed by panel coolant during normal operation at cruise with surface emissivity of 0.8.
3. Unit panel weight includes skin, dry coolant tubes, and tube attachment (solder, weld, braze, etc.)
4. Cooling system weight chargeable to typical panel (4 ft x 20 ft panel). Includes all cooling system components, coolant distribution system, and system coolant weights.
5. Total weight equals summation of dry panel weight plus cooling system weight.
6. Silicone is low density (25 PCF) sprayable overcoat material. T_{max} allowable = 500°F.
7. Kapton is DuPont polyimide film, type "H". T_{max} allowable = 600°F.

FIGURE 86b
MACH 3 THERMO-STRUCTURAL CONCEPT COMPARISON (LOWER SURFACE)

Thermo-Structural Concept	Material		Avg. Temp. During Cruise (K)	Max Abort Temp (K) (1)	Cruise Heat Flux (kW/m^2) (2)	Unit Panel Wt. (kg/m^2) (3)	Wt. of 7.43 m^2 Panel		
	Type	Thickness (mm)					Dry Panel (kg)	Cooling System (kg) (4)	Total (kg) (5)
Baseline Skin	Alum	1.02	366	395	5.3	3.44	25.6	5.7	31.3
Overcoated Skin	(6) Alum Silicone	1.02 1.17	366 408	391 417	3.7	3.83	28.5	4.4	32.9
Overcoated Skin	(7) Alum Kapton	1.02 1.96	366 408	389 413	3.7	6.14	45.6	4.4	50.0

NOTES:

1. Cooling system failure 15 seconds prior to abort. Alum. T_{max} allowable = 478K.
2. Heat flux absorbed by panel coolant during normal operation at cruise with surface emissivity of 0.8.
3. Unit panel weight includes skin, dry coolant tubes, and tube attachment (solder, weld, braze, etc.).
4. Cooling system weight chargeable to typical panel (1.22m x 6.10m panel). Includes all cooling system components, coolant distribution system, and system coolant weights.
5. Total weight equals summation of dry panel weight plus cooling system weight.
6. Silicone is low density (400 kg/m^3) sprayable overcoat material. T_{max} allowable = 533K.
7. Kapton is DuPont polyimide film, type "H". T_{max} allowable = 589K.

FIGURE 87a
MACH 3 THERMO-STRUCTURAL CONCEPT COMPARISON (UPPER SURFACE)

Thermo-Structural Concept	Material		Avg. Temp. During Cruise (°F)	Max. Abort Temp (°F) (1)	Cruise Heat Flux (Btu/sec ft^2) (2)	Unit Panel Wt. (lbm/Ft^2) (3)	Wt. of 80 Ft^2 Panel		
	Type	Thickness (in.)					Dry Panel (lbm)	Cooling System (4) (lbm)	Total (5) (lbm)
Baseline Skin	Alum	0.040	200	251	0.463	0.705	56.4	12.6	69.0
Overcoated Alum	(6) Alum Silicone	 0.040 0.046	 200 275	 244 291	0.326	0.785	62.8	9.8	72.6
Overcoated Skin	(7) Alum Kapton	 0.040 0.077	 200 275	 241 283	0.326	1.258	100.6	9.8	110.4

NOTES:

(1) Cooling system failure 15 seconds prior to abort. Alum T_{max} allowable = 400°F.
(2) Heat flux absorbed by panel coolant during normal operation at cruise with surface emissivity of 0.8.
(3) Unit panel weight includes skin, dry coolant tubes, and tube attachment (solder, weld, braze, etc.)
(4) Cooling system weight chargeable to typical panel (4 ft x 20 ft panel). Includes all cooling system components, coolant distribution system, and system coolant weights.
(5) Total weight equals summation of dry panel weight plus cooling system weight.
(6) Silicone is low density (25 PCF) sprayable overcoat material. T_{max} allowable = 500°F.
(7) Kapton is DuPont polyimide film, type "H". T_{max} allowable = 600°F.

FIGURE 87b
MACH 3 THERMO-STRUCTURAL CONCEPT COMPARISON (UPPER SURFACE)

1) TYPICAL UPPER & LOWER PANELS
   - o PANEL SIZE = 1.2 m x 6.1 m (4 ft x 20 ft)
   - o 1.02 mm (0.04 in.) AL. SKIN
   - o PANEL COOLANT INLET TEMP = 255K (0°F); OUTLET = 322K (120°F)
   - o SYSTEM ΔP = 1.17 MPa (170 psid)
2) PANEL WEIGHTS EXCLUDE SUPPORT STRUCTURE

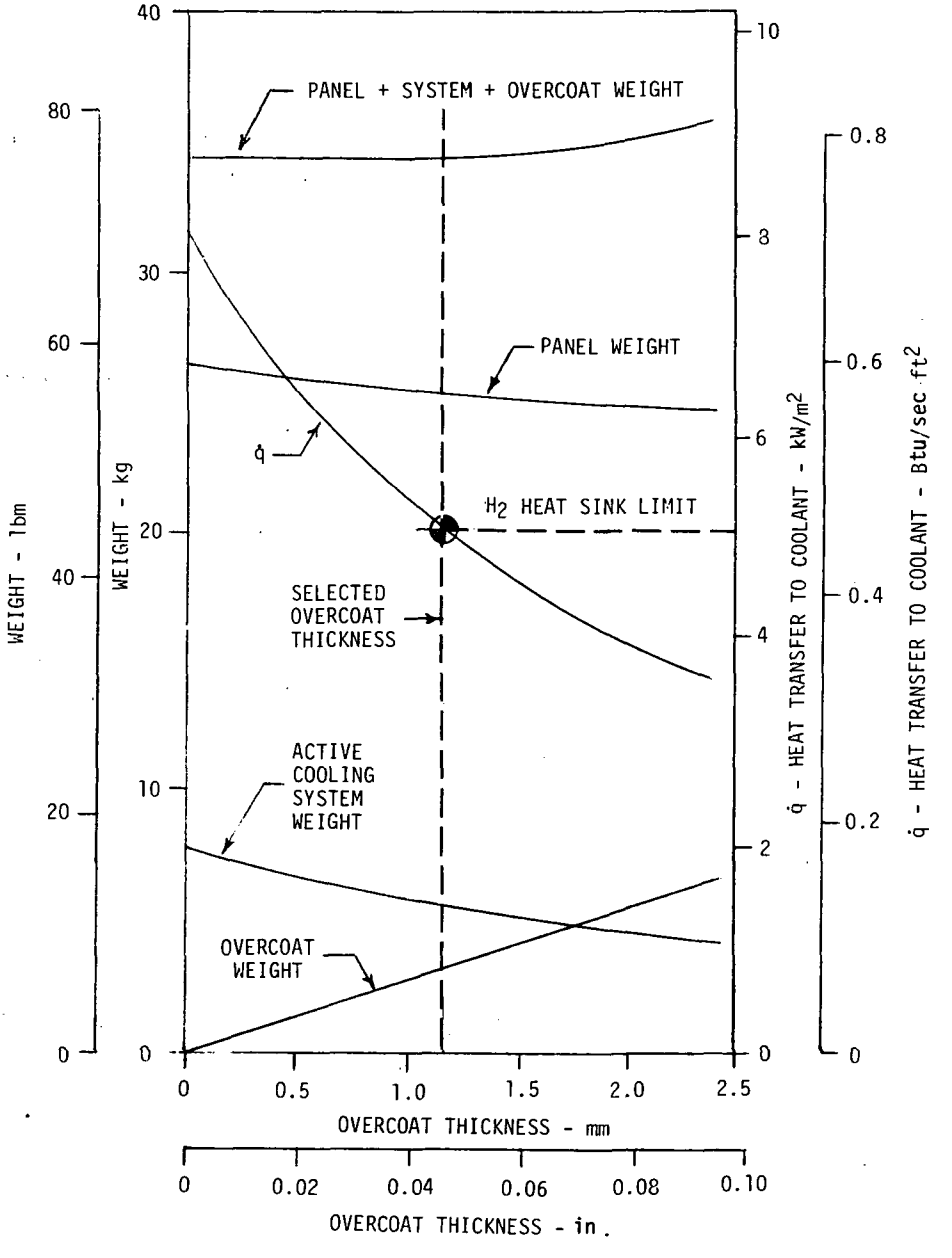

FIGURE 88
MACH 3 CRUISE - SILICONE OVERCOAT

- SILICONE OVERCOAT THICKNESS = 1.17 mm (0.046 in.)
- ALUMINUM SKIN THICKNESS = 1.02 mm (0.04 in.)
- HEAT CAPACITY OF PANEL SUPPORT STRUCTURE AND COOLANT WITHIN TUBES EXCLUDED

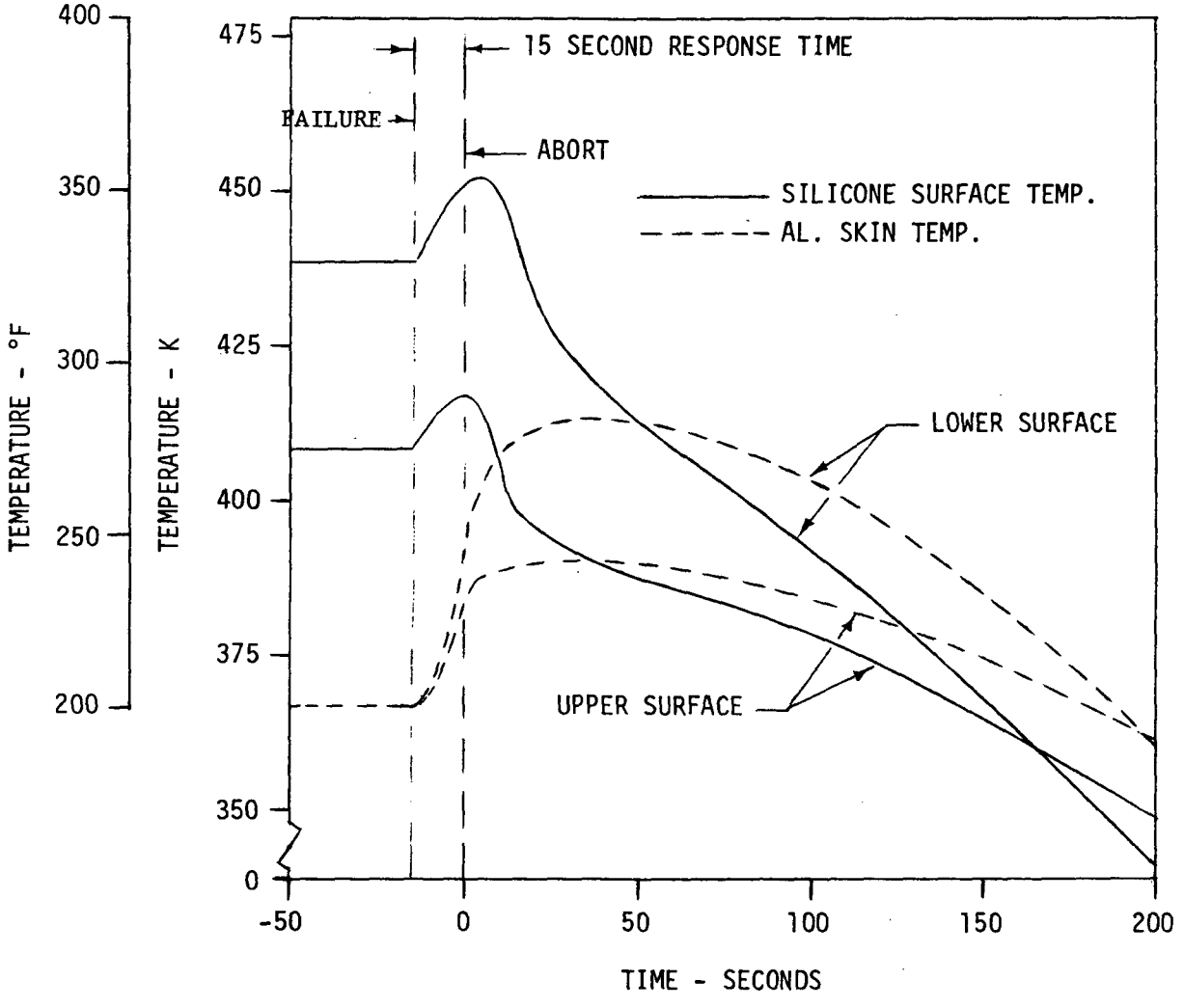

FIGURE 89
SILICONE OVERCOAT CONCEPT ABORT TEMPERATURE RESPONSE (MACH 3 UPPER AND LOWER SURFACES)

o Mach 4.5 Concepts - Figures 90 and 91 present results obtained for Mach 4.5 cruise/abort studies for typical upper and lower surfaces, respectfully.

Upper Surface - The minimum total weight for upper surface panels is shown on Figure 91 to be achieved with the silicone overcoat approach. The weight of the overcoat is offset by reduction in the weight of the cooling system and the tubes (wider tube spacing).

Thermo Structural Concept	Material		Avg. Temp. During Cruise (K)	Max Abort Temp (K) (1)	Cruise Heat Flux (kW/m^2) (2)	Unit Panel Wt. (kg/m^2) (3)	Wt. of 7.43 m^2 Panel		
	Type	Thickness (mm)					Dry Panel (kg)	Cooling System (4) (kg)	Total (5) (kg)
Baseline Skin	Alum	1.02	366	485	16.3	3.94	29.3	12.8	42.1
Thickened Skin	Alum	1.14	366	478	16.3	4.31	32.0	12.8	44.8
Precooled Skin	Alum	1.02	339	470	17.3	3.94	29.3	18.0	47.3
Overcoated Skin	(6) Alum Silicone	1.02 1.91	366 533	451 544	9.0	4.40	32.7	8.6	41.3
Overcoated Skin	(7) Alum Kapton	1.02 6.71	366 584	455 585	5.7	12.99	96.5	6.1	102.6
Overcoated Skin	(7) Alum Kapton	1.02 3.20	366 533	452 535	9.0	8.18	60.8	8.6	69.4
Undercoated Skin	Alum Silicone ($40\%L_iO_2$)	1.02 0.13	366 366	478 478	16.3	4.06	30.2	12.8	43.0

NOTES:

(1) Cooling system failure 15 seconds prior to abort. Alum. T_{max} allowable = 478K.
(2) Heat flux absorbed by panel coolant during normal operation at cruise with surface emissivity of 0.8.
(3) Unit panel weight includes skin, dry coolant tubes, and tube attachment (solder, weld, braze, etc.)
(4) Cooling system weight chargeable to typical panel (1.22m x 6.10m panel). Includes all cooling system components, coolant distribution system, and system coolant weights.
(5) Total weight equals summation of dry panel weight plus cooling system weight.
(6) Silicone is low density (400 kg/m^3) sprayable overcoat material. T_{max} allowable = 533K.
(7) Kapton is DuPont polyimide film, type "H". T_{max} allowable = 589K.

FIGURE 90a
MACH 4.5 THERMO-STRUCTURAL CONCEPT COMPARISON (UPPER SURFACE)

Thermo-Structural Concept	Material		Avg. Temp. During Cruise (°F)	Max. Abort Temp (°F) [1]	Cruise Heat Flux (Btu/sec ft^2) [2]	Unit Panel Wt. (lbm/ft^2) [3]	Wt. of 80 Ft^2 Panel		
	Type	Thickness (in.)					Dry Panel (lbm)	Cooling System [4] (lbm)	Total [5] (lbm)
Baseline Skin	Alum	0.040	200	414	1.435	0.807	64.6	28.3	92.9
Thickened Skin	Alum	0.045	200	400	1.435	0.882	70.5	28.3	98.8
Precooled Skin	Alum	0.040	150	387	1.52	0.807	64.6	39.6	104.2
Overcoated Skin	[6] Alum Silicone	0.040 0.075	200 500	352 519	0.793	0.902	72.2	18.9	91.1
Overcoated Skin	[7] Alum Kapton	0.040 0.264	200 592	359 593	0.505	2.66	212.8	13.4	226.2
Overcoated Skin	[7] Alum Kapton	0.040 0.126	200 499	354 503	0.793	1.676	134.1	18.9	153.0
Undercoated Skin	Alum Silicone ($40\%L_i0_2$)	0.040 0.005	200 200	400 400	1.435	0.831	66.5	28.3	94.8

NOTES:

[1] Cooling system failure 15 seconds prior to abort. Alum T_{max} allowable = 400°F

[2] Heat flux absorbed by panel coolant during normal operation at cruise with surface emissivity of 0.8.

[3] Unit panel weight includes skin, dry coolant tubes, and tube attachment (solder, weld, braze, etc.)

[4] Cooling system weight chargeable to typical panel (4 ft x 20 ft panel). Includes all cooling system components, coolant distribution system, and system coolant weights.

[5] Total weight equals summation of dry panel weight plus cooling system weight.

[6] Silicone is low density (25 PCF) sprayable overcoat material. T_{max} allowable = 500°F.

[7] Kapton is DuPont polyimide film, type "H". T_{max} allowable = 600°F.

FIGURE 90b
MACH 4.5 THERMO-STRUCTURAL CONCEPT COMPARISON (UPPER SURFACE)

Thermo-Structural Concept	Material		Avg. Temp. During Cruise (K)	Max Abort Temp (K) [1]	Cruise Heat Flux (kW/m^2) [2]	Unit Panel Wt. (kg/m^2) [3]	Wt. of 7.43 m^2 Panel		
	Type	Thickness (mm)					Dry Panel (kg)	Cooling System (kg) [4]	Total (kg) [5]
Baseline Skin	Alum	1.02	366	579	26.1	4.24	31.5	17.4	48.9
Thickened Skin	Alum	5.87	366	478	26.1	17.68	131.4	17.4	148.8
	Boron-AL	1.02	422	578	23.1	4.24	31.5	15.2	46.7
	Lockalloy	1.02	422	568	23.1	3.58	26.6	15.2	41.8
Precooled Skin	Alum	4.85	339	579	27.5	14.82	110.2	25.1	135.3
	Boron-AL	1.02	366	564	26.1	4.24	31.5	17.4	48.9
	Lockalloy	1.02	366	554	26.1	3.58	26.6	17.4	44.0
Overcoated Skin	[7] Alum	2.51	366	478	11.93	12.94	96.2	10.3	106.5
	Kapton	3.23	589	599					
	[6] Alum	3.61	366	478	16.1	11.51	85.5	12.7	98.2
	Silicone (Sprayable)	1.07	533	579					
	Alum	2.54	366	478	16.1	12.21	90.8	12.7	103.5
	Silicone ($40\%L_iO_2$)	3.61	533	548					
Insulative Heat Shield	Alum	1.02	366	478	3.73	7.02	52.2	4.7	56.9
	Fiberfrax	6.20	680	689					
	Titanium	0.51	680	689					
Undercoated Skin	Alum	1.02	366	478	26.1	8.41	62.5	17.4	79.9
	Silicone ($40\%L_iO_2$)	4.01	366	478					
Phase Change Material	Alum	1.02	366	478	26.1	6.55	48.7	17.4	66.1
	Alum H/C	12.70	366	478					
	Polyethylene	2.34	366	474					

NOTES:

[1] Cooling system failure 15 seconds prior to abort. Alum T_{max} allowable = 478K. Boron-AL T_{max} allowable = 589K, and Lockalloy T_{max} allowable = 644K.

[2] Heat flux absorbed by panel coolant during normal operation at cruise with surface emissivity of 0.8.

[3] Unit panel weight includes skin, dry coolant tubes, and tube attachment (solder, weld, braze, etc.)

[4] Cooling system weight chargeable to typical panel (1.22m x 6.10m panel). Includes all cooling system components, coolant distribution system, and system coolant weights.

[5] Total weight equals summation of dry panel weight plus cooling system weight.

[6] Silicone is low density (400 kg/m^3) sprayable overcoat material. T_{max} allowable = 533K.

[7] Kapton is DuPont polyimide film, type "H". T_{max} allowable = 589K.

FIGURE 91a
MACH 4.5 THERMO-STRUCTURAL CONCEPT COMPARISON (LOWER SURFACE)

Thermo-Structural Concept	Material: Type	Material: Thickness (in.)	Avg. Temp. During Cruise (°F)	Max. Abort Temp (°F) [1]	Cruise Heat Flux (Btu/sec ft²) [2]	Unit Panel Wt. (lbm/ft²) [3]	Wt. of 80 Ft² Panel: Dry Panel (lbm)	Wt. of 80 Ft² Panel: Cooling System (lbm) [4]	Wt. of 80 Ft² Panel: Total (lbm) [5]
Baseline Skin	Alum	0.04	200	582	2.295	0.869	69.5	38.4	107.9
Thickened Skin	Alum	0.231	200	400	2.295	3.621	289.6	38.4	328.0
	Boron-AL	0.040	300	580	2.032	0.869	69.5	33.6	103.1
	Lockalloy	0.040	300	563	2.032	0.733	58.7	33.6	92.3
Precooled Skin	Alum	0.191	150	400	2.419	3.036	242.9	55.4	298.3
	Boron-AL	0.040	200	556	2.295	0.869	69.5	38.4	107.9
	Lockalloy	0.040	200	537	2.295	0.733	58.7	38.4	97.1
Overcoated Skin	Alum [7]	0.099	200	400	1.051	2.651	212.1	22.7	234.8
	Kapton [7]	0.127	600	619					
	Alum [6]	0.142	200	400	1.417	2.357	188.6	28.1	216.7
	Silicone (Sprayable) [6]	0.042	500	582					
	Alum	0.100	200	400	1.417	2.501	200.1	28.1	228.2
	Silicone ($40\%L_i0_2$)	0.142	500	527					
Insulative Heat Shield	Alum	0.040	200	400	0.329	1.437	115.0	10.4	125.4
	Fiberfrax	0.244	765	780					
	Titanium	0.020	765	780					
Undercoated Skin	Alum	0.040	200	400	2.295	1.722	137.8	38.4	176.2
	Silicone ($40\%L_i0_2$)	0.158	200	400					
Phase Change Material	Alum	0.040	200	400	2.295	1.342	107.3	38.4	145.7
	Alum H/C	0.500	200	400					
	Polyeth-ylene	0.092	200	394					

NOTES:

[1] Cooling system failure 15 seconds prior to abort. Alum T_{max} allowable = 400°F. Boron-AL T_{max} allowable = 600°F, and Lockalloy T_{max} allowable = 700°F.

[2] Heat flux absorbed by panel coolant during normal operation at cruise with surface emissivity of 0.8.

[3] Unit panel weight includes skin, dry coolant tubes, and tube attachment (solder, weld, braze, etc.)

[4] Cooling system weight chargeable to typical panel (4 ft x 20 ft panel). Includes all cooling system components, coolant distribution system, and system coolant weights.

[5] Total weight equals summation of dry panel weight plus cooling system weight.

[6] Silicone is low density (25 PCF) sprayable overcoat material. T_{max} allowable = 500°F.

[7] Kapton is DuPont polyimide film, type "H". T_{max} allowable = 600°F.

FIGURE 91b

MACH 4.5 THERMO-STRUCTURAL CONCEPT COMPARISON (LOWER SURFACE)

The silicone overcoat thickness of 1.905 mm (0.075 in) was based on limiting external surface temperature to 533 K (500°F) during normal cruise. Increased thicknesses resulted in higher surface temperatures which were deemed detrimental to panel operational life. In addition, for this particular case, a thicker overcoat did not decrease total weight, as shown by Figure 92.

Maximum temperatures during abort were well below the allowable short-term material limits assumed, 478 K (400°F) for aluminum skin and 589 K (600°F) for silicone. The initial peak temperature calculated for the bare baseline skin was 485 K (414°F), but a more detailed analysis which included the heat capacity of the honeycomb structure showed that baseline skin temperatures would not exceed 478 K (400°F).

The other upper surface concepts summarized by Figure 90 were either heavier or resulted in higher heat transfer to the panel coolant, thus requiring larger hydrogen fuel flowrates. Use of Kapton as an overcoat and operating during cruise near the assumed 589 K (600°F) limit temperature for long-term exposure, did reduce coolant heat transfer rates because of higher radiation dissipation. However, the weight of the Kapton was prohibitive. At a lower surface temperature, Kapton was more efficient from weight considerations alone.

Lower Surface - As shown by Figure 91, employing Lockalloy as the cooled skin resulted in the lowest weight. A Lockalloy panel designed for operation at 422 K (300°F) during cruise shows a slight advantage over one designed for 366 K (200°F). The same trends apply for the boron-aluminum composite designs. The baseline bare, 1.02 mm (0.04 in), aluminum skin design was not acceptable because of excessive skin temperature during abort. The weight of the thickened aluminum skin concepts is prohibitive, even though some reduction was obtained by precooling, but at the expense of higher cooling system weight and cruise heat flux.

The low density silicone overcoat resulted in lower weight than Kapton, or silicone enriched with lithium oxide. A unique solution was required to define the proper combination of aluminum skin thickness and overcoat thickness in the evaluation of these concepts.

TYPICAL 1.2m x 6.1 m (4 ft x 20 ft) PANEL

PANEL AL. SKIN THICKNESS = 1.02 mm (0.04 in.)

PANEL WEIGHT EXCLUDES SUPPORT STRUCTURE

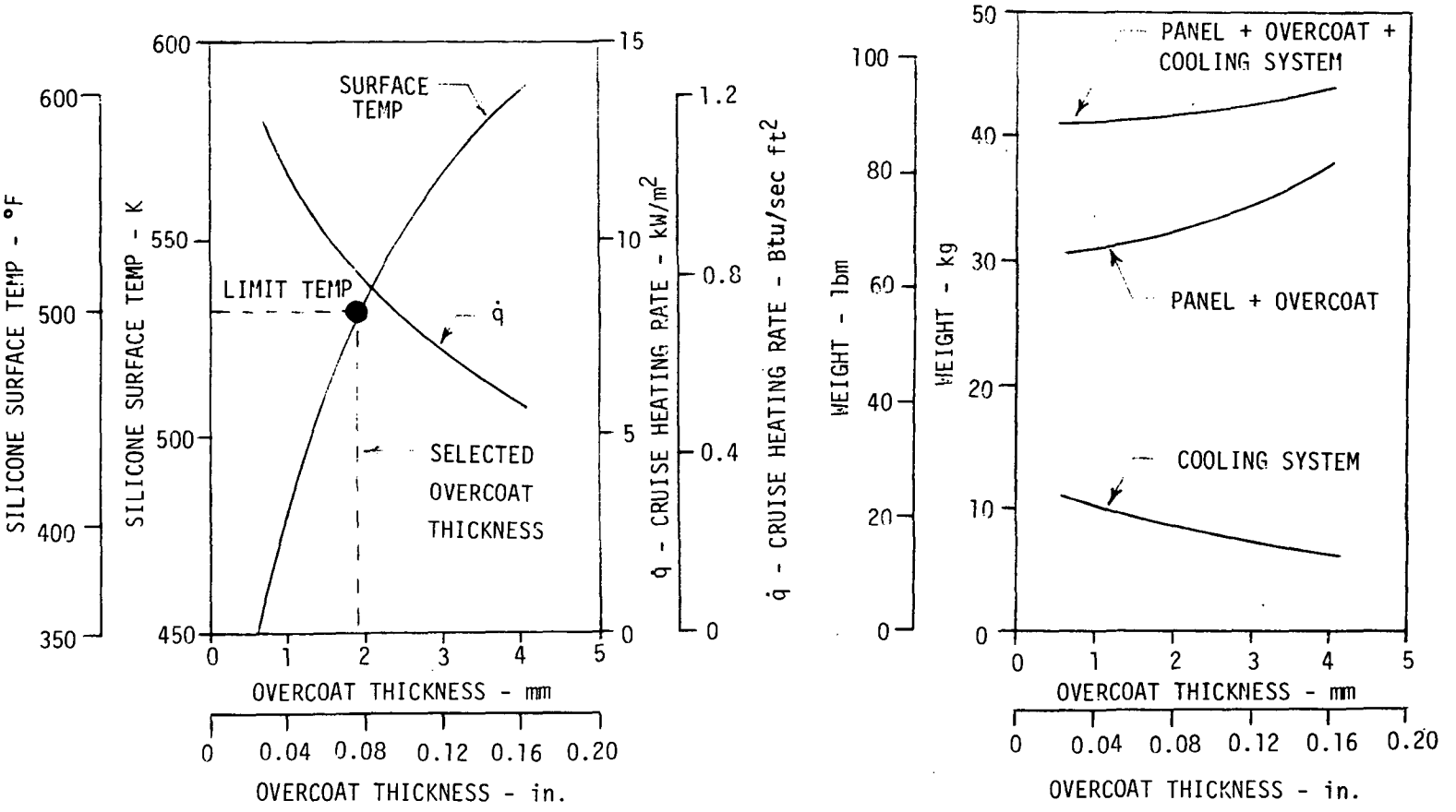

FIGURE 92
MACH 4.5 UPPER SURFACE - SPRAYABLE SILICONE OVERCOAT

The sizing was based on limiting aluminum skin to 478 K (400°F) during abort and limiting overcoat surfaces to their respective maximum values during cruise and abort (i.e., cruise and abort temperatures respectively of 533 K (500°F) and 589 K (600°F) for the silicones and 589 K (600°F) and 644 K (700°F) for Kapton).

Figure 93 illustrates the parametric relationships involved for the sprayable silicone overcoat. The advantage of operating the overcoat at the limit temperature during cruise is apparent from inspection of the figure. Total weight, and heat transfer to the panel coolant, are reduced. Additional increases in overcoat thickness permits a reduction in aluminum skin thickness required to limit abort peak skin temperature to 478 K (400°F), reduces weight, and cooling system heat load. However, this results in exceeding allowable temperature during cruise. The same type of analyses were conducted for the other Mach 4.5 lower surface overcoat candidates. Figure 94 illustrates the transient temperature characteristics of the silicone overcoated concept during abort.

The undercoated skin, utilizing silicone enriched with Lithium oxide, showed a weight reduction, compared to the overcoats. However, it does not reduce cruise heat transfer rates or the hydrogen heat sink required. This concept is unique to the skin/stringer type structural arrangement. It would require a method of containment because the potential reaction of lithium oxide with water causes corrosion.

The insulative titanium heat shield, using Corborundum "Fiberfrax 660" insulation applied to the cooled aluminum skin, is somewhat heavier than the Lockalloy or boron-aluminum composite skin concepts. However, it reduces the cooling system heat loads relative to the unprotected Lockalloy or boron-aluminum skin. This was important because of the basic limitations in availability of fuel heat sink and was taken into account in subsequent evaluations.

An additional advantage of the insulative heat shield concept is that wider coolant tube spacing could be tolerated without exceeding allowable skin temperature levels and gradients. This minimizes potential failure points and failure detection system complexity. Although "Fiberfrax" insulation was used in the analyses, insulations such as Johns-Manville "MIN-K" or "Micro-Fibers" would have provided similar performance.

TIME FROM FAILURE TO ABORT INITIATION = 15 SECONDS
TYPICAL 1.2 m x 6.1 m (4 ft x 20 ft) PANEL
PANEL WEIGHT EXCLUDES SUPPORT STRUCTURE

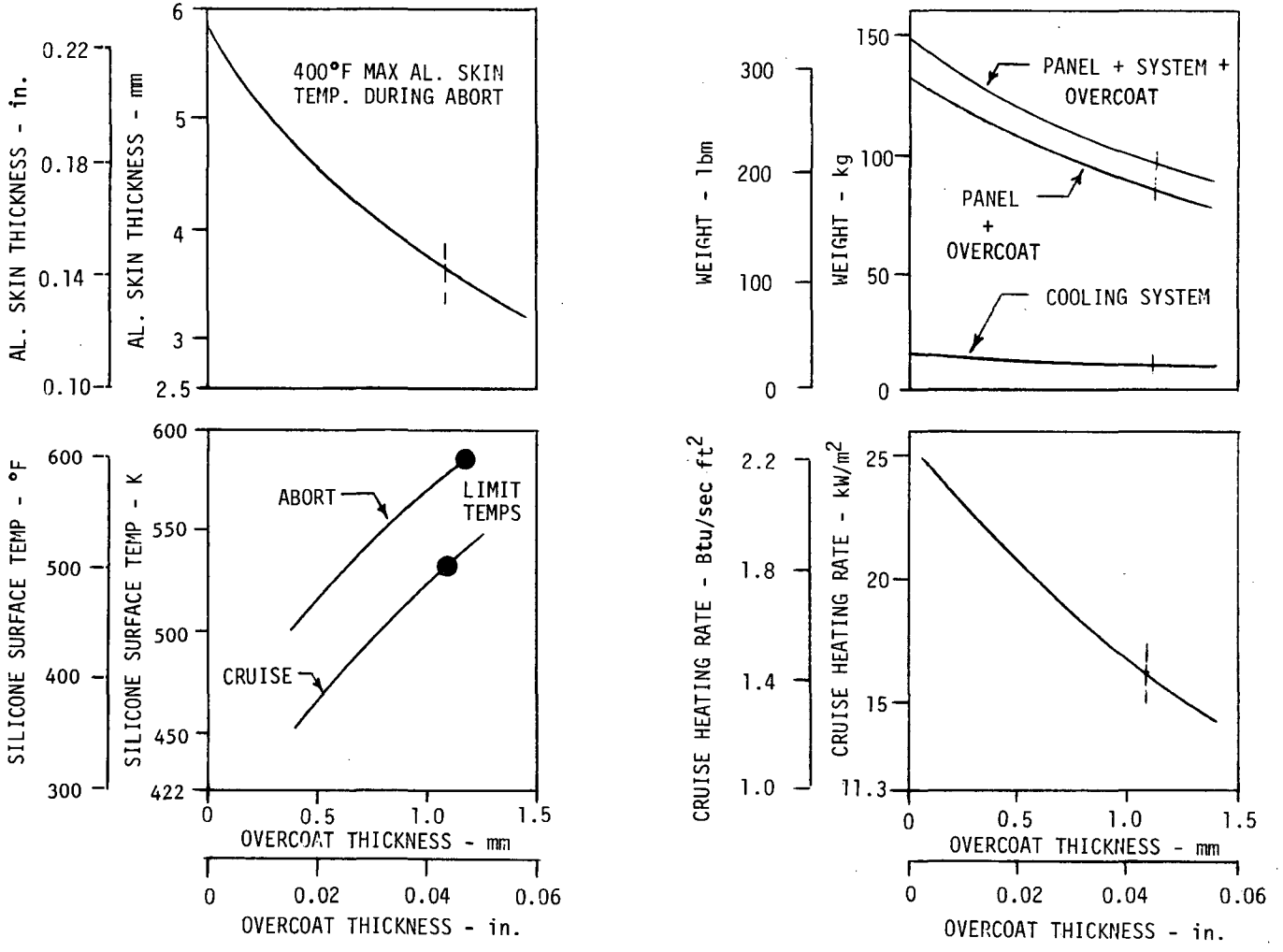

FIGURE 93
MACH 4.5 LOWER SURFACE - SPRAYABLE SILICONE OVERCOAT

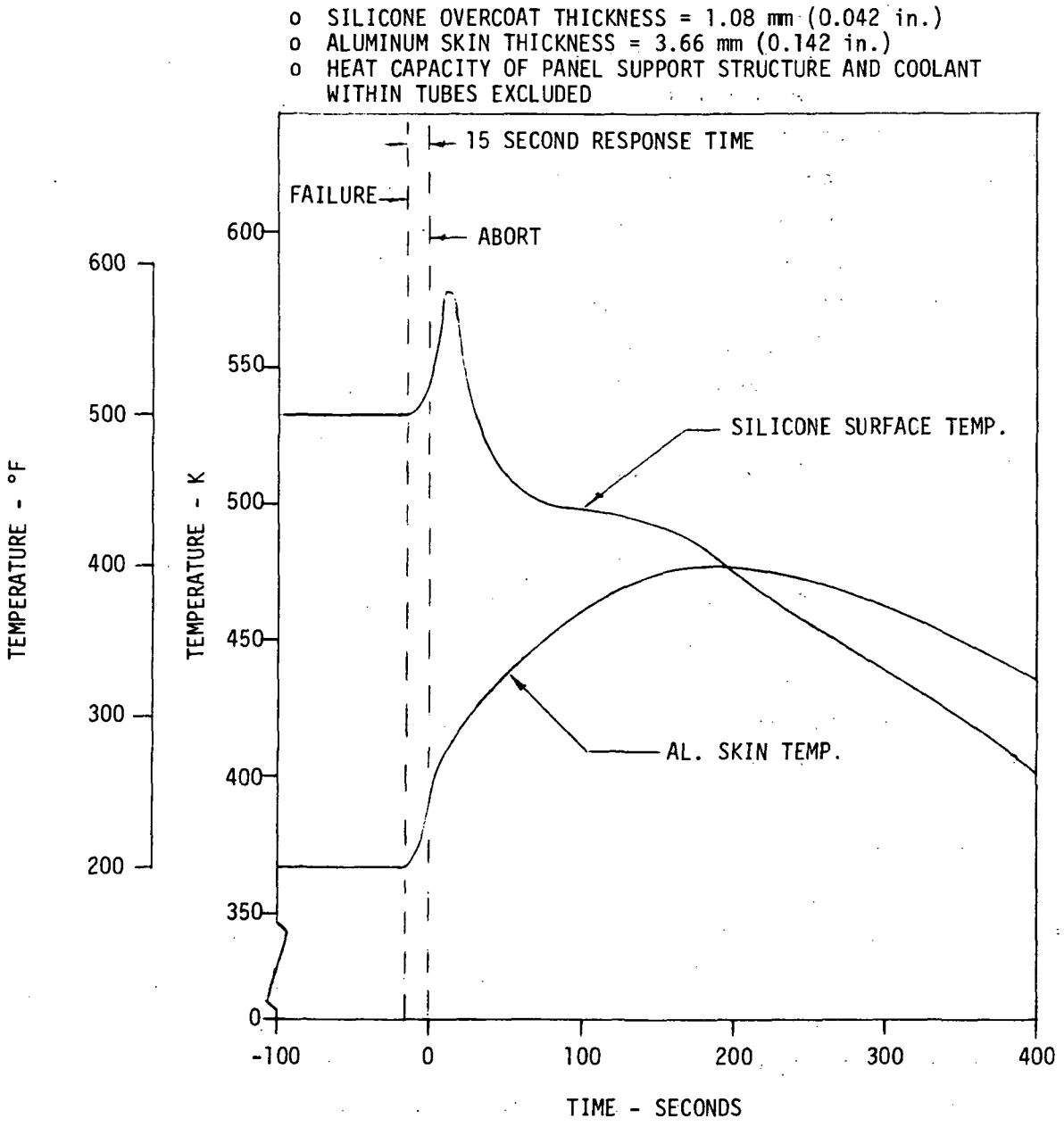

FIGURE 94
SILICONE OVERCOAT CONCEPT ABORT TEMPERATURE RESPONSE (MACH 4.5 LOWER SURFACE)

Insulation degradation due to attachment cut-outs and heat shield supports was accounted for by an initial assumed degradation factor of 2 on the vendor-specified thermal conductivity values. However, a more detailed analysis subsequently conducted, which included heat transfer calculations through actual shield attachments, showed this degradation factor was too conservative. Therefore, a factor of 1.25 was used in later thermal studies.

External surface temperatures were found to be sufficiently low (i.e., 700 K < (800°F)) to permit the use of titanium as the external shield for the typical Mach 4.5 lower surface panel location. Leading edge surfaces, as well as locations further forward than the reference location of 15.2 m (50 ft) aft of the nose tip, subjected to higher cruise and abort heating rates, would likely require a shield material with a higher allowable temperature capability (e.g., Inconel, Rene' 41, etc.).

Typical transient temperatures during Mach 4.5 abort are illustrated by Figure 95. It can be noted that the peak aluminum temperatures occur late in the abort maneuver when structural load factors would be lowest.

The phase change material (PCM) concept utilizing polyethylene in aluminum honeycomb core was heavier than the insulative heat shield and provided no reduction in cruise heat loads. Although aluminum honeycomb was used in the thermal analyses for containing the PCM, the weight shown in Figure 91 did not include the honeycomb. The honeycomb was assumed to be chargeable to structure. An effective thermal conductance and heat capacity for the honeycomb/PCM combination was used in a one-dimensional heat transfer analysis. This approach had been shown to provide good correlation with test data for PCM applications having relatively low transient heating rates, such as the thermal capacitor in the coolant loop of the Skylab Airlock Module, Reference (18). It was judged that the one-dimensional analytical method was an adequate approach for the Mach 4.5 lower surface panel. However, for the much higher transient abort heating rates applicable to the Mach 6 lower surface configuration, a more sophisticated analysis was used to assess PCM performance.

o Mach 6 Concepts - Figures 96 and 97 present results obtained for Mach 6 studies of the typical upper and lower surfaces, respectively. With minor exceptions, the conclusions reached with regard to candidate concept relative weight comparisons are the same as those reached for the Mach 4.5 studies. These conclusions are discussed in following paragraphs.

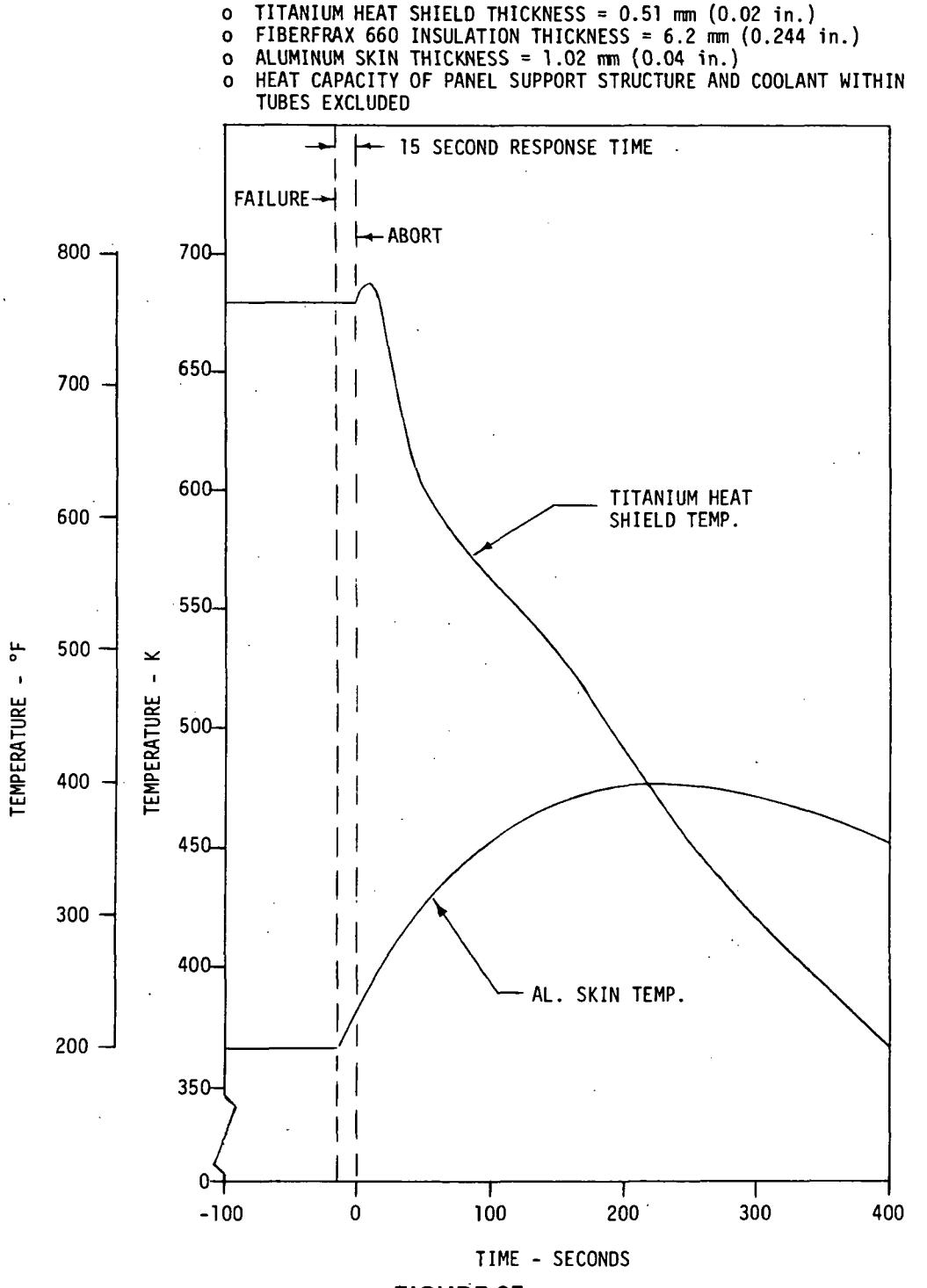

FIGURE 95
INSULATIVE HEAT SHIELD CONCEPT ABORT TEMPERATURE RESPONSE
(MACH 4.5 LOWER SURFACE)

Thermo-Structural Concept	Material Type	Material Thickness (mm)	Avg. Temp. During Cruise (K)	Max Abort Temp (K) (1)	Cruise Heat Flux (kW/m^2) (2)	Unit Panel Wt. (kg/m^2) (3)	Wt. of 7.43 m^2 Panel: Dry Panel (kg)	Wt. of 7.43 m^2 Panel: Cooling System (kg) (4)	Wt. of 7.43 m^2 Panel: Total (kg) (5)
Baseline Skin	Alum	1.02	366	493	17.5	3.98	29.6	13.6	43.2
Thickened Skin	Alum	1.37	366	478	17.5	4.94	36.7	13.6	50.3
Overcoated Skin	(7) Alum / Kapton	1.02 / 2.39	366 / 533	465 / 539	12.1	7.15	53.1	10.3	63.4
	(6) Alum / Silicone	1.02 / 1.42	366 / 533	470 / 555	12.1	4.34	32.2	10.4	42.6
	(7) Alum / Kapton	1.02 / 4.06	366 / 589	468 / 587	9.5	9.41	70.0	8.8	78.8
Undercoated Skin	Alum / Silicone ($40\%L_iO_2$)	1.02 / 0.30	366 / 366	478 / 478	17.5	4.30	31.9	13.6	45.5

NOTES:

(1) Cooling system failure 15 seconds prior to abort. Alum T_{max} allowable = 478K.
(2) Heat flux absorbed by panel coolant during normal operation at cruise with surface emissivity of 0.8.
(3) Unit panel weight includes skin, dry coolant tubes, and tube attachment (solder, weld, braze, etc.)
(4) Cooling system weight chargeable to typical panel (1.22m x 6.10m panel). Includes all cooling system components, coolant distribution system, and system coolant weights.
(5) Total weight equals summation of dry panel weight plus cooling system weight.
(6) Silicone is low density (400 kg/m^3) sprayable overcoat material. T_{max} allowable = 533K.
(7) Kapton is DuPont polyimide film, type "H". T_{max} allowable = 589K.

FIGURE 96a
MACH 6 THERMO-STRUCTURAL CONCEPT COMPARISON (UPPER SURFACE)

Thermo-Structural Concept	Material		Avg. Temp. During Cruise (°F)	Max. Abort Temp (°F) [1]	Cruise Heat Flux (Btu/sec ft^2) [2]	Unit Panel Wt. (lbm/ft^2) [3]	Wt. of 80 Ft^2 Panel		
	Type	Thickness (in.)					Dry Panel (lbm)	Cooling System (lbm) [4]	Total (lbm) [5]
Baseline Skin	Alum	0.040	200	428	1.54	0.816	65.3	29.9	95.2
Thickened Skin	Alum	0.054	200	400	1.54	1.011	80.9	29.9	110.8
Overcoated Skin	[7] Alum Kapton	0.040 0.094	200 500	378 510	1.066	1.464	117.1	22.7	139.8
	[6] Alum Silicone	0.040 0.056	200 500	387 539	1.066	0.888	71.0	22.9	93.9
	[7] Alum Kapton	0.040 0.160	200 600	383 597	0.8354	1.928	154.3	19.5	173.8
Undercoated Skin	Alum Silicone ($40\%L_i0_2$)	0.040 0.012	200 200	400 400	1.54	0.880	70.4	29.9	100.3

NOTES:

[1] Cooling system failure 15 seconds prior to abort. Alum T_{max} allowable = 400°F.
[2] Heat flux absorbed by panel coolant during normal operation at cruise with surface emissivity of 0.8.
[3] Unit panel weight includes skin, dry coolant tubes, and tube attachment (solder, weld, braze, etc.)
[4] Cooling system weight chargeable to typical panel (4 ft x 20 ft panel). Includes all cooling system components, coolant distribution system, and system coolant weights.
[5] Total weight equals summation of dry panel weight plus cooling system weight.
[6] Silicone is low density (25 PCF) sprayable overcoat material. T_{max} allowable = 500°F.
[7] Kapton is DuPont polyimide film, type "H". T_{max} allowable = 600°F.

FIGURE 96b
MACH 6 THERMO-STRUCTURAL CONCEPT COMPARISON (UPPER SURFACE)

Thermo-Structural Concept	Material Type	Material Thickness (mm)	Avg. Temp. During Cruise (K)	Max Abort Temp (K) [1]	Cruise Heat Flux (kW/m^2) [2]	Unit Panel Wt. (kg/m^2) [3]	Wt. of 7.43 m^2 Panel: Dry Panel (kg)	Wt. of 7.43 m^2 Panel: Cooling System (kg) [4]	Wt. of 7.43 m^2 Panel: Total (kg) [5]
Baseline Skin	Alum	1.02	366	736	44.5	4.67	34.7	25.8	60.5
Thickened Skin	Alum Boron-AL Lockalloy	16.13 4.85 2.16	366 422 422	478 589 644	44.5 41.8 41.8	46.49 15.30 6.44	345.5 113.7 47.9	25.8 23.0 23.0	371.3 136.7
Precooled Skin	Boron-AL Lockalloy	3.86 1.78	366 366	589 644	44.5 44.5	12.52 5.64	93.0 42.0	25.8 25.8	118.8
Overcoated Skin	[7] Alum Kapton	11.66 1.22	366 589	478 632	31.4	35.76	265.9	19.9	67.8
	[6] Alum Silicone	12.93 0.48	366 533	478 593	35.3	37.81	281.0	21.6	302.6
Insulative Heat Shield	Alum Fiberfrax Inconel	1.02 20.98 0.51	366 860 860	478 867 867	1.87	11.88	88.3	2.4	90.7
Undercoated Skin	Alum Silicone (40%$L_i{}_2O$)	9.58 7.82	366 366	478 478	44.5	36.51	271.3	25.8	297.1
Phase Change Material	Alum Alum H/C Polyethy-lene	2.26 12.70 10.16	366 366 366	478 478 478	44.5	18.14	134.9	25.8	160.7

NOTES:

[1] Cooling system failure 15 seconds prior to abort. Alum T_{max} allowable = 478K, Boron-AL T_{max} allowable = 589K, and Lockalloy T_{max} allowable = 644K.

[2] Heat flux absorbed by panel coolant during normal operation at cruise with surface emissivity of 0.8.

[3] Unit panel weight inclues skin, dry coolant tubes, and tube attachment (solder, weld, braze, etc.)

[4] Cooling system weight chargeable to typical panel (1.22m x 6.10m panel). Includes all cooling system components, coolant distribution system, and system coolant weights.

[5] Total weight equals summation of dry panel weight plus cooling system weight.

[6] Silicone is low density (400 kg/m^3) sprayable overcoat material. T_{max} allowable = 533K.

[7] Kapton is DuPont polyimide film, type "H". T_{max} allowable = 589K.

FIGURE 97a

MACH 6 THERMO-STRUCTURAL CONCEPT COMPARISON (LOWER SURFACE)

Thermo-Structural Concept	Material		Avg. Temp. During Cruise (°F)	Max. Abort Temp (°F) (1)	Cruise Heat Flux (Btu/sec ft^2) (2)	Unit Panel Wt. (lbm/ft^2) (3)	Wt. of 80 Ft^2 Panel		
	Type	Thickness (in.)					Dry Panel (lbm)	Cooling System (4) (lbm)	Total (5) (lbm)
Baseline Skin	Alum	0.040	200	865	3.92	0.957	76.6	56.9	133.5
Thickened Skin	Alum	0.635	200	400	3.92	9.522	761.8	56.9	818.7
	Boron-AL	0.191	300	600	3.68	3.133	250.6	50.6	301.2
	Lockalloy	0.085	300	700	3.68	1.318	105.5	50.6	156.1
Precooled Skin	Boron-AL	0.152	200	600	3.92	2.564	205.1	56.9	262.0
	Lockalloy	0.070	200	700	3.92	1.156	92.5	56.9	149.4
Overcoated Skin (7)	Alum Kapton	0.459 0.048	200 600	400 678	2.77	7.325	586.1	43.8	629.9
(6)	Alum Silicone	0.509 0.019	200 500	400 607	3.11	7.744	619.5	47.7	667.2
Insulative Heat Shield	Alum Fiberfrax Inconel	0.040 0.826 0.020	200 1088 1088	400 1101 1101	0.165	2.434	194.7	5.2	199.9
Undercoated Skin	Alum Silicone ($40\%L_iO_2$)	0.377 0.308	200 200	400 400	3.92	7.477	598.2	56.9	655.1
Phase Change	Alum Alum H/C Polyethylene	0.089 0.500 0.400	200 200 200	400 400 400	3.92	3.716	297.3	56.9	354.2

NOTES:

(1) Cooling system failure 15 seconds prior to abort. Alum T_{max} allowable = 400°F, Boron-AL T_{max} allowable = 600°F and Lockalloy T_{max} allowable = 700°F.

(2) Heat flux absorbed by panel coolant during normal operation at cruise with surface emissivity of 0.8.

(3) Unit panel weight includes skin, dry coolant tubes, and tube attachment (solder, weld, braze, etc.)

(4) Cooling system weight chargeable to typical panel (4 ft x 20 ft panel). Includes all cooling system components, coolant distribution system, and system coolant weights.

(5) Total weight equals summation of dry panel weight plus cooling system weight.

(6) Silicone is low density (25 PCF) sprayable overcoat material. T_{max} allowable = 500°F.

(7) Kapton is DuPont polyimide film, type "H". T_{max} allowable = 600°F.

FIGURE 97b
MACH 6 THERMO-STRUCTURAL CONCEPT COMPARISON (LOWER SURFACE)

Upper Surface - The silicone overcoat concept resulted in the lowest weight and reduced cruise heating rates below those for the bare aluminum and undercoated skin concepts. Lower heating rates were achieved with a Kapton overcoat designed for a 589 K (600°F) surface temperature at cruise. However, the weight was considerably higher. The baseline 1.02 mm (0.04 in) skin again showed that the 478 K (400°F) limit would not be exceeded, if the heat capacity of the honeycomb structure was included in the analysis.

Lower Surface - The Lockalloy skin concepts were found to be lowest in weight. Designing for a 366 K (200°F) average skin temperature during cruise resulted in a slight weight reduction compared to designing for 422 K (300°F). This reversal (from the results obtained for the Mach 4.5 lower surface) occurred because the assumed minimum gage skins 1.02 mm (0.04 in) were insufficient to limit peak abort temperature to 644 K (700°F). The additional thickness of Lockalloy skin required for the 422 K (300°F) cruise design more than offset the cooling system weight reduction. The same trend was noted for the boron-aluminum composite concepts (Figure 97). The boron-aluminum panel concepts were considerably heavier than the Lockalloy designs.

The Kapton and silicone overcoats do not appear feasible for lower surfaces. The problem with overcoats for the Mach 6 lower surface application was that thin coatings must be used to stay below allowable cruise surface temperatures. Thus, they offer little in the way of abort heat protection. These concepts do not significantly lower heat transfer rates to the coolant during cruise because of the limited thickness.

The undercoated skin utilizing silicone enriched with lithium oxide was not an attractive concept. This was due to its low thermal diffusivity, and high cruise heat load. The main feature of the undercoat material was its high potential heat absorption capability. However, it could only be used in a limited thickness because of low thermal conductivity. This restricts its ability to absorb heat at high rates. The outer skin temperature cannot be kept within limits. The aluminum skin required an increase in thickness to provide additional heat capacity. Figure 98 shows that further lithium oxide enrichment would increase both specific heat and thermal conductivity. Even though this would appear to make the undercoat more competitive (on a weight basis) it was not evaluated further because of the basically poor performance.

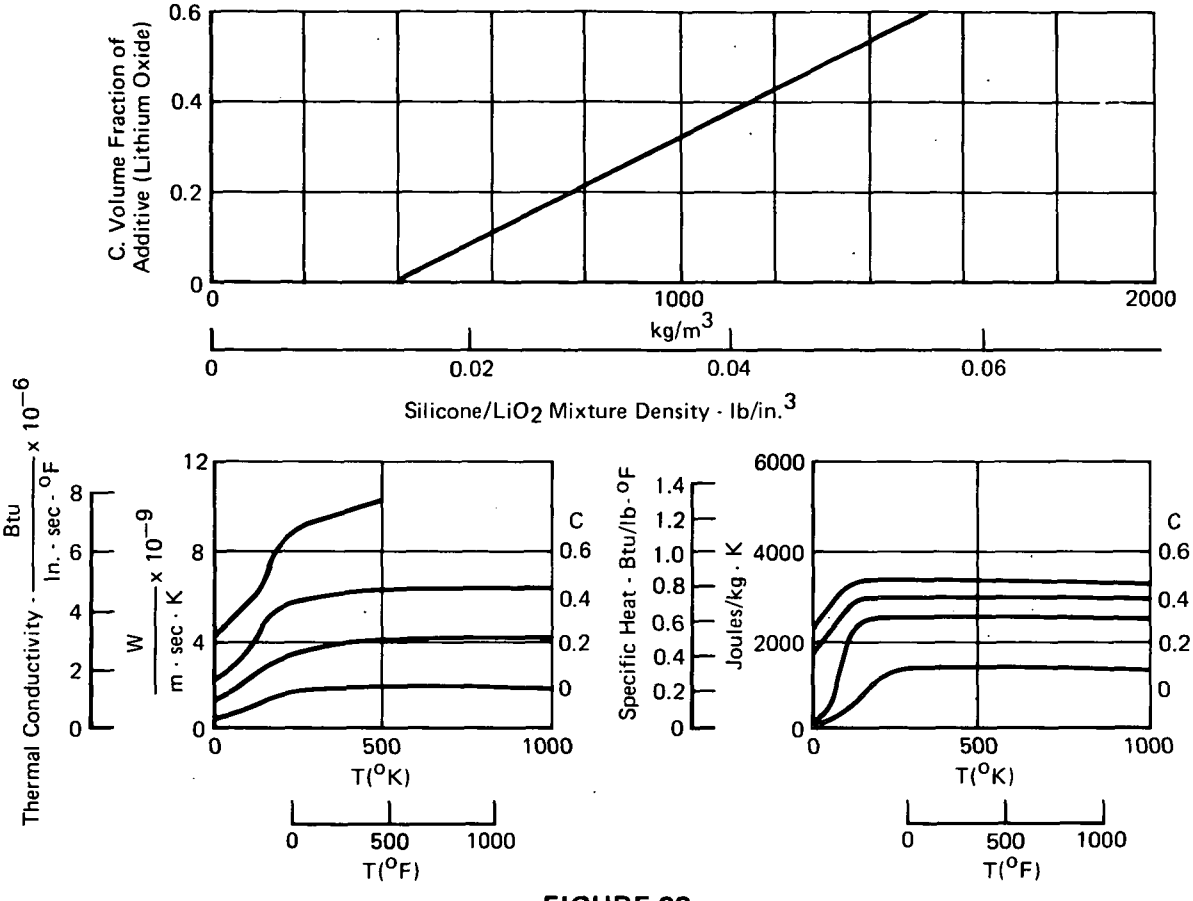

FIGURE 98
ESTIMATED THERMAL PROPERTIES OF OVERCOAT MIXTURES

GP75-0805-31

The insulative heat shield was found to be competitive with the Lockalloy skin on the basis of total weight. The heat shields have the advantage of reducing heat loads to a level which can be absorbed by the available hydrogen. The basic comments relative to the insulative heat shield for the Mach 4.5 lower surface also apply to the Mach 6 lower surface. Due to the higher cruise heating rate, and external surface temperature (1100°F), the radiation shield material was assumed to be constructed of Inconel 625. Subsequent investigations used Rene' 41 because of its superior characteristics. In addition, subsequent studies resulted in lower insulation thicknesses than indicated in Figure 97. This was because of the utilization of a lower insulation degradation factor (1.25 vs. 2.0). These refinements subsequently resulted in the heat shield concept being more competitive with the Lockalloy design on a weight basis. However, these refinements were not implemented until the design integration and optimization phase of the study.

The phase change material (PCM) concept using polyethylene appeared non-competitive during preliminary analyses. Total weight was excessive and cruise heating rates were too high to be absorbed by the available fuel heat sink. Despite these findings, it was felt that the initially employed analysis technique was not sufficiently exact. The initial analyses used effective values for the PCM/honeycomb core thermal conductivity and heat capacity in a one-dimensional heat transfer analysis. Sensitivity analyses using the one-dimensional method showed that the slight variations of thermal conductance assumed between the outer skin and the PCM had a noticeable effect on outer skin and PCM requirements. This was not entirely unexpected because of the highly transient heating rate to the Mach 6 lower surface following a cooling system failure.

Therefore, in order to further refine the analysis, a detailed 31 node thermal model was utilized which included the actual geometry and specific heat transfer paths of the honeycomb core and PCM. Because of symmetry, it was sufficient to consider only 1/6 of a honeycomb cell. The basic cell size was 3.175 mm (0.125 inch), with a 0.0178 mm (0.0007 inch) foil or cell wall thickness (typical of a 49.66 kg/m^3 (3.1 lbm/ft^3) core design). A 12.7 mm (0.5 inch) total core depth, filled to 80 percent with PCM, was used (based on the preliminary one-dimensional analysis results). The 20 percent cell void was allowed for PCM expansion during the phase change. The polyethylene properties used in the PCM analyses are depicted by Figure 99. These were derived from data contained in Reference (19).

An effective specific heat was employed to account for the material heat capacity during the phase change transition. Parametric analyses were conducted for several outer aluminum skin thicknesses and honeycomb cell wall thicknesses. The transient results, shown by Figure 100 illustrate the temperature levels and gradients for two different values of cell wall thickness, with a 1.02 mm (0.04 inch) outer aluminum skin. Peak skin temperature reductions (from those shown on Figure 100) of only 7 K (12°F) and 3.3 K (6°F) were achieved for cell wall thicknesses of 0.0178 mm (0.0007 inch) and 0.038 mm (0.0015 inch), respectively, by increasing outer skin thickness to 1.53 mm (0.06 inch). Therefore, the most efficient PCM design, which would limit peak temperature during abort to 478 K (400 °F), would include a 1.02 mm (0.04 inch) outer skin and a honeycomb core cell wall thickness of approximately 0.306 mm (0.012 inch).

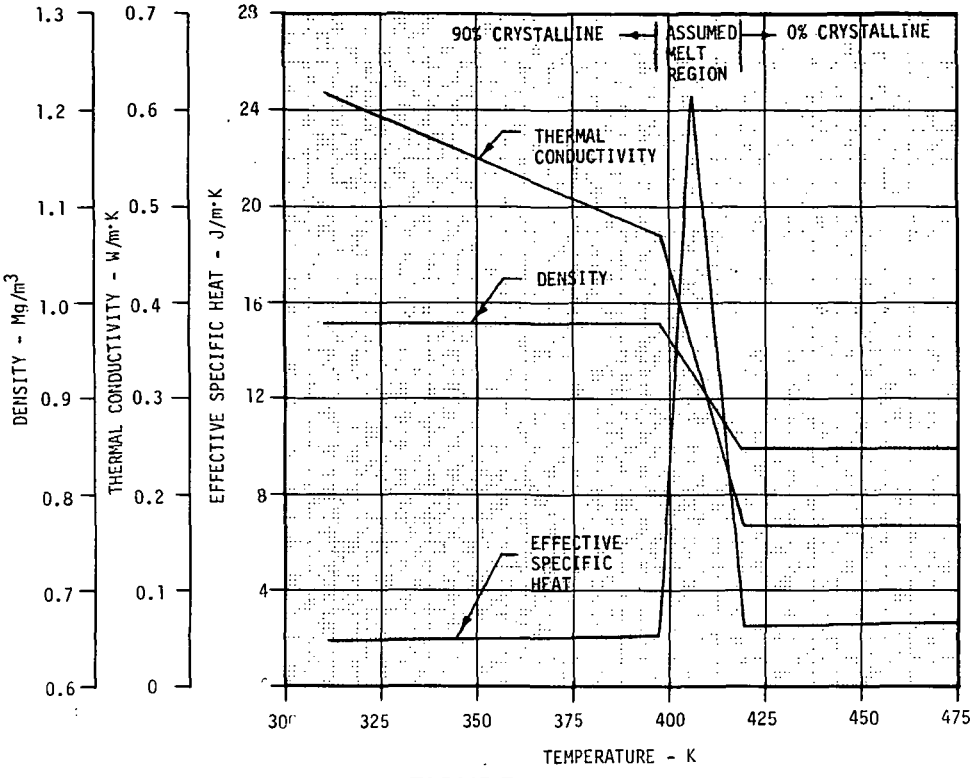

FIGURE 99a
POLYETHYLENE PROPERTIES EMPLOYED IN PCM ANALYSES

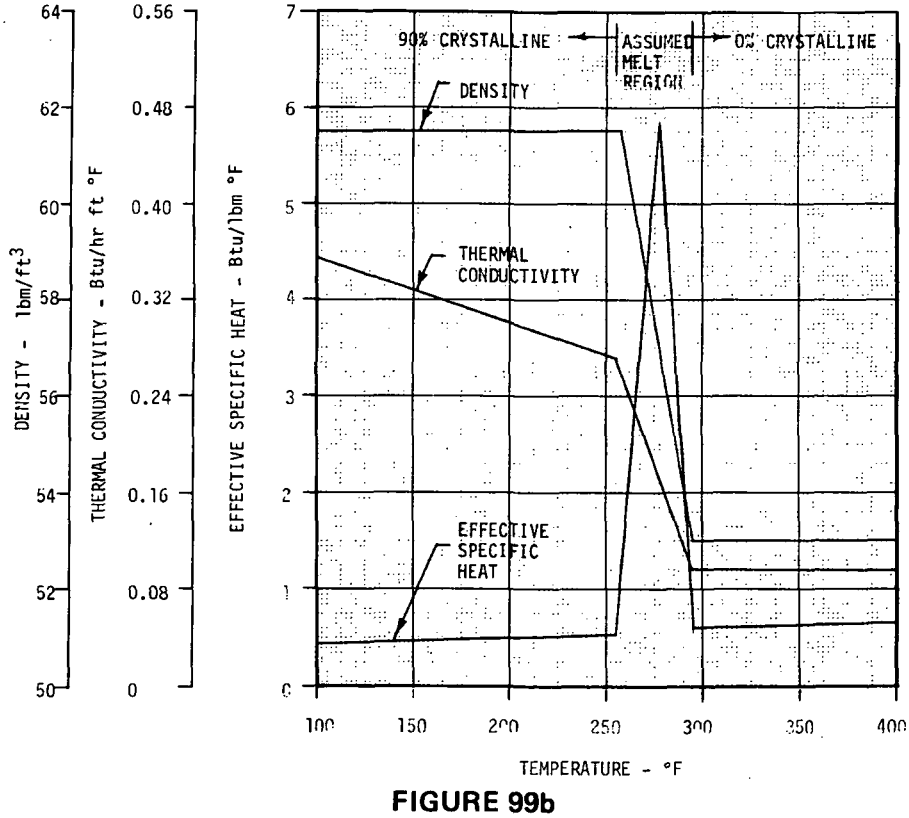

FIGURE 99b
POLYETHYLENE PROPERTIES EMPLOYED IN PCM ANALYSES

FAILURE RESPONSE TIME = 15 SEC.
- o FAILURE @ -15 SECONDS
- o ABORT @ 0 SECONDS

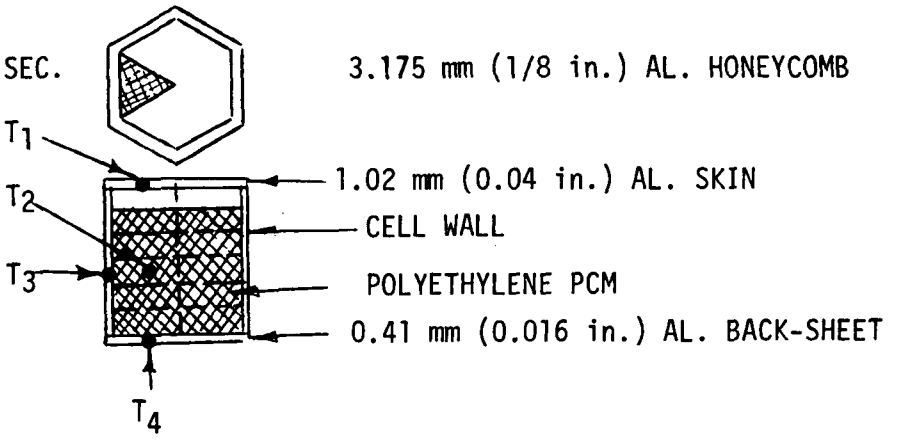

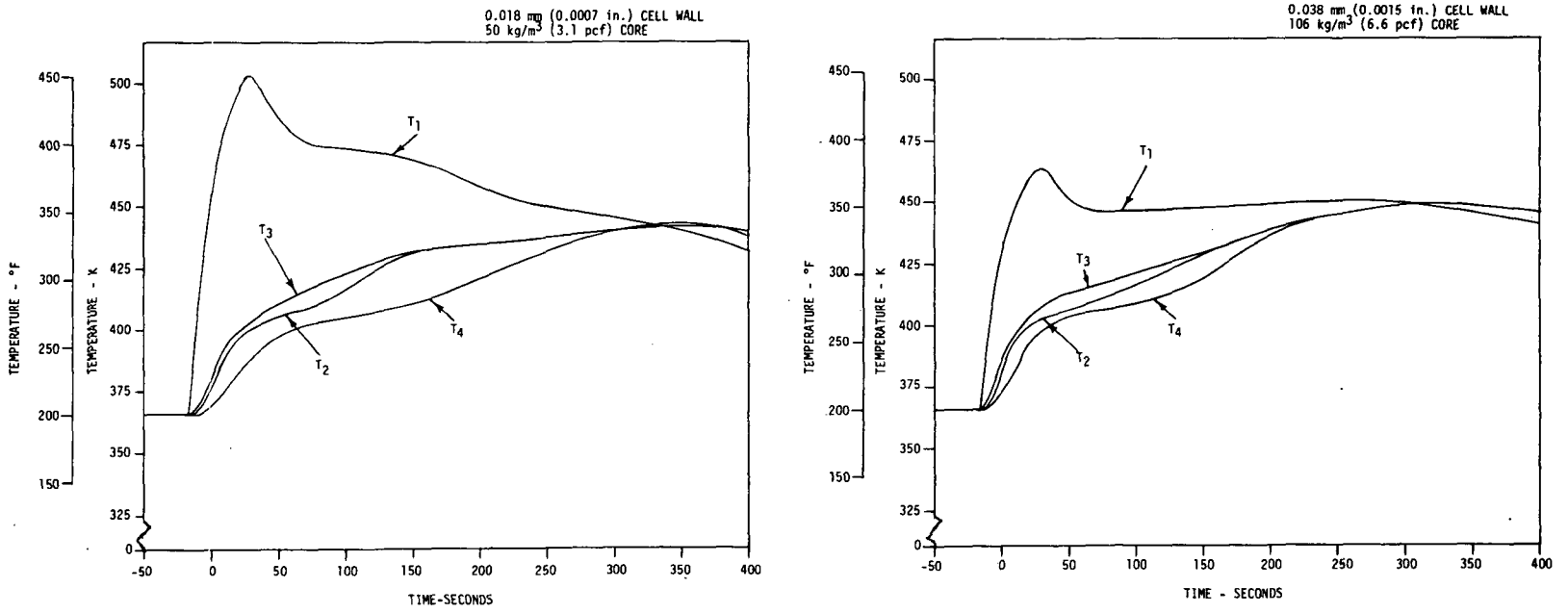

FIGURE 100
POLYETHYLENE PCM TEMPERATURES DURING ABORT
Mach 6 Lower Surface

Although subsequent analyses showed that the typical honeycomb panel core depth required for structural integrity was on the order of 30.48 mm (1.2 inches) and the inner face sheet approximately 1.02 mm (0.04 inch), no further thermal analyses were made. The basic non-competitiveness of the PCM concept relative to other candidates eliminated PCM as a viable approach.

o Sensitivity Analyses - Sensitivity analyses were conducted to illustrate thermal response characteristics and effects on design parameters caused by variations of reaction time for abort initiation and in nominal cruise/abort heating rates. The Mach 6 configurations were used since the effects are more pronounced, and present a larger design impact, than the lower Mach number configurations. Figures 101 and 102 show the sensitivity of candidate Mach 6 designs to failure response time (i.e., the elapsed time between cooling system failure and abort initiation). The nominal designs were based on a 15 second response.

Figure 102 illustrates the weight increase, on a unit panel basis, required to limit material temperatures to their maximum allowables for variable response times. The insulated designed have the advantage of being less weight sensitive to longer times for abort initiation than the unprotected bare surface concepts. The Lockalloy lower surface concept is shown to be lighter than the insulative heat shield approach for response times less than about 60 seconds.

Figure 103 shows panel weight requirement as a function of cruise cold wall heating rate. This figure illustrates sensitivity of other lower surface location designs compared to the typical location (15.2 m (50 ft) aft of nose tip) assumed for this study. Actively cooled panels located further forward on the aircraft would be required to accommodate higher cruise and abort heating rates. The weight increase required for the panel locations having higher heating rates is shown by Figure 103. The insulated heat shield requires less weight increase than the Lockalloy skin.

o Combined Upper and Lower Surface Concepts - Selected combinations of upper and lower surface concepts were devised to provide visibility into the potential of each thermostructural concept (from the standpoint of overall aircraft integration). Figures 104, 105, and 106 present the baseline aircraft configuration total cooled area (2980 m^2 (32,134 ft^2)) weight chargeable to the combination concepts (dry panel weight exclusive of structural support plus active cooling system weight). The average heat transfer to the coolant,

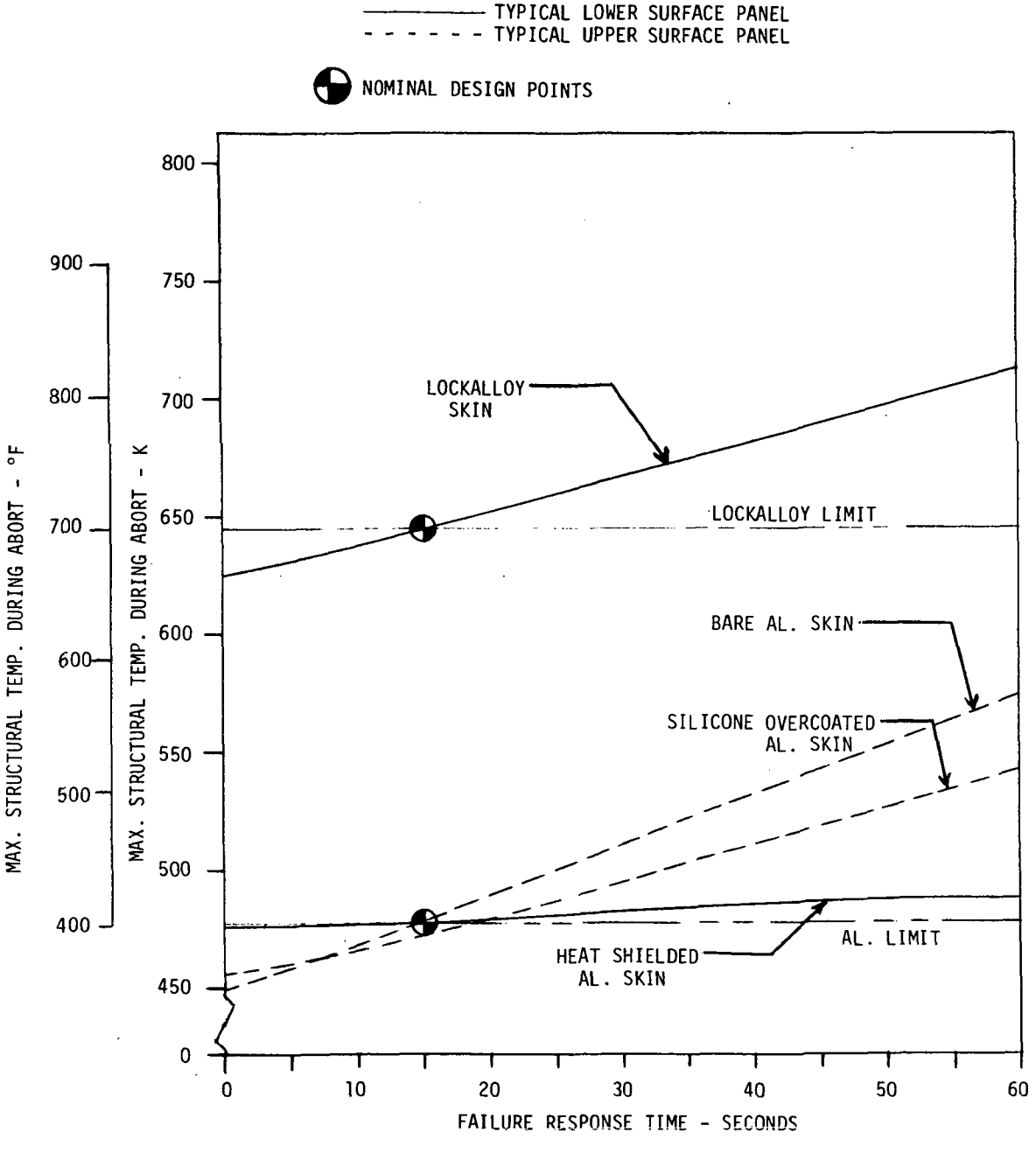

FIGURE 101
MAXIMUM STRUCTURAL TEMPERATURE vs FAILURE RESPONSE TIME
(MACH 6 CONCEPTS)

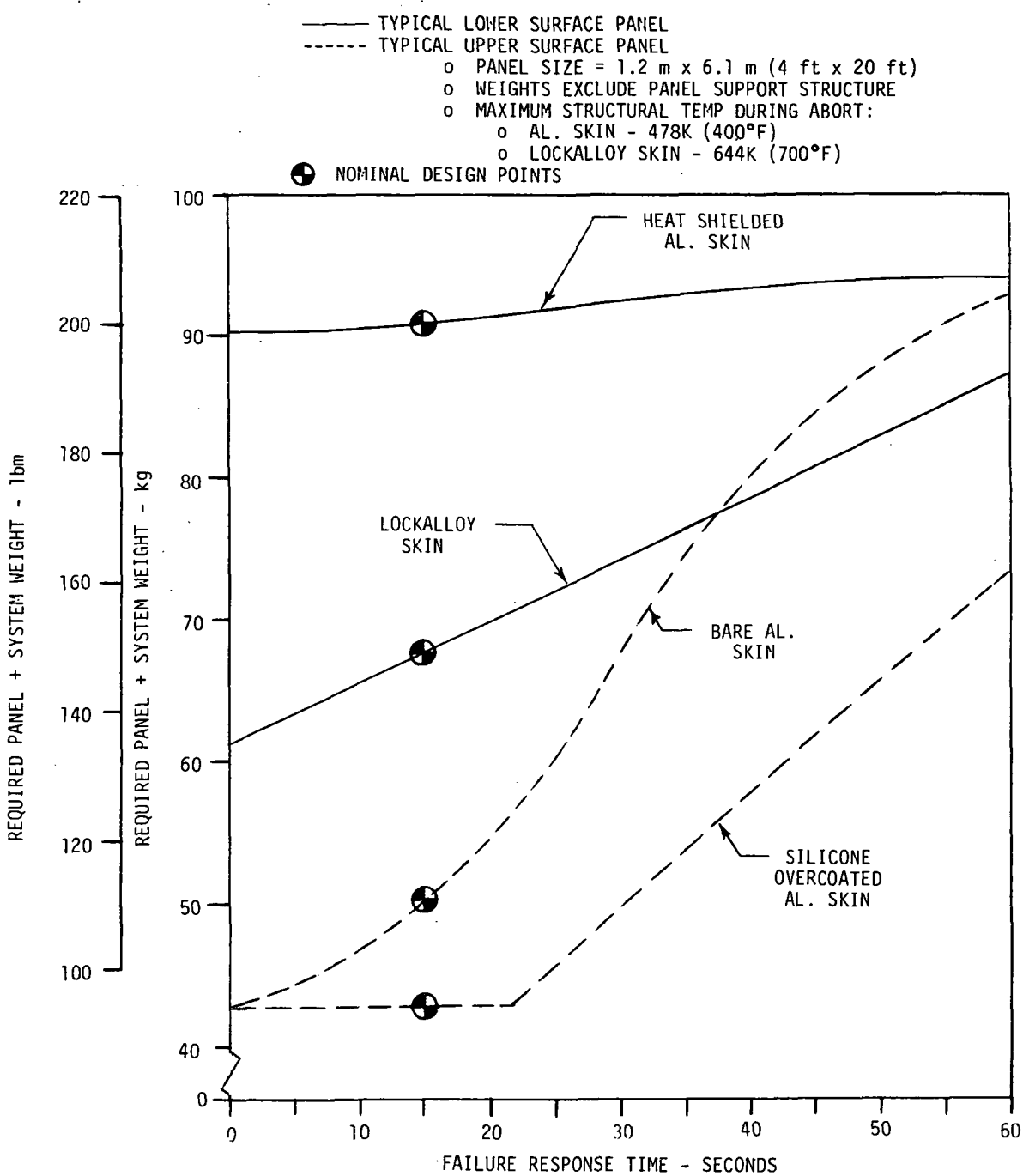

FIGURE 102
PANEL PLUS SYSTEM WEIGHT vs FAILURE RESPONSE TIME
(MACH 6 CONCEPTS)

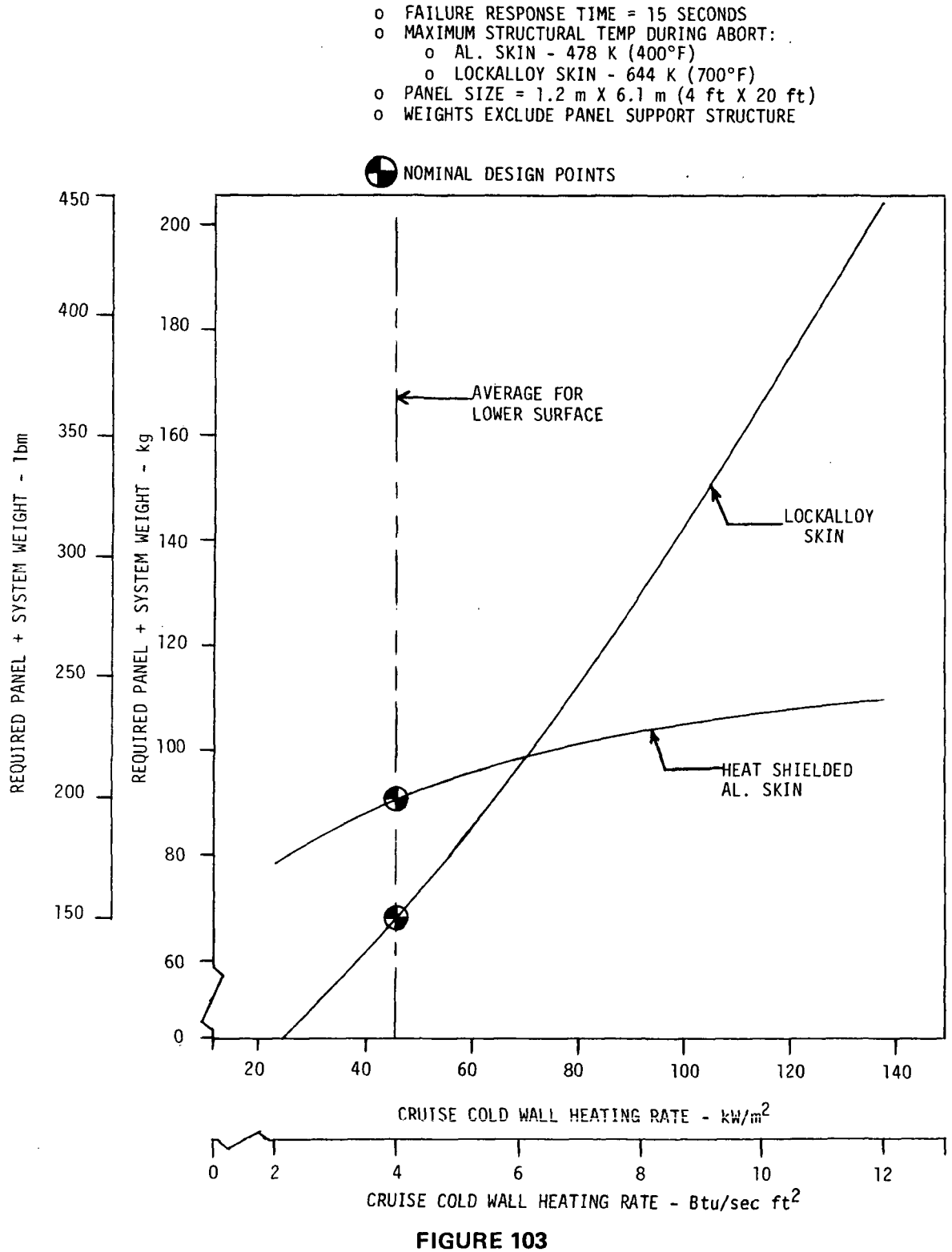

FIGURE 103
PANEL PLUS SYSTEM WEIGHT SENSITIVITY TO CRUISE HEATING RATE/LOCATION (MACH 6 LOWER SURFACE CONCEPTS)

- FAILURE RESPONSE TIME = 15 sec
- TOTAL COOLED AREA = 2985 m^2 (32,134 ft^2)
  - 1621 m^2 (17,449 ft^2) UPPER SURFACE
  - 1364 m^2 (14,685 ft^2) LOWER SURFACE
- PANEL SUPPORT STRUCTURE WEIGHT EXCLUDED

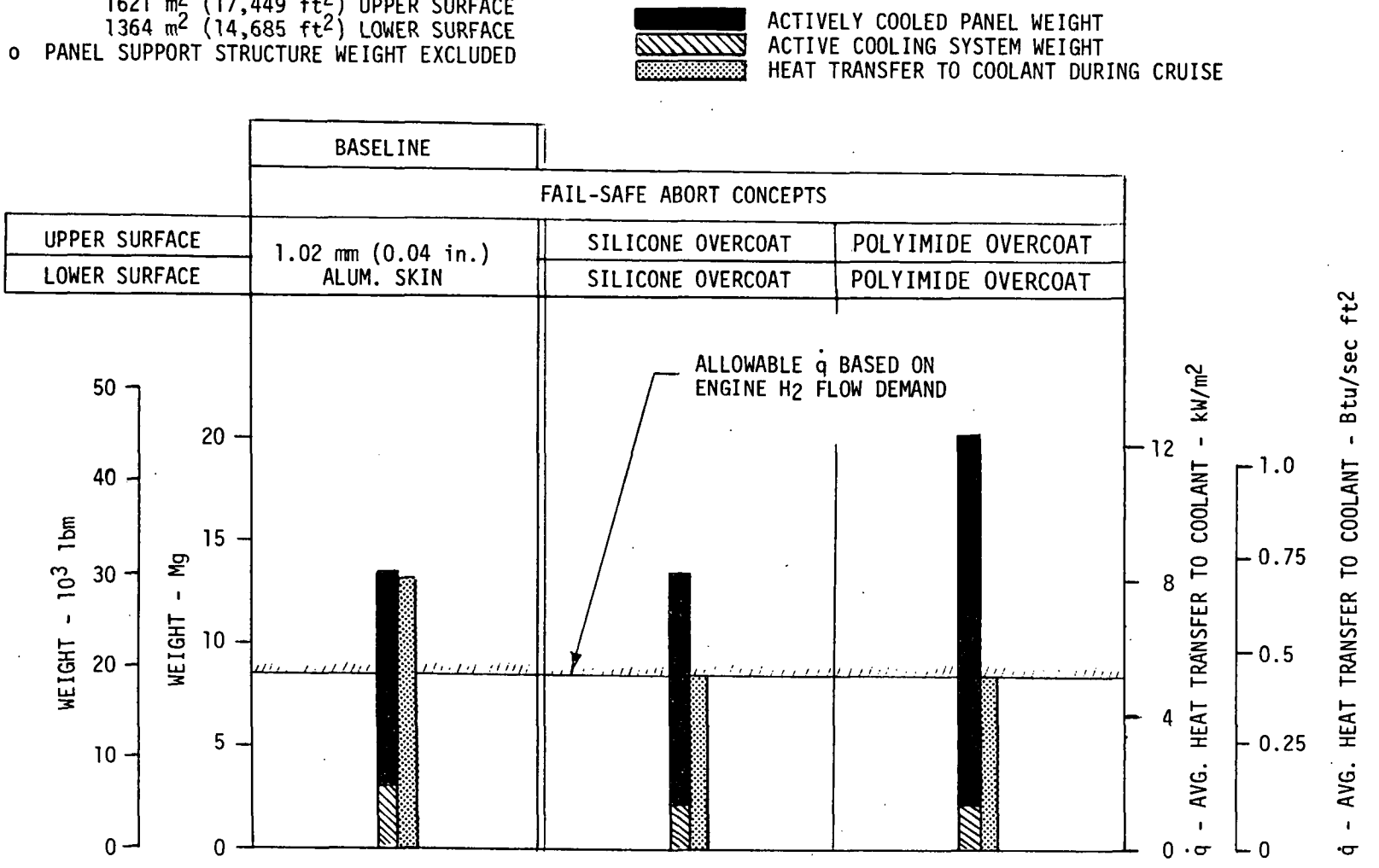

FIGURE 104
MACH 3 THERMO-STRUCTURAL CONCEPTS

- o FAILURE RESPONSE TIME = 15 sec
- o TOTAL COOLED AREA = 2985 m^2 (32,134 ft^2)
  - 1621 m^2 (17,449 ft^2) UPPER SURFACE
  - 1364 m^2 (14,685 ft^2) LOWER SURFACE
- o PANEL SUPPORT STRUCTURE WEIGHT EXCLUDED

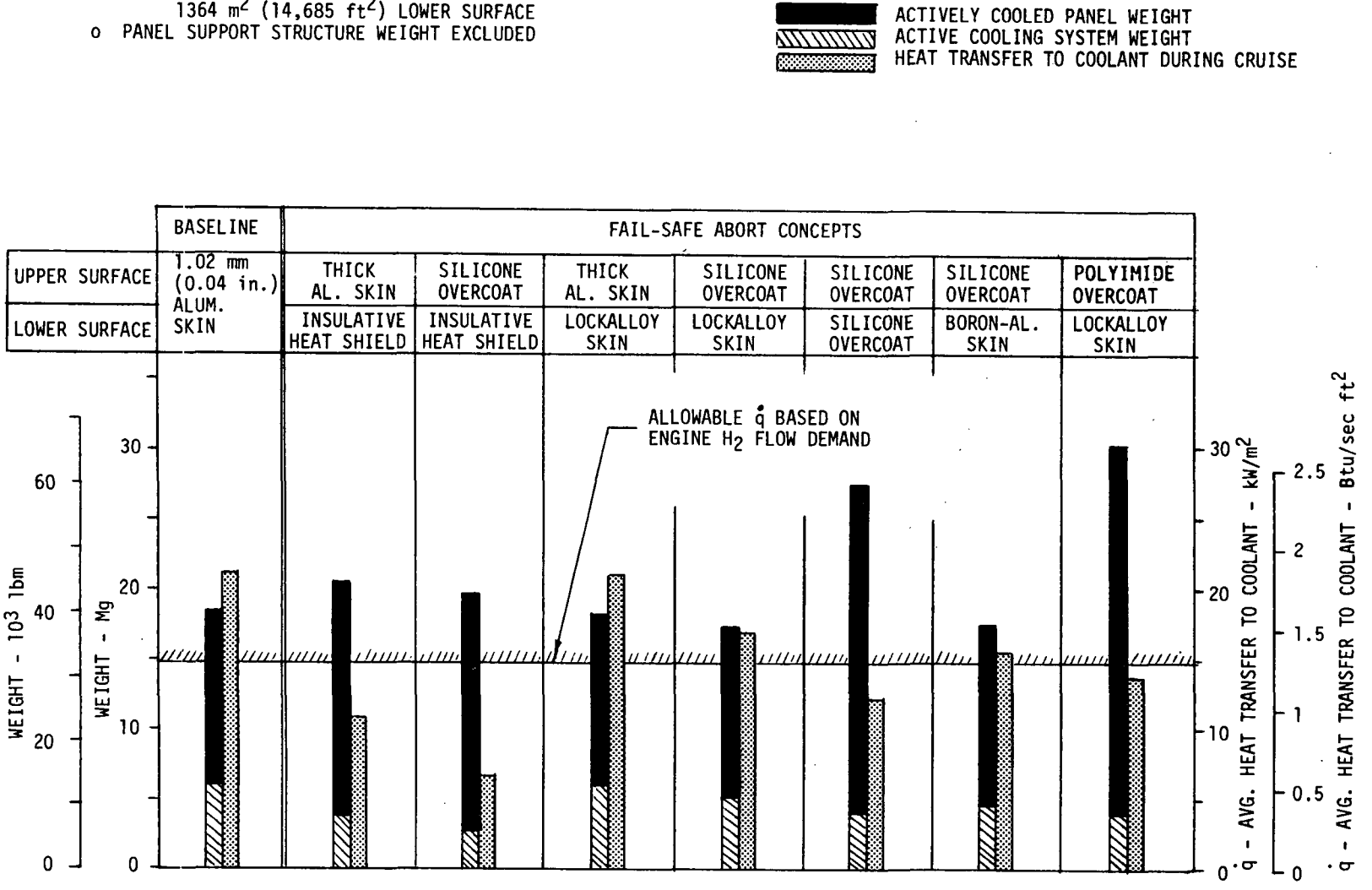

FIGURE 105
MACH 4.5 THERMO-STRUCTURAL CONCEPTS

- FAILURE RESPONSE TIME = 15 sec
- TOTAL COOLED AREA = 2985 m^2 (32,134 ft^2)
  - 1621 m^2 (17,449 ft^2) UPPER SURFACE
  - 1364 m^2 (14,685 ft^2) LOWER SURFACE
- PANEL SUPPORT STRUCTURE WEIGHT EXCLUDED

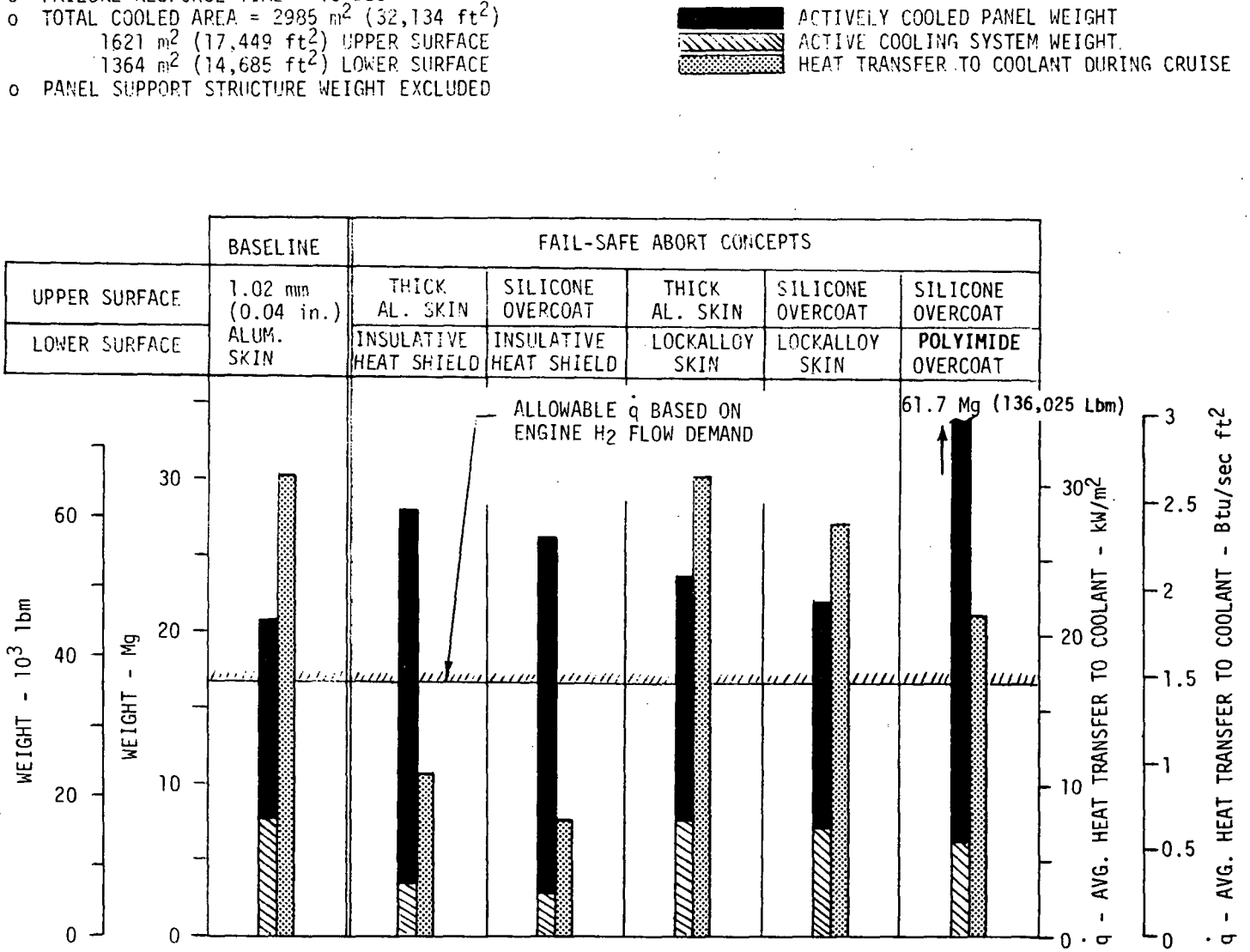

FIGURE 106
MACH 6 THERMO-STRUCTURAL CONCEPTS

for each upper/lower surface combination, is shown on the figures. An area-averaged approach was used in the comparison, where it was assumed that the typical upper and lower surface panels contributed 54.3 percent and 45.7 percent, respectively, of the total aircraft surface area. All configurations shown are capable of an abort from cruise, initiated 15 seconds after a total cooling system failure, without exceeding allowable material temperatures. Specific material temperatures and dimensions were summarized in the preceding section.

Mach 3 Concepts - As shown by Figure 104, the total weight of a silicone overcoat concept, when applied to both upper and lower surfaces, was found to be approximately the same as the baseline. In addition, average heat transfer to the coolant during cruise would be reduced to a level which can be absorbed by the hydrogen demanded by the aircraft engines. Weight of the Kapton overcoat concept was found to be considerably higher.

Mach 4.5 Concepts - The only combinations which resulted in a match between system heat load and available hydrogen heat sink utilize insulative heat shields or overcoats (Figure 105). An insulative heat shield on the lower surface, combined with a silicone overcoated upper surface could provide minimum cooling system heat load and would not be appreciably heavier than the baseline configuration. A bare Lockalloy lower surface combined with a silicone overcoated upper surface resulted in minimum total weight, but excessive cooling system heat transfer.

The combined concept of silicone overcoated upper surface with a boron-aluminum lower surface also resulted in an attractive total weight. However, the heat transfer to the coolant was again judged excessive.

Mach 6 Concepts - Utilization of any thermostructural concept on the lower surface other than an insulative heat shield results in excessive system heat loads, as shown by Figure 106.

4.3.4 Thermostructural Concept Selection - A concept ranking process was performed to select candidate finalist concepts for each of the three abort Mach numbers. The concepts surviving the ranking/selection process were carried into a final systems integration and optimization phase.

Concept ranking required the establishment of a consistent and meaningful rating system if the end results were to be credible. Therefore, figures of merit were utilized in the concept ranking process which recognized the prime

areas of importance. Wherever possible the merits of each design were quantified. This was easily done for weight and relative initial cost of the thermostructural concept-cooling system combinations. However, other figures of merit such as operating cost and reliability are functions of design complexity, damage resistance, damage tolerance, inspectability, maintainability and life, which could only be rated qualitatively. Thus, a concept ranking system allowing both quantitative and qualitative evaluations of the candidate thermostructural fail-safe concepts was established.

The structural concept applicable to each thermostructural approach were defined before proceeding with the ranking. Figure 107 shows the aircraft lower surface concepts configured for Mach 6 abort. Concepts for all other abort Mach numbers and surface locations were similar to one or another of the Mach 6 lower surface concepts. Some of the concepts considered will require considerable development; particularly the concepts using boron-aluminum, Lockalloy, surface coatings, or phase change materials. It was assumed that all required development could be successfully accomplished.

Each concept was rated in three major categories; operating cost, initial cost, and reliability. The considerations in the establishment of an operating cost figure-of-merit were total weight chargeable to a given concept (this included cooling system weight), damage resistance, inspectability, and maintainability. The initial cost figure-of-merit considered weight, and material and fabrication cost. The reliability figure-of-merit considered design tolerance to damage, design complexity and inspectability. These three figures-of-merit were then grouped into one overall figure-of-merit to provide a relative ranking of the concepts.

A number of basic assumptions and criteria for making the ratings were common to all the rated concepts and are summarized as follows:

o The type failure detection system utilized, the fluid filled (phase change) tube elements, was assumed common to all concepts.

o No attempt was made to provide a correlation; i.e., the ratings for the Mach 3 upper surface concepts have no relationship with ratings for other Mach numbers and surfaces. No attempt was made to provide a correlation between columns on a given chart. In fact, an effort was made to preclude such correlation; i.e., the maintainability ratings were considered independent of the damage tolerance or inspectability ratings, etc. The rating of 10 is

CONCEPT	DESCRIPTION
(A) BASELINE 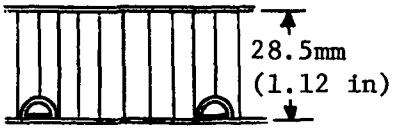	Honeycomb Panel, 2024-T81 Al. Skins, 5056-H34 Al. Core, 6061-T6 Al. Tubes, Adhesive Bonded.
(B) 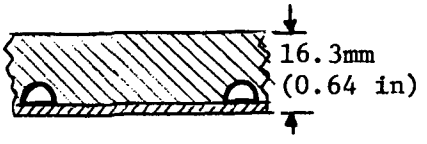	2024-T81 Al. Plate With Integral Coolant Passage, 2024-T81 Outer Skin Welded or Weld-Bonded on Plate. No other Stiffening Rqd. No heat treatment after welding.
(C) 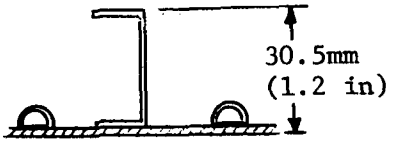	All Parts Boron-Aluminum. Metallurgical Joined.
(D) 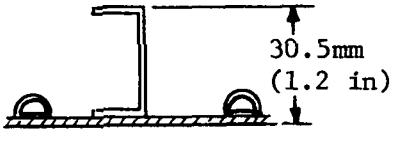	Lockalloy Outer Skin (requires joining of relatively small size sheets), Lockalloy formed stiffeners, 6061-0 tube brazed to skin. No heat treatment after brazing.
(E) 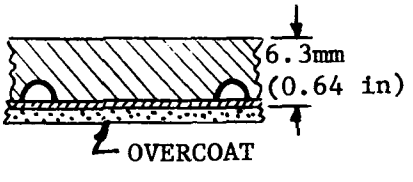	2024-T81 Plate with Integral Coolant Passage, 2024-T81 Outer Skin Welded or Weld-Bonded in place. No other stiffening required. No heat treatment after welding.
(F) 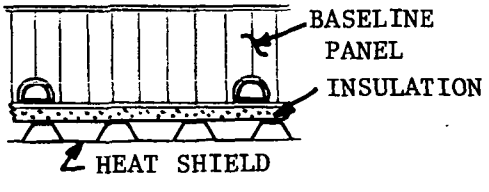	Baseline Panel with Insulation and Preloaded Monolithic Heat Shield.

FIGURE 107
MACH 6 LOWER SURFACE STRUCTURAL CONCEPTS

CONCEPT	DESCRIPTION
Ⓖ 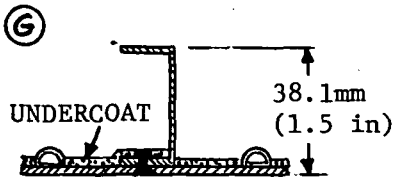	2024-T81 Aluminum Skin and Stiffener. 6061-T6 Tube. Tube adhesive bonded to skin. Stiffener riveted to skin.
Ⓗ 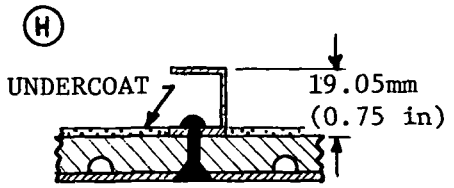	2024-T81 Plate with Integral Coolant Passage. 2024-T81 Outer Skin Welded or Weld-Bonded in place. 2024-T81 Stiffener riveted to skin. Probably could reduce frame spacing slightly and eliminate stiffeners. However, did not account for eliminating stiffeners. No heat treatment after welding.
Ⓘ 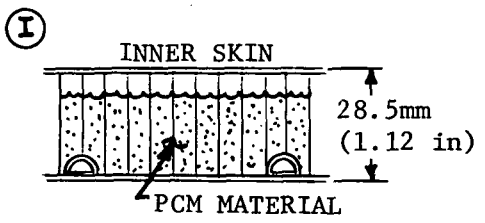	2024-T81 Skins, 5056-H34 Core, 6061-T6 tubes. Adhesive Bonded. Core filled with phase change material before bonding inner skin in place. Increased honeycomb core void reduces PCM effectiveness.

NOTE: STRUCTURAL CONCEPTS Ⓐ, Ⓑ, Ⓒ, Ⓓ, Ⓔ, Ⓕ, Ⓖ, Ⓗ AND Ⓘ APPLICABLE TO THERMOSTRUCTURAL DESIGNS FOR ALL ABORT MACH NUMBERS AND AIRCRAFT SURFACES

FIGURE 107 (Continued)
MACH 6 LOWER SURFACE STRUCTURAL CONCEPTS

assigned to concepts considered best or most desirable for each figure of merit. Panels were assumed to be 1.2m x 6.1m (4 x 20 ft) and of gentle contour.

o The weight ratings are indicative of relative concept weights. Weights include dry panel and system weights plus estimated additional panel weight required for strength, joining to substructure and adjacent panels, and manifolds. These additional weights are based on previous actively cooled panel design studies, References (6) and (20). The added weight increment for a 7.43m^2 (80 ft^2) panel, for each of the structural concepts identified by Figure 107 were as follows: Concepts Ⓐ, Ⓕ and Ⓘ 76.2 kg (168 lb_m); Concepts Ⓑ, Ⓔ and Ⓗ 11.34 kg (25 lb_m); Concepts Ⓒ, Ⓓ 72.6 kg (160 lb_m); and Concept Ⓖ 85.28 kg (188 lb_m). These structural weight increments were refined during selected concept integration and optimization.

o The material and fabrication cost ratings included as part of the initial cost figure-of-merit were estimated on an initial investment production basis. Factors which were included were raw material, fabrication, and tooling costs for producing and inspecting the detail parts, assembling them into a panel and installing the panel on an airframe. Development costs are not considered in this rating. In addition, it was determined that active cooling system components (that portion of the total active cooling system chargeable to a given panel concept) should be factored into the concept material and fabrication initial cost. Two approaches to evaluation of the material fabrication cost parameter were utilized dependent upon the thermostructural concept material. If all concepts for a given typical aircraft surface and a given Mach number were based on the use of aluminum structure the following form of the material/fabrication cost parameter was used:

$$\left[\begin{array}{c}\text{Material/Fabrication Cost} \\ \text{Parameter}\end{array}\right] = \left[\frac{\text{Panel Weight}}{\text{Fabrication Ease Factor}}\right] + 5\left[\begin{array}{c}\text{Active Cooling} \\ \text{Sys. Wt.}\end{array}\right]$$

This expression was based on the assignment of a relative cost factor of 1 to typical aluminum structure. The fabrication ease factor, (based on the ease with which required forming, cutting, and joining operations could be accomplished and shown on the rating charts for each abort Mach number/aircraft surface combination), provided a fabrication efficiency impacting concept cost; the higher the fabrication efficiency, the lower the cost. The cost of active cooling system (ACS) components, based on current environmental control system component costs, are estimated to be at least 10 times the basic cost of typical aluminum structure. However, the active cooling system weight charged to a concept included ducting and residual coolant. Thus, a factor of 5 on total charged active cooling system weight seemed reasonable. The concept resulting in the lowest value of the material/fabrication cost parameter was assigned a score of 10 for this parameter. The score for the remaining compared concepts was determined by ratioing the values of the material/fabrication cost parameter to that parameter for the concept scoring 10.

In cases where the concept comparisons included materials other than aluminum for structure, i.e., boron-aluminum or Lockalloy, or the use of titanium or Inconel heat shields, a modification of the expression for the material/fabrication cost parameter was used. This modified expression is:

$$\left[\begin{array}{c}\text{Material/Fabrication Cost} \\ \text{Parameter}\end{array}\right] = \frac{C_N\ (\text{Panel Wt.})}{C_1} + 5\ (\text{ACS Wt.})$$

where: C_1 = Relative cost of aluminum structure = 1

C_N = C_1, C_2, C_3, C_4 or C_5 dependent on concept

C_2 = Relative cost of boron-aluminum structure = 12

C_3 = Relative cost of Lockalloy structure = 10

C_4 = Relative cost of heat shielded (titanium or Inconel single sheet beaded skin) aluminum structure = 1.5

C_5 = Relative cost of Phase Change Material concepts a minimum of 1.5

o Reliability considered overall characteristics of a concept which enabled it to perform its intended function without requiring undue attention or corrective effort.

o Damage tolerance rating indicates the ability to continue to carry structural and thermal loads for a reasonable period of time after sustaining damage.

o Inspectability ratings were based on the ease with which evidence of damage could be detected during normal service operations or routing maintenance checks.

o Maintainability ratings were based on the ease with which a damaged panel could be repaired and removed or penetrated for access to other subsystems.

o A damage resistance rating was used to distinguish between a concept's ability to resist damage due to handling or foreign object impact from its ability to remain in service (damage tolerance) after sustaining damage.

The following sections present the overall ranking of the concepts considered for each of the aircraft surface/Mach number cases. In addition, the concept compatibility with available hydrogen heat sink (is absorbed heat flux equal to, or less than, available heat sink?) is indicated. The ratings and the weighting factors reflect our considered opinion. The weight ratings

and the heat sink compatibility factor are the only ones based on a quantitative evaluation. Still it is felt that this rating properly identifies concepts that must be further evaluated.

a. Mach 3 Thermostructural Concept Selection - Figures 108 and 109 present the ranking charts for the Mach 3 concepts. As shown by Figure 108, the prime lower surface concept was an aluminum honeycomb panel with the outer face sheet overcoated with a silicone elastomer. The second and third ranked concepts, the Kapton polyimide film overcoated panel and the bare aluminum panel, rated approximately the same. The bare aluminum panel concept was retained, along with the silicone elastomer overcoated panel, for final optimization and comparison even though it was not compatible with available heat sink. There was no point in retaining the Kapton coated panel due to its obvious inferiority compared to the silicone elastomer coated concept.

Figure 109 shows the rankings for the Mach 3 aircraft upper surface concepts. Again, the silicone overcoated panel was the superior concept and the bare aluminum panel design retained for comparative purposes.

b. Mach 4.5 Thermostructural Concept Selection - Figure 110 illustrates the ranking of Mach 4.5 aircraft lower surface concepts. The concept rated number one, the baseline bare aluminum panel, was rejected because the initial abort descent temperature analyses (see Figure 91) indicated a maximum abort temperature of 579K (582°F) for this concept and because of the incompatibility with available heat sink. The concept ranked number two, the insulative heat shielded panel, was retained along with the fourth highest rated concept (silicone overcoated) for optimization. The concept rated as third, the lithium oxide filled silicone elastomer undercoat, was rejected as a candidate for optimization because of the potential reactions with moisture and incompatibility with the available hydrogen heat sink.

Figure 111 shows the ranking for the aircraft upper surface concepts. The two concepts retained for final optimization were the silicone overcoated panel and the thickened aluminum skin concept. The bare thickened aluminum skin concept, considered on its own merits, rated number two out of seven concepts. However, it is shown to be incompatible with the available heat sink.

THERMO-STRUCTURAL CONCEPT	TYPE STRUCTURE (1)	MATERIAL		FABRICATION EASE FACTOR	OPERATING COST "A"					INITIAL COST "B"			RELIABILITY "C"				CONCEPT RANKING		COMPATIBLE WITH AVAILABLE LH_2 HEAT SINK
		TYPE	THICKNESS mm (in.)		WEIGHT*(0.75)	DAMAGE RESISTANCE(0.05)	INSPECTABILITY(0.1)	MAINTAINABILITY(0.1)	SUBSCORE (1/3)	WEIGHT(0.2)	MATERIAL AND FABRICATION COST(0.8)*	SUBSCORE (1/3)	DAMAGE TOLERANCE(0.5)	COMPLEXITY(0.3)	INSPECTABILITY(0.2)	SUBSCORE (1/3)	TOTAL SCORE $\frac{A+B+C}{3}$	RELATIVE RATING	
BASELINE SKIN	A	ALUM	1.02 (0.040)	10	** 9.9	8	10	10	9.8	9.9	7.2	7.7	9	10	10	9.5	9	3 √	NO
OVERCOATED SKIN	A	ALUM SILICONE	1.02 (0.040) 1.17 (0.046)	8	10	9.5	8	9	9.7	10	10	10	10	8	8	9	9.6	1 √	YES
OVERCOATED SKIN	A	ALUM KAPTON	1.02 (0.040) 1.96 (0.077)	8	8.7	10	9	9	8.8	8.7	9.5	9.3	9.5	8	9	8.95	9.02	2	YES

NOTE: (1) - TYPE STRUCTURE INDICATED BY LETTER IDENTIFIER PER FIGURE 107.
* - NUMBER IN PARENTHESES IS IMPORTANCE FACTOR.
** - TEN IS MOST DESIRABLE, ONE IS LEAST DESIRABLE.
√ - SELECTED CONCEPT(S).

FIGURE 108
THERMO-STRUCTURAL CONCEPT RANKING
AIRCRAFT LOWER SURFACE - MACH 3 CRUISE

THERMO-STRUCTURAL CONCEPT	TYPE STRUCTURE (1)	MATERIAL: TYPE	MATERIAL: THICKNESS mm (in.)	FABRICATION EASE FACTOR	OPERATING COST "A": WEIGHT (0.75)*	OPERATING COST "A": DAMAGE RESISTANCE (0.05)	OPERATING COST "A": INSPECTABILITY (0.1)	OPERATING COST "A": MAINTAINABILITY (0.1)	OPERATING COST "A": SUBSCORE (1/3)	INITIAL COST "B": WEIGHT (0.2)	INITIAL COST "B": MATERIAL AND FABRICATION COST (0.8)*	INITIAL COST "B": SUBSCORE (1/3)	RELIABILITY "C": DAMAGE TOLERANCE (0.5)	RELIABILITY "C": COMPLEXITY	RELIABILITY "C": INSPECTABILITY (0.2)	RELIABILITY "C": SUBCORE (1/3)	CONCEPT RANKING: TOTAL SCORE (A+B+C)/3	CONCEPT RANKING: RELATIVE RATING	COMPATIBLE WITH AVAILABLE LH_2 HEAT SINK
BASELINE SKIN	A	ALUM	1.02 (0.040)	10	** 10	8	10	10	9.9	10	8.3	8.6	9	10	10	9.5	9.33	2 √	NO
OVERCOATED SKIN	A	ALUM SILICONE	1.02 (0.040) 1.17 (0.046)	8	9.9	9.5	8	9	9.6	9.9	10	10	10	9	8	9.3	9.63	1 √	YES
OVERCOATED SKIN	A	ALUM KAPTON	1.02 (0.040) 1.96 (0.077)	8	8.5	10	9	9	8.7	8.5	9.2	9.1	9.5	9	9	9.25	9.02	3	YES

NOTE: (1) - TYPE STRUCTURE INDICATED BY LETTER IDENTIFIER PER FIGURE 107.
* - NUMBER IN PARENTHESIS IS IMPORTANCE FACTOR.
** - TEN IS MOST DESIRABLE, ONE IS LEAST DESIRABLE.
√ - SELECTED CONCEPT(S).

FIGURE 109
THERMO-STRUCTURAL CONCEPT RANKING
AIRCRAFT UPPER SURFACE - MACH 3 CRUISE

THERMO-STRUCTURAL CONCEPT	TYPE STRUCTURE (1)	MATERIAL TYPE	MATERIAL THICKNESS MM (in.)	FABRICATION EASE FACTOR	OPERATING COST "A" WEIGHT*(0.75)	OPERATING COST "A" DAMAGE RESISTANCE (0.05)	OPERATING COST "A" INSPECTABILITY (0.1)	OPERATING COST "A" MAINTAINABILITY (0.1)	OPERATING COST "A" (1/3) SUBSCORE	INITIAL COST "B" WEIGHT (0.2)	INITIAL COST "B" MATERIAL AND FABRICATION COST (0.08)*	INITIAL COST "B" (1/3) SUBSCORE	RELIABILITY "C" DAMAGE TOLERANCE (0.5)	RELIABILITY "C" COMPLEXITY (0.3)	RELIABILITY "C" INSPECTABILITY (0.2)	RELIABILITY "C" (1/3) SUBSCORE	CONCEPT RANKING $\frac{A+B+C}{3}$ TOTAL SCORE	CONCEPT RANKING RELATIVE RATING	COMPATIBLE WITH AVAILABLE LH_2 HEAT SINK
BASELINE SKIN	A	ALUM	1.02 (0.040)	8.5	9.4**	7.5	10	9	9.33	9.4	8.6	8.76	7.5	8.7	10	8.36	8.82	1	NO
THICKENED SKIN	G	ALUM	5.87 (0.231)	8	5	10	10	8.5	6.1	5	4.67	4.74	10	10	10	10	6.95	9	NO
	A	BORON-AL	1.02 (0.040)	2	9.6	8	5	4	8.5	9.6	2.24	3.71	7	7	5	6.6	6.27	11	NO
	A	LOCKALLOY	1.02 (0.040)	3	10	8	10	8	9.7	10	2.98	4.38	7.5	8	10	8.15	7.41	7	NO
PRECOOLED SKIN	G	ALUM	4.85 (0.191)	10	5.3	10	10	8.5	6.33	5.3	4.32	4.52	9.9	10	10	9.95	6.93	10	NO
	A	BORON-AL	1.02 (0.040)	2	9.4	8	5	4	8.35	9.4	2.19	3.63	7	7	5	6.6	6.19	12	NO
	A	LOCKALLOY	1.02 (0.040)	3	9.8	8	10	8	9.55	9.8	2.89	4.27	7.5	8	10	8.15	7.32	8	NO
OVERCOATED SKIN	G	ALUM / KAPTON	2.51 (0.099) / 3.23 (0.127)	9.5	6.2	9.8	8.5	7	6.69	6.2	6.9	6.76	9.6	9.1	8.5	9.23	7.56	5	YES
	G	ALUM / SILICONE	3.61 (0.142) / 1.07 (0.042)	9.5	6.4	10	8	7.5	6.85	6.4	6.9	6.8	9.7	9.5	8	9.3	7.65	4 √	YES
	G	ALUM / SILICONE ($40\%L_iO_2$)	2.54 (0.10) / 3.61 (0.142)	9.5	6.3	9.9	8	7.5	6.77	6.3	6.6	6.54	9.8	9.3	8	9.29	7.53	6	YES
INSULATIVE HEAT SHIELD	F	ALUM / FIBERFRAX / TITANIUM	1.02 (0.040) / 6.35 (0.25) / 0.66 (0.076)	8	6.9	7	7.5	8.9	7.17	6.9	10	9.38	9	8.5	7.5	8.55	8.37	2 √	YES
UNDERCOATED SKIN	G	ALUM / SILICONE ($40\%L_iO_2$)	1.02 (0.040) / 4.01 (0.158)	9.5	7.2	8	9	9	7.6	7.2	6.8	6.88	8.5	8.8	9	8.69	7.72	3	NO

NOTE: (1) - TYPE OF STRUCTURE INDICATED BY LETTER IDENTIFIER PER FIGURE 107.
* - NUMBER IN PARENTHESIS IS IMPORTANCE FACTOR.
** - TEN IS MOST DESIRABLE, ONE IS LEAST DESIRABLE.
√ - SELECTED CONCEPT(S).

FIGURE 110
THERMO-STRUCTURAL CONCEPT RANKING
AIRCRAFT LOWER SURFACE - MACH 4.5 CRUISE

THERMO-STRUCTURAL CONCEPT	TYPE STRUCTURE (1)	MATERIAL TYPE	MATERIAL THICKNESS mm (in.)	FABRICATION EASE FACTOR	OPERATING COST "A" WEIGHT*(0.75) **	OPERATING COST "A" DAMAGE RESISTANCE(0.05)	OPERATING COST "A" INSPECTABILITY(0.1)	OPERATING COST "A" MAINTAINABILITY(0.1)	INITIAL COST "B" (1/3) SUBSCORE	INITIAL COST "B" WEIGHT(0.2)	INITIAL COST "B" MATERIAL AND FABRICATION COST(0.08)*	INITIAL COST "B" (1/3) SUBSCORE	RELIABILITY "C" DAMAGE TOLERANCE(0.5)	RELIABILITY "C" COMPLEXITY(0.3)	RELIABILITY "C" INSPECTABILITY(0.2)	RELIABILITY "C" (1/3) SUBSCORE	CONCEPT RANKING TOTAL SCORE $\frac{A+B+C}{3}$	CONCEPT RANKING RELATIVE RATING	CONCEPT RANKING COMPATIBLE WITH AVAILABLE LH_2 HEAT SINK
BASELINE SKIN	A	ALUM	1.02 (0.040)	8	9.9	8	10	10	9.7	9.9	6.5	7.18	8	10	10	9	8.63	3	NO
THICKENED SKIN	A	ALUM	1.14 (0.045)	8	9.7	8.2	10	10	9.69	9.7	6.5	7.14	8.2	10	10	9.1	8.64	2 √	NO
PRECOOLED SKIN	A	ALUM	1.02 (0.040)	8	9.5	8	10	10	9.4	9.5	4.7	5.66	8	9.5	10	8.85	7.97	7	NO
OVERCOATED SKIN	A	ALUM / SILICONE	1.02 (0.040) / 1.93 (0.076)	7.5	10	9.5	8	9	9.68	10	9.4	9.52	9	9	8	8.8	9.33	1 √	YES
	A	ALUM / KAPTON	1.02 (0.040) / 6.71 (0.264)	7	6.6	10	8	8	7.05	6.6	10	9.32	8.8	8	8	8.4	8.26	6	YES
	A	ALUM / KAPTON	1.02 (0.040) / 6.71 (0.126)	7	8.1	9.9	8	8	8.2	8.1	8.6	8.5	8.5	8	8	8.25	8.32	4	YES
UNDERCOATED SKIN	G	ALUM / SILICONE ($40\%L_1O_2$)	1.02 (0.040) / 0.114 (0.0045)	9	9.2	8	9	8	9	9.2	6	6.64	10	8	9	9.2	8.28	5	NO

NOTE: (1) - TYPE OF STRUCTURE INDICATED BY LETTER IDENTIFIER PER FIGURE 107.
* - NUMBER IN PARENTHESIS IS IMPORTANCE FACTOR.
** - TEN IS MOST DESIRABLE, ONE IS LEAST DESIRABLE.
√ - SELECTED CONCEPT(S).

FIGURE 111
THERMO-STRUCTURAL CONCEPT RANKING
AIRCRAFT UPPER SURFACE - MACH 4.5 CRUISE

It would be possible to make this concept applicable if the lower surface concept utilized with it could be configured to restrict the overall absorbed heat to a level compatible with the hydrogen heat sink. Therefore, the thickened skin approach was retained.

c. Mach 6 Thermostructural Concept Selection - Figure 112 presents the Mach 6 aircraft lower surface concept ranking. As shown, only one concept was retained. This concept, the insulative heat shielded panel, was the only one that can provide a realistic match with available heat sink. It is of interest to note that the total score for this concept was, for all practical purposes, the same as the bare unprotected baseline aluminum panel. The bare aluminum panel can neither survive an abort or match absorbed heat flux with available heat sink.

Figure 113 shows the results of the ranking of Mach 6 aircraft upper surface concepts. Two were retained for optimization, the silicone overcoated panel and the bare thickened aluminum skin panel. The thickened skin concept was retained primarily for comparative purposes. This concept rated only sixth out of six. However, the concept ranked number two, based on initial analyses would not meet the 478K (400°F) maximum abort temperature requirement and would not be compatible with available heat sink. The concepts ranked third, fourth, and fifth are clearly inferior to the prime concept, the silicone overcoated panel. Thus, the thickened skin concept was retained for comparison.

d. Summary of Selected Thermostructural Concepts - On the basis of the ranking of concepts, and the compatibility with available heat sink, the thermostructural concepts listed on Figure 114 were selected for further optimization.

4.4 FAIL-SAFE SYSTEM INTEGRATION AND OPTIMIZATION

The results of previous analyses were utilized to select realistic fail-safe abort systems for each of the three cruise Mach number abort conditions.

4.4.1 Complete System Evaluation - Thermostructural concepts, failure detection concepts, and abort trajectory maneuver techniques, were integrated and refined to achieve fail-safe abort systems. The thermostructural concepts selected were the most promising candidates for this final optimization. Infrared scanning and liquid (phase change) filled sensors, and eutectic salt elements, the prime failure detection system approaches (Section 4.1.4), were

THERMO-STRUCTURAL CONCEPT	TYPE STRUCTURE ①	MATERIAL TYPE	MATERIAL THICKNESS MM (in.)	FABRICATION EASE FACTOR	OPERATING COST "A" WEIGHT*(0.75)	OPERATING COST "A" DAMAGE RESISTANCE(0.05)	OPERATING COST "A" INSPECTABILITY(0.1)	OPERATING COST "A" MAINTAINABILITY(0.1)	OPERATING COST "A" (1/3) SUBSCORE	INITIAL COST "B" WEIGHT(0.2)	INITIAL COST "B" MATERIAL AND FABRICATION COST(0.08)*	INITIAL COST "B" (1/3) SUBSCORE	RELIABILITY "C" DAMAGE TOLERANCE(0.5)	RELIABILITY "C" COMPLEXITY(0.3)	RELIABILITY "C" INSPECTABILITY(0.2)	RELIABILITY "C" (1/3) SUBSCORE	CONCEPT RANKING $\frac{A+B+C}{3}$ TOTAL SCORE	CONCEPT RANKING RELATIVE RATING	COMPATIBLE WITH AVAILABLE LH_2 HEAT SINK
BASELINE SKIN	A	ALUM	1.02 (0.040)	8.5	** 10	7	9	8.5	9.6	10	8.81	9.05	7.5	8	9	7.95	8.87	1	NO
THICKENED SKIN	B	ALUM	16.13 (0.635)	10	3.6	9	10	10	5.15	3.6	3.29	3.35	10	10	10	10	6.17	8	NO
	C	BORON-AL	4.85 (0.191)	2	6.5	8.1	5	2	5.98	6.5	1	2.1	7	5	5	6	4.69	11	NO
	D	LOCKALLOY	2.16 (0.085)	3	9.5	8	9	7.5	8.18	9.5	2.43	3.84	7.5	8.5	9	8.1	7.04	4	NO
PRECOOLED SKIN	C	BORON-AL	3.86 (0.152)	2	7.2	8	5	2	6.5	7.2	1.16	2.37	7	5	5	6	4.96	10	NO
	D	LOCKALLOY	1.78 (0.070)	3	9.8	7.9	9	7.5	9.4	9.8	2.63	4.06	7.4	8.5	9	8.05	7.17	3	NO
OVERCOATED SKIN	E	ALUM KAPTON	11.66 (0.059) 1.22 (0.048)	9.8	4.6	10	8.5	7	5.5	4.6	3.95	4.08	9.7	9.7	8.5	9.46	6.35	6	NO
	E	ALUM SILICONE	12.93 (0.509) 0.49 (0.0193)	9.7	4.4	9.8	8.5	7	5.34	4.4	3.71	3.85	9.9	9.8	8.5	9.59	6.26	7	NO
INSULATIVE HEAT SHIELD	F	ALUM FIBERFRAX INCONEL	1.02 (0.040) 20.98 (0.826) (0.51 (0.020)	8	8.2	7	8	8.4	8.14	8.2	10	9.64	9	9	8	8.8	8.86	2 ✓	YES
UNDERCOATED SKIN	H	ALUM SILICONE (40%L_2O_3)	9.58 (0.377) 7.82 (0.308)	9.5	4.4	8.9	9.5	9.5	5.65	4.4	3.61	3.77	8.5	9.5	9.5	9	6.14	9	NO
PHASE CHANGE MATERIAL	I	ALUM ALUM H/C POLY-ETHYLENE	2.26 (0.089) 12.7 (0.50) 10.16 (0.40)	7	6.8	7.5	8	8	7.08	6.8	4.36	4.85	8	7.5	8	7.85	6.59	5	NO

NOTE: ① - TYPE OF STRUCTURE INDICATED BY LETTER IDENTIFIER PER FIGURE 107.
* - NUMBER IN PARENTHESIS IS IMPORTANCE FACTOR.
** - TEN IS MOST DESIRABLE, ONE IS LEAST DESIRABLE.
✓ - SELECTED CONCEPT(S).

FIGURE 112
THERMO-STRUCTURAL CONCEPT RANKING
AIRCRAFT LOWER SURFACE - MACH 6 CRUISE

THERMO-STRUCTURAL CONCEPT	TYPE STRUCTURE (1)	MATERIAL		OPERATING COST					INITIAL COST				RELIABILITY				CONCEPT RANKING		COMPATIBLE WITH AVAILABLE LH_2 HEAT SINK
		TYPE	THICKNESS mm (in.)	FABRICATION EASE FACTOR	WEIGHT* (0.75)	DAMAGE RESISTANCE (0.05)	INSPECTABILITY (0.1)	MAINTAINABILITY (0.1)	(1/3) SUBSCORE	WEIGHT (0.2)	MATERIAL AND FABRICATION COST (0.08)*	(1/3) SUBSCORE	DAMAGE TOLERANCE (0.5)	COMPLEXITY (0.3)	INSPECTABILITY (0.2)	(1/3) SUBSCORE	TOTAL SCORE $\frac{A+B+C}{3}$	RELATIVE RATING	
BASELINE SKIN	A	ALUM	1.02 (0.040)	7.5	** 10	8	10	9	9.8	10	7.39	7.91	7.5	9	10	8.45	8.72	2	NO
THICKENED SKIN	A	ALUM	1.37 (0.054)	7.5	9.4	8.1	10	9	9.35	9.4	7.3	7.72	7.5	9	10	8.45	8.51	6 √	NO
OVERCOATED SKIN	A	ALUM KAPTON	1.02 (0.040) 2.39 (0.094)	7	8.5	9.5	8.5	8.5	8.55	8.5	9.1	8.98	8.5	8	8.5	8.35	8.63	4	YES
	A	ALUM SILICONE	1.02 (0.040) 1.42 (0.056)	7	10	9.5	8	8.5	9.62	10	9.4	9.52	9	8.5	8	8.65	9.26	1 √	YES
	A	ALUM KAPTON	1.02 (0.040) 4.06 (0.160)	7	7.7	10	8.5	8	7.92	7.7	10	9.54	8	8	8.5	8.1	8.52	5	YES
UNDERCOATED SKIN	G	ALUM SILICONE ($40\%L_1O_2$)	1.02 (0.040) 0.305 (0.012)	10	9.1	8.5	9	9	9.05	9.1	7.4	7.74	9	10	9	9.3	8.7	3	NO

NOTE: (1) - TYPE OF STRUCTURE INDICATED BY LETTER IDENTIFIER PER FIGURE 107.
* - NUMBER IN PARENTHESIS IS IMPORTANCE FACTOR.
** - TEN IS MOST DESIRABLE, ONE IS LEAST DESIRABLE.
√ - SELECTED CONCEPT(S).

FIGURE 113
THERMO-STRUCTURAL CONCEPT RANKING
AIRCRAFT UPPER SURFACE - MACH 6 CRUISE

CRUISE/ABORT MACH NUMBER	TYPICAL AIRCRAFT SURFACE	THERMOSTRUCTURAL CONCEPT	BACK-UP STRUCTURE
3 ↓	UPPER	SILICONE OVERCOATED ALUMINUM SKIN	ALUMINUM HONEYCOMB
	LOWER	SILICONE OVERCOATED ALUMINUM SKIN	ALUMINUM HONEYCOMB
4.5 ↓	UPPER	SILICONE OVERCOATED ALUMINUM SKIN (PRIME)	ALUMINUM HONEYCOMB
		THICKENED ALUMINUM SKIN (SECONDARY)	ALUMINUM HONEYCOMB
	LOWER	TITANIUM HEAT SHIELDED ALUMINUM SKIN (PRIME)	ALUMINUM HONEYCOMB
		SILICONE OVERCOATED THICK ALUMINUM SKIN (SECONDARY)	SKIN/STRINGER
6 ↓	UPPER	SILICONE OVERCOATED ALUMINUM SKIN (PRIME)	ALUMINUM HONEYCOMB
		THICKENED ALUMINUM SKIN (SECONDARY)	ALUMINUM HONEYCOMB
	LOWER	INCONEL HEAT SHIELDED ALUMINUM SKIN (PRIME)	ALUMINUM HONEYCOMB
		(NO SECONDARY CONCEPT)	

FIGURE 114
THERMO-STRUCTURAL CONCEPTS SELECTED FOR OPTIMIZATION

re-evaluated for concept compatibility. The optimized abort trajectories reported in Section 4.2.3 were utilized for this integration-optimization process.

Part a) of this section presents the results of structural analyses of the selected concepts. Part b) presents the results of the thermal analyses. Part c) provides the re-evaluation of the most promising failure detection approaches.

a. Structural Analyses - Strength analysis of the finalist thermo-structural concepts were conducted to insure structural adequacy of the designs for both normal aircraft operation and for abort situations.

To maintain continuity, and to provide a basis for comparison with present actively cooled panel programs (References (6) and (20)), typical design load requirements of the Reference (5) Concept 3 aircraft (baseline aircraft for this study) were used to optimize the structural panels. These design loads are consistent with the References (6) and (20) studies. Figure 115 summarizes the design load requirements.

Eight of the nine finalist concepts were adhesively bonded aluminum honeycomb sandwich with coolant manifolds and dee-shaped tubes. Figure 116 shows the construction of a typical actively cooled panel of the type analyzed. The skins were assumed 2024-T81 and the tubes 6061-T6 aluminum. A two foot intermediate frame spacing was used in the analysis. The coolant pressure in the tubes was assumed consistent with panel designs from References (6) and (20). The honeycomb core was assumed to be 49.7 kg/m^3 (3.1 lbm/ft^3) material. Utilizing geometric inputs provided by thermal analysis of panel requirements (Figure 117), the honeycomb structural panels

DESIGN LIMIT LOADS: $n_x = \pm 210.2$ kN/m (1200 lb$_f$/in.)

Pressure = ± 6.9 kPa (1.0 psi)

ULTIMATE LOADS = 1.5 times design limit loads

FATIGUE AND FRACTURE MECHANICS DESIGN CRITERIA:

a) Cyclic loading of ± 210.2 kN/m (1200 lb$_f$/in.) (stress ratio = -1)
b) 5000 cycles at limit design temperatures (20,000 cycles with a scatter factor of 4)
c) Constant uniform lateral pressure load, 6.9kPa (1.0 psi)
d) Cracks will not grow through the wall thickness of coolant passages in 20,000 cycles.

FIGURE 115
STRUCTURAL PANEL LOAD REQUIREMENTS

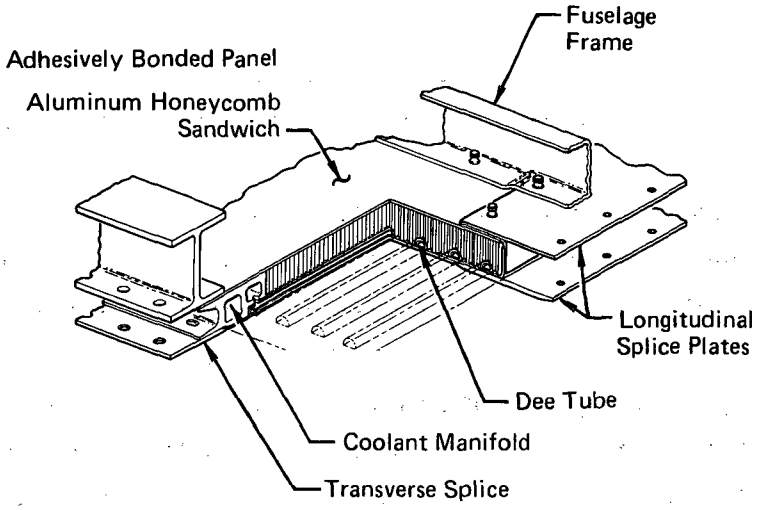

FIGURE 116
ACTIVELY COOLED PANEL CONSTRUCTION

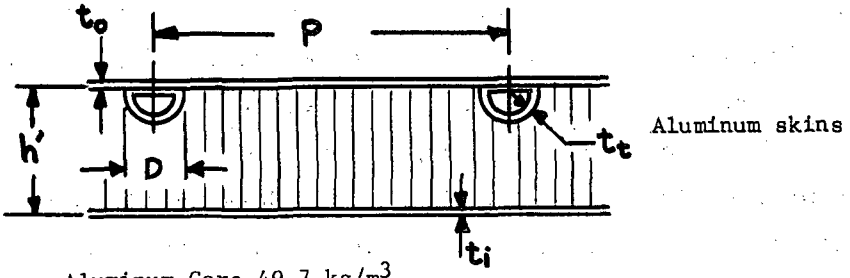

Aluminum Core 49.7 kg/m^3
(3.1 lbm/ft^3)

MACH NO.	AIRCRAFT SURFACE	P(PITCH) cm (in)	D mm (in)	t_t mm (in)	t_o mm (in)	SKIN MATERIAL
3	Upper(U)	10.67 (4.2)	6.35 (0.25)	0.89 (0.035)	1.02 (0.040)	Aluminum
	Lower(L)	7.49 (2.95)	(0.25)	↓	↓	↓
4.5	(U)	6.73 (2.65)	(0.25)			
	(L)(Insul)	10.16 (4.00)	(0.25)			
6	(U)	6.02 (2.37)	(0.25)			
	(L)(Insul)	10.16 (4.00)	(0.25)			

FIGURE 117
STRUCTURAL PANEL THERMAL INPUTS

were optimized. The resulting honeycomb panel structural weights are summarized in Figure 118. These weights are for the structural panel only. They do not include overcoat material, heat shield, or insulation weights. Heat shield (and attachment) weights for the radiative insulated heat shield concepts are shown in the notes of Figure 118.

For an abort condition, FAR (Part 25) (Reference (21)) specified that the structure must be capable of carrying 80% of the design limit loads. All the panels are capable of carrying more than 100% design limit loads at 478K (400°F). Based on analyses of the Reference (20) study, the thermal stresses due to transient abort conditions are small. This was also found to be the case for the thermostructural concepts investigated herein. An adhesive having adequate thermal conductivity and good shear strength at or above 478K (400°F) is expected to be available in the future. Projecting the properties of current adhesives, it was assumed the advanced adhesive would result in skin-to-manifold splice joints in the aluminum skin panels with an ultimate shear stress allowable greater than 19.15 kPa (400 psi) at 478K (400°F). Any panels subjected to temperatures exceeding 450K (350°F) during abort will experience a permanent reduction in mechanical properties.

One thermostructural concept (the Mach 4.5 aircraft lower surface candidate with silicone overcoated aluminum skin) was assumed to be of skin/stringer construction. This concept was evaluated for the same load requirements as the honeycomb structure. Results showed that a skin/stringer panel would be about the same weight as a comparable honeycomb panel. The actual panel concept construction would have a thick, 3.56mm (0.14 in.), skin due to thermal requirements. The weight of this concept was 15.48 kg/m^2 (3.17 lbm/ft^2), about 22 percent heavier than an equivalent honeycomb panel. Thus, the skin-stringer concept was judged to be more than adequate from a structural viewpoint if designed to meet the thermal requirements.

The aircraft considered in the study experiences a wide range of heating rates over the various surfaces. This is not expected to significantly impact actively cooled panel weights for the abort concepts. As shown by Figure 118, panel structural weight was found to be insensitive to absorbed

MACH NO.	AIRCRAFT SURFACE	h' cm (in)	(2) t_i mm (in)	UNIT STRUCTURAL WEIGHT kg/m^2 (lbm/ft^2)			
				OUTER SKIN + TUBES	CORE + INNER SKIN	(3)	TOTAL PANEL (DRY)
3	(U)Upper	3.15 (0.24)	1.07 (0.042)	3.213 (0.658)	4.453 (0.912)	4.98 (1.02)	12.65 (2.59)
	(L)Lower	3.15 (1.24)	1.02 (0.040)	3.384 (0.693)	4.282 (0.877)	4.98 (1.02)	12.65 (2.59)
4.5	(U)	3.0 (1.18)	1.02 (0.040)	3.447 (0.706)	4.218 (0.864)	4.98 (1.02)	12.65 (2.59)
	(L) (4) Insulated	3.15 (1.24)	1.07 (0.042)	3.232 (0.662)	4.433 (0.908)	4.98 (1.02)	12.65 (2.59)
6	(U)	3.0 (1.18)	0.99 (0.039)	3.520 (0.721)	4.145 (0.849)	4.98 (1.02)	12.65 (2.59)
	(L) (5) Insulated	3.15 (1.24)	1.07 (0.042)	3.232 (0.662)	4.433 (0.908)	4.98 (1.02)	12.65 (2.59)

NOTES: (1) OVERCOAT, HEAT SHIELD AND INSULATION WEIGHTS MUST BE ADDED TO STRUCTURAL WEIGHT INCREMENTS.

(2) TYPICAL VALUES OF PANEL GEOMETRY, WHERE:

h'= DISTANCE BETWEEN CENTROIDS OF OUTER AND INNER SKIN.
t_i= THICKNESS OF INNER SKIN

(3) WEIGHT INCREMENT FOR MANIFOLDS, PANEL ATTACHMENTS, AND NONOPTIMUMS.

(4) ADD 2.43 kg/m^2(0.498 lb_m/ft^2) FOR TITANIUM HEAT SHIELD (CORRUGATION STIFFENED BEADED SKIN) AND SUPPORTS.

(5) ADD 4.35 kg/m^2(0.89 Lb_m/ft^2) FOR RENE' 41 HEAT SHIELD (CORRUGATION STIFFENED BEADED SKIN) AND SUPPORTS.

FIGURE 118
HONEYCOMB PANEL STRUCTURAL WEIGHT SUMMARY

heat flux. This is further verified by the results of an analysis to determine the basic structural weight sensitivity to a wide range of absorbed heat flux. These results are presented as Figure 119.

b. Actively Cooled Panel Thermal Analyses - Additional analyses of a more detailed nature were conducted on each of the selected upper and lower surface thermostructural concepts for each Mach number. The analyses included the revised cruise and abort heating rates applicable to the refined Mach 4.5 trajectory. Although a slight reduction in abort heating

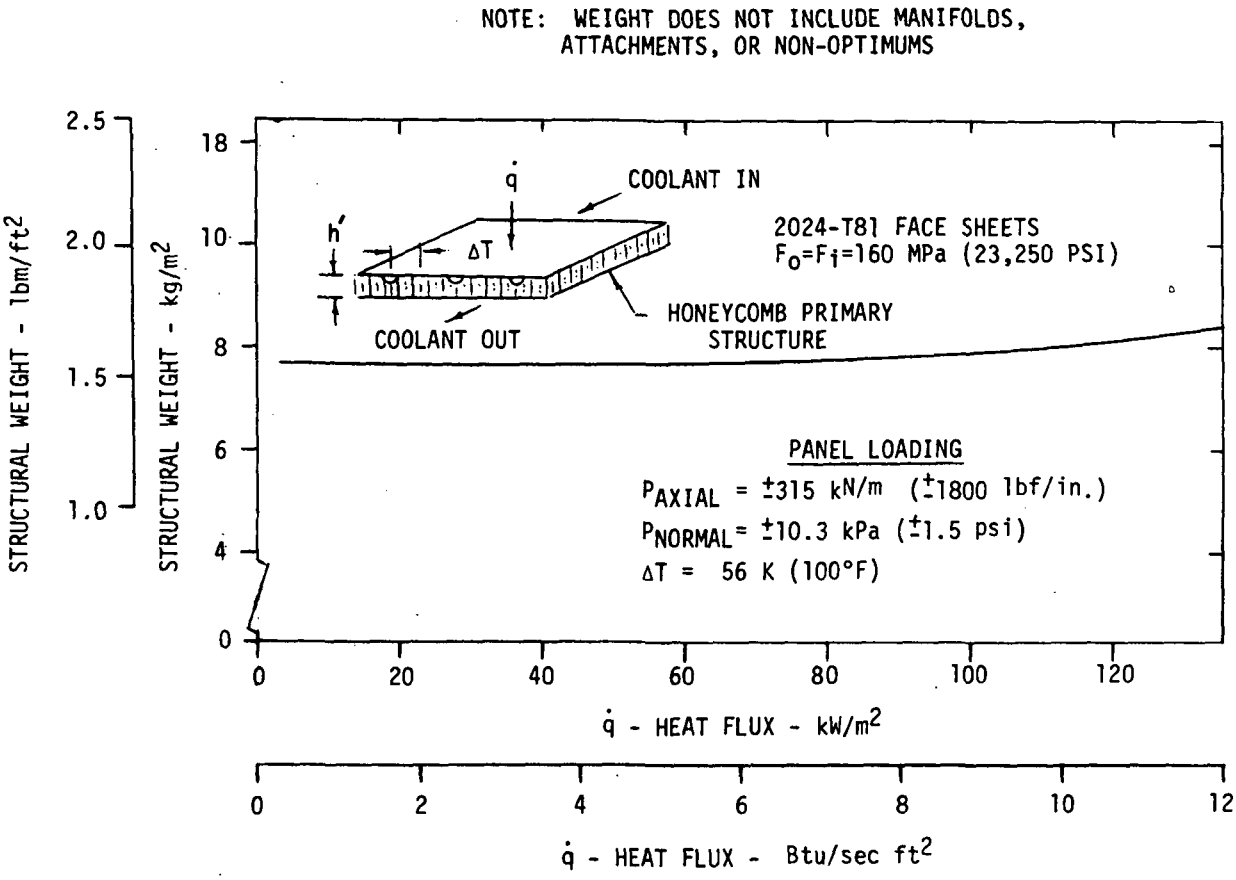

FIGURE 119
SENSITIVITY OF STRUCTURAL WEIGHT TO HEAT FLUX

rates was shown to be possible for the Mach 3 case (Section 4.2.3), the reduction was not deemed significant enough to impact study results. Furthermore, abort heating rates were low enough for the Mach 3 configurations that the panel designs were dictated by cruise heating rates. These were essentially unchanged from the initial values. The final design cruise and abort heating rates for the Mach 6 configurations were unchanged from prior studies.

The actively cooled panel back-up structures defined for each configuration were included in the refined thermal analyses. As expected, the additional heat capacity of the aluminum honeycomb structural configurations resulted in somewhat lower temperatures during abort. Panel skin temperature levels and gradients during sustained cruise were not significantly affected by the presence of the back-up honeycomb structure.

All of the thermostructural concepts selected employed some form of insulation on the outer surface (silicone overcoats or insulative heat shields), thus reducing both absorbed heat and required coolant flowrates. Therefore, smaller coolant tubes could be used, without resulting in excessive panel coolant pressure drop. Detailed analyses were conducted for the baseline 8.64mm (0.34 inch) I.D. dee-tube as well as the final selected 6.35mm (0.25 inch) dee tube. It was determined, in some cases, that the use of a smaller coolant tube, even with the same pitch as the larger one, resulted in slightly lower panel skin temperatures during cruise because of higher internal heat transfer coefficients. This was due to the increased Reynolds number of the coolant flow.

A few changes were made relative to insulation performance used for the Mach 4.5, and Mach 6, lower surface insulative heat shield concepts. Johns-Manville Micro-Fibers Felt (Type E) insulation was judged to be a better choice for the Mach 4.5 lower surface than Fiberfrax or Min-K. Its lower density, 64.1 kg/m^3 (4 lbm/ft^3), and its 922K (1200°F) continuous use temperature level was adequate. Fiberfrax 660 insulation was retained for the Mach 6 lower surface, although flexible high-temp Min-K 2000 could have been used. Based on earlier preliminary analyses a degradation factor of 2 on thermal conductivity was used to account for heat short effects of shield supports, support cut-outs and other installation details. As a result of a more detailed analyses of shield support heat leak, the degradation factor was modified to a factor of 1.25.

The insulation was placed directly on the cooled panel face sheet without gaps between the aluminum skin and insulation, or between the insulation package and the heat shield. Thus, boundary leakage was not considered a factor in the overall insulative degradation factor used.

Figures 120, 121 and 122 present details of the panel design, coolant parameters, and maximum temperatures for each candidate. The final selections are indicated in the figures by check marks.

Figure 123 presents a weight comparison of the concepts. The selected configurations are checked. In some cases the final selected configuration exhibits a slight weight penalty when compared to the alternate concept.

AIRCRAFT SURFACE	THERMOSTRUCTURAL CONCEPT	ACTIVELY COOLED PANEL GEOMETRY						COOLANT PARAMETERS			MAX PANEL TEMPERATURE		
		P cm (in.)	D mm (in.)	t_s mm (in.)	ΔX_{SIL} mm (in.)	h cm (in.)	t_i mm (in.)	HEATING RATE kW/m^2 (Btu/sec ft^2)	FLOW RATE PER TUBE g/s (lb/hr)	COOLANT ΔP kPa (psid)	MATERIAL	CRUISE TEMP K (°F)	ABORT TEMP K (°F)
UPPER √	SILICONE OVERCOAT OVER AL. SKIN (HONEYCOMB PANEL)	10.6 (4.2)	6.35 (.25)	1.02 (.04)	1.17 (.046)	3.2 (1.26)	1.02 (.04)	4.17 (0.367)	10.84 (86)	22 (3.2)	AL. SKIN	383 (230)	386 (235)
											SILICONE	414 (285)	421 (299)
	BARE AL. SKIN (HONEYCOMB PANEL)	10.6 (4.2)	6.35 (.25)	1.02 (.04)	-- --	3.2 (1.26)	1.02 (.04)	5.71 (0.503)	16.9 (134)	46 (6.7)	AL. SKIN	378 (221)	388 (239)
LOWER √	SILICONE OVERCOAT OVER AL. SKIN (HONEYCOMB PANEL)	10.2 (4)	6.35 (.25)	1.02 (.04)	1.17 (.046)	3.07 (1.21)	0.97 (.038)	6.36 (0.56)	17.65 (140)	49 (7.1)	AL. SKIN	386 (235)	403 (266)
											SILICONE	451 (353)	455 (360)
	BARE AL. SKIN (HONEYCOMB PANEL)	(2.95)	6.35 (.25)	1.02 (.04)	-- --	3.07 (1.21)	0.97 (.038)	11.55 (1.018)	23.8 (189)	81.4 (11.8)	AL. SKIN	386 (235)	416 (290)

t_s = COOLED PANEL SKIN THICKNESS

P = COOLANT TUBE PITCH

D = COOLANT DEE TUBE DIAMETER

h = STRUCTURAL HONEYCOMB DEPTH

t_i = HONEYCOMB BACK-FACE SHEET THICKNESS

ΔX_{SIL} = SILICONE OVERCOAT THICKNESS

√ SELECTED CONFIGURATIONS

FIGURE 120
MACH 3 THERMO-STRUCTURAL CONCEPTS

AIRCRAFT SURFACE	THERMOSTRUCTURAL CONCEPT	ACTIVELY COOLED PANEL GEOMETRY								COOLANT PARAMETERS			MAX PANEL TEMPERATURE		
		P cm (in.)	D mm (in.)	t_s mm (in.)	ΔX_{SIL} mm (in.)	h cm (in.)	t_i mm (in.)	t_o mm (in.)	ΔX_{ins} mm (in.)	HEATING RATE kW/m^2 (Btu/sec ft^2)	FLOW RATE PER TUBE g/s (lbm/hr)	COOLANT ΔP kPa (psid)	MATERIAL	CRUISE TEMP K (°F)	ABORT TEMP K (°F)
UPPER √	SILICONE OVERCOAT OVER AL. SKIN	8.89 (3.5)	6.35 (.25)	1.02 (.04)	1.91 (.075)	3.1 (1.22)	0.91 (.036)	--	--	8.19 (0.722)	20 (159)	59 (8.6)	AL. SKIN	388 (239)	409 (276)
													SILICONE	533 (499)	537 (507)
	BARE AL. SKIN	6.73 (2.65)	6.35 (.25)	1.02 (.04)	-- --	3.1 (1.22)	0.91 (.036)	-- --	-- --	14.44 (1.272)	26.4 (209)	95 (13.8)	AL. SKIN	392 (246)	424 (303)
LOWER √	INSULATED HEAT SHIELD	10.2 (4)	6.35 (.25)	1.02 (.04)	-- --	3.15 (1.24)	1.07 (.042)	0.41 (.016)	6.35 (.25)	3.59 (0.316)	9.71 (77)	20 (2.9)	AL. SKIN	380 (224)	420 (296)
													TIT. SKIN	663 (734)	677 (759)
	SILICONE OVERCOAT OVER AL. SKIN (SKIN/STRINGER)	8.89 (3.5)	6.35 (.25)	3.61 (.142)	1.3 (.051)	-- --	-- --	-- --	-- --	13.69 (1.206)	32.5 (258)	141 (20.4)	AL. SKIN	370 (207)	437 (327)
													SILICONE	541 (515)	602 (624)

t_s = COOLED PANEL SKIN THICKNESS

P = COOLANT TUBE PITCH

D = COOLANT DEE TUBE DIAMETER

h = STRUCTURAL HONEYCOMB DEPTH

√ SELECTED CONFIGURATIONS

t_i = HONEYCOMB BACK FACE SHEET THICKNESS

ΔX_{SIL} = SILICONE OVERCOAT THICKNESS

ΔX_{INS} = INSULATION THICKNESS

t_o = TITANIUM HEAT SHIELD MATERIAL THICKNESS

FIGURE 121
MACH 4.5 THERMO-STRUCTURAL CONCEPTS

AIRCRAFT SURFACE	THERMOSTRUCTURAL CONCEPT	P cm (in.)	D mm (in.)	t_s mm (in.)	ACTIVELY COOLED PANEL GEOMETRY ΔX_{SIL} mm (in.)	h cm (in.)	t_i mm (in.)	t_o mm (in.)	ΔX_{ins} mm (in.)	COOLANT PARAMETERS HEATING RATE kW/m^2 (Btu/sec ft^2)	FLOW RATE PER TUBE g/s (lb/hr)	COOLANT ΔP kPa (psid)	MAX PANEL TEMPERATURE MATERIAL	CRUISE TEMP K (°F)	ABORT TEMP K (°F)
UPPER √	SILICONE OVERCOAT OVER AL. SKIN	7.47 (2.92)	6.35 (.25)	1.02 (.04)	1.42 (.056)	3.07 (1.21)	0.91 (.036)	-- --	-- --	12 (1.057)	24.59 (195)	85.5 (12.4)	AL. SKIN	391 (244)	443 (337)
													SILICONE	554 (537)	563 (554)
	BARE AL. SKIN	6.02 (2.37)	6.35 (.25)	1.02 (.04)	-- --	3.07 (1.21)	0.91 (.036)	-- --	-- --	17.64 (1.554)	29.5 (234)	121 (17.5)	AL. SKIN	391 (244)	454 (358)
LOWER √	INSULATED HEAT SHIELD	10.2 (4)	6.35 (.25)	1.02 (.04)	-- --	3.15 (1.24)	1.07 (.042)	0.41 (.016)	5.84 (.23)	4.26 (0.375)	11.73 (93)	26 (3.8)	AL. SKIN	379 (222)	465 (377)
													RENE SKIN	850 (1070)	866 1100)

t_s = COOLED PANEL SKIN THICKNESS

P = COOLANT TUBE PITCH

D = COOLANT DEE TUBE DIAMETER

h = STRUCTURAL HONEYCOMB DEPTH

t_i = HONEYCOMB BACK FACE SHEET THICKNESS

ΔX_{SIL} = SILICONE OVERCOAT THICKNESS

ΔX = INSULATION THICKNESS

t_o = RENE' 41 HEAT SHIELD MATERIAL THICKNESS

√ SELECTED CONFIGURATIONS

FIGURE 122
MACH 6 THERMO-STRUCTURAL CONCEPTS

MACH NO.	AIRCRAFT SURFACE	CONFIGURATION	COOLED SKIN, TUBES, AND STRUCTURE	WEIGHTS FOR 7.43 m^2 PANEL - kg					PANEL UNIT WEIGHT kg/m^2
				MANIFOLDS AND NON-OPTIMUMS	HEAT SHIELD AND INSULATION	ACTIVE COOLING SYSTEM	FAILURE DETECTION SYSTEM	TOTAL	
3	UPPER	√ SILICONE OVERCOAT OVER AL. SKIN	57.0	37.0	3.5	4.8	1.2	103.5	13.91
		BARE AL. SKIN	57.0		0	6.1	0.6	100.7	13.57
	LOWER	√ SILICONE OVERCOAT OVER AL. SKIN	57.0		3.5	6.6	1.3	105.4	14.16
		BARE AL. SKIN	57.0		0	10.1	0.6	104.7	14.11
4.5	UPPER	√ SILICONE OVERCOAT OVER AL. SKIN	57.0		5.7	8.1	1.5	109.3	14.70
		BARE AL. SKIN	57.0		0	11.7	0.6	106.3	14.31
	LOWER	√ INSULATED HEAT SHIELD	57.0		21.1	4.4	1.3	120.8	16.26
		SILICONE OVERCOAT OVER AL. SKIN	77.9		3.9	11.3	1.5	131.6	17.72
6	UPPER	√ SILICONE OVERCOAT OVER AL. SKIN	57.0		4.2	10.3	1.7	110.2	14.84
		BARE AL. SKIN	57.0		0	13.7	0.6	108.3	14.55
	LOWER	√ INSULATED HEAT SHIELD	57.0		40.6	4.9	1.3	140.8	18.94

NOTES: √ SELECTED CONFIGURATIONS
(1) FLUID FILLED TUBE (VAPOR PRESSURE) FAILURE DETECTION ELEMENTS. WEIGHT BASED ON TUBE PITCH. SYSTEM WEIGHT IS 0.168 kg/m^2 FOR 10.2 cm PITCH (TYP.)
(2) INFRARED SCANNING FAILURE DETECTION SYSTEM WEIGHT IS 0.64 kg PER PANEL

FIGURE 123a
THERMO-STRUCTURAL CONCEPT WEIGHTS

MACH NO.	AIRCRAFT SURFACE	CONFIGURATION	COOLED SKIN, TUBES, AND STRUCTURE	WEIGHT FOR 80 ft^2 PANEL -lbm					PANEL UNIT WEIGHT lbm/ft^2
				MANIFOLDS AND NON-OPTIMUMS	HEAT SHIELD AND INSULATION	ACTIVE COOLING SYSTEM	FAILURE DETECTION SYSTEM	TOTAL	
3	UPPER	✓ SILICONE OVERCOAT OVER AL. SKIN	125.6	81.6	7.7	10.6	2.6	228.1	2.85
		BARE AL. SKIN	125.6		0	13.4	1.4	222.0	2.78
	LOWER	✓ SILICONE OVERCOAT OVER AL. SKIN	125.6		7.7	14.5	2.8	232.2	2.90
		BARE AL. SKIN	125.6		0	22.2	1.4	231.0	2.89
4.5	UPPER	✓ SILICONE OVERCOAT OVER AL. SKIN	125.6		12.5	17.8	3.2	241.0	3.01
		BARE AL. SKIN	125.6		0	25.9	1.4	234.5	2.93
	LOWER	✓ INSULATED HEAT SHIELD	125.6		46.5	9.6	2.8	266.1	3.33
		SILICONE OVERCOAT OVER AL. SKIN	171.8		8.5	25.0	3.2	290.1	3.63
6	UPPER	✓ SILICONE OVERCOAT OVER AL. SKIN	125.6		9.3	22.8	3.8	243.1	3.04
		BARE AL. SKIN	125.6		0	30.1	1.4	238.7	2.98
	LOWER	✓ INSULATED HEAT SHIELD	125.6		89.6	10.8	2.8	310.4	3.88

NOTES: ✓ SELECTED CONFIGURATIONS

(1) FLUID FILLED TUBE (VAPOR PRESSURE) FAILURE DETECTION ELEMENTS. WEIGHT BASED ON TUBE PITCH. SYSTEM WEIGHT IS 0.0345 lbm/ft^2 FOR 4 in. PITCH (TYP.)

(2) INFRARED SCANNING FAILURE DETECTION SYSTEM WEIGHT IS 1.4 lbm PER PANEL

FIGURE 123b
THERMO-STRUCTURAL CONCEPT WEIGHTS

In these cases, the selected system resulted in a reduction in absorbed heat flux compared to the alternate concept and was selected to provide a more realistic match between absorbed heat flux and available heat sink.

Figures 124 through 135 present configuration details and thermal analyses results for the selected panel configurations. All analyses were based on initiation of the abort trajectory 15 seconds after cooling system failure. It was assumed that the failure resulted in instantaneous depletion of the coolant within the tubes of the actively cooled panel. Due to geometric and flow rate symmetry (i.e. same flow rate through each tube and constant tube spacing), only a portion of each panel was analyzed in detail. In addition, the abort heating transient analyses were conducted on those panel segments which were determined to exhibit the highest skin temperature during cruise.

Inspection of Figures 125 through 135 show that all material temperatures during cruise and abort are within allowable values. It is noted that in a few cases, the cruise peak skin temperature occurred at an intermediate segment of the panel, rather than at the exit where coolant temperature is highest. This was due to the presence of laminar coolant flow in the tube up to and including this panel segment, with turbulent flow further downstream. The lower laminar flow heat transfer coefficient offsets the effect of the lower coolant temperature at this point. Laminar flow was assumed to apply below Reynolds numbers of 2100, with a step change to turbulent flow at higher Reynolds numbers. A higher flow rate, or smaller tubes, would result in peak skin temperature further down the length of the panel, at the expense of higher coolant pressure drop. The maximum cooled skin temperature gradients were near the 56K (100°F) target level and occurred at the panel inlet, where local heating rates were slightly higher. Only moderate temperature gradients were present in the honeycomb structure during cruise and, in general, declined rather rapidly upon loss of cooling.

c. Failure Detection Integration - The evaluation of failure detection methods (Section 4.1.4) identified three methods as the most promising. These were: Infrared scanning of external surfaces (rated number one); Fluid filled tube elements (phase change) (rated number two); and Eutectic salt elements (rated number three).

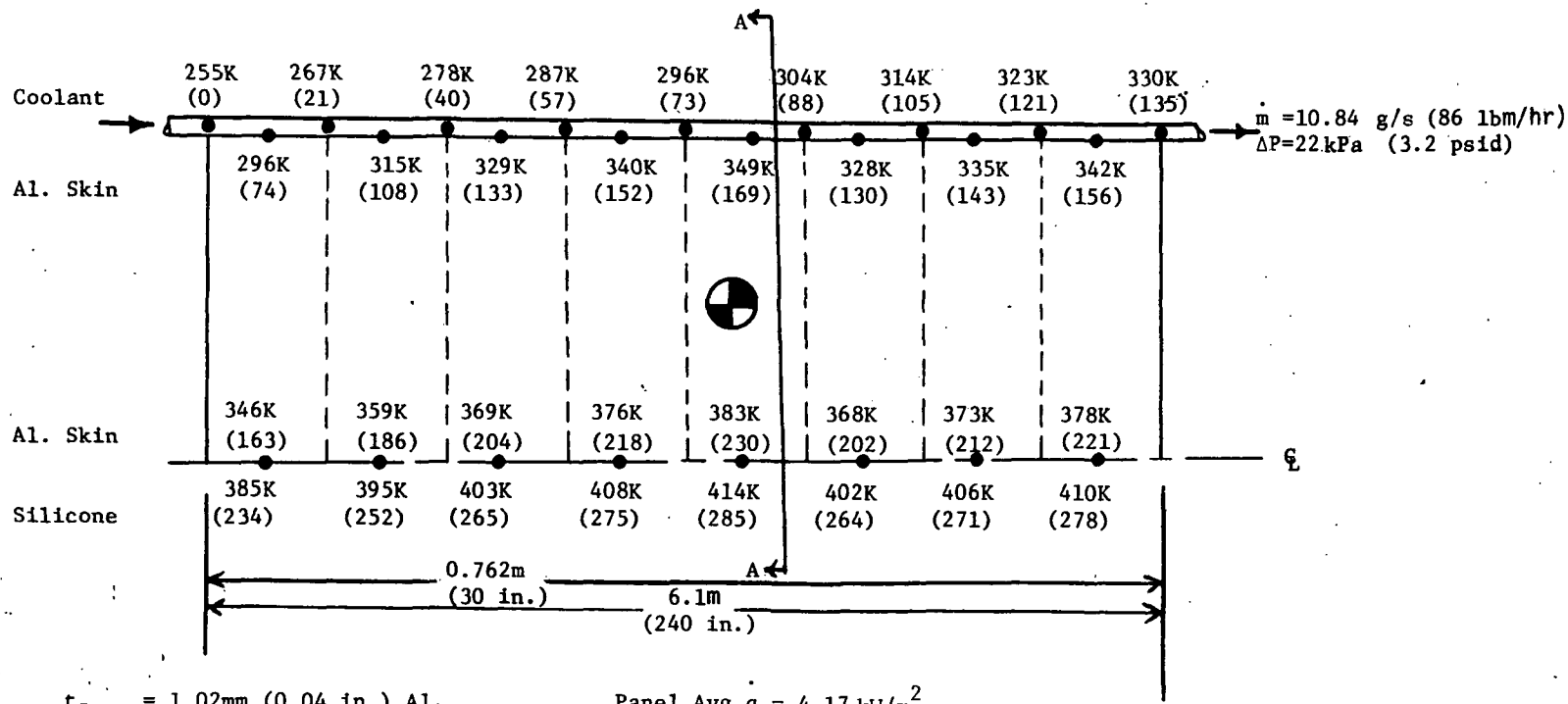

t_s = 1.02mm (0.04 in.) Al.

ΔX_{SIL} = 1.17mm (0.046 in.) Silicone

h = 3.2cm (1.26 in.) Al. H/C

t_i = 1.02mm (0.04 in.) Al.

D = 6.35mm (0.25 in.) Dee-Tube

P = 10.6cm (4.2 in.) Pitch

Hottest Panel Segment

Panel Avg q = 4.17 kW/m^2 (0.367 Btu/sec ft^2)

Note: Temperatures in parentheses are °F

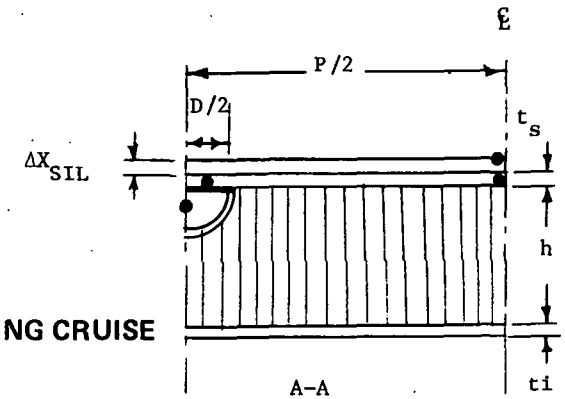

FIGURE 124
MACH 3 UPPER SURFACE TEMPERATURES DURING CRUISE (SILICONE OVERCOAT CONCEPT)

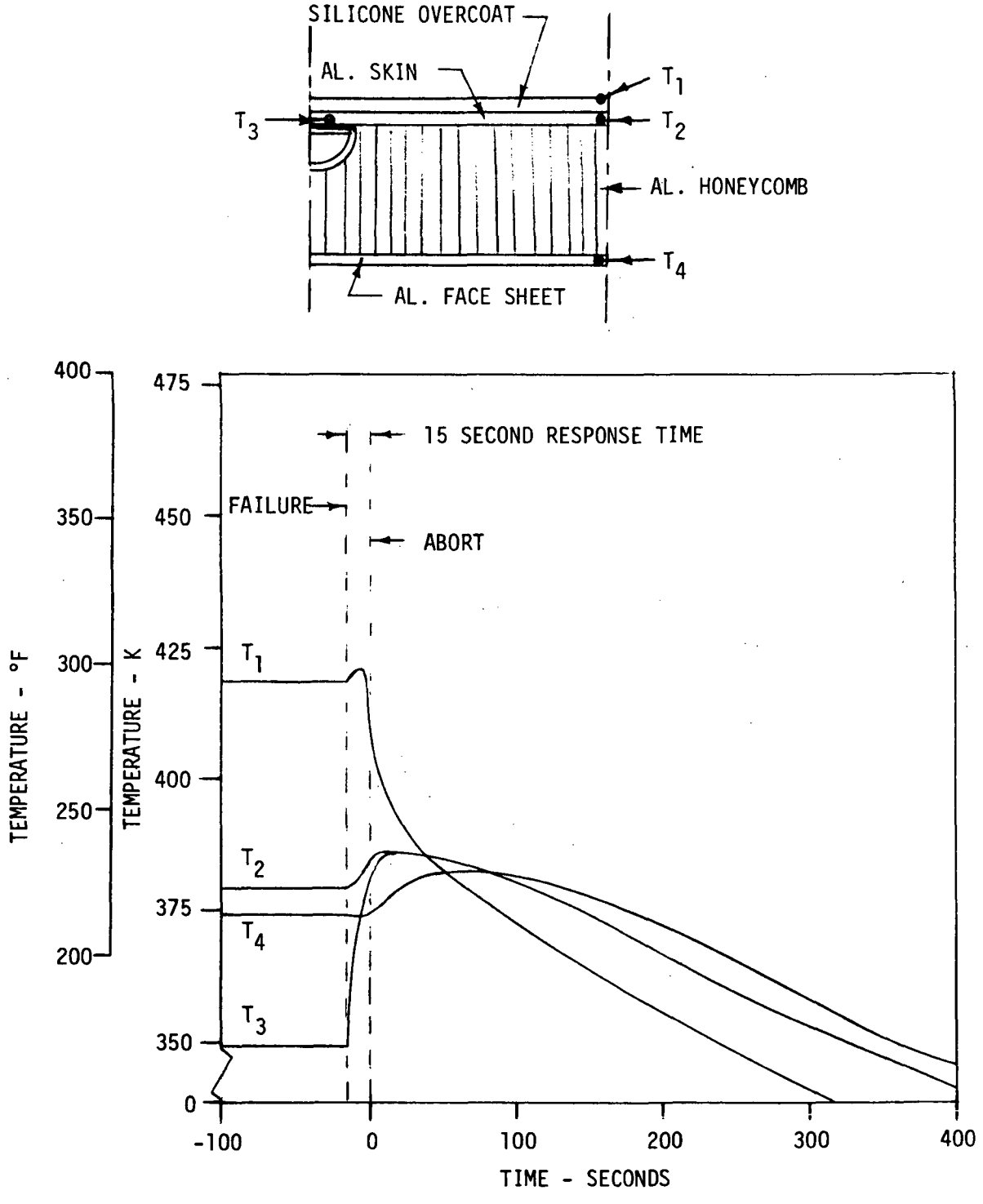

FIGURE 125
MACH 3 UPPER SURFACE TEMPERATURES DURING ABORT
(SILICONE OVERCOAT CONCEPT)

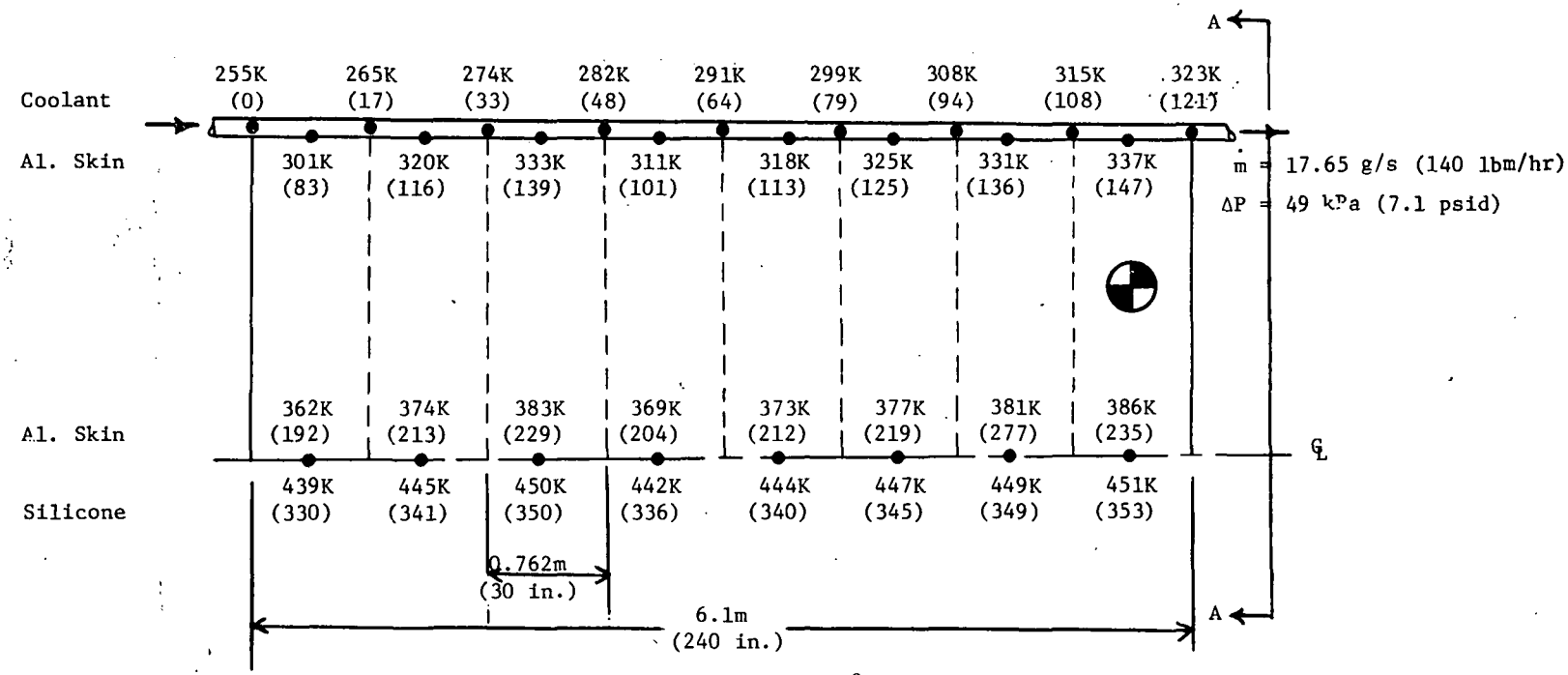

t_s = 1.02 mm(0.04 in.) Al. Panel Avg. $\dot{q}$ = 6.36 kW/m^2

ΔX_{SIL} = 1.17 mm(0.046 in.) Silicone (0.56 Btu/sec ft^2)

h = 3.07 cm(1.21 in.) Al. H/C

t_i = 0.97 mm(0.038 in.) Al.

D = 6.35 mm(0.25 in.) Dee-Tube

P = 10.2 cm(4 in.) pitch

Hottest Panel Segment

Note: Temperatures in parentheses are °F

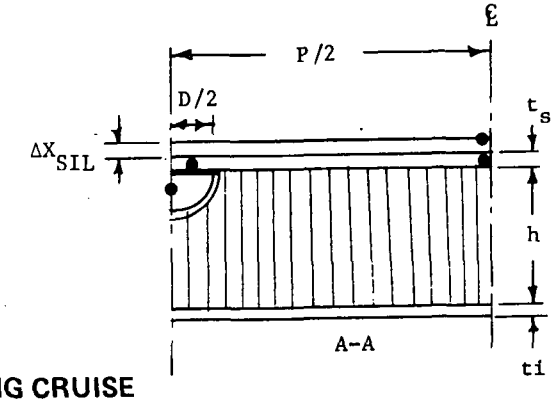

FIGURE 126
MACH 3 LOWER SURFACE TEMPERATURES DURING CRUISE
(SILICONE OVERCOAT CONCEPT)

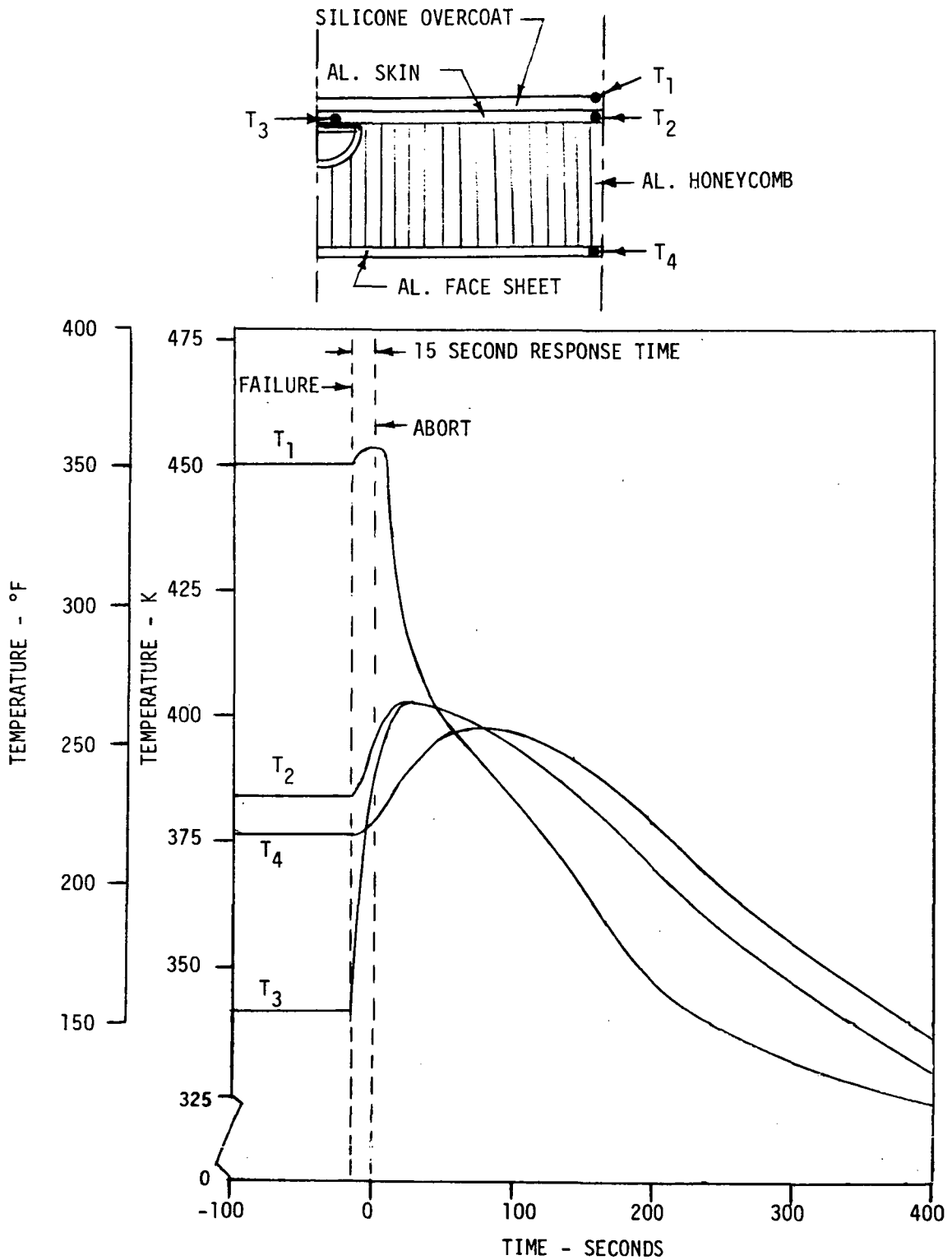

FIGURE 127
MACH 3 LOWER SURFACE TEMPERATURES DURING ABORT
(SILICONE OVERCOAT CONCEPT)

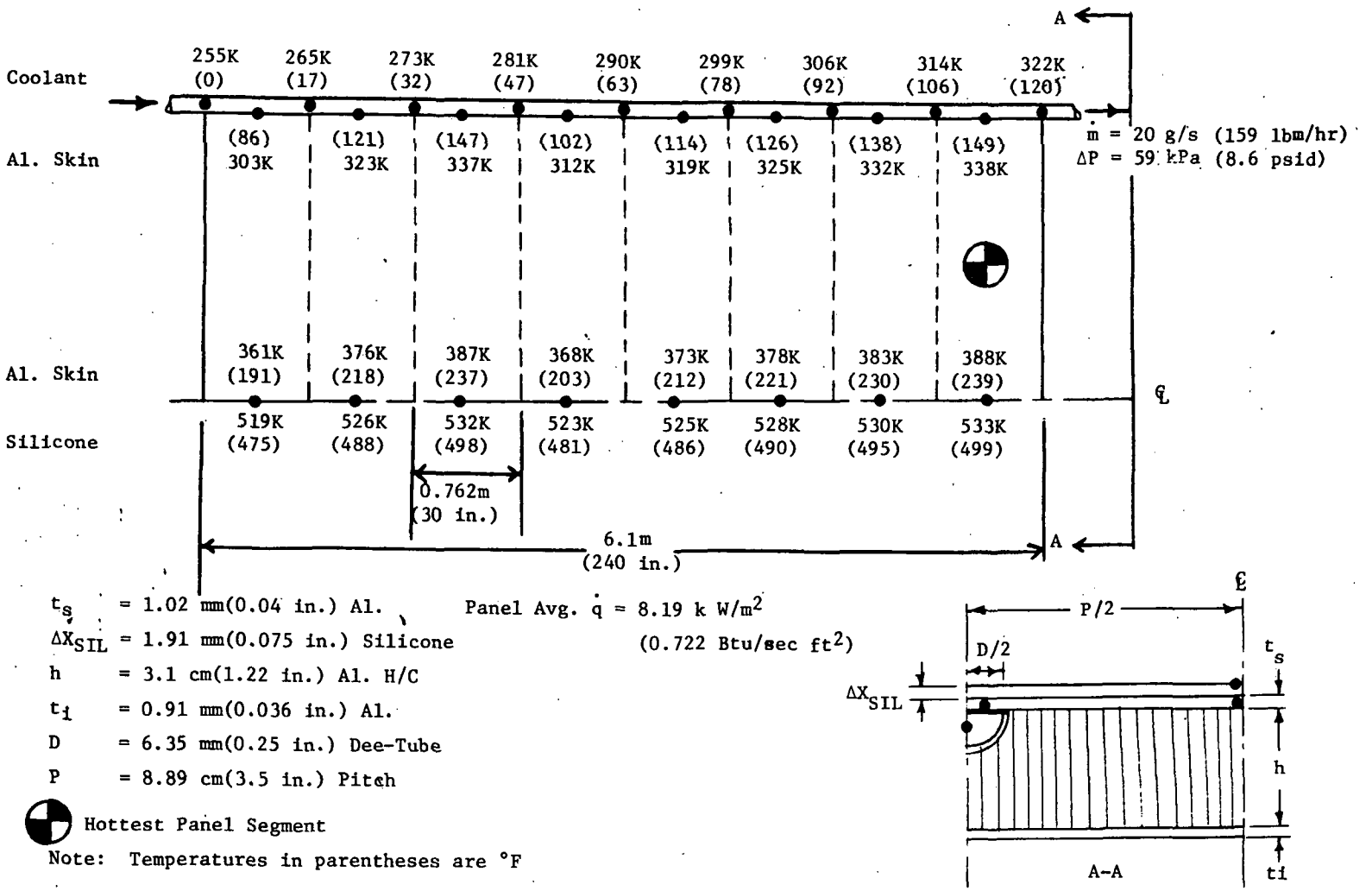

FIGURE 128
MACH 4.5 UPPER SURFACE TEMPERATURES DURING CRUISE
(SILICONE OVERCOAT CONCEPT)

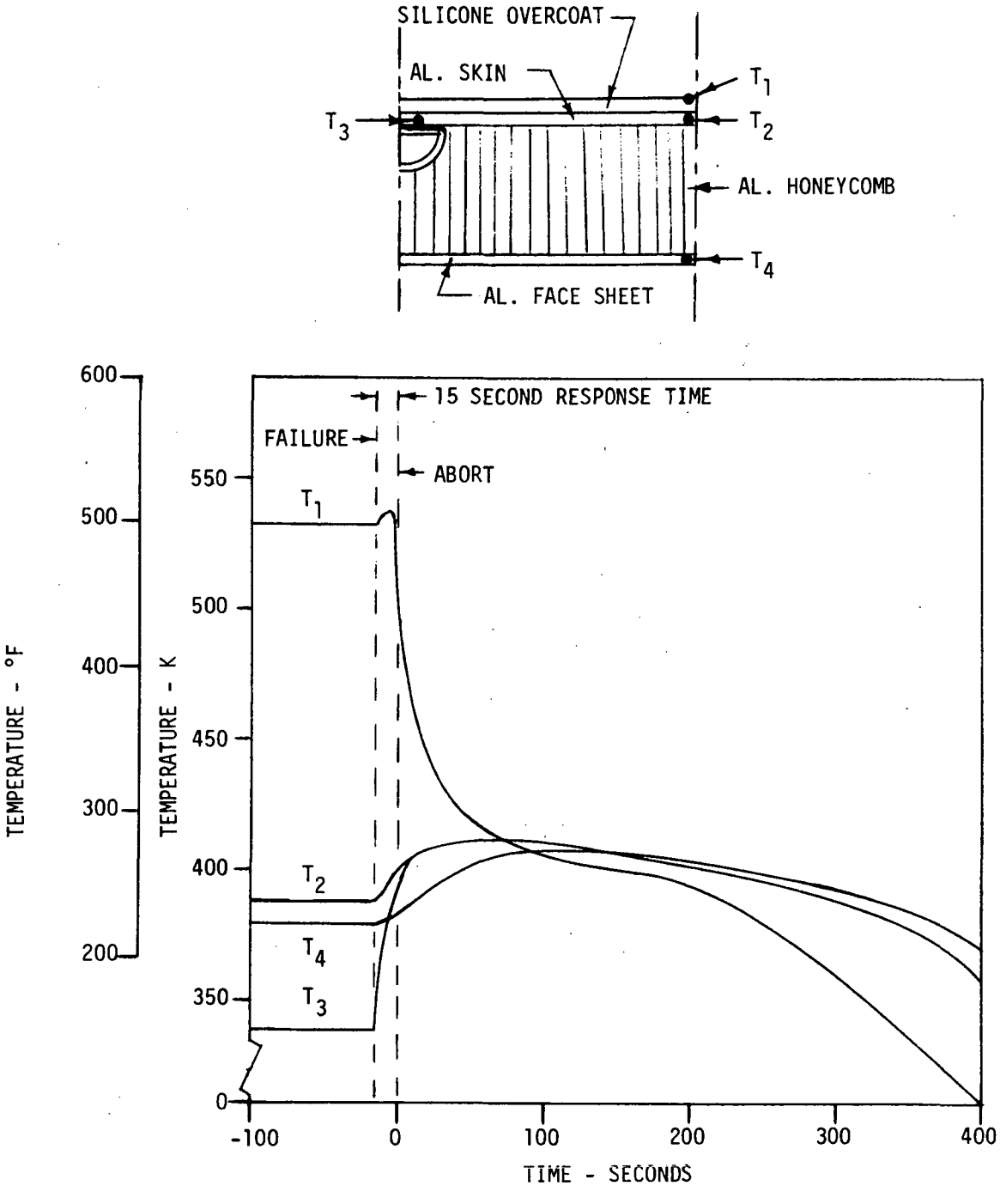

FIGURE 129
MACH 4.5 UPPER SURFACE TEMPERATURES DURING ABORT
(SILICONE OVERCOAT CONCEPT)

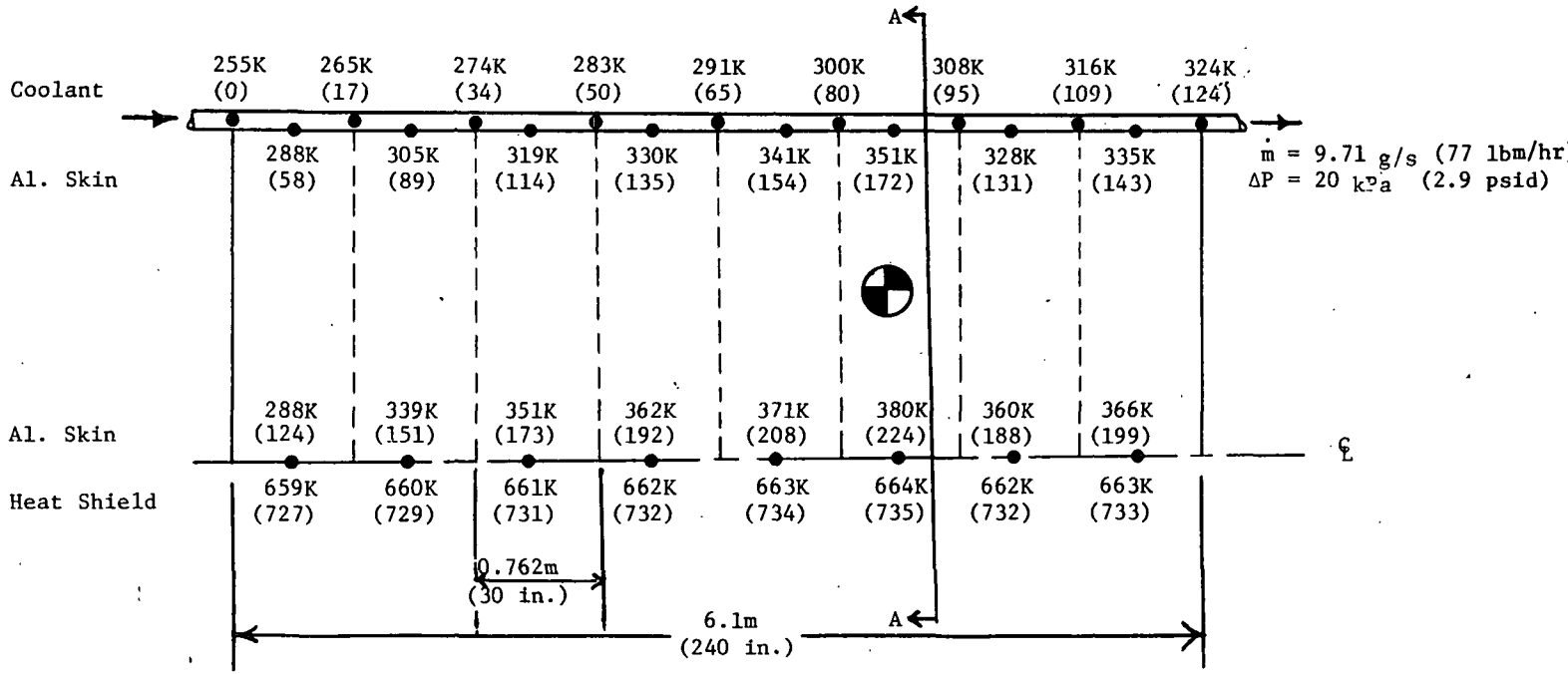

t_s = 1.02 mm(0.04 in.) Al.

ΔX_{INS} = 6.35 mm(0.25 in.) J.M. Micro-Fibers

t_o = 0.41 mm(0.016 in.) Titanium

h = 3.15 cm(1.24 in.) Al. H/C

t_i = 1.07 mm(0.042 in.) Al.

D = 6.35 mm(0.25 in.) Dee-Tube

P = 10.2 cm(4 in.) Pitch

Hottest Panel Segment

Note: Temperatures in parentheses are °F

Panel Avg. $\dot{q}$ = 3.59 k W/m^2 (0.316 Btu/sec ft^2)

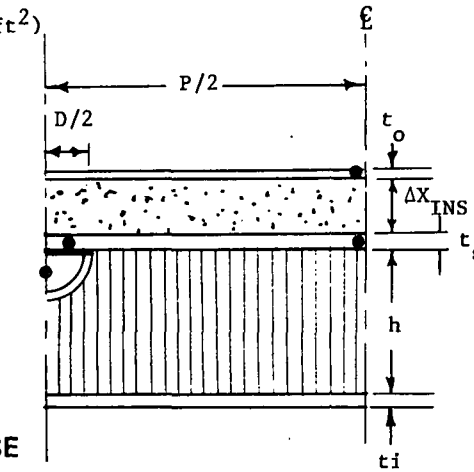

FIGURE 130
MACH 4.5 LOWER SURFACE TEMPERATURES DURING CRUISE

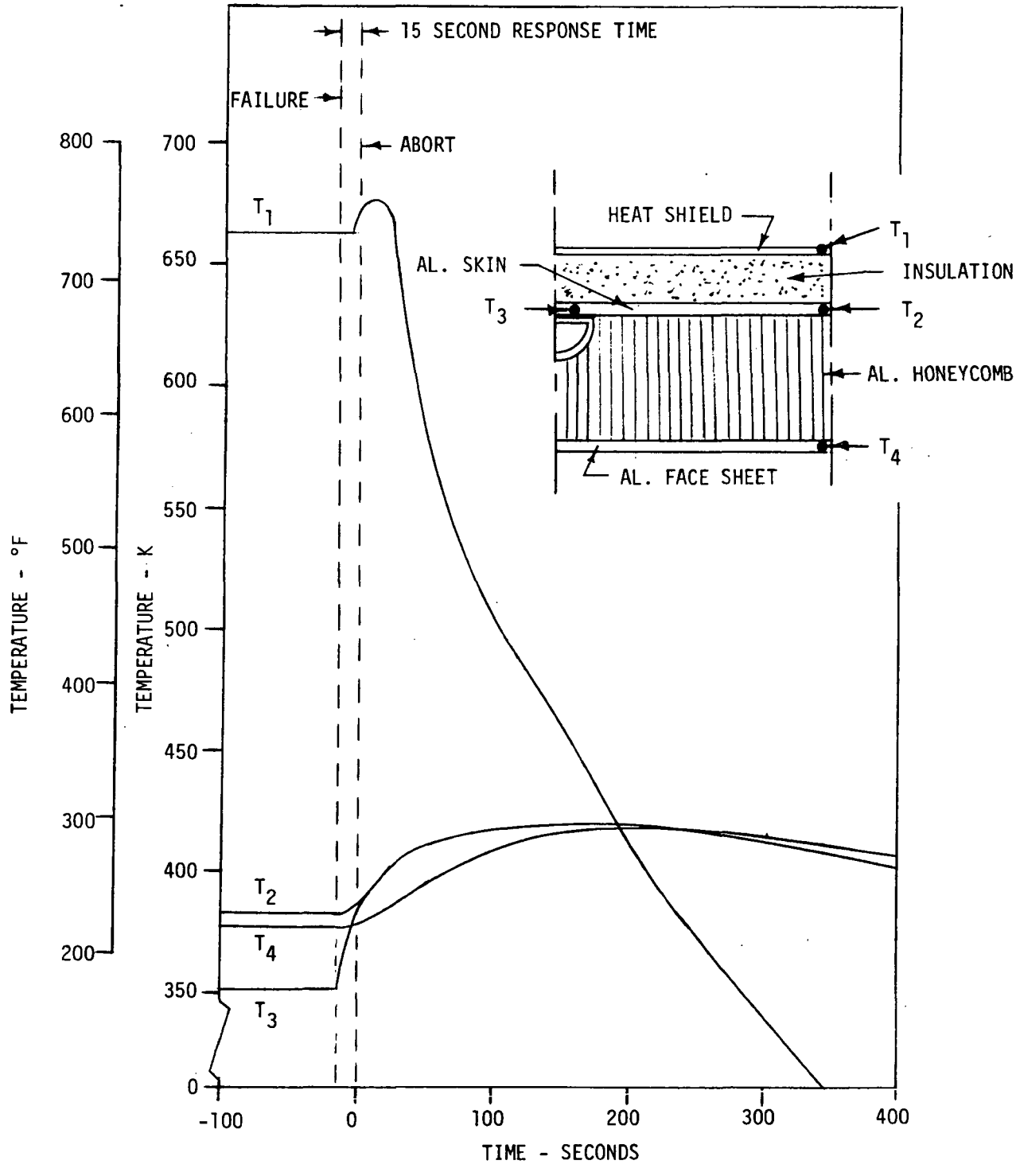

FIGURE 131
MACH 4.5 LOWER SURFACE TEMPERATURES DURING ABORT
(INSULATIVE HEAT SHIELD CONCEPT)

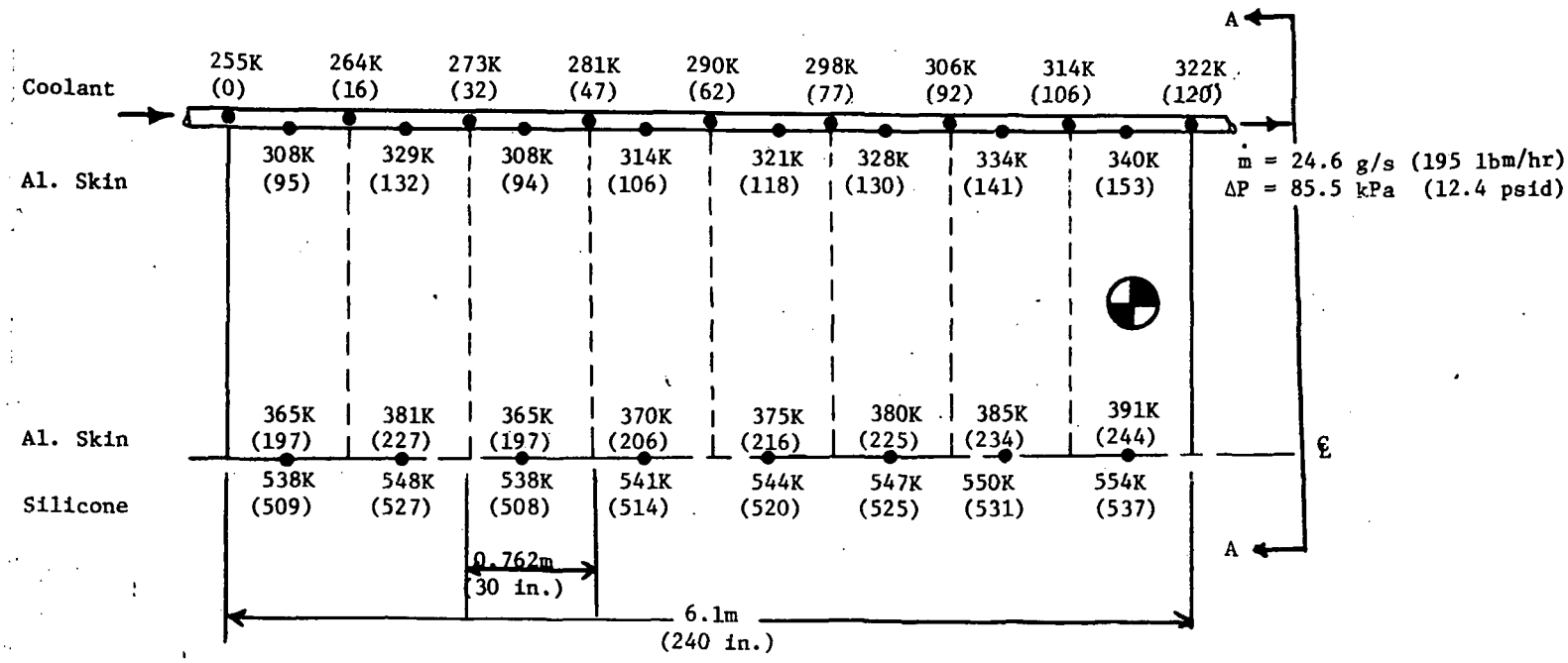

t_s = 1.02 mm(0.04 in.) Al. Panel Avg. $\dot{q}$ = 12 kW/m^2

ΔX_{SIL} = 1.42 mm(0.056 in.) Silicone (1.057 Btu/sec ft^2)

h = 3.07 cm(1.21 in.) Al. H/C

t_i = 0.91 mm(0.036 in.) Al.

D = 6.35 mm(0.25 in.) Dee-Tube

P = 7.47 cm(2.92 in.) Pitch

Hottest Panel Segment

Note: Temperatures in parentheses are °F

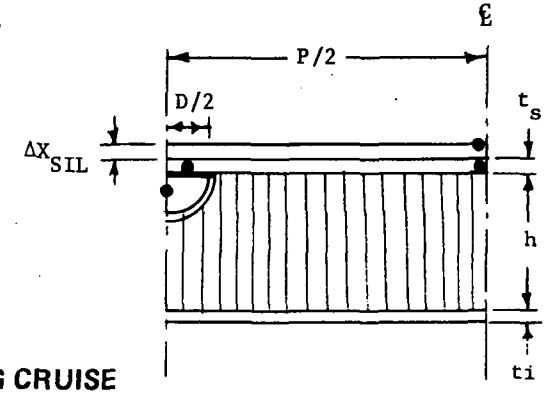

FIGURE 132
MACH 6 UPPER SURFACE TEMPERATURES DURING CRUISE
(SILICONE OVERCOAT CONCEPT)

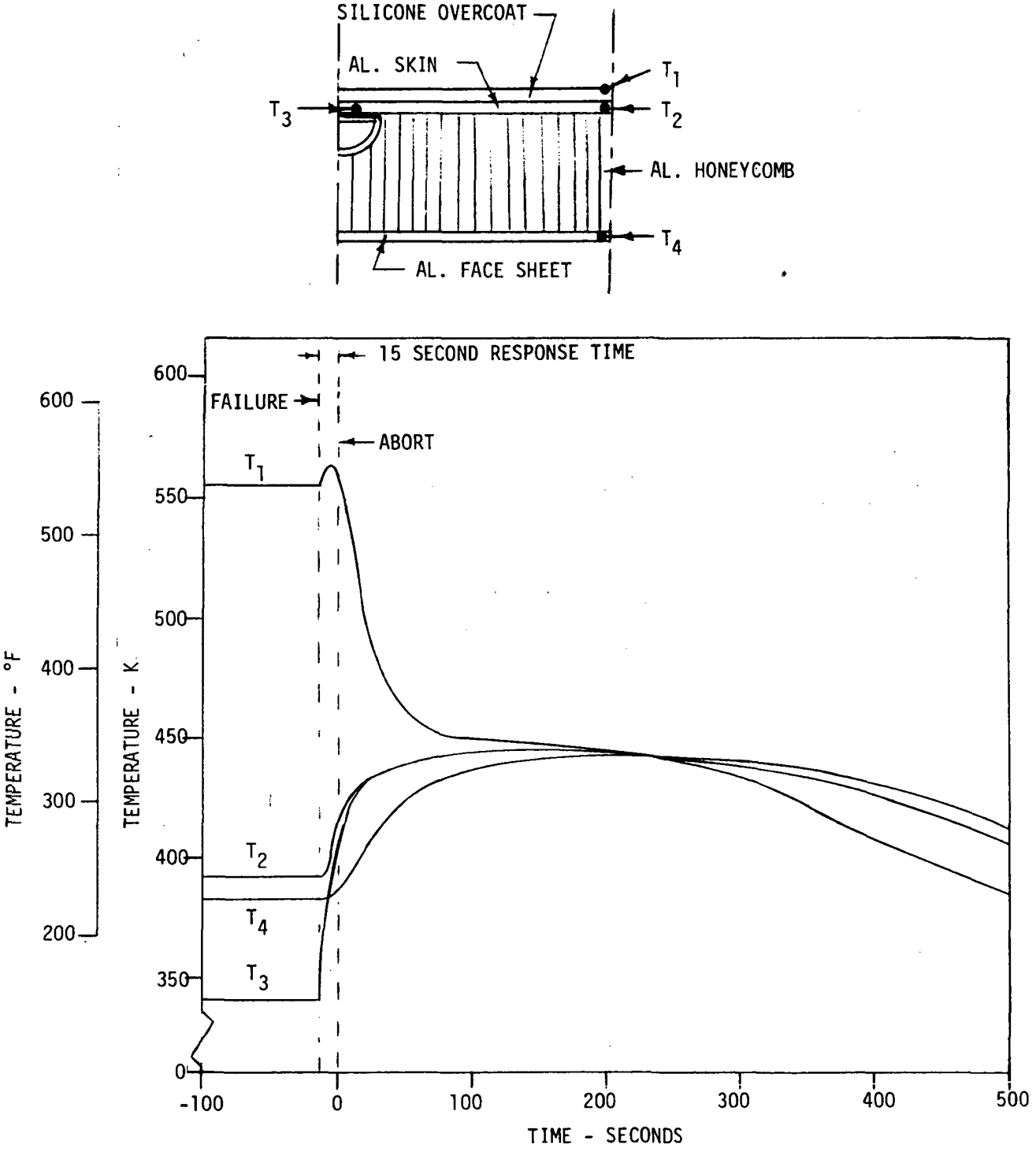

FIGURE 133
MACH 6 UPPER SURFACE TEMPERATURES DURING ABORT
(SILICONE OVERCOAT CONCEPT)

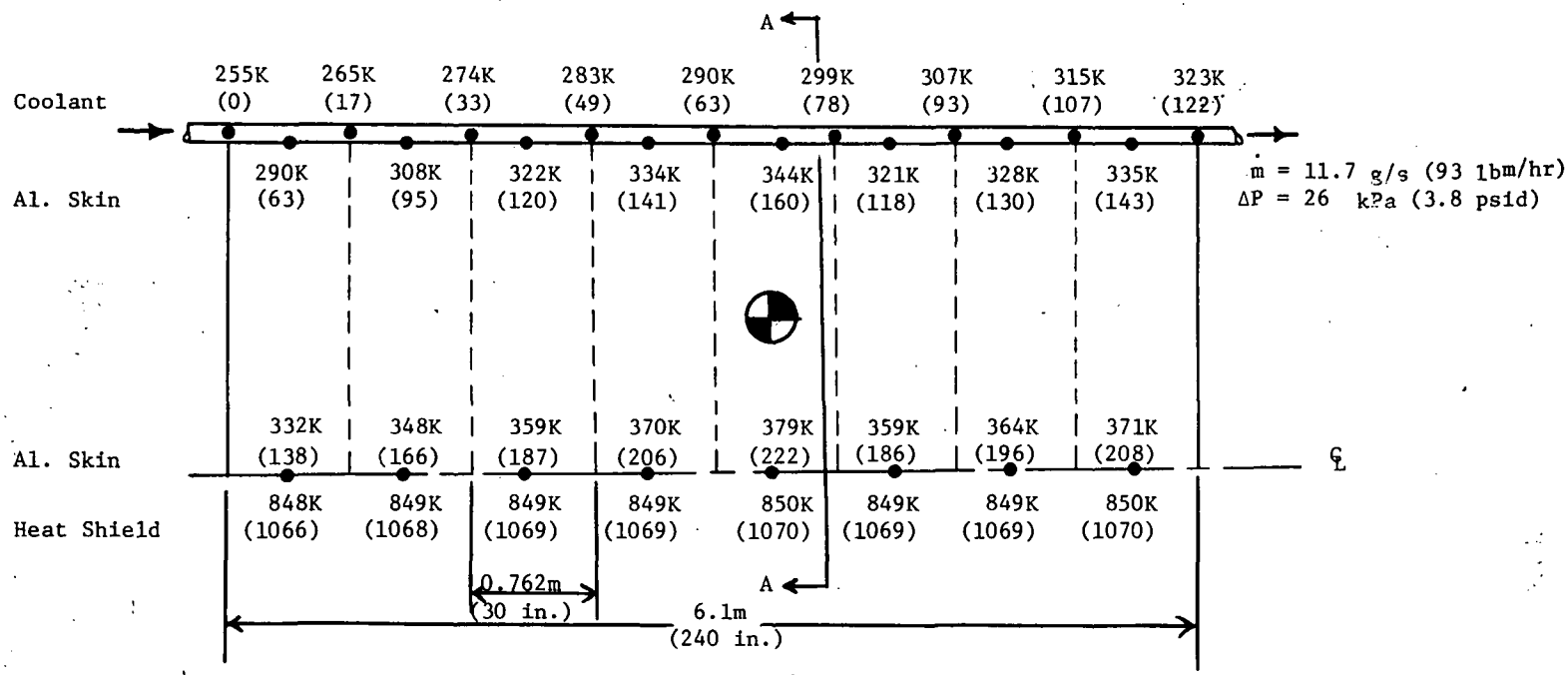

t_s = 1.02 mm(0.04 in.) Al.

ΔX_{INS} = 5.84 mm(0.23 in.) Fiberfrax 660

to = 0.41 mm(0.016 in.) Rene' 41

h = 3.15 cm(1.24 in.) Al. H/C

t_i = 1.07 mm(0.042 in.) Al.

D = 6.35 mm(0.25 in.) Dee-Tube

P = 10.2 cm(4 in.) Pitch

Panel Avg. $\dot{q}$ = 4.26 k W/m^2 (0.375 Btu/sec ft^2)

Hottest Panel Segment

Note: Temperatures in parentheses are °F

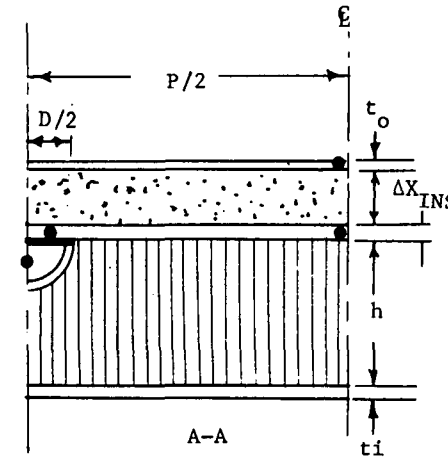

FIGURE 134
MACH 6 LOWER SURFACE TEMPERATURES DURING CRUISE (INSULATIVE HEAT SHIELD CONCEPT)

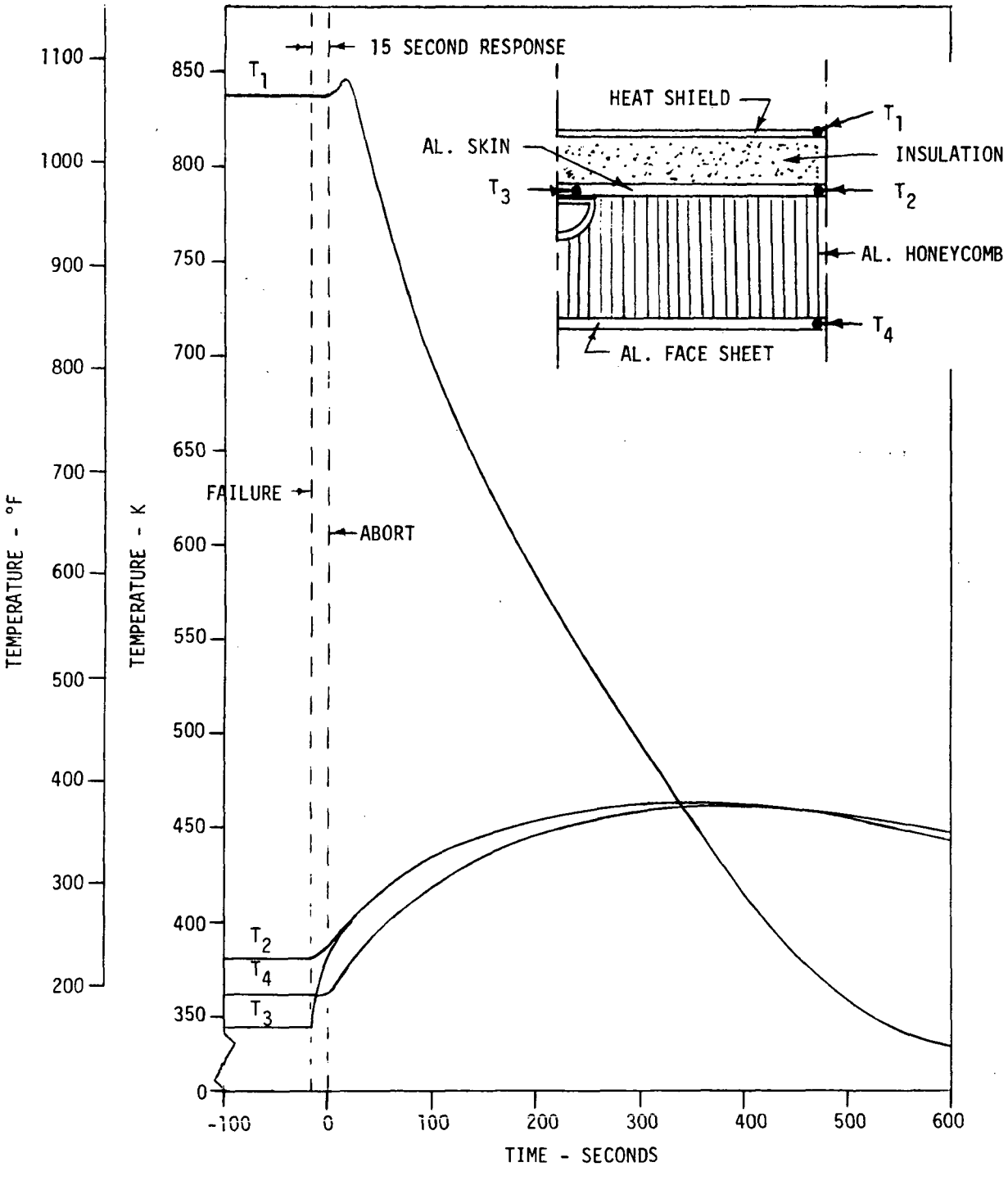

FIGURE 135
MACH 6 LOWER SURFACE TEMPERATURES DURING ABORT
(INSULATIVE HEAT SHIELD CONCEPT)

These approaches were re-evaluated for compatibility with the candidate thermostructural concepts.

The infrared scanning technique was examined on the basis of ability to detect changes in external surface temperature resulting from loss of cooling of an individual panel.

Figures 125, 129, and 133 present temperature response characteristics of typical aircraft upper surfaces that could be scanned with infrared detection equipment. As shown by Figure 125, the Mach 3 case, the surface temperature change during the assumed 15 second delay between loss of cooling and abort initiation is very small, only on the order of 2 to 3 K (4 to 5°F). Such minor changes could result from normal variations in aircraft attitude and altitude.

The use of a longer response time would provide a greater surface temperature change, but would also increase structural temperature levels prior to abort. In the Mach 3 case, this would not have a significant impact because the protection concepts (silicone overcoat) are designed by cruise considerations rather than abort. During abort, the maximum structural temperatures reach only 386K (235°F) and 403K (266°F) for the upper and lower surfaces, respectively. Thus, a longer delay could be tolerated. However, in this case, the increase in structural temperature could be detected by contact thermometry. Thus, infrared scanning does not appear to have any inherent advantage over the use of temperature sensitive elements in contact with the structural skin except for a small weight savings. In view of the extensive development that would be required, the infrared scanning approach may not be justifiable.

Again for the Mach 4.5 aircraft upper surface, Figure 129 shows only limited temperature response of the overcoat surface during a 15 second delay. Both the upper surface and lower surface thermostructural concepts could tolerate a longer delay but the arguments applicable to the Mach 3 case would also be applicable.

The Mach 6 aircraft upper surface also shows only limited temperature response during the abort delay (Figure 133). This concept, however, could not tolerate increases in delay time because, with the 15 second delay, the structural temperature reaches 443K (337°F). The critical temperature for reuse of the structure is 450K (350°F) due to the permanent reduction in

mechanical properties after exposure to higher temperatures. Therefore, due to the expected difficulties that an infrared scanning system would encounter in discriminating relatively minor surface overtemperatures, the infrared scanning technique was eliminated from further consideration.

The remaining two candidate approaches for failure detection, the eutectic salt elements and the fluid filled tube elements, were examined in more detail. Because of overall potential, the fluid filled tube elements were considered first.

To provide complementary data for evaluating the sensing elements, the Mach 6 upper and lower surface panels were analyzed to define temperature response, assuming no abort maneuver initiation. Figure 136 presents the results of this analysis. The 15 second response time is shown on the figure for reference. If the instrumentation provides a warning signal at a temperature level 28K (50°F) above the normal operation maximum design value of 394K (250°F), it will take 20 seconds to detect a failure in the upper surface and 75 seconds for the lower surface. Therefore, the initiation of the abort maneuver would exceed the baseline 15 second response time.

An analysis was conducted of the fluid (Freon 21) filled tube elements (phase change) attached to the aluminum skin of the silicone overcoated upper surface Mach 6 concept. The assumption of loss of coolant in only one tube provides a more severe case (in terms of failure detection) than total loss of panel cooling. Figure 137 shows the temperature distributions in the skin at the instant of failure and 15 seconds after failure. This distribution illustrates that the most desirable sensor element location would be next to the coolant tube rather than at the mid-point between tubes.

A sensor element, 0.305m (1 ft) in length, at the location adjacent to the coolant tube, with its low combined mass of aluminum and Freon (9.52 g/m (0.0064 lbm/ft)), would experience a temperature rise of about 5 K/sec (9°F/sec). This temperature rise is due to the excess heat input (heat in excess of that absorbed by adjacent tubes) at this location. The heat required to boil the Freon is about 312 to 347 $\frac{J}{m}$ (0.09 to 0.1 Btu/ft). With a 22K (40°F) temperature rise of the element, the total heat input required to boil the Freon would be about 4.85 kJ/m (1.4 Btu/ft). The excess heat available for this function would be 894 J/m's (0.257 Btu/ft sec). Thus, the sensor would provide the desired signal about 5 seconds after failure.

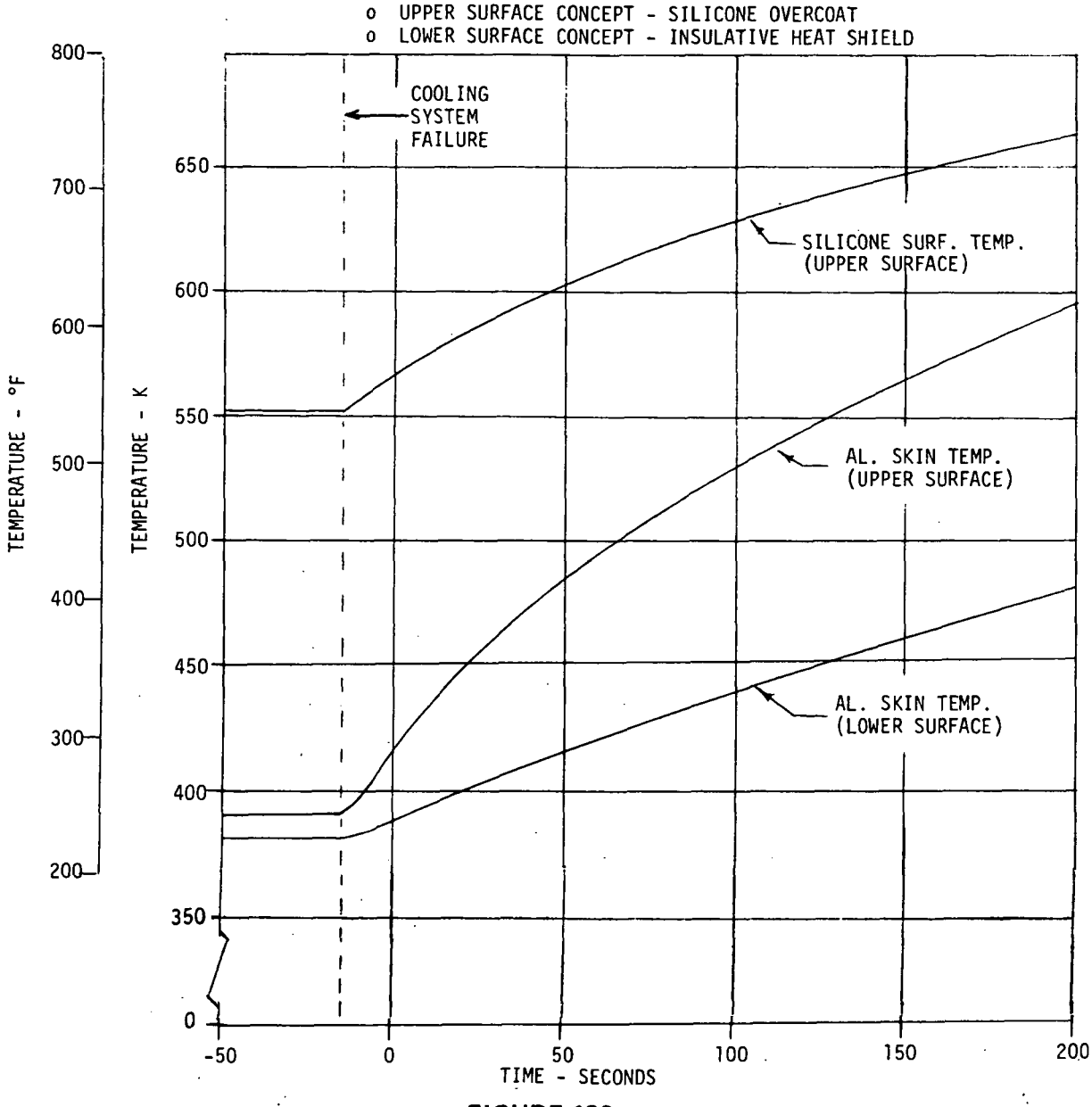

FIGURE 136
MACH 6 PANEL TEMPERATURE RESPONSE TO FAILURE DURING CRUISE (SYSTEM FAILURE WITH NO ABORT)

The element on the lower surface would experience a temperature rise of about 2 K/sec (4°F/sec). Assuming a 22 K (40°F) temperature rise of the sensor element, again the total heat input required for sensor initiation would be 4.85 kJ/m (1.4 Btu/ft). The excess heat in this case would be 435 J/m·s (0.125 Btu/ft sec). Therefore, the sensor would initiate the pressure signal in about 11 seconds.

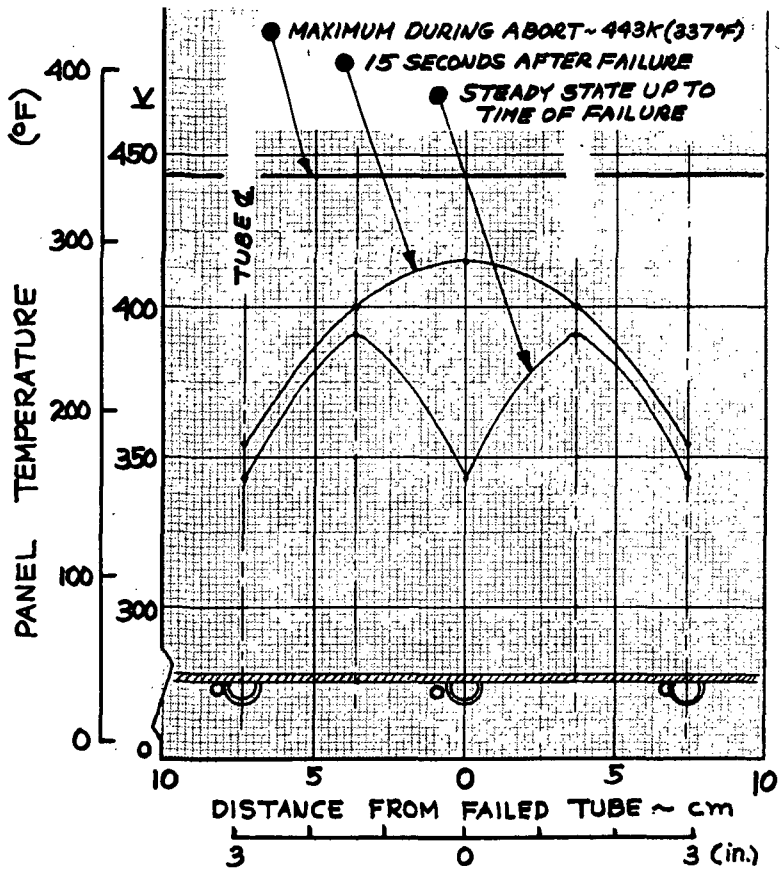

FIGURE 137
UPPER SURFACE PANEL TEMPERATURE DISTRIBUTION
(LOSS OF COOLING FROM ONE TUBE - MACH 6)

Examination of the Mach 3 and Mach 4.5 thermostructural concepts selected (Figures 120 and 121) shows that the normal absorbed heat flux is about the same as for Mach 6 concepts. Therefore, the Freon filled tube elements will provide comparable sensor response times.

It is concluded that the Freon filled tube elements will provide adequate sensor response times for the range of conditions investigated.

An examination of the eutectic salt elements, located adjacent to the coolant tubes, for a set point temperature of 403 K (265°F) and a sensor mass of 56.4 g/m (0.0358 lbm/ft), indicated sensor response times equivalent to those of the Freon filled tubes.

It was also judged that the eutectic salt elements could provide the failure detection function within the Mach 3 and Mach 4.5 aircraft with sensor response times about the same as the Freon filled tubes.

The eutectic salt elements would result in a penalty (fixed weight increase) of 1.79 Mg (3952 lbm) to the aircraft (2980 m^2 (32,134 ft^2 of cooled surface area). The Freon filled tube elements would result in a penalty of 0.5 Mg (1109 lbm).

Thus, the Freon filled tubes would be superior to the eutectic salt elements. In addition, the eutectic salt element can only provide failure indication whereas the Freon tubes provide a continuous monitoring capability.

The eutectic salt elements are state-of-the-art. The Freon filled tube element approach, to our knowledge, has never been considered for application as a failure detection device and would require considerable development. The risk appears low insofar as the engineering technology is concerned. The major cost/risk factor would be in the fabrication and installation of a reliable functioning system. The impact on panel fabrication cost (assuming a fully developed tube system) is estimated to be approximately the same for either approach. It may prove that some fluid other than Freon will be more desirable in this application. However, Freon illustrates the basic principle of operation. Determination of the optimum fluid to use is considered as part of the required development.

The conclusion was that the potential payoff of the Freon filled sensors, a safe aircraft system, appears to justify the selection of this approach for integration into advanced technology aircraft.

4.4.2 Selected Fail-Safe Systems - This section presents the selected fail-safe system concepts for each of the three typical cruise Mach number conditions. The selected concepts include the three basic factors required to assure safety of flight: A failure detection system capable of detecting failures or malfunctions in the active cooling system as well as failures in individual actively cooled panels; an abort trajectory capable of providing a near minimum heat load to the aircraft during descent from cruise Mach number; and thermostructural design approaches which minimize both the weight and the maximum structural temperature during an abort descent.

Figure 138 presents a weight summary of the selected fail-safe systems on the basis of the weight chargeable to one individual 1.2 m x 6.1 m (4 ft x 20 ft) actively cooled panel. Figure 139 presents a similar summary for the baseline actively cooled aluminum/active cooling systems for the three cruise

MACH NO.	AIRCRAFT SURFACE	CONFIGURATION (HONEYCOMB PANEL GEOMETRY)	FAIL-SAFE SYSTEM WEIGHT PER 7.43 m^2 (80 ft^2) PANEL ~ kg (lbm)						UNIT WEIGHT kg/m^2 (lbm/ft^2)
			COOLED SKIN, TUBES, AND STRUCTURE	MANIFOLDS AND NON-OPTIMUMS	HEAT SHIELD AND INSULATION	ACTIVE COOLING SYSTEM (1)	FAILURE DETECTION SYSTEM (2)	TOTAL	
3	UPPER	SILICONE OVERCOAT OVER AL. SKIN	57.0 (125.6)	37.0 (81.6)	3.5 (7.7)	4.8 (10.6)	1.2 (2.6)	103.5 (228.1)	13.91 (2.85)
	LOWER	SILICONE OVERCOAT OVER AL. SKIN	57.0 (125.6)	37.0 (81.6)	3.5 (7.7)	6.6 (14.5)	1.3 (2.8)	105.4 (232.2)	14.16 (2.90)
4.5	UPPER	SILICONE OVERCOAT OVER AL. SKIN	57.0 (125.6)	37.0 (81.6)	5.7 (12.5)	8.1 (17.8)	1.5 (3.2)	109.3 (241.0)	14.70 (3.01)
	LOWER	INSULATED HEAT SHIELD OVER AL. SKIN	57.0 (125.6)	37.0 (81.6)	21.1 (46.5)	4.4 (9.6)	1.3 (2.8)	120.8 (266.1)	16.26 (3.33)
6	UPPER	SILICONE OVERCOAT OVER AL. SKIN	57.0 (125.6)	37.0 (81.6)	4.2 (9.3)	10.3 (22.8)	1.7 (3.8)	110.2 (243.1)	14.84 (3.04)
	LOWER	INSULATED HEAT SHIELD OVER AL. SKIN	57.0 (125.6)	37.0 (81.6)	40.6 (89.6)	4.9 (10.8)	1.3 (2.8)	140.8 (310.4)	18.94 (3.88)

NOTES: (1) SYSTEM HEAT LOAD IS EQUAL TO, OR LESS THAN, AVAILABLE HYDROGEN FUEL FLOW HEAT SINK CAPACITY.

(2) FLUID FILLED TUBE (PHASE CHANGE) FAILURE DETECTION ELEMENTS. WEIGHT BASED ON TUBE PITCH. SYSTEM WEIGHT IS 0.168 kg/m^2 (0.0345 lbm/ft^2) FOR 10.4 cm (4 in.) TUBE PITCH. COOLING SYSTEM WEIGHT INCLUDES FAILURE DETECTION WEIGHT FOR BASIC COOLING SYSTEM.

FIGURE 138
FAIL-SAFE SYSTEM WEIGHTS

MACH NO.	AIRCRAFT SURFACE	CONFIGURATION (HONEYCOMB PANEL GEOMETRY)	BASELINE WEIGHT PER 7.43 m^2 (80 ft^2) PANEL ~ kg (lbm)						UNIT WEIGHT kg/m^2 (lbm/ft^2)
			COOLED SKIN, TUBES, AND STRUCTURE	MANIFOLDS AND NON-OPTIMUMS	HEAT SHIELD AND INSULATION	ACTIVE COOLING SYSTEM (1)	FAILURE DETECTION SYSTEM (2)	TOTAL	
3	UPPER	BASELINE AL. SKIN AT AVERAGE Tw = 366K (200°F)	57.9 (127.7)	37.0 (81.6)	---	6.1 (13.5)	---	101.0 (222.8)	13.59 (2.79)
	LOWER	SAME AS ABOVE	58.3 (128.6	37.0 (81.6)	---	10.1 (22.3)	---	105.4 (232.5)	14.19 (2.91)
4.5	UPPER	SAME AS ABOVE	59.0 (130)	37.0 (81.6)	---	13.2 (29.0)	---	109.2 (240.6)	14.70 (3.01)
	LOWER	SAME AS ABOVE	59.7 (131.7)	37.0 (81.6)	---	17.6 (38.9)	---	114.3 (252.2)	15.38 (3.15)
6	UPPER	SAME AS ABOVE	59.0 (130.1)	37.0 (81.6)	---	13.7 (30.2)	---	109.7 (241.9)	14.76 (3.02)
	LOWER	SAME AS ABOVE	60.7 (133.8)	37.0 (81.6)	---	26.0 (57.3)	---	123.7 (272.7)	16.65 (3.41)

NOTES: (1) ACTIVE COOLING SYSTEM HEAT LOADS EXCEED AVAILABLE HYDROGEN FUEL FLOW HEAT SINK CAPACITY.

(2) SYSTEMS DO NOT HAVE CAPABILITY FOR DETECTION OF INDIVIDUAL PANEL FAILURES.

FIGURE 139
BASELINE SYSTEM WEIGHTS

Mach numbers, for comparative purposes. The weights shown are for the typical upper and lower surface locations with heating rates, at cruise, equal to the average for the entire aircraft upper, or lower, surface, respectively. As shown by the figures, the unit weights are not radically different.

To provide additional insight into the basic differences between the fail-safe systems and the baselines, the systems for each cruise Mach number are discussed in following paragraphs.

a. Mach 3 Fail-Safe System - The fail-safe system selected for Mach 3 cruise utilized conventional instrumentation for monitoring of active cooling system parameters to provide warning of system malfunction or failure. The failure detection system components used to detect failures (loss of cooling) of individual actively cooled panels were Freon filled tube elements. These elements (sensors) have the potential to provide a continuous record of average panel temperature. With loss of panel cooling (or individual coolant tube) the Freon vaporizes, providing a pressure pulse signal to a pressure transducer. The system of tube elements use a common Freon reservoir to provide volume for thermal expansion of the Freon. Pressure is maintained at a constant level by a compensator within the liquid Freon reservoir during normal operation. The pressure pulse is experienced only with boiling of the Freon due to loss of panel cooling. Sensor response times were estimated at less than 15 seconds for the upper and lower surfaces of the aircraft. These response times were adequate for the structural heat protection provided.

The abort descent trajectory used provided a low heat load to the aircraft during abort. This trajectory used a constant "g-load" pull-up to a high-lift coefficient glide condition. Engine power was cut at initiation of abort.

The thermostructural concepts selected for the Mach 3 system was a silicone insulative overcoat. The coating thickness was an average of 1.17 mm (0.046 in). Maximum temperatures of the aluminum structure during abort were well under the reuse limit of 450 K (350°F).

Figure 140 presents a comparison of the fail-safe system with a Mach 3 bare aluminum skin baseline system. As shown, the fail-safe capability resulted in a fixed weight increase of 0.5 Mg (847 lbm) over the total weight of the baseline system, about 168 g/m^2 (0.0264 lbm/ft^2) if cooling requirements are not considered.

	SYSTEM WEIGHTS - Mg (lbm) (1)	
	BASELINE SYSTEM	FAIL-SAFE SYSTEM
STRUCTURE (2)	38.2 (84,243)	39.2 (86,320)
ACTIVE COOLING SYSTEM (3)	3.3 (7,285)	2.3 (4,974)
FAILURE DETECTION SYSTEM (4)	NONE	0.5 (1,081)
SUBTOTAL	41.5 (91,528)	42.0 (92,375)
ADDITIONAL HYDROGEN REQUIRED FOR COOLING (5)	32.1 (70,900)	NONE
TOTAL	73.6 (162,428)	42.0 (92,375)
	HEAT LOADS - MW (Btu/sec) (1)	
COOLING SYSTEM HEAT LOAD (START OF CRUISE) (6)	25 (2.37 X 10^4)	15.4 (1.46 X 10^4)
HYDROGEN FUEL FLOW HEAT SINK CAPACITY (CRUISE) (7)	15.4 (1.46 X 10^4)	15.4 (1.46 X 10^4)

NOTES:
(1) ALL WEIGHTS AND HEAT LOADS BASED ON EQUAL AIRCRAFT CONFIGURATIONS WITH 2980 m^2 (32,134 ft^2) OF COOLED SURFACE AREA. VALUES SHOWN ARE DERIVED FROM AVERAGE VALUES FOR 1618 m^2 (17,449 ft^2) WITH CRUISE HEATING RATE EQUAL TO TYPICAL UPPER SURFACE AVERAGE AND 1362 m^2 (14,685 ft^2) WITH CRUISE HEATING RATE EQUAL TO TYPICAL LOWER SURFACE AVERAGE.
(2) ACTIVELY COOLED PANELS, ATTACHMENTS, NON-OPTIMUMS, HEAT SHIELDS AND INSULATION (OR OTHER HEAT PROTECTION) WHERE APPLICABLE.
(3) ALL COMPONENTS, INSTRUMENTATION, COOLANT, COOLANT DISTRIBUTION LINES, ETC.
(4) ALL COMPONENTS INTEGRATED INTO AIRCRAFT
(5) BASED ON (6) (7) FOR MACH 3 CRUISE FOR 7.41 Mm (4000 NM). DOES NOT INCLUDE HYDROGEN CONTAINMENT.
(6) BASELINE HAS UNPROTECTED ALUMINUM SKIN AT AVERAGE OF 366 K (200°F) AT CRUISE.
(7) BASED ON TYPICAL VALUES FOR DUCT BURNING TURBOFAN ENGINES, ΔT_f = 33 K TO 311 K (500°F).

FIGURE 140
COMPARISON OF MACH 3 CRUISE SYSTEMS

If hydrogen heat sink is considered, the fail-safe system has the lower weight. The baseline system, for the assumed cruise range, 74.1 Mm (4000 NM), would require an additional 32.1 Mg (70,900 lbm) of hydrogen to provide adequate cooling. Weight for containment of the excess hydrogen is not included in this additional weight. Note the differences (Figure 140) between the baseline and fail-safe systems in terms of system heat load versus available

hydrogen fuel heat sink capacity. The baseline system, at start of Mach 3 cruise, would require approximately 162% of available heat sink. Thus, this system would not be capable of operation unless additional hydrogen were provided or a large portion of the cooled area were heat shielded in some manner, with an attendant increase in weight. The fail-safe system heat load matches the heat sink availability and is a viable system for Mach 3 operation.

b. Mach 4.5 Fail-Safe System - The selected Mach 4.5 cruise fail-safe system was configured with the same failure detection devices as the Mach 3 system. The same type of abort descent trajectory was utilized to reduce descent heat load.

The thermostructural approach on this aircraft was to use the silicone overcoat material on the upper surfaces (average thickness of 1.91 mm (0.075 in)) and a titanium heat shield, with insulation (6.35 mm (0.25 in) thick), on the lower surfaces. Maximum abort temperatures were under the limit for reuse of 450K (350°F). The corrugation stiffened beaded skin titanium heat shield-insulation package-cooled panel assembly does not use radiation gaps and this minimizes boundary layer leakage.

Figure 141 compares the fail-safe system with the bare unprotected aluminum skin baseline system. In this case, the addition of fail-safe capability increased the fixed weight by 1.7 Mg (3734 lbm), or 0.57 kg/m^2 (0.116 lbm/ft^2), compared to the no-abort-capability, and insufficient cooling capability, baseline.

The baseline system heat load, at start of cruise at Mach 4.5, was approximately 123% of the available fuel heat sink capacity. The fail-safe system heat load was about 41% of fuel heat sink capacity. Figure 141 shows that an additional 10.7 Mg (23,600 lbm) of hydrogen would be required for the baseline system to meet the cooling demand. The fail-safe system, for the same cruise range, would reduce the total weight nearly 9.1 Mg (20,000 lbm).

c. Mach 6 Fail-Safe System - This system again used the same type of failure detection methods and abort trajectory as the Mach 3 and 4.5 systems. A silicone overcoated (1.42 mm (0.056 in) thickness) upper surface and a Rene' 41 corrugated stiffened beaded skin heat shield and insulation on the lower surface were combined to provide abort heat protection of the aluminum

	SYSTEM WEIGHTS - Mg (lbm) (1)	
	BASELINE SYSTEM	FAIL-SAFE SYSTEM
STRUCTURE (2)	38.7 (85,303)	42.9 (94,481)
ACTIVE COOLING SYSTEM (3)	5.6 (12,301)	2.6 (5,645)
FAILURE DETECTION SYSTEM (4)	NONE	0.5 (1,212)
SUBTOTAL	44.3 (97,604)	46.0 (101,338)
ADDITIONAL HYDROGEN REQUIRED FOR COOLING (5)	10.7 (23,600)	NONE
TOTAL	55.0 (121,204)	46.0 (101,338)
	HEAT LOADS - MW (Btu/sec) (1)	
COOLING SYSTEM HEAT LOAD (START OF CRUISE) (6)	54.7 (5.19×10^4)	18.1 (1.72×10^4)
HYDROGEN FUEL FLOW HEAT SINK CAPACITY (CRUISE) (7)	44.4 (4.21×10^4)	44.4 (4.21×10^4)

NOTES:
(1) ALL WEIGHTS AND HEAT LOADS BASED ON EQUAL AIRCRAFT CONFIGURATIONS WITH 2980 m^2 (32,134 ft^2) OF COOLED SURFACE AREA. VALUES SHOWN ARE DERIVED FROM AVERAGE VALUES FOR 1618 m^2 (17,449 ft^2) WITH CRUISE HEATING RATE EQUAL TO TYPICAL UPPER SURFACE AVERAGE AND 1362 m^2 (14,685 ft^2) WITH CRUISE HEATING RATE EQUAL TO TYPICAL LOWER SURFACE AVERAGE.
(2) ACTIVELY COOLED PANELS, ATTACHMENTS, NON-OPTIMUMS, HEAT SHIELDS AND INSULATION (OR OTHER HEAT PROTECTION) WHERE APPLICABLE.
(3) ALL COMPONENTS, INSTRUMENTATION, COOLANT, COOLANT DISTRIBUTION LINES, ETC.
(4) ALL COMPONENTS INTEGRATED INTO AIRCRAFT
(5) BASED ON (6) (7) FOR MACH 4.5 CRUISE FOR 7.41 Mm (4000 NM). DOES NOT INCLUDE HYDROGEN CONTAINMENT.
(6) BASELINE HAS UNPROTECTED ALUMINUM SKIN AT AVERAGE OF 366 K (200°F) AT CRUISE.
(7) BASED ON TYPICAL VALUES FOR TURBORAMJET ENGINES (RAMJET MODE AT CRUISE) ΔT_f = 33 K TO 311 K (500°F).

FIGURE 141
COMPARISON OF MACH 4.5 CRUISE SYSTEMS

actively cooled panels, and to provide a reduction in absorbed heat flux at cruise conditions. The maximum structural temperatures during abort (total loss of cooling) would be approximately 443K (337°F) for the upper surfaces and 465K (377°F) for the lower surface.

Figure 142 illustrates the weight differences between the fail-safe system and the unprotected baseline system. Fail-safe capability resulted in a fixed weight increase over the baseline weight of 3.3 Mg (7162 lbm) if cooling requirements are neglected. This is about 1.11 kg/m^2 (0.229 lbm/ft^2). System

	SYSTEM WEIGHTS - Mg (lbm) (1)	
	BASELINE SYSTEM	FAIL-SAFE SYSTEM
STRUCTURE (2)	38.9 (85,734)	46.1 (101,703)
ACTIVE COOLING SYSTEM (3)	7.7 (17,105)	3.2 (6,955)
FAILURE DETECTION SYSTEM (4)	NONE	0.6 (1,343)
SUBTOTAL	46.6 (102,839)	49.9 (110,001)
ADDITIONAL HYDROGEN REQUIRED FOR COOLING (5)	29.4 (64,700)	NONE
TOTAL	76.0 (167,539)	49.9 (110,001)
	HEAT LOADS- MW (Btu/sec) (1)	
COOLING SYSTEM HEAT LOAD (START OF CRUISE) (6)	90.6 (8.59×10^4)	25.2 (2.39×10^4)
HYDROGEN FUEL FLOW HEAT SINK CAPACITY (CRUISE) (7)	54.2 (5.14×10^4)	54.2 (5.14×10^4)

NOTES:
(1) ALL WEIGHTS (AND HEAT LOADS) BASED ON EQUAL AIRCRAFT CONFIGURATIONS WITH 2980 m^2 (32,134 ft^2) OF COOLED SURFACE AREA. VALUES SHOWN ARE DERIVED FROM AVERAGE VALUES FOR 1618 m^2 (17,449 ft^2) WITH CRUISE HEATING RATE EQUAL TO TYPICAL UPPER SURFACE AVERAGE AND 1362 m^2 (14,685 ft^2) WITH CRUISE HEATING RATE EQUAL TO TYPICAL LOWER SURFACE AVERAGE.
(2) ACTIVELY COOLED PANELS, ATTACHMENTS, NON-OPTIMUMS, HEAT SHIELDS AND INSULATION (OR OTHER HEAT PROTECTION) WHERE APPLICABLE.
(3) ALL COMPONENTS, INSTRUMENTATION, COOLANT, COOLANT DISTRIBUTION LINES, ETC.
(4) ALL COMPONENTS INTEGRATED INTO AIRCRAFT
(5) BASED ON (6) (7) FOR MACH 6 CRUISE FOR 7.41 Mm (4000 NM). DOES NOT INCLUDE HYDROGEN CONTAINMENT.
(6) BASELINE HAS UNPROTECTED ALUMINUM SKIN AT AVERAGE OF 366 K (200°F) AT CRUISE.
(7) BASED ON TYPICAL VALUES FOR TURBORAMJET ENGINES (RAMJET MODE AT CRUISE) ΔT_f = 33 K TO 311 K (500°F).

FIGURE 142
COMPARISON OF MACH 6 CRUISE SYSTEMS

heat loads for the unprotected baseline were 167% of available fuel heat sink capacity at start of cruise conditions. In this case, the baseline system with adequate onboard hydrogen would be about 26.1 Mg (57,500 lbm) heavier than the fail-safe system. The fail-safe system requires only 46.5% of available fuel heat sink capacity.

Figure 143 presents a comparison of Reference (15) results and this study. As shown, the "Fail-Safe Abort System" total unit weight is approximately 90% of the unit weight of the Reference (15) unshielded 366K (200°F) structure with redundant cooling systems, which requires 10.44 Mg (23,000 lbm) of excess hydrogen for cooling. The additional 4.54 Mg (10,000 lbm) required for containment of the excess hydrogen is not included in the weight summary. The 10.44 Mg (23,000 lbm) of excess hydrogen is for a Mach 6 cruise range of about 5.87 Mm (3170 NM). The fail-safe system aircraft has a cruise range of over 7.41 Mm (4000 NM). If the Reference (15) concept were placed on an equal basis, approximately 13.16 Mg (29,000 lbm) of excess hydrogen would be required. The "Fail-Safe" concept does not require any additional hydrogen for cooling, using only 46.5% of available fuel heat sink at start of cruise conditions. The Reference (15) shielded structure (about 33% of area is shielded) concept with redundant cooling systems is shown in the figure to have lower unit weight than the "Fail-Safe" system concept. However, this system does not have the abort capability, or the capability to detect loss of cooling within the individual actively cooled panels. Loss of cooling could result in structural failure if undetected. Addition of heat protection to the unshielded areas would add approximately 0.619 kg/m^2 (0.1268 lbm/ft^2) to the presented weights of the Reference (15) shielded concept for a total unit weight of 16.697 kg/m^2 (3.4207lbm/ft^2). This weight increase considers the cooling system weight reductions due to reduced heat load and the elimination of excess hydrogen. A comparison of this unit weight with the "Fail-Safe" system unit weight of 16.713 kg/m^2 (3.423 lbm/ft^2) indicates that "Fail-Safe" capability results in unit weights approximately equal to an equivalent all shielded concept with redundant cooling systems. In addition, it appears that the failure detection system could be added to the shielded redundant cooling system concept for very little penalty, only 0.204 kg/m^2 (0.0418 lbm/ft^2. This would be expected to result in an actively cooled structure concept with outstanding safety capability.

	UNIT WEIGHT - kg/m² (lbm/ft²)					
	REFERENCE (15) UNSHIELDED 366 K (200°F) STRUCTURE, REDUNDANT COOLING SYSTEM		REFERENCE (15) SHIELDED 366 K (200°F) STRUCTURE, REDUNDANT COOLING SYSTEM		FAIL-SAFE SYSTEM 366 K (200°F) STRUCTURE	
STRUCTURE	12.651 [1]	(2.5912)	12.651 [1]	(2.5912)	15.452 [2][3]	(3.1649)
COOLING SYSTEM	2.697	(0.5524)	1.798	(0.3682)	1.057	(0.2164)
FAILURE DETECTION SYSTEM	NONE		NONE		0.204	(0.0418)
OTHER	3.303 [1][4]	(0.6765)	1.594 [1][5]	(0.3265)	NONE	
SUBTOTAL [5]	18.651	(3.8201	16.043	(3.2859)	16.713	(3.4231)
ADDITIONAL HYDROGEN HEAT SINK [6][7]	0.860	(0.1760)	0.039	(0.0080)	NONE	
TOTAL	19.511	(3.9961)	16.082	(3.2939)	16.713	(3.4231)

NOTE:
[1] 3159 m² (34,000 ft²) OF COOLED SURFACE, CRUISE RANGE 5.87 Mm (3170 NM)
[2] 2980 m² (32,134 ft²) OF COOLED SURFACE, CRUISE RANGE 7.41 Mm (4000 NM)
[3] INCLUDES RENE'41 HEAT SHIELDS ON LOWER SURFACE, SILICONE ELASTOMER OVERCOAT ON UPPER SURFACES. BASIC STRUCTURE LESS HEAT PROTECTION IS 12.65 kg/m² (2.59 lbm/ft²).
[4] EXCESS HYDROGEN [10.44 Mg (23,000 lbm)] FOR COOLING, DOES NOT INCLUDE HYDROGEN CONTAINMENT.
[5] HEAT SHIELDING [4.5359 Mg (10,000 lbm)] PLUS 0.4539 Mg (100 lbm) EXCESS HYDROGEN FOR COOLING, DOES NOT INCLUDE HYDROGEN CONTAINMENT.
[6] ALL FOR MACH 6 CRUISE AIRCRAFT.
[7] ADDITIONAL HYDROGEN FOR COOLING FOR ΔTIME (0.23 HOURS) TO GIVE TOTAL CRUISE RANGE OF 7.41 Mm (4000 NM). DOES NOT INCLUDE HYDROGEN CONTAINMENT.

FIGURE 143
MACH 6 CRUISE TRANSPORT AIRCRAFT WEIGHT SUMMARY

5. CONCLUSIONS

The potentials of a "Fail-Safe Abort System" for use in actively cooled, hydrogen fueled, supersonic and hypersonic aircraft were examined. This concept depends on three basic elements:

o Detection of cooling system malfunctions, including individual actively cooled structural panels; with reliable and responsive sensors.

o An abort descent trajectory which minimizes the aircraft descent heat load.

o Fail-safe thermostructural concepts which minimize the increase in structural temperatures during abort at minimum weight.

Conclusions relative to these elements follow:

a. Detecting Cooling System Failure is State-of-the-art - Basic cooling system malfunctions, or failure, can be detected by the use of conventional instrumentation such as pressure transducers, flow meters, thermistors and thermocouples, and liquid level indicators for measuring system parameters.

b. Detecting Loss of Cooling in the Airframe Panels is Feasible - Failure (loss of cooling) of individual actively cooled structural panels can be detected by temperature sensitive elements attached to the aluminum skins of the cooled panels. The temperature sensor response times appear to be such that no significant weight penalty will be experienced due to delay between failure and failure detection. The temperature sensing elements required for detection of individual panel loss of cooling, and the associated system components, are relatively complex and require development. The potential benefits of these sensors appear to justify the development risk.

c. Abort Trajectories Significantly Reduce Heat Load - Abort trajectories using constant g-load pull-up maneuvers result in descent heat loads sufficiently low that abort heating does not result in significant thermostructural weight penalties.

d. No Weight Penalty Required for Fail-Safe Features - No thermostructural weight penalty due to abort heating is incurred for Mach 3 or Mach 4.5 cruise aircraft. Design of the thermostructural system to provide a match between absorbed heat and hydrogen fuel heat sink capacity provides a thermostructural design capable of abort descent. The weight penalty due to Mach 6 abort is offset by reductions in weight of the active cooling system. The

"Fail-Safe" concept, compared to an unprotected 366K (200°F) aluminum structure aircraft carrying adequate hydrogen to meet all cooling requirements, will result in a reduction of the combined structural/cooling system/required heat sink weight.

e. Aircraft is Reusable After Abort - Structural temperatures during abort from Mach 3 and Mach 4.5 can be kept below 450K (350°F), the practical limit for reuse of the aluminum structure. The thermostructural design at these Mach numbers is dictated by cruise Mach number considerations. The maximum structural temperatures encountered during Mach 6 abort are a function of the type of failure and the time required to sense the failure. Basic cooling system malfunction, or failure of an upper surface panel to receive adequate cooling will result in maximum abort temperature levels on the order of 443K (337°F) and 465K (377°F), for the typical upper surface and lower surface structural concepts studied.

f. THE BASIC CONCEPT OF "FAIL-SAFE ABORT SYSTEMS" IS COMPLETELY FEASIBLE THROUGHOUT THE MACH 3 TO MACH 6 SPEED RANGE.

In addition to the primary conclusions stated above, a comparison of results of this study with those of Reference (15) resulted in several pertinent observations. These are:

o The addition of "Fail-Safe" capability to an actively cooled Mach 6 cruise transport design results in total system unit area weights approximately equal to the total system unit area weights for a heat shielded design with redundant cooling systems.

o A marriage of a redundant cooling system approach with the "Fail-Safe Abort" concept appears possible with minimal weight impact. An integrated system of this type would have outstanding overall safety capability.

o The structural heat protection required to provide the "Fail-Safe Abort" capability allows a reduction in aircraft heat loads to a point where normal engine fuel flow demands can provide more than adequate heat sink.

6. REFERENCES

1. C. J. Pirrello and R. L. Herring, Study of a Fail-Safe Abort System for an Actively Cooled Hypersonic Aircraft - Technical Summary, NASA CR-2652 January 1976.
2. J. E. Stone, A Fuselage/Tank Structure Study for Actively Cooled Hypersonic Cruise Vehicles, Active Cooling System Analysis, NASA CR-132669, June 1975.
3. R. A. Jones, D. O. Braswell and C. B. Richie, Fail-Safe System for Actively Cooled Supersonic and Hypersonic Aircraft, NASA TM X-3125, January 1975.
4. T. Nobe, A Fuselage/Tank Structure Study for Actively Cooled Hypersonic Cruise Vehicles, Aircraft Design Evaluation, NASA CR-132668, June 1975.
5. A. H. Baker, A Fuselage/Tank Structure Study for Actively Cooled Hypersonic Cruise Vehicles, Structural Analysis, NASA CR-132670, June 1975.
6. Design and Fabrication of an Actively Cooled Panel, NASA Contract No. NAS1-12919, 1974.
7. GE5/J26-Study C, Report SS-65-2, General Electric Company Flight Propulsion Division, December 1965. (Confidential)
8. Gillies, J. A., A Text Book of Aviation Physiology, Pergamon Press, 1975.
9. Brewer, G. D. and Morris, R. E., Study of Active Cooling for Supersonic Transports, NASA CR 132573, February 1975.
10. Pierce L. Lawing, Analysis of Various Descent Trajectories for a Hypersonic Cruise, Cold-Wall Research Airplane, NASA TN D-7860, June 1975.
11. J. V. Becker, New Approaches to Hypersonic Aircraft, ICAS Paper presented at the 7th Congress of ICAS, Rome, Italy, September 1970.
12. W. A. McConarty and F. M. Anthony, Design and Evaluation of Active Cooling Systems for Mach 6 Cruise Vehicle Wings, NASA CR-1916, December 1971.
13. R. G. Helenbrook, W. A. McConarty, and F. M. Anthony, Evaluation of Active Cooling Systems for a Mach 6 Hypersonic Transport Airframe, NASA CR-1917, December 1971.
14. R. G. Helenbrook and F. M. Anthony, Design of a Convective Cooling System for a Mach 6 Hypersonic Transport Airframe, NASA CR-1918, December 1971.

15. F. M. Anthony, W. H. Dukes, and R. G. Helenbrook, Data and Results from a Study of Internal Convective Cooling Systems for Hypersonic Aircraft, NASA CR-132432, June 1974.

16. D. V. Hale, M. J. Hoover, and M. J. O'Neill, PHASE CHANGE MATERIALS HANDBOOK, NASA CR-61363, September 1971.

17. H. D. Altis and L. L. Pagel, Hypersonic Vehicle Study, Volume III - Thermodynamics, MDC Report F666, October 1967 (S).

18. G. A. Niblock, C. C. Miller, and J. S. Holmgron, STUDY OF STRUCTURAL ACTIVE COOLING AND HEAT SINK SYSTEMS FOR SPACE SHUTTLE, MDC Report E0638, June 1972.

19. D. W. VanKrevelen, Properties of Polymers, Correlations with Chemical Structure, Elsevier Publishing Company, 1972.

20. DESIGN AND FABRICATION OF RADIATIVE-ACTIVELY COOLED STRUCTURAL PANEL, NASA Contract NAS1-13939, 1975.

21. Federal Aviation Regulations, Volume III, Part 25 Airworthiness Standards: Transport Category Airplanes.